Denudation history and palaeogeography of the Pyrenees and their peripheral basins: an 84-million-year geomorphological perspective

Marc Calvet, Yanni Gunnell, Bernard Laumonier

Denudation history and palaeogeography of the Pyrenees and their peripheral basins: an 84-million-year geomorphological perspective

Marc Calvet[a]
Yanni Gunnell[b]
Bernard Laumonier[c]

[a] Université de Perpignan—Via Domitia, CNRS UMR 7194 Histoire Naturelle de l'Homme Préhistorique, 52 avenue Paul Alduy, F-66860 Perpignan, France

[b] Université de Lyon—Lumière Lyon 2, CNRS UMR 5600 Environnement-Ville-Société, 5 Avenue P. Mendès-France, F-69676 Bron, France

[c] École des Mines de Nancy, GeoRessources, UMR 7359, Université de Lorraine, Campus ARTEM, CS14234, F-54042 Nancy, France

Abstract

This review provides a synthesis of the evolution of the Pyrenees since ~84 Ma and is uniquely focused on analysing jointly and comparatively its peripheral pro-foreland, retro-foreland and Mediterranean basins. The reconstructions adopt a geomorphological perspective focused on the waxing and waning of palaeorelief, and is underpinned by (i) the denudation history of the mountain belt encoded in the sedimentary record of its basins, (ii) rock-cooling histories inferred from low-temperature thermochronology, and (iii) the age and spatial distribution of tectonic and erosional landforms. Existing geological reconstructions of the Pyrenees commonly terminate at the end of the syntectonic collision period (early Miocene). Here, the no-less eventful post-shortening period of the last 25–30 m.y. is also addressed. Accordingly, emphasis is given to the record provided by nonmarine clastic sequences, and to the often understated depositional biochronology documented by the continental fossils they contain. Sedimentological and provenance analysis of coarse clastic deposits further documents the fine-scale palaeogeography of sources and sinks, and is correlated with different generations of eustatic, tectonic, and volcanic features, as well as extant populations of land surfaces such as rock pediments, palaeovalleys, and other

landforms indicative of palaeoelevation and palaeotopography. These interconnected and age-bracketed diagnostic features are correlated with independent evidence concerning the structural evolution of the orogenic belt at crustal and lithospheric scale. They show that the Ancestral (i.e., Paleogene) Pyrenees were in many aspects dissimilar to the successor mountain range we observe today. They also suggest that, despite its prima facie topographic continuity from the Mediterranean to the Atlantic, the modern mountain range, particularly in its eastern half, is in a transient topographic state. This would appear to have been driven by large-scale asthenospheric flows contributing to regional uplift and erosion of not just the mountain range but also its foreland basins during the last ~12 m.y.

Contents

1 Introduction

This review offers a fully integrated analysis of the Pyrenees from a geomorphological perspective, i.e., understanding the cycles and chronology of mountain growth and decay through the record of landforms as well as rocks. The emphasis, therefore, is on reconstructing the successive states of the Pyrenees as a mountain range, thus deviating from the more conventional approach which consists in presenting the Pyrenees as a belt of crustal deformation with limited concern for its topographic features and transformations. Like the mythical six blind men of Hindustan whose task was to characterise the complete features of an elephant by each exploring one part of its anatomy, geoscience reviews of the Pyrenees have tended recurrently to be delivered in spatially, conceptually, or chronologically limited bundles. Because the mountains extend across several nations, divisions have often fallen not just along linguistic (e.g., French, Spanish, Catalan, English) and disciplinary lines (e.g., structural geology, solid-earth geophysics, stratigraphy,

142 sedimentology, palaeontology, geochronology, geomorphology, surface process modelling)
143 but also along scientific divides within identical disciplines (e.g., in terms of understanding
144 the metamorphic geology, displacement distances between Europe and Iberia, magnitudes
145 of crustal shortening, sequence stratigraphy, glacial geomorphology, alluvial sequence
146 analysis, karst evolution, etc.). As a result, our understanding of the palaeogeography and
147 topographic evolution of the Pyrenees has remained stubbornly piecemeal. The most robust
148 portrayals are often inferred from basin analysis but are equally often restricted to selected
149 subregions or geological epochs, and thus fall short of producing a narrative that spans the
150 late Mesozoic to the Present, extends from the highest peaks in Hercynian basement to the
151 most distal Neogene molasse deposits of the Ebro and Aquitaine basins, and deals with
152 Cenozoic and Quaternary landform assemblages from the Mediterranean to the Bay of
153 Biscay.
154 Some of the cutoff lines in this fragmented narrative have been of a spatial nature:
155 (i) Relative overemphasis on the Ebro Basin and the pro-wedge compared to the retro-
156 wedge and the Aquitaine Basin;
157 (ii) emphasis on the Mesozoic basin architecture of the Aquitaine foreland — in line with the
158 goals of petroleum exploration — with only a subsidiary focus on the record provided by
159 the overlying Cenozoic sequences;
160 (iii) emphasis on the central Pyrenees, where (since 1985) the ECORS-Pyrenees deep seismic
161 profile has spawned a model of crustal architecture which, however, does not
162 adequately describe the orogen's architecture further to the west (some data available
163 from the 1989 ECORS-Arzacq profile) or to the east (no data of a similar nature);
164 (iv) emphasis on the ECORS-inspired subsurface crustal architecture of the Axial Zone in the
165 central Pyrenees rather than on the subaerial geometry of the orogen, which for 30 years
166 has been invariably portrayed as a thick and tight-folded anticlinal stack of basement
167 nappes despite growing evidence that other geometric reconstructions involving a lesser
168 magnitude of vertical crustal thickening, and possibly of horizontal shortening, can be
169 accommodated;
170 (v) emphasis on basin analysis in discrete, strike-perpendicular foreland segments or swaths,
171 fostering a potential for information offsets and apparent along-strike discrepancies —
172 e.g., between the Eocene foredeeps of Catalonia and Aragón, and among the fossil-poor
173 continental depositional records; and for similar inconsistencies in mapping criteria for

various Cenozoic deposits among different generations of geological maps in the French Pyrenees.

(vi) emphasis on summit erosion surfaces, but without descending to the outer sierras and foothills below elevations of 1000 m, where important geomorphological clues of a similar nature also occur.

Other recurring cutoff lines are of a chronological nature:

(i) emphasis on the Alpine structures without sufficient consideration for Hercynian tectonic inheritance; or, conversely, emphasis on Hercynian inheritance with insufficient recognition of Alpine overprints. This has entailed major delays in the publication of certain geological maps and impacted the publication agenda of synthetic and integrated monographs about the Pyrenees (Barnolas and Chiron, 1996, 2018);

(ii) emphasis on the synorogenic (syntectonic) Pyrenees, i.e., on the late Cretaceous and Paleogene epochs until the cessation of fold-and-thrust deformation, as if the post-orogenic period (interchangeably also termed post-shortening period in this review), which spans the Neogene and Quaternary, had remained uniquely uneventful and could satisfy the expedient assumption of a topographic steady state;

(iii) emphasis on the orogen as if it were a closed plate-boundary system driven exclusively by crustal thickening, erosion, and peripheral sedimentation — when actually the orogen is also influenced by an independent chronology of Cenozoic intraplate and asthenospheric processes affecting large tracts of Iberia, the French Massif Central, the Western Mediterranean, and impacting on base-level changes within the mountain range as well as its peripheral lowlands.

This matrix of spatial and chronological cutoff lines arises from a fragmentation of the scientific cultures involved in documenting the Pyrenees. In 1789, geologist Louis Ramond de Carbonnières wrote:

> *"I doubt that there exists a mountain range better suited than the Pyrenees to the observation by a naturalist of its structure and rock disposition. Because it is simple and regular throughout most of its extent, the order which presided over the formation of its peaks and the laws which govern their degradation will soon become apparent. The relief will eventually be reduced to shapeless accumulations of debris, and its pattern to a strange*

labyrinth. Through the location, proportion and elevation of its different parts, the naturalist will readily understand the constants and laws over which he had stumbled in other settings" (translation into English: this study).

Despite these early hopes for a unified understanding of the mountain range, over 200 years later we find that the investigation of the Pyrenees has suffered from the usual disconnect between geological and geomorphological approaches, between orogen-scale desktop modelling and local-scale field observations, between a focus on Alpine tectonics and a neglect of Quaternary neotectonics, with many of its consequences listed above. Restricting research to the confines of the time or spatial bundles listed above has generated persistent blind spots with an entrenched risk of confirmation bias. This review attempts to transcend some of those conventional boundaries of inquiry by operating from two key angles: (i) we address the metabolism of the orogen as a mountain range rather than just as a crustal wedge or mosaic of geological structures, and thus focus on its erosional history, topographic evolution, and landform assemblages; (ii) we articulate the geodynamic history of the Pyrenees with the palaeogeography of its Ebro, Aquitaine and Mediterranean sedimentary basins simultaneously, spanning the earliest plate convergence episodes of the latest Mesozoic to glaciation in the Pleistocene. As a result, rather than a small, asymmetrically bi-vergent orogen captured over simplifyingly short intervals of geological time, it portrays instead a mountain range evolving continuously by lateral and longitudinal growth or destruction through a succession of three quite distinct avatars defined hereafter as the Proto-Pyrenees, the Ancestral Pyrenees, and the Modern Pyrenees — respectively and schematically during the late Cretaceous, Paleogene and Neogene–Quaternary. Each of these Pyrenean ranges has displayed transient periods of crustal and topographic symmetry and asymmetry, successions of range-parallel and range-transverse drainages, the construction and unequal preservation of range-front megafans, uneven intensities of crustal uplift and depths of rock denudation, unequal depths of fluvial incision and patterns of alluvial deposition, and unequal intensities of glacial imprint in more recent time. Many place names (massifs, peaks, towns, etc.) mentioned in the text are located in the figures, but for precision and completeness it is recommended to use an Earth navigation browser.

2. An outline of Pyrenean tectonics

The natural landscapes of the Pyrenees became the focus of scientific investigation (e.g., Palassou, 1781–1823; Ramond de Carbonnières, 1789; Pasumot, 1797) somewhat before gaining appeal as a cultural, aesthetic and touristic attraction in the 19th century (overviews by Briffaud, 1994; Besson, 2000). Like the European Alps, the Pyrenees were approached from the early days of geology as a reference model that would help geologists to understand mountain building processes more generally. The mountain range has accordingly attracted a vast effort of international research into its Hercynian basement fabric, its Meso-Cenozoic cover rocks, and into the many thrusts and folds that shaped it from the Cretaceous to the early Neogene. Among the earlier books, "Études pyrénéennes" (de Margerie, 1946) constitutes a good starting point. More recent overviews include books by Canerot (2008), Barnolas and Chiron (1996), Barnolas and Chiron (2018; but is 20 years out of date despite its publication in 2018), and review papers: e.g., Mattauer (1968), Mattauer and Henry (1974), Souquet et al. (1977), Choukroune (1992), Roure and Choukroune (1998), Damotte (1998), Vergés et al. (2002), Teixell et al. (2018), and Muñoz (2002, 2019).

Work on the geomorphology of the Pyrenees has been less abundant than in the case of hard-rock geology, lithostratigraphy, tectonics and solid-earth geophysics, but it began almost at the same time as the early geological work. The landscape of the Pyrenees has been attracting geomorphologists since the late 19th century and has involved scholars from Germany (Penck, 1886, 1894; Ashauer, 1934; Panzer, 1926, 1933), the Netherlands (Pannekoek, 1935; Boissevain, 1934; de Sitter, 1952, 1954, 1961; Kleinsmiede, 1960; Zandvliet, 1960; Hartevelt, 1970), Switzerland (Nussbaum, 1930, 1931, 1943), Spain (García Sainz, 1940; Solé Sabaris, 1951) and France (de Martonne, 1910; Blanchard, 1914; Sorre, 1913; Birot, 1937; Goron, 1941a, b; Sermet, 1950; Taillefer, 1951; Viers, 1960, 1961; Barrère, 1963). For more detailed reference lists covering work before 1990, see Birot (1937) and Calvet (1996).

2.1. First-order structure of the orogenic wedge

An Alpine orogenic belt roughly striking E–W and nearly 1700 km long extends from the Galicia Bank in NW Spain to the western Alps in Provence. The Pyrenean orogen (Fig. 1)

forms the median segment of this orogenic belt over a length of 450 km between the Bay of Biscay (Atlantic Ocean) and the Gulf of Lion (Mediterranean Sea), but crustal deformation extends westward, uninterrupted, to the Cantabrian Mountains, and northeastward beyond the Corbières virgation into coastal belt of Languedoc. The Cantabrian Mountains to the west, which are topographically continuous with the Pyrenees, had until recently been treated as a distinct morphotectonic system. Initially interpreted as resulting from southward subduction of the Bay of Biscay's oceanic crust (e.g., Boillot and Capdevila, 1977), the Cantabrian mountain belt is now viewed as a westward continuation of Pyrenean structures because it also involves northward underthrusting of the Iberian crust (Pedeira et al., 2003, 2007, 2015; Carballo et al., 2015; Teixell et al., 2018). A component of southward oceanic underthrusting, of limited magnitude in the east but which amplifies westward towards Galicia (Teixell et al., 2018), is nonetheless also involved.

The Pyrenees result overall from the protracted and complex evolution of the mobile crustal belt situated between Eurasia and Iberia during the Triassic, then from the late Jurassic to the late Cretaceous, with collisional tectonics from the late Cretaceous to the early Miocene. As an Alpine mountain range, the Pyrenees thus defined are relatively small and extend for 370 km between Pic d'Orhy in the west and Cap de Creus in the east (the Basque Country, which differs substantially from the rest of the orogen: e.g., Razin, 1989, is not analysed in detail in this structural presentation). The mountain belt strikes N110°E, varies in width from 75 to 150 km, and between the Aquitaine Basin in the north and the Ebro Basin in the south is structurally divided into a classic succession of five tectonostratigraphic belts. These are known as the Sub-Pyrenean Zone, North-Pyrenean Zone (NPZ), Axial Zone (AZ), Nogueres Zone, and South-Pyrenean Zone (SPZ). From a more strictly tectonic viewpoint, the orogen presents two major domains (Fig. 2):

- the European domain, where Alpine structures are north-vergent. It consists of most of the NPZ, which overrides the Aquitaine retro-foreland basin along the North-Pyrenean Frontal Thrust (NPFT). The southern edge of the Aquitaine Basin south of the North-Pyrenean Front (Fig. 2) is also substantially crumpled over a blind thrust (the so-called Sub-Pyrenean Thrust), which connects at depth with the NPFT and marks the outermost limit of the crustal wedge. This outer tectonic belt is the Sub-

Pyrenean Zone and coincides with a fold-and-thrust belt geographically known as the Petites Pyrénées.

- the Iberian domain, where Alpine structures are south-vergent. From north to south, it consists of the southwestern part of the NPZ, the Axial Zone, the Nogueres Zone (a small and controversial unit), and the SPZ; the SPZ overrides the Ebro Basin and terminates at the South-Pyrenean Frontal Thrust (SPFT); between the Axial Zone and the SPZ lies the Nogueres Zone — to which we return in Section 2.3.3.2.2. The rock sequences of the Ebro Basin itself are variously deformed, thus displaying an element of symmetry with the situation in the Sub-Pyrenean Zone of the Aquitaine Basin (Fig. 3).

In the central and eastern Pyrenees, cover-rock outcrops in the narrow southern fringe of the NPZ are intensely deformed and underwent low-pressure–high-temperature (LP–HT) metamorphism during the Alpine orogeny. Known as the Internal Metamorphic Zone (IMZ), this belt of metamorphic outcrops can be considered as a sixth structural unit (Fig. 3), not recognised as such in earlier literature. It defines the structural centreline of the orogen. It derives directly from a hyperextended mid-Cretaceous rift, on the floor of which the lithospheric mantle (today exposed as small outcrops of lherzolite) became exhumed (Jammes et al., 2009; Lagabrielle et al., 2010). The Axial Zone and IMZ are abruptly separated by the North-Pyrenean Fault (NPF), which has long been considered as the locus of the Europe–Iberia plate boundary (e.g., Le Pichon et al., 1970; Choukroune et al., 1973). As discussed in Section 2.3.1, however, matters are somewhat more complex.

The synorogenic Cretaceous and Cenozoic sequences are remarkably well preserved, and this has made the Pyrenean orogen a very attractive area for studying thin- and thick-skinned synsedimentary tectonics. Another outstanding feature of the Pyrenees, however, is also its extensive outcrop of Paleozoic rocks. The crystalline rocks of the Paleozoic basement make up most of the Axial Zone, for this reason also known as the ‘Haute Chaîne Primaire’ (Paleozoic High Range), and are also exposed in several North-Pyrenean massifs (part of the North-Pyrenean Zone) and in the Mouthoumet massif (part of the Sub-Pyrenean Zone). The Mesozoic and Cenozoic cover sequences of the Axial Zone were removed by nappe displacement and/or by erosion during the Alpine tectonic cycle.

2.2. The Pyrenees before the Pyrenees: pre-orogenic plate reconstructions

2.2.1. Geological fabric of the Hercynian basement

The Pyrenees contain a segment of the southern outer zones of the vast Hercynian mountain belt (Barnolas and Chiron, 1996). The Hercynian orogeny (~330–290 Ma, possibly 360–290 Ma according to Casas et al., 2019) resulted in the deformation of sedimentary and volcanic rock sequences of Ediacaran to early Carboniferous age (~580–325 Ma) and of (mainly) Ordovician intrusive rocks (~475–445 Ma). LP–HT regional metamorphism was widespread, intensifying with depth to anatexis and represented by micaschists, marble, paragneisses, metagranitic orthogneisses, and even migmatites. Large granitic plutons cross-cutting the metamorphic country rock were emplaced mainly between 310 and 295 Ma. Inherited rock textures, thrusts, large upright and recumbent folds, detachment faults, mylonitic zones, and large dome structures such as the Canigou–Carançà in the eastern Pyrenees have been well studied (e.g., Carreras and Capella, 1994; Laumonier et al., 2014).

Magnitudes of orogenic denudation were greater in the eastern and central Axial Zone than in the west. As a result, the western Axial Zone is dominated by carbonate-rich, low-grade Devonian and Carboniferous series, whereas crustal rocks exposed in the eastern half of the Axial Zone are on average older and display deeper facies such as the Ediacaran Canaveilles Group (schists and carbonates), the Cambrian Jujols Group (schists), and the Ordovician Canigou metagranite. In the east, younger Hercynian rocks are rare and confined to narrow synclines (e.g., Silurian, Devonian and Carboniferous at Villefranche-de-Conflent). The Hercynian plutons (Saint-Laurent-de-Cerdans, Quérigut, Mont-Louis, Maladeta, Néouvielle, etc.) cross-cut all of these series at all crustal levels. The Hercynian cycle ended in Permian time with an abundant production of late-orogenic molasse and volcanic deposits under an extensional to right-lateral tectonic regime; today these are mostly preserved along the southern edge of the Axial Zone.

At least in the eastern half of the Axial Zone, the Hercynian structures and fabrics are generally easy to distinguish from the more recent Alpine structures. The only exceptions concern the reverse to dextral strike-slip mylonite belts along the Mérens Fault, the Têt valley, and from the Col du Perthus to the eastern part of the Axial Zone. It is likely that they are of Hercynian age but were reactivated during the Alpine orogeny. Among some locally exposed Paleozoic granulite outcrops of the NPZ, major low-angle detachment fault planes

361 have been detected and attributed to extension during the Cretaceous followed by Alpine
362 tectonic inversion rather than to Hercynian inheritance (Laumonier, 2015; Cochelin et al.,
363 2018).

364

365 ***2.2.2. Mesozoic palaeogeography***

366

367 Outcrops of the pre-orogenic sedimentary sequences are diversely distributed throughout
368 the orogen as a result of nondeposition, postdepositional erosion or tectonics, or because of
369 burial beneath Cenozoic sequences in the pro- and retro-foreland basins (for a synthesis, see
370 Puigdefàbregas and Souquet, 1986; Canérot, 2008). Like its Germanic counterpart, the
371 Triassic sequence (250–200 Ma) records a major transgression–regression cycle within the
372 widespread context of rifting prevalent throughout western Europe at the time (rapid
373 subsidence in the Aquitaine Basin): red fluvial Buntsandstein, covered by lagoonal and
374 marine Muschelkalk carbonates and terminating with Keuper evaporites and ophites
375 (hypovolcanic tholeiitic dolerites) (López-Gómez, 2019).

376 The Jurassic (200–145 Ma) records another major transgression–regression cycle, succeeded
377 by the lowermost Cretaceous transgression (145–125 Ma). The Jurassic carbonate shelf
378 sequence occupies the western confines of the Alpine Tethys and consists entirely of marl
379 and carbonate. Although the early and middle Jurassic were tectonically stable epochs, a
380 new rifting episode started during the late Jurassic and continued into the early Cretaceous,
381 depositing carbonate rocks (e.g., Urgonian limestone facies during Barremian time) in the
382 context of an extensive marine transgression — but this time cleary related to the opening
383 of the southern North Atlantic in the west.

384 In the future North-Pyrenean Zone, rifting intensified during Aptian and Albian times (125–
385 110 Ma), peaking during the Albian and Cenomanian (110–95 Ma). Mantle lherzolites
386 became exposed as a result of extreme crustal thinning in rapidly subsiding grabens (e.g.,
387 Jammes et al., 2009; Lagabrielle et al., 2010; Tugend et al., 2014; Clerc and Lagabrielle, 2014;
388 Lagabrielle et al., 2019), and syn-rift sedimentation reached thicknesses of 4–6 km in some
389 depocentres. Sediment fill was lithologically quite varied, ranging from fine-textured clastic
390 deposits (Aptian 'Black marls', and Middle Albian to Lower Cenomanian 'Black flysch'
391 turbidites) to coarse breccia around the basin margins (e.g., 'Poudingues de Mendibelza')

(Souquet et al., 1985; Debroas and Azambre, 2012). Alkaline mafic magmatism also erupted in the area of the (future) North-Pyrenean Zone.

During the early Cretaceous, the region corresponding to the future Axial Zone was largely a land area, though not a mountain range. From middle Cenomanian time, rifting slackened rapidly, and within a regional context of sea-level rise the North Pyrenean foredeep widened northward (Cenomanian and Turonian 'Grey flysch': ~95–90 Ma, displaying a turbidite facies with breccia; followed by Coniacian 'Fucoid flysch': ~90–85 Ma). Meanwhile, to the south, i.e., over the future western end of the Axial Zone, the former land area became submerged and the new environment favoured the establishment of a carbonate platform ('Calcaires des canyons', today forming the Arres d'Anie massif, for example). These are post-rift deposits, well documented as such by the sharp Cenomanian angular unconformity which used to be erroneously interpreted as the termination of a pre-Cenomanian orogenic event. Metamorphic transformation of the Black flysch in the Internal Metamorphic Zone occurred around this time (~100–90 Ma) in a yet poorly understood tectonic context. After 85 Ma, the retro-foreland area evolved into a strike-parallel marine foredeep, which performed as a receptacle for north-prograding clastic sequences. The foredeep filled sequentially from east to west during the Campanian–Maastrichtian, in step with the Axial Zone in the east progressively rising above sea level in response to early Pyrenean compressional deformation. The foredeep sequences and part of the Axial Zone were soon covered by continental red beds known regionally as the Garumnian series (e.g., Rosell et al., 2001). Meanwhile, the west of the Pyrenees remained below sea level (see palaeogeographic map sequence in Plate I). The end of the Cretaceous is thus the transitional period during which syn-orogenic sedimentation took over from the pre-orogenic episodes and gave rise to the Proto-Pyrenees.

2.2.3. Geodynamic conditions in Cretaceous time

The kinematics of the Iberian Plate from the late Jurassic to the late Cretaceous (~160–84 Ma) remain difficult to reconstruct in terms of its strike-slip motion, angular distance of anticlockwise rotation, and separation distance with the European Plate. Left-lateral strike-slip motion of Iberia, for example, has been judged negligible by some authors — often

geologists on the basis of land-based criteria; but substantial by others — usually marine geophysicists who focus on the kinematics of Atlantic sea-floor spreading between Iberia and Newfoundland. In contrast, the ~35° anticlockwise rotation of Iberia associated with the opening of the Bay of Biscay remains fairly uncontested, but its precise age (i.e., entirely, or only partly, Aptian) remains debated (e.g., Gong et al., 2008; Vissers and Meijer, 2012a; Tavani et al., 2018). The width of the rift zone between Iberia and Europe and the causes for lherzolite exhumation are also controversial: whereas strike-slip motion would accommodate small pull-apart basins but seems incompatible with transverse crustal thinning, orthogonal plate extension (NNE–SSW) would be more compatible with the exposure of mantle rocks. The existence of oceanic crust in this rift zone, though currently undocumented, remains unlikely. A triangle of partly compatible end-member models is thus still under scrutiny, with one model inferring > 500 km of transcurrent motion along an ancient transform fault which has been conflated with the NPF (Le Pichon et al., 1970); another advocating minimal motion in the Pyrenean region (particularly the strike-slip component: 100 km at most), thus implying that Iberia never was a truly independent microplate (Souquet et al., 1977; Canérot, 2016); and a third envisaging throughout the Cretaceous the opening and subsequent subduction of a true oceanic domain, which could have attained a width of 500 km in the east (Vissers et al., 2012). Some recent studies, among them Olivet (1996) as a precursor, have attempted to reconcile the geological and geophysical evidence. Nirrengarten et al. (2018), for example, estimate that the Pyrenean rift was ~100 km wide and separated southern France from an Ebro microplate rather than from all of Iberia. The Ebro microplate itself was separated from the rest of Iberia on its south side by another Cretaceous rift, now inverted and forming the Iberian Range. Opening of the Pyrenean rift and exposure of a lherzolite outcrop a few tens of kilometres wide occurred during Albian to Cenomanian time, i.e., after left-lateral transcurrent motion of the Ebro microplate and most of Iberia's rotation during the early Cretaceous had ended (in this model, its cumulative lateral throw is 300–400 km); it was also coeval with the opening of the Bay of Biscay and associated ocean-floor spreading (rotation of Iberia was still ongoing). All of these events occurred during the early Late Cretaceous.

The continuation eastward of the (future) Pyrenees depends on how the orogen connected before the late Cretaceous to what lies further east. One scenario suggests that the future

Pyrenees simply continued between Provence and the Sardinia–Corsica bloc (which in this case would be part of the Iberian Plate: this is the classic model); another scenario suggests instead that the eastern extension of the future Pyrenees connected with expanses of the Alpine Tethys to the southeast via a transform fault zone passing somewhere between the Pyrenees and Sardinia prior to Sardinia's rotation in the Miocene (discussion in Tavani et al., 2018). In that case, the Sardinia–Corsica bloc would be part of the European Plate, but what filled the palaeogeographic space east of Iberia and south of France (continental or oceanic crust?) is unknown. It could have been an arm of the Tethys Ocean in Jurassic time.

2.3. Tectonic legacies of plate convergence

The Pyrenean crustal wedge began to form in mid Santonian time (~84 Ma). Convergence was relatively rapid during two successive episodes, namely from the Santonian to the Maastrichtian (~84–68 Ma) and subsequently from the early Eocene to the Aquitanian (~55–20 Ma). Convergence rates slackened during the Paleocene sensu lato (~68–55 Ma) and have done so once again since the Burdigalian. The mountain range thus grew in two pulses, first during latest Cretaceous time (previously referred to as the Laramide phase at least in French literature because of its coincidence with mountain building in the Laramide Rockies) and producing the Proto-Pyrenees, then from the Eocene to the Oligocene (including the classic late Eocene Pyreneo-Provençal phase) and producing the Ancestral (or Paleogene) Pyrenees. The earlier period of crustal convergence caused tectonic inversion of the mid-Cretaceous rift zone, whereas the second period corresponds to the collision itself. Note that this chronology was established in, and is thus valid for, the central Pyrenees, but cannot substitute for other, less well documented parts of the mountain range. Tectonic collision in the Basque Country (westernmost Pyrenees), for example, had barely begun in mid-Eocene time, whereas in the eastern Pyrenees collision had all but ended by early Oligocene time and was being overprinted by a new deformation cycle impinging as a consequence of north-west Mediterranean extensional dynamics.

Despite fairly good agreement over the broad geodynamic sketch presented above, much disagreement still persists around some of its key aspects, some of which were highlighted in the 1970s but with no ensuing consensus. Below we outline those persistent uncertainties.

2.3.1. The North-Pyrenean Fault (NPF): plate boundary between Iberia and Europe?

The NPF is a conspicuous crustal discontinuity separating the Axial Zone from the Internal Metamorphic Zone of the NPZ, and is at least 250 km long. The NPF was originally interpreted as a Hercynian fault reactivated during Pyrenean collision by a modest component of vertical displacement (Mattauer, 1968), but after the advent of plate tectonics theory it was reinterpreted as a major continental transform fault that had undergone several hundreds of kilometres of left-lateral motion — despite being undetectable in the western Pyrenees (Le Pichon et al., 1970; Choukroune et al., 1973; Boillot et al., 1973). Others still have emphasized instead a case of asymmetry in the Cretaceous rift, with most of the crustal thinning occurring on the European margin (i.e., the present-day NPZ) while the Iberian Plate conserved its original thickness (the asymmetry could, of course, potentially also result from long-distance left-lateral slip bringing together two plate edges with different crustal thicknesses). Despite the ECORS profiles, understanding the depth and angle of the NPF has also proved challenging: the NPF may reach the mantle and offset the Moho (e.g., Choukroune, 1992), but the prevailing view is that it is cross-cut by the NPFT — which is the major south-dipping thrust that has transported the NPZ and part of the Axial Zone northward over the retro-foreland (Fig. 3). Currently, the NPF is considered to be just one among other north-facing Cretaceous normal faults belonging to the Iberian side of the rift and later inverted, the true plate boundary being concealed beneath the Internal Metamorphic Zone. In the western part of the Axial Zone, the NPF could also be the root zone of the south-verging Cotiella-Peña Montañesa system, which was thrust southward over the Axial Zone (e.g., Espurt et al., 2019). At least in the eastern Pyrenees, reactivation of the NPF in late Eocene time could be the main cause for raising the Axial Zone relative to the NPZ. Consistent with this view is the fact that the NPF terminates with the Axial Zone in the west.

2.3.2. The late Cretaceous to Paleocene mountain range, or Proto-Pyrenees

The Proto-Pyrenean mountain range rose above sea level only in the eastern part of where the current range now stands, and is not well documented. The south-vergent Campanian

516 thrust of Bóixols in the central SPZ developed during this period. It results from an inversion
517 of the Cretaceous Organyà graben's southern boundary fault and has generated a fault-bend
518 fold (Sant Corneli ramp anticline) (Berástegui et al., 1990; Bond and McClay, 1995; Mencos
519 et al., 2015). The Bóixols thrust is covered by the unfaulted Garumnian series. Other thrusts
520 probably formed during Campanian–Maastrichtian time in the (future) NPZ, i.e., in and
521 around the highly thinned crust of the Cretaceous rift. The thrusts in the NPZ were either
522 north-vergent: i.e., the (still poorly-documented) Internal Metamorphic Zone overriding the
523 non- or weakly metamorphic segment of the NPZ and the incipient NPFT; or south-vergent:
524 i.e., the incipient Lakora Thrust and the probable root zone of the incipient Supra-Axial
525 Thrust (or SAT; Figs. 2, 3; see further specifications Section 2.3.3). At greater depths, most of
526 the lithospheric mantle disappeared as a result of either northward or southward
527 underthrusting (e.g., Teixell et al., 2016; Espurt et al., 2019; Ternois et al., 2019). By
528 Paleocene time, these convergent plate motions (several tens of kilometres of crustal
529 shortening) had resulted in (i) cancelling out the crustal extension generated by Cretaceous
530 rifting, (ii) restoring an almost normal-thickness crust beneath the NPZ, and (iii) accelerating
531 subsidence in the North Pyrenean foredeep.

532

533 ***2.3.3. The Eocene–Oligocene mountain range, or Ancestral Pyrenees***

534

535 A number of gently dipping tectonic boundaries (thrusts, reverse faults) carve up the
536 Hercynian basement and its cover sequence. Three categories of tectonic unit can be
537 distinguished at currently exposed erosional depths. Some units are cover-rock nappes,
538 consisting exclusively of pre- to syn-orogenic sedimentary sequences. For these cover
539 nappes, the Keuper beds (where present) have usually played a major role as a lubricant on
540 thrust planes or in diapiric fold evolution. Other tectonic units, often among the thickest, are
541 mixed: they consist of Hercynian basement and cover-rock packages (pre- to synorogenic
542 strata), concerning both the Axial Zone and the SPZ (Gavarnie nappe at the centre of the
543 range; Canigou–Vallespir and Cadí nappe in the east). Lastly, some units are basement
544 nappes and are confined to the Axial Zone (they may continue unexposed beneath cover
545 sequences in portions of the SPZ). Those three categories of tectonic unit may be termed
546 upper, middle, and lower, respectively, but scholars have stumbled on the difficulty of

correlating the basement units of the Axial Zone with the cover units of the SPZ (for the eastern Pyrenees: e.g., Muñoz et al., 1986; Fontboté et al., 1986; Laumonier, 1987, 2015; Laumonier et al., 2015; for the central Pyrenees: Vergés and Muñoz, 1990; Muñoz, 1992; Muñoz et al., 2018; for the western Pyrenees: Labaume et al., 2016a; Labaume and Teixell, 2018).

A major consequence of the middle-late Eocene to early Oligocene tectonic movements has been the uplift of the Axial Zone relative to the NPZ and SPZ, especially in the eastern part of the mountain belt (see Section 2.3.1 above). As a result, the Axial Zone presents itself as a vast basement window while also hosting the root zones of the middle and lower tectonic units. Unlike the NPF, the limit between the Axial Zone and the SPZ presents itself as a large range-front flexure, interpreted schematically as the frontal ramp fold affecting the basement of the Ancestral Pyrenees. This tectonic structure of the Axial Zone was associated with the emplacement of part of the middle units, and lastly of the lower units. Another consequence of the late uplift of the Axial Zone is that the upper units of the SPZ are klippen preserved in the frontal-ramp syncline and 'floating' on the Paleogene of the middle units (Fig. 3D). The position of their root zones, perhaps within but, equally possibly, north of the Axial Zone, is uncertain because the connection with the southern klippen has been removed by denudation (Section 2.3.3.2).

2.3.3.1. Crustal architecture of the European domain

North of the Axial Zone, the Pyrenean retro-wedge consists of masses of Hercynian basement (the North-Pyrenean massifs: Barousse; Arize; Saint-Barthélemy, also named Montagne de Tabe; Trois-Seigneurs; Agly), and Mesozoic cover sequences (within the NPZ and the Sub-Pyrenean Zone). The NPZ is narrow (10–15 km) and highly deformed in the east; it widens (15–30 km) and has been well studied in the central Pyrenees along the ECORS-Pyrenees profile (Baby, 1988; Ford et al., 2016; Rougier et al., 2016). The NPZ is the result of tectonic basin inversion during the late Cretaceous (Proto-Pyrenees: ~80–66 Ma), and most of all during the Eocene (~56–35 Ma). In the west, the NPZ corresponds with the moderately deformed and inverted Cretaceous basins that today form the south-vergent 'Chaînons béarnais' (Béarn Ranges) and north-vergent Mauléon Ranges (Teixell et al., 2016; Canérot,

2017; Saspiturry et al., 2019). Here outcrops of the Axial Zone and NPF pinch out, and the NPZ and SPZ find themselves in direct contact with one another, the former being thust over the latter.

The North-Pyrenean Frontal Thrust (conspicuously exposed, e.g., at Pic de Bugarach) was instrumental, mainly during end-Cretaceous and Eocene time, in displacing the NPZ, the NPF, and part of the Axial Zone northward by 25–30 km. The narrow Sub-Pyrenean Zone consists of folded synorogenic late Cretaceous and Eocene sedimentary series. Deformation of the Sub-Pyrenean Zone was partly controlled by the Sub-Pyrenean Thrust — a blind thrust which connects at depth with the NPFT (Fig. 3). In the western Pyrenees, the Sub-Pyrenean Zone corresponds to the Arzacq Basin. North of the Sub-Pyrenean Zone, the synorogenic sequences of the Aquitaine Basin remain weakly deformed or undeformed. In the European Pyrenees, salt tectonics appear to play a major role (Canérot et al., 2005; Labaume and Teixell, 2020; Ford and Vergés, 2020).

In the far east, the retro-wedge configuration changes abruptly: (i) the southern part of the NPZ (i.e., the Internal Metamorphic Zone, Fig. 2) disappears in the Gulf of Lion as result of the extensional tectonics prevalent since Oligocene time in this region; the eastward continuation of the IMZ has nonetheless been detected offshore (Guennoc et al., 2000). (ii) The northern part of the NPZ bends around and strikes in a NNE–SSW direction, forming the large orocline known as the eastern Corbières nappe, and some Mesozoic thrust packages at the southern tip of Provence (Cap Sicié) have been interpreted as a distant eastward continuation of the NPZ (Jolivet et al., 2020). (iii) The Sub-Pyrenean Zone widens considerably and also displays a basement outcrop (the Mouthoumet massif). E–W-striking Pyrenean structures also impinge on the southern edge of the Massif Central, the most obvious consequence of thrust tectonics being the Mazamet–Tantajo reverse fault, which forms the boundary of the Montagne Noire (Fig. 1).

2.3.3.2. Crustal architecture of the Iberian domain

The Iberian pro-wedge is chiefly a south-vergent thrust sequence consisting of upper, middle and lower tectonic units. The South-Pyrenean Frontal Thrust schematically represents the leading edge of the middle and/or lower thrusts. This configuration is very clear in the

southeastern Iberian domain, where the orogenic pro-wedge ceased to grow outward during the early Oligocene; but less so in the southern and southwestern domains, where collisional deformation continued until the early Miocene. Here, deformed pro-foreland sedimentary sequences became incorporated into the SPZ tectonic unit (South Jaca Basin, also known as Guarga Syncline) by dint of the deepest, most recent and most southerly thrusts such as the Upper Guarga thrust (surfacing at the Sierras Exteriores) and the Lower Guarga blind thrust propagating southward into the Ebro Basin (Labaume and Teixell, 2018). Considerable lateral variation along the strike of the orogen gains from a segmented examination of the main structures from east to west.

2.3.3.2.1. Structure of the southeastern Pyrenees

From top to bottom, the eastern Pyrenees display the following tectonic units, mapped in Figures 2 and 3:

(i) the Aspres upper unit, which is an Axial Zone upper basement nappe;

(ii) the upper SPZ units (Pedraforca nappe; klippen of Coustouges, Bac Grillera, Biure, and the Empordà, further east), which are preserved within the Ripoll fault-bend syncline (i.e., the frontal-ramp of the Ancestral Pyrenees);

(iii) the Canigou nappe: a thick and extensive middle unit, which incorporates a large component of Axial-Zone basement rocks (as well as the Mesozoic sequence of the so-called Amélie-les-Bains Basin, which is the only remaining evidence of pre-orogenic cover rocks in the eastern Axial Zone) and most of the SPZ (Cadí units). The thin and discontinuous Vallespir unit is the basal portion of the Canigou nappe in the Axial Zone;

(iv) some lower units displaying outcrops of their basal thrust planes (Albères and Roc de France units; Freser duplex structure);

(v) components of the lowermost unit (mainly the Saint-Laurent-de-Cerdans unit), whose floor thrust (but no known outcrops of it) forms the base of the pro-wedge and functions as the lowermost imbricate for the overlying frontal ramps;

(vi) the small and lowermost Serrat unit, concealed under the Cadí units.

In the Axial Zone, the lower units are visible beneath the Canigou nappe in the vast Albères and smaller Freser windows (Laumonier, 2015). The eastern segment of the SPFT is known by its local name as the Vallfogona Thrust, where the lower and middle thrusts join up. The Pedraforca nappe and upper Bac Grillera klippe have no established root zones within the Axial Zone (Figs. 2, 3). As in the case of the Bóixols unit (see below), it makes good sense nonetheless (i) to situate their pre-tectonic home area in the northern part of the Axial Zone, north of the Soldeu–L'Hospitalet fault in the case of the Upper Pedraforca unit (Fig. 2); and (ii) to envisage that they were transported southward by means of a major thrust, named here Supra-Axial Thrust (SAT), which forms the base of a Supra-Axial nappe overspanning the Axial Zone (noted Supra-Axial Thrust Sheet in Fig. 3). The SAT was rooted north of the Axial Zone in an area perhaps corresponding to the IMZ but today obscured by the FNP, which in the eastern Pyrenees displays the attributes of a post-SAT reverse fault despite having the geometric appearance of a backthrust (Fig. 3D), as discussed above (Section 2.3.1.). The Coustouges, lower Bac Grillera and Biure klippen were originally connected to the Aspres unit in the Axial Zone, but also perhaps to the SAT. The Empordà composite nappe (Bilotte et al., 1979), which mirrors the northern Corbières nappe, is also linked to the SAT.

The orogen in the southeastern Ancestral Pyrenees began to acquire its characteristic architecture (i) in early Ypresian time (Ilerdian) with the formation of the narrow Ripoll foredeep. This continued (ii) through the middle Eocene (late Ypresian–early Lutetian) with the leading edges of the upper units advancing as far as the foredeep (e.g., Muñoz et al., 1986; Vergés and Martínez, 1988; Pujadas et al., 1989; Vergés and Muñoz, 1990; Martínez et al., 1997). Crustal deformation continued (iii) through the middle Lutetian to Bartonian, a time when the Canigou–Vallespir–Cadí nappe advanced southward and the Ripoll foredeep itself became a piggyback basin. The lower thrust units were emplaced (iv) mainly during Bartonian and Priabonian time (late Eocene), contributing to form the Ripoll fault-bend flexure (soon to become the Ripoll syncline) and to raise the Axial Zone topographically. The Vallfogona Thrust remained active until the early Oligocene.

2.3.3.2.2. Structure of the south-central Pyrenees

The central Pyrenees present a classic sequence of thrust units from north to south (review in Oliva-Urcia, 2018): (i) within the Axial Zone, the Gavarnie Thrust shears the Paleozoic basement internally but also overrides the Mesozoic sequences to the south, along the border between the Axial Zone and the SPZ. The thrust plane separates the Gavarnie nappe from the underlying Benasque–Orri nappe (includes here the Bielsa, Ribagorçana and Bono units), which itself overrides the Rialp nappe (Fig. 3); (ii) just south of the Axial Zone, along the fault-bend flexure, the Nogueres Zone is the leading edge of a nappe and consists of basement units with a thin tegument of Permo-Triassic sediments; (iii) the central SPZ is a vast, lobate allochtonous thrust sheet known as the South-Pyrenean Central Unit (SPCU; actually a lateral continuation of the Pedraforca unit; Fig. 2), and its Serres Marginals unit is effectively the western continuation into the central Pyrenees of the lowermost Pedraforca nappe (Fig. 2). The SPCU mainly consists of the Montsec unit, which also incorporated the Upper Cretaceous Bóixols unit.

After the pioneering work of Séguret (1972), interpretations of the SPCU were strongly influenced by results from the deep seismic ECORS-Pyrenees profile produced in 1985–1986. From this major work emerged a ‘standard model’ of the central Pyrenean crust (Fig. 3B; Muñoz, 1992; Beaumont et al., 2000), which advocates the following geometry: (i) the Gavarnie nappe extends southward via the Nogueres Zone, which is why the Gavarnie Thrust has been renamed Nogueres Thrust in that area; (ii) the Axial Zone is interpreted as a thick and vigorously compressed anticlinal nappe stack in which syn-orogenic thrust planes, such as the eastern end of the Gavarnie (Nogueres) Thrust, have been tilted almost vertically; (iii) the putative home area of the SPZ allochtonous units (particularly the Cretaceous Organyà Basin) was given to be the Rialp basement unit, i.e., south of the present-day Axial Zone. A partly similar model has been proposed for the Pedraforca nappe further east (Vergés et al., 1995).

Despite having gained wide currency, this crustal model is vulnerable to a number of caveats (Soler et al., 1998; Laumonier, 2015), particularly features such as the tight anticlinal stack of the Axial Zone, and the series of major upturned Alpine thrusts both in the Axial Zone and within the allochtonous South-Pyrenean units (whether above the Axial Zone basement or in areas south of it). The revision of the ‘standard model’ shown in Fig. 3B, first elaborated by Laumonier (2015) and illustrated in Fig. 3C, emphasizes instead:

(i) the absence in the east-central part of the Axial Zone, i.e., between the Gavarnie and Aspres thrusts, of a major Alpine thrust, whether upturned or not;

(ii) the need for the basal thrust plane of the SPCU–Pedraforca units to be rooted north of the Axial Zone, implying the existence of a major overspanning nappe — the Supra-Axial Thrust unit (SAT) — overriding an Axial Central Unit (ACU, newly coined for the occasion; Figs. 2, 3), i.e., from the NPZ to the SPZ. Here, the ACU lumps together the eastern parts of the Gavarnie and Benasque–Orri units and the basement of the Canigou nappe;

(iii) the need for the Nogueres units to form a basal duplex structure linked to the Supra-Axial Thrust unit. This redefines the overspanning SAT unit as the true 'Nogueres Thrust' sensu Teixell et al. (2018), which further south becomes the basal thrust of the SPCU (Fig. 3C). For future reference it seems preferable, however, to avoid the term 'Nogueres Thrust', which has been employed to mean too many different things in the past.

From these reconsiderations it follows that crustal shortening within the Axial Zone was more limited in the new than in the 'standard' model, and the home area of the SPCU–Pedraforca nappe system was not situated south of the current Axial Zone but rather above and overspanning it (Fig. 2). The home area of the Bóixols–Upper Pedraforca units (vertical green and pink hatching in Fig. 2) lay north of the Gavarnie–Lladorre–Soldeu–l'Hospitalet line, whereas the home area of the Montsec–Lower Pedraforca units lay south of this fault line (southward displacement during Eocene time noted by white arrows in Fig. 2). In this model, the (future) Bóixols Thrust represents the upper portion of the Lladorre Fault, i.e. the mid-Cretaceous normal fault that became inverted at the end of the Cretaceous and was initially instrumental in forming the Bóixols Anticline. Subsequently during Eocene time, the SAT, which was rooted north of the Axial Zone (Fig. 3D), transported the entire Axial Zone's cover sequence southward over a distance of 40–50 km to its present-day position (i.e., the SPCU and Pedraforca klippen). Meanwhile, crustal shortening within the underlying basement itself (or Axial Central Unit: ACU, Figs. 2, 3D) was negligeable. In its broad principle, this model in analogous to the scenario advocated by Teixell et al. (2018, Fig. 20 therein) for the west-central Pyrenees. The Gavarnie–L'Hospitalet fault zone would thus be the deeper portion of the Bóixols / Lladore Fault, first inverted at the end of the Cretaceous

and with the Bóixols unit subsequently transported southward by the Supra-Axial Thrust; the home areas of the Montsec and Lower Pedraforca units were located south of the Gavarnie–L'Hospitalet fault zone. Furthermore, unlike the standard model of Muñoz (1992), the nappe stack does not form a thick anticlinal hump and is, instead, flatter and thinner (compare cross-sections B and C, Fig. 3). Independent work compatible with the revised model is currently emerging (Angrand, 2017; Cochelin et al., 2018, Figs. 9d and 9e therein; Teixell et al., 2018; Espurt et al., 2019; Ternois et al., 2019). This has potential implications in terms of estimating the total depths of denudation required to exhume the crystalline Paleozoic rocks of the Axial Zone, and also bears on establishing when debris from the exposed Axial Zone began to feed into the conglomerate sequences of the pro- and retro-foreland. These corollary aspects would require further investigation, but Cochelin et al. (2018, their Fig. 10) have already shown from independently published thermochronological data (Fitzgerald et al., 1999; Sinclair et al., 2005) that the putative 'Nogueres' and Orri units shared similar exhumation histories (rapid exhumation between 35 and 30 Ma), thus accrediting the view that the central Pyrenees form a single tectonic unit (the ACU, Fig. 3C) delimited by the NPF in the north, rather than the duplex structure of the 'standard' model shown in Figure 3B. Because of its décollement seated in the Keuper evaporites, the SPCU has propagated much further southward (and in a somewhat unclear manner) than its lateral SPZ extensions in the east (Pedraforca, via the Segre ramp) and west (via the Ainsa Oblique Zone) (Fig. 2) (Muñoz et al., 2013).

2.3.3.2.3. Structure of the southwestern Pyrenees

The western Pyrenees of today stand where the Axial Zone plunges beneath its envelope of Cretaceous cover rocks. The Béarn Ranges ('Chaînons béarnais': Canérot et al., 1978; Teixell, 1990; Teixell et al., 2016), long held to belong to the southern part of the NPZ where structural vergence is directed southward, directly override the SPZ (Lakora nappe, which involves the basement and the cover sequence). This occurred before uplift of the Axial Zone. The Lakora Thrust is thus the exact equivalent of the Supra-Axial Thrust (sensu hic) in the central and eastern Pyrenees (i.e., the 'Nogueres Thrust' sensu Teixell et al., 2018). Despite their position within the NPZ, the Béarn Ranges therefore really belong to the

763 Iberian side of the Cretaceous rift (southern NPZ) and not to its European side (northern
764 NPZ). The succession of small thrust slivers ('Écailles bordières') along the northern edge of
765 the Axial Zone also belongs to the Iberian domain (these can be interpreted as basal horses
766 beneath the Supra-Axial Thrust).

767 The Gavarnie nappe (Axial Zone and northern half of the SPZ to the Oturia Thrust)
768 propagated southward during the late Eocene and early Oligocene. It incorporates the
769 Larra–Sierras Interiores–Ordesa–Monte Perdido system, which is the westward extension of
770 the Serres Marginals thrust unit via the Ainsa Oblique Zone (Fig. 2), and has been dated to
771 the middle Eocene (Labaume et al., 2016a; Labaume and Teixell, 2018). This entire crustal
772 mass was subsequently transported on the back of the Guarga–Sierras Exteriores Thrust
773 during the Oligocene and earliest Miocene. The southern Jaca Basin has been transported
774 piggyback on the Guarga thrust unit (see also section 3.2.3).

775

776 ***2.3.4. Some unresolved issues***

777 As revealed by the geological research presented above, the structure of the Proto-Pyrenees
778 and Ancestral Pyrenees is complex and still imperfectly understood. Three areas of
779 uncertainty are highlighted below, all dependent on tectonic models and their prior
780 assumptions.

781 (i) The successive stages of crustal wedge construction during the late Cretaceous (Proto-
782 Pyrenees) and Paleogene (Ancestral Pyrenees), and thus their respective legacies in the
783 mountain architecture, are still debated, particularly on the European side of the orogen.
784 The NPFT may have been at its most active during the late Cretaceous, contributing
785 substantially to mid-Cretaceous rift inversion and to the production of a pop-up
786 structure; whereas displacement along it, as likewise along the Sub-Pyrenean Thrust,
787 slackened during the Paleogene. Establishing the magnitude and chronology of the
788 vertical movements which were associated with these thrust displacements, and
789 whether they occurred above or below sea level, is important for interpreting the north-
790 Pyrenean conglomerate sequences (see Section 3.1 and Fig. 5), but constraints are still
791 imprecise.

(ii) Structural interpretations of the Iberian side of the Ancestral Pyrenees continue to stumble on the links between the Axial Zone and SPZ thrust units (Fig. 2). Establishing the geometries of the various units has bearing on the age of displacement on those thrusts and on the true magnitude of Alpine shortening. For example, according to current stratigraphic and structural evidence, the eastern middle thrusts of Canigou–Vallespir and Cadí were mostly active during middle Lutetian and Bartonian times (~45–38 Ma), whereas maximum displacement on the Gavarnie and Oturia thrusts farther west (Fig. 2) occurred during the Bartonian and Rupelian (~40–30 Ma). Such lags in the evolution of the crustal wedge emphasize an east-to-west polarity in the construction of the orogen. A similar lag is recorded in the progressive shaping of the orogen's southern boundary flexure, and thus in the uplift and erosion of the Axial Zone and the out-of-step discharge of foreland conglomerate sequences. Crustal shortening terminated overall much earlier in the east (middle Oligocene, ~28 Ma) than in the west (base of the Middle Miocene, ~16 Ma). These diachronous events are not clearly recorded by thermochronological datasets (see Section 4.1.3), which mainly document a N–S age progression during those periods of the Paleogene. The thermochronological record does likewise not clearly reflect the east-to-west polarity in range-front conglomerate sequence ages, particularly along the retro-wedge (evidence is somewhat clearer along the pro-wedge; Whitchurch et al., 2011) (see sections 3.1 and 3.2 and Fig. 5). It would thus be spurious to establish direct causal links between crustal shortening magnitudes and the production of continental clastic sequences, and thus to calibrate them too systematically, on fission-track-derived denudation patterns in the mountain range.

(iii) Whether based on balanced cross-sections or on magnetic anomalies in the Atlantic, estimates of maximum synorogenic crustal shortening remain highly variable (Choukroune, 1992; Muñoz, 1992; Roure and Choukroune, 1998; Vergés et al., 1995, 2002; Beaumont et al., 2000; Sinclair et al., 2005; Vissers and Meijer, 2012b; Mouthereau et al., 2014; Teixell et al., 2016, 2018; Grool et al., 2018). Values adduced for the central Pyrenees vary by a factor of almost 2 (90 to 165 km), and depend for example on whether the band of exhumed mantle rocks flooring the pre-orogenic rift is considered to be narrow (15–20 km) or much wider. Depending on the tectonic model of crustal convergence, total shortening is also considered to have been greatest either in the eastern or in the central Pyrenees. As a result, crustal shortening rates also vary widely

(0.5 to 5 mm/yr) depending on the time interval of interest. A consensus nonetheless exists around low convergence rates (<1 mm/yr) during the Paleocene, and on peak rates (3–5 mm/yr) during the middle and late Eocene and (at least in the west-central Pyrenees) during the Oligocene. This scenario concurs with the convergence rates between Africa, Iberia and Europe reconstructed from magnetic anomalies in the Atlantic (e.g., Rosenbaum et al., 2002; Schettino and Turco, 2011; Vissers and Meijer, 2012b; Macchiavelli et al., 2017). Other authors, basing their inferences on thermochronological data, have advocated a different chronology (e.g., Mouthereau et al., 2014), but converting rock exhumation ages and rates to crustal shortening rates remains a complex, assumption-laden exercise. For a wide-ranging discussion of these issues, see Teixell et al. (2018) and Grool et al. (2018).

2.4. From the Ancestral to the Modern Pyrenees: insights from geophysics and geodynamics

The Pyrenees have benefited from a number of geophysical studies aimed at (i) detecting the subsurface continuation of surface structures (e.g., folds and faults in the Aquitaine Basin, of importance for fossil hydrocarbon exploration); (ii) understanding the crustal- and lithospheric-scale structure of the orogenic wedge; (iii) untwining the pre- and synorogenic components of the detected structures; and (iv) reconstructing the more recent, post-orogenic evolution of the crustal wedge, most of all in its atypical eastern region.

2.4.1. Western and central Pyrenees

Important data were acquired in the 1970s. Gravity surveys revealed a strong negative Bouguer anomaly striking E–W beneath the high range, suggesting the existence of a crustal root perhaps 50 km thick. Positive anomalies detected along the north side of the range from the Labourd to Saint-Gaudens also suggested the presence of shallow dense crustal bodies, at the time believed to be Mesozoic alkaline volcanics. Seismic surveys (synthesis in Daignières et al., 1980–81) also revealed greater Moho depths beneath the Axial Zone than beneath the NPZ. In the eastern half of the orogen, the vertical dip of the NPF was promptly

interpreted as resulting from an abrupt juxtaposition between a thicker Iberian crust (45–50 km) and a thinner European crust (~30 km).

A historic milestone in 1985–86 was the ECORS-Pyrenees deep seismic profile, the first of its kind through a mountain range (ECORS Pyrenean Team, 1988). Crustal thickening beneath the Axial Zone showed up for the first time as a north-dipping underthrust of the Iberian lower crust beneath the European lithosphere, later confirmed by complementary surveys in 1988 (Anguy et al., 1991). The European lithosphere, with thinner crust than in the Axial Zone, acted as a rigid backstop in the collision with Iberia. Despite being thinner, the European crust acted as a rigid backstop in the collision with its Iberian counterpart. The NPF was detected to depths of only 10 km, thus mitigating its importance as a primary plate boundary. The ECORS-Arzacq profile was generated in 1988 but only on the French side, and yielded somewhat disappointing results (Daignières et al., 1994).

Although the ECORS-Pyrenees schema became the cornerstone for interpreting the architecture of the entire Pyrenean edifice, the implementation of other geophysical methods also spawned new questions and opened new perspectives. For example, a dense eclogitic root at the base of the Iberian Plate's leading edge has been inferred (e.g., Vacher and Souriau, 2001; Dufréchou et al., 2018). Magnetotelluric surveys along the ECORS profile have signalled the likely occurrence of partial melting of the lithospheric root (Pous et al., 1995a, b). Campanyà et al. (2012, 2018) likewise detected a low-resistivity zone between 20 and 70 km beneath the central Pyrenees, also interpreting it as a region of partial melting. Whether the melting recorded in the central Pyrenees is endemic to the orogenic subduction itself, or whether it results from externally driven asthenospheric processes impinging, without volcanism, on the base of the lithosphere in the central area as it does, with volcanic activity, in the eastern Pyrenees and Languedoc, is unclear (Gunnell et al., 2008; Jolivet et al., 2020). Either way, the evidence is an indication of transience in the orogen's post-orogenic metabolism, which is further discussed in sections 4 to 6.

Tomographic imaging has recently generated higher-resolution, lithospheric-scale interpretations of the orogen's deep structure (Chevrot et al., 2015, 2018; Teixell et al., 2018) (Fig. 4). Through the central Pyrenees, the Iberian Moho is detected at 32 km beneath the Ebro Basin, and plunges beneath the SPZ (37 km), the Axial Zone (40–50 km), the NPZ (50–60 km), reaching 60–70 km below the Sub-Pyrenean Zone (Fig. 4D, panels A, B, C). The

885 European Moho, in contrast, is irregular in detail but occurs at average depths of 30–35 km.
886 The subduction plane lies at a depth of 30 km beneath the northern Axial Zone, and 50–70
887 km beneath the Sub-Pyrenean Zone, thus dipping north by at least 25–30°. It links up very
888 clearly with the basal thrust of the South-Pyrenean crustal taper. Many aspects of the
889 orogen's deep architecture nonetheless still remain debated, such as (i) the mode of slip
890 propagation (and partitioning) from the subduction plane to the shallower crustal thrusts;
891 and (ii) the dip and total length of the Iberian slab (e.g., Souriau and Granet, 1995; Souriau et
892 al., 2008): is it exclusively shallow-angle, or does it become vertical at greater depths, and if
893 so how deep does it go? Lengths of 100 km, and even > 200 km in numerical models, have
894 been proposed for a dense and unstable lithospheric root beneath the Pyrenees (e.g.,
895 Vanderhaeghe and Grabkowiak, 2014), dragging down the orogenic wedge until its
896 gravitational detachment caused vertical relaxation of the mountain range. A deep, vertical
897 Iberian slab does not, however, appear on recent seismic tomographies, and the Pyrenean
898 asthenospheric underworld is conspicuously absent from the global inventory of slab
899 graveyards detected in the Earth's mantle (van der Meer et al., 2018). A 'lost' slab has
900 nonetheless been detected beneath the Reggane anomaly in Saharan Africa and tentatively
901 deemed compatible with this scenario given the northward migration of both the African
902 and European plates since early Cretaceous time (Visser et al., 2016).

903

904 ***2.4.2. Eastern Pyrenees***

905

906 From the time of the earliest studies in the east (Gallart et al., 1980, 1982; Daignières et al.,
907 1980–1981), it became apparent that the eastern Pyrenees were different. For example, the
908 gravity anomaly beneath the Axial Zone of the central Pyrenees pinches out in the east, and
909 at the longitude of Mt. Canigou the Moho beneath the Axial Zone and the NPZ rises to
910 depths of 30 km or less. At the Mediterranean coast, 50 km farther east, gravity and seismic
911 signatures (Moho at 20–22 km) already share more characteristics with those of the Gulf of
912 Lion than with those of an orogen wedge. Some faults, such as the North Mouthoumet and
913 Tech faults, additionally display offsets in the Moho. These strong indications of crustal
914 thinning are also clear at lithospheric scale, with a lithosphere–asthenosphere boundary
915 (LAB) at depths of 180 km beneath the central Pyrenees thinning to ~120 km in the eastern

Pyrenees (Gunnell et al., 2008; Fig. 4B, C). Unfortunately, the eastern Pyrenees have never benefited from an ECORS transect. Recent tomographic imaging (Diaz et al., 2018; Chevrot et al., 2018) nonetheless fully confirms those earlier studies (Fig. 4D), dispelling any notion that the orogen is cyclindrical or in any way a homothetic transformation of the ECORS-Pyrenees model. The crustal root beneath the Axial Zone, which reaches depths of <45 km beneath Andorra (itself situated 40 km to the east of the ECORS-Pyrenees profile), disappears entirely 100 km to the east of the ECORS traverse, i.e., below Mt. Canigou where the Moho is <35 km deep (Fig. 4D, panels D and E). At this longitude, the flexural bend of the plunging Iberian Moho has flattened out and the subduction plane is undetectable. A 5–7 km vertical offset in the Moho beneath the Axial Zone could be the indication of a south-vergent thrust (Fig. 4D, panel E), although it could also be the locus of the Têt Fault, also a major discontinuity in the fabric of the orogen (Figs. 1, 2).

The causes and detailed breakup kinematics of the orogen in the Western Mediterranean during the Neogene are also a matter of debate. Breakup was a result of southward trench rollback of the Apennine subduction slab, and was guided by the Catalan Transfer Zone (Rehault et al., 1984; Mauffret et al., 2001; also previously named accident Paul Fallot (Durand-Delga and Fontboté, 1980) and, more recently, North Balearic Transform Zone (Advocaat et al., 2014; see palaeogeographic maps presented in Plate I). This transfer zone is a deep crustal fault striking NW–SE and along which the Corsica–Sardinia block sheared itself away from the remainder of the Pyrenees. The resulting Gulf of Lion is a back-arc basin in which a NW to SE gradient of intensifying crustal extension has been inferred. The Pyrenean crust thus thins rapidly just 20 km east of the current Roussillon coastline, then yields progressively offshore to necking in the lower crust, then to exhumed lower crust and/or serpentinised upper mantle in the Provençal Basin (the presence of an aborted oceanic ridge between Provence and Corsica is currently speculative; Granado et al., 2016; Canva et al., 2020; Jolivet et al., 2020). As a result of crustal extension giving birth to the Western Mediterranean, a dozen extensional basins were also generated on the continental seaboard and in the eastern Pyrenees (Fig. 1), fragmenting the topography and progressively tearing open the orogen from east to west along its Axial Zone. The first stage of extension affected the Mediterranean back-arc during the late Oligocene–early Miocene (resulting onshore basins: Roussillon, Conflent, Vallès-Penedès, Narbonne-Sigean and several other smaller

basins in the Corbières). The second episode extended into the core of the Axial Zone during the late Miocene (resulting intermontane basins: Cerdagne, Capcir, Seu d'Urgell, Val d'Aran–Pruëdo), but also impacted the Mediterranean onshore area of Catalonia (Selva, Empordà), where the older basins closest to the coast (Vallès, Roussillon) were also reactivated during the late Miocene and Pliocene (see Section 3.3).

2.4.3. Crustal roots and their implications for geomorphology

The history of the orogen's deep structures and their differences from east to west and north to south are important for understanding (i) crustal behaviour during the orogenic period, and (ii) vertical movements during the post-orogenic period. Implications for the geomorphological evolution of the Pyrenees as a mountain range are essential and will be examined more specifically from that angle in Section 4.

On a N–S cross-section through the west-central Pyrenees, it now remains fairly straightforward to associate the deep crustal structures (underthrusting of the Iberian lower crust beneath the European lithospheric mantle, etc.) with the structures in the mid- and upper crust (i.e., the Pyrenean orogenic wedge), even though estimates of total crustal shortening at depth and at the surface (at least ~100 km, see above) are highly variable. Should it be inferred from the more recent crustal tomographies that plate convergence in the eastern Pyrenees was very limited, thus failing to produce a crustal root? Such a conclusion would violate the evidence from the nappe structures, which indicates magnitudes of crustal shortening comparable to the central Pyrenees (e.g., Laumonier, 2015; Grool et al., 2018). The major lateral architectural changes in the crustal wedge, which (among other features) involves lateral heterogeneities in the European Moho (Chevrot et al., 2015; Wang et al., 2016), require some other explanation, and these have been addressed by a few publications (e.g., Gunnell et al., 2008; Chevrot et al., 2018; Jolivet et al., 2020).

The most commonly proposed scenario is that the crustal root beneath the eastern Pyrenees was initially no different to that detected farther west, but that it was destroyed by the impinging extensional tectonics (e.g., Séranne, 1999; Lacombe and Jolivet, 2005). Gunnell et

977 al. (2008) speculated that the root was delaminated or thermally eroded by an influx of hot
978 asthenosphere channelled southward from the Massif Central (see Barruol et al., 2004).
979 Jolivet et al. (2020) proposed instead that the processes responsible for lithospheric thinning
980 beneath the eastern Pyrenees and for the hyperextended crust in the Gulf of Lion were
981 linked, and occurred on a mode reminiscent of metamorphic core complexes but also
982 involving asthenospheric processes at the lithosphere–asthenosphere boundary.

983 It still remains surprising that the basic orogenic structure, and particularly the superposition
984 of the respective Mohos, should have been so completely erased by these processes.
985 According to Chevrot et al. (2014, 2018), important differences in the pre-orogenic
986 Cretaceous rift structure (see also Tugend et al., 2014; Wehr et al., 2018) could explain why
987 compressional deformation might have been less focused and spatially more distributed in
988 the east of the orogen, particularly east of the Toulouse Fault — thus not forming a single,
989 massive crustal root. This scenario provides an alternative to the option advocating post-
990 orogenic eradication of a previously formed crustal root, but its authors do not adduce more
991 specific structural correlations or constraints with the surface geology.

992 A third scenario, until now never discussed, is also possible. Its premise, advocated by Teixell
993 et al. (2016) in the west-central Pyrenees, is that the formation of the Pyrenean crustal root
994 occurred after (i) restoration of normal crustal thickness in the Cretaceous rift zone, (ii)
995 subduction of the formerly exhumed mantle of the rift floor, and (iii) lower-crust
996 underthrusting (proto-collision) of the Iberian leading edge. Root-forming collision thus
997 occurred broadly after mid-Eocene time, but this third scenario emphasizes that collision in
998 the eastern Pyrenees was mostly associated with the lower thrust units, active during the
999 Priabonian and Rupelian; whereas farther west thrust displacement continued until the early
1000 Miocene, i.e., for a further 10 m.y. This alone could explain why the crustal root was smaller
1001 in the east than anywhere else documented until now.

1002 Clearly, the hypothesis of a smaller initial root in the eastern Pyrenees does not rule out the
1003 additional prospect of its full eradication during the Neogene, whether by purely brittle,
1004 more ductile, or melt-related processes. Both scenarios are thus compatible with one
1005 another. Previous work in the central Pyrenees had argued that the mountain range was
1006 isostatically overcompensated, i.e., mean elevation was less than predicted by Airy's model,
1007 perhaps because of a dense eclogitic root dragging it downward in that region (Vacher and

Souriau, 2001). With a crust just ~30–35 km thick, evidence suggests instead that topography in the eastern Pyrenees is not supported by a crustal root of sufficient thickness for isostatic compensation of the mountain range to be occurring at the Moho. The notion that elevations in the eastern Pyrenees are anomalously high (Gunnell et al., 2008) is of special interest from a geomorphological perspective because it implies that this segment of the mountain range, where the lithosphere–asthenosphere boundary is relatively shallow (Fig. 4), is dynamically supported and is thus likely in a transient rather than in an equilibrium topographic state (Calvet and Gunnell, 2008; see point 3.3. for further discussion).

2.5. Synthesis of Pyrenean tectonics

The Pyrenees constitute a good example of a mountain range affected by multiple orogenic overprints. The long Variscan history of the region (Barnolas and Chiron, 1996) ended in the complete destruction of the Hercynian mountain belt and the burial of its residual topography under a mass of clastic debris (initially purple-coloured Permo-Triassic claystone and sandstone). A new chapter then began with the Alpine orogenic cycle (Barnolas and Chiron, 2018). This started with a long period of marine shelf sedimentation extending from the Trias (~240 Ma) to the Barremian (~125 Ma). A period of rifting then transformed the Europe–Iberia mobile belt, but convergence, collision and underthrusting of the Iberian Plate beneath the European Plate followed in a succession of stages between the late Cretaceous and at least the late Oligocene. A subsequent phase of crustal extension during the Neogene is recorded, impinging on the eastern half of the orogen (Barnolas and Chiron, 2018; Jolivet et al., 2020).

We now possess a fairly satisfactory understanding of the orogenic growth and decay patterns of the Pyrenees through geological time (Teixell et al., 2018). The crustal wedge widened and thickened in three distinct stages, before partially undergoing hyperextensional collapse in a fourth (Jolivet et al., 2020):

(i) late Cretaceous: burial of lithospheric mantle rocks initially exposed as a result of overstretched crust, and inversion of the earlier Cretaceous rifts structures;

(ii) early to middle Eocene in the east, middle Eocene to early Oligocene in the west: tectonic convergence under a distinctly tangential regime (low dip angles of most thrusts), with formation of complex nappes structures (Canigou, Gavarnie, etc.);

(iii) late Eocene and early Oligocene in the east, late Oligocene to early Miocene in the west: development, particularly in the Iberian domain, of more strongly dipping thrusts, giving the mountain range its final geometry of a collisional orogenic wedge. This process involved vertical uplift of the Axial Zone relative to the NPZ and SPZ, but also of the NPZ relative to the Sub-Pyrenean Zone, with development of a crustal root produced by underthrusting and subduction of the Iberian lower crust beneath the overriding European Plate.

(iv) Oligocene to Neogene: post-orogenic hyperextension in the east as a consequence of Mediterranean trench rollback and slab tear along the Paul Fallot–North Balearic Transform Zone (Jolivet et al., 2020). This transformed the segment of the Pyrenees currently collapsed in the Gulf of Lion but also the entire eastern onshore part of the modern orogen, even as compression was continuing in its western part. The eastern Pyrenees are thermally the hottest part of the orogen, impacted by asthenospheric flow and volcanic activity. The cooler Pyrenees further west currently appear less directly impacted by these processes.

3. A view from the basins: a proxy record of mountain uplift and erosion

The denudation history of a mountain belt is recorded in the depositional history and stratigraphic architecture of its adjacent and intermontane sedimentary basins (e.g., García-Castellanos and Cloetingh, 2012). Constraints on the chronostratigraphy of the foreland sequences are usually provided by the marine and continental fossil record, and various methods of basin analysis help to reconstruct the tectonic regime and depositional systems through time (Allen and Allen, 2013). These clues yield indirect evidence about the topographic energy of the mountain range in the past. The facies characteristics of the sedimentary rocks also document the succession of palaeoclimatic conditions that presided over the erosional decay of the orogen.

In the case of the Pyrenees, however, the post-shortening (i.e., late Cenozoic) environmental conditions are paradoxically less well documented than the earlier periods of Mesozoic rifting and Paleogene collision. Focus on the older geological periods has arisen from the

priorities set by petroleum exploration. In a compilation which tries to make sense of several hundred local studies published in French, Spanish, Catalan and English but never previously linked up into a coherent narrative (recent partial exceptions: Garcés et al., 2020; Ortiz et al., 2020), we provide here a synthesis of the evolution of the Pyrenees captured through (i) the clastic record of denudation of the orogenic wedge in all of its peripheral and intermontane basins (this Section 3), (ii) the rock-cooling record of its Hercynian basement core (Section 4), and (iii) the denudation of the foreland basins themselves in relation to base-level changes affecting them. Whereas most reviews of the Pyrenean foreland basins focus on information provided by marine deposits and magnetostratigraphy, in this review we also highlight the rich biochronological evidence provided by continental fossil assemblages. Marine deposition ceased after the Priabonian on the Iberian side of the range, after the Ypresian in eastern Aquitaine, and occurred only intermittently in western Aquitaine during the Oligocene and Miocene. The reason for granting continental biostratigraphy pride of place in this review is that palaeontological data from nonmarine sequences are available from all three basin environments of the Pyrenees, i.e., the Ebro, Aquitaine, and Mediterranean. This allow consistent short- as well as long-distance correlations within a coherent and accredited reference frame. Furthermore, issues of endemism are not recognised as a potential barrier to robust comparisons because components of Iberian endemism among mammalian taxa only concern the Atlantic west and the Meseta. The literature has long established that the faunas in the southern Pyrenees were very similar to those of France and other parts of Europe, whether during the Eocene (Badiola et al., 2009) or the Oligocene and Burdigalian (Alvarez Sierra et al., 1990).

The stratigraphic ages for clastic sedimentary sequences will follow the European Land Mammal Age (ELMA) scales of Vandenberghe et al. (2012) for the Paleogene, and Hilgen et al. (2012) for the Neogene, while also considering local updates or recalibrations from more recent magnetostratigraphic research in the Ebro Basin. The excellent documentation of the Ebro foreland by magnetostratigraphic research is unmatched everywhere else, mostly because of comparatively unsuitable open-air exposures and sampling conditions north and east of the mountain range.

3.1. Chronology of clastic supply to the Aquitaine retro-foreland

3.1.1. State of the art and data sources

After 1950, the Aquitaine Basin became the focus of a large number of studies based on seismic surveys and drilling in the context of oil and gas exploration (see Biteau et al., 2006). Given that oil plays tend to occur in the deeper stratigraphy, the Cenozoic molasse deposits were often ignored as overburden of little key interest (Cenozoic cover rocks are nonetheless addressed, for example, in Winnock et al., 1973; Kieken, 1973; Schoeffler, 1971, 1973; Cavelier et al., 1997; Gély and Sztrakos, 2000; Serrano et al., 2001; Rougier et al., 2016; Barnolas and Chiron, 2018; Ortiz et al., 2020). The study of the clastic Cenozoic sequences by other means, however, is hampered by the dense vegetation, and by the widespread and often thick blanket of Quaternary regolith. The chronostratigraphy of the continental deposits in the Aquitaine retro-foreland is nonetheless suitably constrained at some localities by the frequent occurrence of interlayers of marine beds (Fig. 5), which recur between ~56 (Ypresian) and ~12 Ma (middle Miocene). Accommodation space and the wavelength of lithospheric flexural response to sedimentary loads seem to have varied along strike as a function of heterogeneities in pre-orogenic rift inheritance, and particularly magnitudes of Cretaceous crustal extension. Overall, flexural rigidity is found to decrease southwestward from the eastern Aquitaine Basin to the Arzacq subbasin (Angrand et al., 2018).

The body of work devoted to the Eocene marine record is the largest (e.g., Plaziat, 1984; Sztrakos et al., 1998), but a few overviews also exist for the Oligocene and the Miocene (Cahuzac et al., 1995, 1996, 1999, 2010; Sztrakos and Steurbaut, 2017). Note that the Aquitaine Basin is the locus of two type sections of the International Stratigraphic Scale, namely the Aquitanian (defined in 1858 by K. Mayer Eymar) and the Burdigalian (defined in 1892 by Depéret) (for recent reviews on this topic, see Parize et al., 2008, and Londeix, 2014). The Aquitaine Basin also turns out to be an extremely rich repository of continental fossils, with an inventory of several hundred sites — whether in fluvio-lacustrine stratified context or in a karst setting. Some of these are benchmark sites used in the indexation of Paleogene (MP) and Neogene (MN) biozones of the ELMA scale (Richard, 1948; Crouzel, 1957; Bergounioux and Crouzel, 1960; Sudre et al., 1992; Duranthon, 1991, 1993; Muratet et al., 1992; Muratet and Cavelier, 1992; Antoine et al., 1997, 2011; Legendre et al., 1997; Duranthon and Cahuzac, 1997; Astruc et al., 2003; etc.). The most significant among these

reference sites, however, are situated in the distal, often lacustrine molasse deposits of the basin. This potentially weakens the quality of some chronostratigraphic correlation with the more proximal conglomerate sequences of the Pyrenean retro-foreland, but opportunities for multiple constraints are nonetheless plentiful, and Ortiz et al. (2020) have provided an areally extensive, integrated basin analysis of the onshore western Aquitaine–offshore Bay of Biscay continuum.

3.1.2. Synorogenic conglomerate beds: the Paleogene Palassou Series

The Palassou conglomerate sequence (Fig. 5) has been well studied in the eastern foothills area (Crochet, 1991), particularly the narrow band of almost vertically upturned beds between the Arize and Ariège rivers (here in the Sub-Pyrenean Zone). The outcrop broadens substantially to the east of the Ariège and into the Aude river catchment, where the sequence also underwent Alpine folding. The Palassou Series is > 2 km thick and has been subdivided into three units interpreted as three successive intervals of tectonic activity, each separated by syn-sedimentary unconformities that display fanning dip angles and grade into sharper angular unconformities nearer the mountain front. The conglomerate beds display point-bar facies typical of meandering or wandering streams on large range-front alluvial fans. In the Ariège, clast abrasion criteria imply a minimum transport distance of 6 to 7 km for limestone pebbles, and 30 km in the case of quartz (Crochet, 1991). The pebbles are large (D_{99} = 164 mm), with a marked up-sequence increase in size (D_{99} in youngest beds: 403 mm) and the largest debris in excess of 600 mm. Petrographic composition indicates that the alluvium has sampled the entire lithological assortment of the Ancestral Pyrenees in varying proportions. Inputs from the Axial Zone are in a minority (< 10%) in the older Palassou Unit 1 and at the base of middle Unit 2, but become dominant (and at places exclusively so) in the remainder of Unit 2 (90%, including granite and metamorphic rocks). Debris from the Axial Zone are very scarce in uppermost Unit 3.

The age of the Palassou sequence has been established on the basis of (i) its stratigraphic continuity with the marine and coastal Lower Ypresian (i.e., Ilerdian) beds, (ii) a series of mammalian fossil deposits (particularly in the Aude syncline and in the distal molasse deposits between Castelnaudary and Castres), and (iii) a selection of freshwater and terrestrial *Mollusca*. Unit 1 lies conformably over the Ilerdian (Lower Ypresian) and contains

in its basal beds some mammalian assemblages ascribable to MP 7 and MP 8–MP 9 (Marandat, 1991; Marandat et al., 2012), i.e., 54–52 Ma (Legendre and Lévêque, 1997; Escarguel et al., 1997; Vandenberghe et al., 2012). Unit 1 continues into the early Lutetian. The middle Palassou (Unit 2) spans the late Lutetian and Bartonian. The top of upper unit 3 contains the mammalian fossil deposits of Mas-Saintes-Puelles (MP 19, ~35 Ma) and Villeneuve-la-Comtal (MP 20, ~34 Ma), and is thus compatible with a Priabonian age. The Bartonian and Priabonian sequences extend as far north as the Castres Basin, where they consist of finer Pyrenean molasse known as 'Molasse de Blan' and 'Molasse de Saix' (Mouline, 1978, 1989). These formations contain about 60 mammalian fossil sites (3 Lutetian, 39 Bartonian, and 16 Priabonian).

The Palassou Series continues into the early Oligocene (Rupelian). This Unit 4 was not described by Crochet (1991) and is barely reported in the literature apart from a brief mention by Astre (1933). Its outcrops occur between the Hers valley and the Lauragais ('Poudingues de Vals'), and continue towards the Castres Basin ('Poudingues de Puylaurens' and 'Molasses de Briatexte'; Mouline, 1967). The Rupelian beds around Castres contain 41 mammalian sites. The 'Poudingues de Vals' are at least 200 m thick (though a lot less at Puylaurens) and exhibit very low dips. At Vals, pebble provenance is predominantly limestone from the outermost Pyrenean fold belts, with very little input from the Axial Zone. Palaeochannels containing small pebbles of weathered gneiss and granite are nonetheless frequent in the Lauragais and Puylaurens areas, with no proven provenance from the Montagne Noire. This pulse of clastic debris from the Pyrenees overlies distal lacustrine limestone beds than contain biozones MP 19 and MP 20 (34–33 Ma) at the seuil de Naurouze; and the top of the conglomerate unit itself contains biozones MP 24–25 at Puylaurens (~30–28 Ma). Palassou 4 is the outermost occurrence of conglomerates supplied by the Paleogene Pyrenean orogeny (Mouline, 1978). The clastic wedge may have reached these distal areas because of a decline in subsidence rate and accommodation space, forcing the rivers from Rupelian time to prograde northwards across the overfilled retro-foreland. A further age bracket is provided by the continuous sequence of the Bélesta and Briatexte lacustrine limestone beds capping Unit 4. This limestone formation can be traced southward to Belpech (at the Aude–Ariège border). The outcrop is probably time transgressive but includes biozones MP 24–25 and 26 (28–27 Ma) at the northern site of St-Martin-de-Casselvi, where two fossil exposures occur one above the other (Astruc et al., 2003). This

lacustrine environment could be an indication of diminished clastic output from the Pyrenees, where topography may have therefore attained a state of subdued relief and moderate energy.

The Chattian molasse overlying the Bélesta limestone is fine-textured and extremely monotonous in the Lauragais and Toulouse areas. The stratigraphic position of the distal facies above the Puylaurens conglomerate clearly indicates a decline in river-load clast sizes and, by inference, in catchment steepness in the Pyrenees. The thickness of this late Oligocene molasse has been overestimated by Astre (1959, 1964), who conflated this formation with the younger Aquitanian molasse (which admittedly displays an identical facies but whose age has been revised based on a reintepretation of its fossil assemblage; Baudelot and Olivier, 1978; Duranthon, 1991, 1993). The base of the Aquitanian stage has now been recorded in a borehole sunk for the Toulouse underground train network at depths corresponding to 114–122 m a.s.l. (Antoine et al., 2006). The underlying Chattian beds attain estimated thicknesses of 180 to 380 m according to Astre (1959), i.e., 180 m if we assume that their dips decrease westward (a fact recently confirmed by excavations for the Toulouse underground metro network). The Chattian facies was described by Astre (1959) as that of silty to sandy shale floodplain deposits containing a few limestone beds, sporadically associated with broad, well-defined shoestring sand channels occasionally containing coarser sand and gravel. The presence of muscovite, biotite and tourmaline in the sand fraction imply some provenance from the Hercynian outcrops.

The Oligocene molasse deposits of Pyrenean origin thus extend far into the Aquitaine Basin. In the lower plains of the Tarn and Aveyron rivers, four depositional units separated by disconformities have been described (Muratet and Cavelier, 1992; Muratet et al., 1992), and the most conspicuous erosional lacuna has been attributed to the late Rupelian eustatic fall. Northwest of the Tarn–Garonne river junction, the Pyrenean molasse outcrops disappear beneath the ‘Calcaires blancs’ (Aquitanian lacustrine beds of white limestone) of the Agen region, and eventually reappear and connect laterally with the fossil-rich marine (highstand: ca. 30 Ma) Rupelian limestone (Asteries Limestone) of the Bordeaux region (Sztrakos and Steurbaut, 2017).

3.1.3. Western analogues of the Palassou beds: the Jurançon sequence

Outcrops of proximal Paleogene conglomerates, which are otherwise mostly obscured by Neogene overburden west of the Ariège River, occur around the city of Pau, where they are known as 'Poudingues de Jurançon'. Jurançon is the type locality described in 1819 by Palassou himself, whose surname was used after 1862 by Leymerie, as a tribute to Palassou, to describe occurrences of this geological formation in the east (i.e., the outcrops examined in Section 3.1.2). The outcrops reported in the Garonne, Ariège and Aude catchments were considered to be Eocene by Noulet in 1858 (see Crochet, 1991). The western outcrops of this conglomerate formation, however, were renamed 'Jurançon' by Douvillé (1924), thereby not only dissociating it from the Palassou sequences but also ascribing it a Miocene age without any clear justification. A Tortonian age was even prescribed based on the notion that it was a proximal facies of the Neogene molasse (Crouzel, 1957). The Neogene age of the Jurançon Formation was then (spuriously) extended to the more distal, 1200 m-thick molasse sequences that fill the Arzacq Basin between the Gave de Pau and the Adour River.

More recent investigations, however, have worked towards correlating the 'Poudingues de Jurançon' and 'Molasses d'Arzacq' formations with the synorogenic Paleogene units of the Palassou Series described in Section 3.1.2. Its westernmost outcrops near Lahontan extend laterally to (and are thus broadly coeval with) a facies of palaeontologically-dated Upper Eocene marine molasse and limestone (Boulanger and Poignant, 1970). Seismic profiles and borehole logs also evidence the lateral facies changes from the conglomerates to the Paleogene molasse beds in the Arzacq syncline. Age brackets are provided in the west by marine Oligocene beds (Schoeffler, 1969, 1971, 1973) and by the overlying Lower Rupelian 'Faluns de Gaas' (shelly sand) (Sztrakos and Steurbaut, 2017). In the east, the top of the 400-m-thick continental molasse beds of Arzacq has been dated by mammalian fossil indicators at Nassiet/Le Bourgadot (Rupelian, MP 23: Sudre et al., 1992; Viret, 1938; Glangeaud, 1938; Schoeffler, 1969); and its base likewise dated at Horsarieux/Pédelail (Eocene–Oligocene boundary: Stehlin, 1910, in Capdeville, 1997), just above the marine Bartonian beds.

Like the Palassou Series units 1 to 3, the Jurançon conglomerates fall into three units, and a Paleogene age has been confirmed by two fossil invertebrate assemblages — one from the basal unit, which rests conformably on Upper Ypresian marine sandstone and Lutetian shale, and the other from the middle unit (Bartonian; Hourdebaigt et al., 1986; Hourdebaigt, 1988). As with the Palassou, lower and upper Jurançon units contain an assemblage of pebbles almost exclusively of outer-Pyrenean fold-belt provenance. Contributions from the Axial

Zone, particularly from granite outcrops, are substantial in the middle sequence. This suggests that there has not been a simple or progressive pattern of denudation of the Axial Zone, whether in the east or the west of the orogen. With a D_{99} of 500 mm, the beds also include metre-sized boulders. Clast roundedness is less than among the Ariège Palassou sequences.

Given that at Ossun and Pau the marine-to-continental transition occurred during the late Ypresian, it can be inferred that, from the Corbières in the east across to the Béarn in the west, the westward marine regression was fast along the strike of the orogen (see palaeogeographic maps in Plate I). West of Pau, the Paleogene piedmont of the Ancestral Pyrenees was a deep furrow undergoing a slower rate of sedimentation, mainly in the form of west-prograding deltaic sequences (Cavelier et al., 1997, Fig. 4 therein; Serrano et al., 2001). At Peyrehorade, continental upper Palassou beds display intercalations with Priabonian marine beds. In the lower Adour valley and on the Basque coast at Biarritz, the Paleogene marine sequence is continuous from the Eocene to the Oligocene. It contains at best a few sandstone and conglomerate beds, and olistoliths of middle Eocene age (Kieken, 1973). In this area, the mountain belt undergoing crustal deformation at the time descended directly into the sea in a way reminiscent of the modern Cantabrian Ranges. Debris conveyed out of the rising Ancestral Pyrenees were thus delivered directly to the Bay of Biscay, which at the time formed a gulf extending much further east into the Aquitaine Basin than today (see palaeogeographic maps in Plate I). By the end of the Oligocene, these Pyrenean debris were evacuated directly via a submarine canyon (Bélus–Saubrigues canyon), ancestor to the present-day Gouf de Capbreton (Cirac et al., 2001). This canyon was cut during Oligocene time into the Saubrigues anticline up to 35 km east of the modern coastline, but soon became filled with sediment by late Chattian to Aquitanian time (Kieken, 1973; Cahuzac et al., 1995; Sztrakos and Steurbaut, 2017).

3.1.4. The early and middle Miocene molasse

By comparison with the Paleogene foreland deposits, their Neogene successors are thin and exhibit shallow dips. On seismic profiles, the Neogene cover sequence never exceeds thicknesses of a few hundred metres (Schoeffler, 1971, 1973) — on average 200–300 m, with localised depocentres attaining 600 m at the Landes coastline or beneath the middle

Adour valley, 500 m north of Tarbes, 540 m north of Auch, and 560 m at Lézat (i.e., 15 to 30 km north of the NPF).

During the early and middle Miocene, marine sedimentation prevailed in the west and produced interlayers with the ongoing continental deposit accumulations farther east. Three marine transgressions have been recorded, each forming a wide triangular gulf advancing up to 150 km into the interior of the Aquitaine Basin, with its depocentres situated between 100 and 75 km north of the Pyrenean mountain front. This configuration suggests that Pyrenean tectonics were no longer directly influencing the pattern and chronology of sea-level changes. The most extensive transgression occurred in Aquitanian time (Londeix, 2014), its easternmost vertex reaching the city of Agen and depositing a bed of paralic, oyster-rich marls sandwiched between white lacustrine limestones ('Calcaires blancs') at their base and grey limestones ('Calcaires gris') at their top. This 'trilogie agenaise' is a distinctive geological feature of the region, totalling a thickness of 30 to 60 m and containing two mammalian sites (Paulhiac and Laugnac) emblematic of biozones MN 1 and MN 2 (Fig. 5, Ariège transect).

The palaeogeography of the Burdigalian transgression was comparable, although slightly less extensive (Cahuzac and Poignant, 2004). The middle Miocene transgression invaded land somewhat farther to the south and reached Lectoure, also forming a narrow gulf along the base of the western Pyrenees around Orthez and Salies-de-Béarn. This shallow sea, also known as 'Mer des Sables fauves' (Tawny Sands in Figure 5), has fallen foul of contradictory interpretations. Although initially assumed to be a Tortonian feature (Crouzel, 1957), its Langhian to Serravallian age (~16–11 Ma) is now well established despite persistent uncertainty concerning the palaeogeography of its two successive highstands. According to some authors, the gulf of Lectoure was a Serravallian feature (Cahuzac et al., 1995; Cahuzac and Poignant, 1996), whereas for others this marine highstand occurred in Langhian time, the Serravallian ingress being the lesser of the two eustatic rises. Because of local flexural deformations in the Aquitaine Basin itself ('Celtaquitanian flexure'), the Serravallian deposits occur as a series of drowned valley fills cut into the northern edge of the marine Langhian series and its underlying Aquitanian molasse (i.e., the 'trilogie agenaise') (Magné et al., 1985; Rey et al., 1997; Gardère, 2002, 2005; Gardère et al., 2002; Gardère and Pais, 2007). The southward migration of the marine depocentre as a result of this tectonic downwarp, which influenced the positions of two successive palaeoshoreline highstands, could be the

manifestation of a slight reactivation of Pyrenean retro-wedge crustal loading during the middle Miocene.

The carbonate-rich continental molasse sequences of the Miocene continue the trends previously observed in their marine counterparts. Geologists have reported 17 levels of younger deposits overlying the Aquitanian 'trilogie agenaise', 13 of them made conspicuous by the recurrence of a distinctive variety of lacustrine limestone and attaining a total thickness of 328 m (Crouzel, 1957). As the depozone narrowed progressively towards the south during the Miocene, the resulting furrow collected the most recent components of the foreland fill sequence. These can be observed at Saint-Gaudens and Montréjeau, and occur at the base of the Pyrenean mountain range, directly against the NPF. This southward rollover of the continental molasse depocentre could be the result of renewed subsidence of the Pyrenean foredeep, and thus of a brief revival of tectonic convergence in the central and western Pyrenees. All of these clastic levels contain mammalian fossils, for which revised biozone nomenclatures broadly confirms the stratigraphy originally established by Crouzel (1957). The site ages range from early Burdigalian (MN 3, at Estrepouy) to late Serravallian / early Tortonian (MN 8, at St-Gaudens and Montréjeau, where the faunal assemblages are precursors to the Vallesian but do not contain *Hipparion*). No site ascribable to MN 9 has yet been established (Antoine et al., 1997). The stratigraphic datum containing *Hipparion* (*Hippotherium primigenius*) has been debated (Sen, 1990), but the first known record of this indicator fossil at the Vallesian type locality in Catalonia set its age at 11.1 Ma (Garcés et al., 1997; Agustí et al., 2001). Based on this indirect criterion, the Neogene molasse sequence of the Aquitaine Basin is older than 11 Ma.

Crucially, stratigraphic facies characteristics throughout the entire Neogene sequence all exhibit fine-textured debris (molasse) transported to low-energy depositional environments, indicative of substantially subdued relief in the Pyrenees and its piedmont in Neogene time. Deposit lithology ranges from siltstone to fine sand and greywacke, cross-cut by mica-rich sand-filled palaeochannels. The latter occasionally contain coarser sand and gravel, with very rare pebble beds (pebble size: 2–5 cm) barely 1 m thick, particularly in the Montréjeau–St Gaudens molasse. Unlike earlier periods of the Paleogene, when fine-textured debris accumulated mostly in the more distal, northern parts of the Aquitaine Basin, lacustrine marl and limestone formations were now being deposited in a proximal position, in direct, nonconformable contact with the Sub-Pyrenean fold structures buried beneath them. This

1356 configuration, for example, occurs in the case to the Aquitanian to early Burdigalian cover
1357 rocks at La Lèze ('Saint-Ybars Limestone', see Fig. 5: Aude and Ariège transects), or of the
1358 Serravallian–Tortonian basal beds at Montréjeau and Saint-Gaudens.
1359 The only coarser-textured facies in a proximal position to the mountain range occur at the
1360 base of the Neogene sequence near Pamiers. Here, the conglomerate outcrop forms a
1361 homoclinal scarp, and exposures on the scarp face exhibit an upward-fining fluvial sequence
1362 in which palaeochannels at the base of the unit contain large pebbles (long axis: 10–40 cm),
1363 whereas palaeochannels at the top contain 5–10-cm-sized pebbles (maximum) amid thick
1364 reddish clay beds. Mammalian fossil assemblages within the beds correlate these strata with
1365 the late Oligocene (MP 29) and Aquitanian (MN 1 and MN 2; Addé-Lacomme, 1935;
1366 Bergounioux and Crouzel, 1971; Duranthon, 1991, 1992). The pebbles are almost exclusively
1367 quartz-rich (granite, gneiss, micaschist), and their identifiable provenance links them to large
1368 swaths of the Axial Zone. Such a wide distribution of quartz-rich debris from the interior of
1369 the Pyrenean mountain belt provides strong evidence that the Sub-Pyrenean outer fold
1370 belts, by this time, no longer acted as barriers to the conveyance of debris from the eroding
1371 mountain range.
1372 As the overfilled synclines of the Petite Pyrénées were undergoing burial by the mass of
1373 incoming debris (thereby raising local base levels) the intervening anticline ridges rising
1374 slightly above the fill sequence underwent erosional thinning and truncation. The entire
1375 assemblage thus formed a composite area of low relief, perhaps at places a continuous
1376 topographic ramp between the mountain range and the Aquitaine Basin.
1377 Miocene deposition did not extend eastward much beyond the Ariège valley, and the
1378 stratigraphy exhibits a number of lacunae. For example, all of biozone MN 3, and perhaps
1379 the base of MN 4, are missing, i.e., 3 million years of Burdigalian biostratigraphy (Duranthon,
1380 1991). The geodynamic cause of this stratigraphic lacuna has never been discussed, but a
1381 eustatic fall is ruled out because a Burdigalian transgression was occurring at the same time
1382 farther west in the Aquitaine Basin. A tectonic influence thus seems more likely, the lacunae
1383 in that case being erosional: with east-facing faults of the Mediterranean rift system
1384 transforming the eastern Pyrenees exactly at that time and the west-facing Toulouse Fault
1385 array also undergoing reactivation (Astre, 1959), the land in between from Carcassonne to
1386 Castelnaudary stood as a horst exposed to denudation. This possibility is supported by the
1387 discovery at Bourg-Saint-Bernard (Astre, 1953, 1959), 22 km east of Toulouse, of a mastodon

tooth (*Turicius turicensis simorrensis* Osborn), i.e., a genus whose arrival in Europe from Africa occurred ~18 Ma (Tassy, 1990; van der Made and Mazo, 2003), trapped in a fissure of exposed Chattian molasse (i.e., >23 Ma). This stratigraphically anomalous occurrence of a younger fossil in an older geological bed suggests erosion and redeposition of younger rocks across the land surface, here in a context of extensional crustal strain.

3.1.5. Sharp regime change during the late Miocene

3.1.5.1. Stratigraphic aspects

Compared to the earlier Neogene molasse, the late Neogene stratigraphic sequence (Fig. 5) is radically different from anything that preceded it in at least two respects. Firstly, the sedimentology is characterised by an abrupt influx of almost pure siliciclastic debris, which furthermore always lack a carbonate matrix in their depositional settings. Secondly, the base of the sequence usually displays evidence of a sharp disconformity involving networks of channels vertically incised into the underlying molasse depositional sequences. This ravinement surface has been well described by Crouzel (1957, Fig. 38 therein), who nonetheless erroneously extended this observation to the base of the marine 'Sables fauves' farther out into the Aquitaine Basin. This highly irregular boundary has sporadically been refuted and interpreted instead as a Pliocene or early Pleistocene weathering front (Icole, 1973). However, the erosional stratigraphic boundary is well documented throughout the foreland basin where decalcified, pebble-bearing clay deposits form a disconformable blanket across every existing geological structure from the Neogene molasse sequences (whether marine or continental) to the Paleogene Palassou conglomerate beds and the Cretaceous fold structures of the Sub- and North-Pyrenean zones.

3.1.5.2. Growth of range-front megafans

The late Neogene cover sequence (Fig. 5, Ariège and Béarn transects) extends as far out from the Pyrenees as the Landes plateau and the Entre-deux-Mers (between Dordogne and Garonne) near Bordeaux. Closer to the Pyrenean mountain front, it formed large alluvial fans

at the mouths of the main Pyrenean valleys. Among these: the Lannemezan megafan (Neste River) (Boule, 1894; Patin, 1967; Icole, 1968, 1969), the Ger megafan (Gave de Pau) (Fig. 1, Fig. 5 Béarn transect), and lesser fans such as the Cieutat–Orignac (Adour River), the Gave d'Ossau, the Lasserre-Lahitère (Salat River), and residual strips of formerly much larger fans coaxial with the Arbas, Arize and Ariège rivers. The Ariège and Garonne rivers, however, have comparatively large watersheds and were relatively more efficient at exporting most of the bedload to the outer piedmont. In the Basque Country, the extensive limestone catchment lithology has limited the abundance of clastic supply. Fan debris accumulations attain 60–80 m in the Ger and Orignac–Cieutat, 90–110 m in the central and eastern Lannemezan, and 170 m in the western Lannemezan. The cumulative thickness of the Ger megafan attains 100–120 m.

Four sedimentary units have been identified in some of those clastic sequence, with evidence of internal disconformities. The three uppermost units, clearly defined within the Ger megafan (Karnay et al., 1998; Capdeville et al., 1998), belong to the Pliocene. The basal unit of the late Neogene cover sequence is varyingly named 'Clay-with-pebbles' or 'Variegated clays' depending on the 1:50,000 scale map sheet concerned and on its proximal or distal position, respectively. The reported thickness of this unit ranges from 20 to 60 m. Its base is well dated at Orignac, where a lignite bed has yielded a rich assemblage of mammalian fossils (known since 1865) containing *Hipparion* (Astre, 1932; Richard, 1948; Crouzel, 1957). It can thus be assigned a Vallesian age (MN 10; Antoine et al., 1997), i.e., ~9.9 Ma. The botanical fossils in the lignite (Sauvage, 1969) are similar to those at Capvern (Bugnicourt et al., 1988) as well as near Pau and Mont-de-Marsan, i.e., rich in warmth-loving plants such as palms. The stratigraphically equivalent beds at Arjuzanx, on the southern Landes plateau, have also yielded an Upper Miocene mammalian fossil (*Dorcatherium*) amidst similar floral assemblages which include the cinnamon tree (*Cinnamomum polymorphum*; Huart and Lavocat, 1963). The systematic presence of marine phytoplancton in the same formation near Mont-de-Marsan suggests a close proximity to the Tortonian shoreline at the time (Capdeville, 1990). The three upper units of the Ger alluvial fan each contain 2 to 4 upward-fining depositional sequences, but mean pebble size increases from Unit 1 (2–5 cm) to Unit 3 (15 cm; maximum: 25–30 cm). The age of the megafan top is currently unknown, but its surface itself is cut and filled by shallow alluvial channel deposits containing even coarser debris than Unit 3.

The stratigraphy beneath the Landes area (Dubreuilh et al., 1995; Corbier et al., 2010; Bosq et al., 2019), where four fluvial sequences have cut and filled the underlying 'Variegated clays' of late Miocene age, attain a total thickness of 130 m. These formations, known respectively as Arengosse, Onesse–Beliet, Belin, and Castet, all contain lignite beds which document the decline in abundance, and ultimate extinction, of the warmth-loving plants still present in the slightly older strata elsewhere.

- The Arengosse unit cuts deep into the underlying sequence and is consistent with a Pliocene age. Warmth-loving species record a sharp decline in the topmost beds. The Arengosse Formation is typical of a deltaic environment and includes marine sand containing assemblages of foraminifera. Borehole cores indicate a marine gulf in the south of the Landes extending ~10 km east of the current coastline during the Pliocene (Kieken et al., 1975).
- The Onesse–Beliet unit, which was previously assigned chronostratigraphically to the Gelasian–Calabrian boundary (~1.8 Ma; Dubreuilh et al., 1995) but now considered older (i.e., closer to the Gelasian–Piacenzian boundary: 2.5–2.6 Ma; Corbier et al., 2010), includes only rare non-temperate taxa.
- The Belin unit outlines an early floodway of the Garonne River, already established in its northern position at the time, thus suggesting an onset of fluvial incision of the Lannemezan clastic sequence.
- The topmost Castet unit consists of reworked sediment from the older units. Despite having been formerly interpreted as an early Pleistocene fluvial unit (Corbier et al., 2010), it has recently been reinterpreted as an aeolian formation (a mid-latitude erg) and consists of a range of dated middle Pleistocene deposits (Marine Isotope Stages 10, 8 and 6; Sitzia, 2014; Sitzia et al., 2015).

Based on the coarse calibre of the debris forming the late Neogene megafan deposits, these landforms have been ascribed by most authors to a tectonic pulse in the Pyrenees. Taillefer (1951) took exception to this doctrine and ascribed them to a climatic cause. The current position of the top of the marine Langhian beds in Armagnac, which lie at 230 m (former gulf of Lectoure), nevertheless implies a magnitude of 200 m of post-Langhian uplift (conveniently, the Langhian was also the Miocene eustatic maximum, so the tectonic cause of this relative base-level rise is beyond doubt; see also Miller et al., 2011). Based on this

criterion, projecting the gradient of the Langhian baseline up the Adour River from Aire-sur-l'Adour obtains a 0.4% post-Langhian tilt of the (originally horizontal) marine beds and projects the southward continuation of this line to an elevation of 400 m in the foothills of the Pyrenees. This altitude grades to the base of retro-foreland's megafan accumulations, and thus documents a post-Langhian tilt of the Pyrenean piedmont and a minimum uplift value of the Pyrenean retro-wedge since that time.

The Neogene clastic wedge on the inner continental shelf of the Bay of Biscay (Landes) thickens offshore (Pujos-Lamy, 1984) and its aggradation rate appears to have increased through time. A 500-m-thick Miocene sequence and a 1000-m-thick Pliocene and Quaternary sequence were detected at the Ibis borehole (Kieken, 1973). Seismic profiles and more recent borehole data compiled by Ortiz et al. (2020), which provide a clear 3D reconstruction of the margin, now reveal that the post-Miocene wedge offshore is, on average, similar in thickness and volume to its Miocene predecessor (volume not quantified precisely by Ortiz et al.). Given that it was emplaced in just ~5 Ma (i.e., 3 to 4 times faster than its underlying Miocene sequence), with bypass to the abyssal domain by this time already substantial; and given, moreover, that it occurred prior to the acceleration of global cooling in the Pleistocene, the overall evidence is compatible with some form of tectonic reactivation in the Pyrenees and Massif Central starting in the late Neogene, with contributions from each of their river systems in currently unspecified proportions. The Pyrenees thus undoubtedly contributed to rapid Miocene, Pliocene and Quaternary sequence progradation in the south of the Aquitaine continental shelf zone (Bellec, 2003; Bellec et al., 2009).

3.2. Chronology of clastic supply to the Iberian foreland

3.2.1. State of the art and data sources

In contrast to the Aquitaine Basin, exceptionally good outcrop exposures permitted by the much drier climate in the Iberian foreland have promoted many opportunities for extensive and detailed stratigraphic and sedimentological studies of the fill sequences. This has also spawned the description and naming of a multitude of lithostratigraphic units of local extent, resulting in a complicated inventory of place-based terminologies. Appearances of regional uniformity have been inferred on the basis of long-distance lithostratigraphic correlations,

but unforeseen complications have arisen because many of those locally-defined units have turned out to be diachronous.

The record of Paleogene clastic sequences in the pro-foreland setting can broadly be divided into two palaeogeographic segments from east to west (Barnolas et al., 2019): (i) the Southeast Pyrenean Foreland Basin, which is confined to eastern and central Catalonia and includes the large Ripoll piggyback basin (Fig. 5, Catalunya transect), cradled by the Canigou–Vallespir–Cadí nappe unit (Figs. 2, 3); and (ii) the South Pyrenean Foreland Basin in western Catalonia and onward into Aragón, which as far west as Pamplona is also a collection of piggyback basins — large (Ainsa, Jaca) and small (Pobla, Tremp, Ager), cradled by the SPZ thrust systems (Figs. 3, 5).

As with the Aquitaine Basin, we emphasize clast provenance and the diachronous patterns of basin fill generated by the rising Pyrenees. Progress in clarifying the basic lithostratigraphic correlations has been gained from sequence stratigraphy, magnetostratigraphy, U–Pb and fission-track ages of detrital zircon crystals (Whitchurch et al., 2011; Thomson et al., 2017; Roigé et al., 2019), and from the correlation of various continental fossil assemblages to ELMA biozones. For example, 8 tectono-sedimentary units (TSUs) have been identified in the Iberian foreland (3 for the Paleogene, and 5 for the Neogene: Villena et al., 1992; Pérez-Rivaréz et al., 2018). The inventory, however, is confined to the Ebro basin itself and does not include the folded Eocene sequences that were being cannibalised and incorporated into the orogen by outward growth of the pro-wedge. In the Southeast Pyrenean Foreland Basin, 8 sequences were inventoried just within the Eocene series (Puigdefábregas et al., 1986). The pioneering work of Reille (1971) was updated by a more recent synthesis (Barnolas and Gil-Peña, 2001), which defines only 4 sequences within the Eocene series. Friend et al. (1996) have provided a comprehensive analysis of the continental deposits spanning the Priabonian to the Lower Miocene.

Obtaining age constraints for these various depositional systems and their lithofacies assemblages has proven difficult chiefly for two reasons. Firstly, marine environments on the Iberian side of the orogen only endured until the Eocene. After ~36 Ma, the Ebro Basin became internally drained. Accordingly, the sedimentary sequences acquired thereafter a continental character, thus ruling out all prospect of chronostratigraphic constraints from marine indicator fossil evidence (reliable and independent constraints for the Neogene are even more tenuous than for the Paleogene, with only one radiometric age in the form of a

19.7±0.3 Ma cinerite bed; Pérez-Rivaréz et al., 2018). Secondly, mammalian faunal assemblage sites have turned out to be (i) much less abundant than in the Aquitaine Basin despite a growing inventory through the years, (ii) comparatively poorer in species diversity, and (iii) very unevenly distributed through basin space and stratigraphic time. A synthesis produced by Cuenca et al. (1992) listed at the time a total of 123 fossil sites, mostly situated in the south and southeast of the Ebro Basin. They were much scarcer in the outer pro-wedge, and even more so within the tectonically deformed clastic sequences of the inner pro-wedge (for the Paleogene, see also: Crusafont and Golpe-Posse, 1973; Golpe-Posse, 1981a; Sudre et al., 1992; Antunes et al., 1997; Cuesta et al., 2006; Badiola et al., 2009; Bonilla-Salomon et al., 2016; and for the Neogene: Crusafont et al., 1966; Crusafont and Pons, 1969; Cuenca et al., 1989; Alvarez-Sierra et al., 1990; Agustí et al., 1994, 2011).

As a result of these key differences with the Aquitaine Basin, palaeogeographic reconstructions of the Ebro Basin have relied on magnetostratigraphy as the core method for tuning the record of continental deposits to index fossils in existing marine sequences (Garcés et al., 2020). Divergences of interpretation from one local study to another are understandably numerous (e.g., Burbank et al., 1992a, b; Costa et al., 2010, 2011; Hogan and Burbank, 1996; Arenas et al., 2001; Oliva-Urcia et al., 2016, 2019; Roigé et al., 2019), and the most robust chronological constraints in the case of continental deposits are obtained when magnetostratigraphic results are combined with ELMA-based evidence (Barberà et al., 2001; Larrasoaña et al., 2006). Resulting palaeogeographic interpretations and palaeogeographic maps for the Ebro foreland using either approach usually concur remarkably well. The most recent synthesis by Garcés et al. (2020) favours magnetostratigraphic evidence and prioritises correlations with the Geomagnetic Polarity Time Scale (GPTS). Within that particular reference frame, some offsets or mismatches with existing ELMA-based chronostratigraphic data, particularly at the fossil-rich sites of Sossis and Sant Jaume de Frontanyà, are not considered or discussed, and thus remain currently unresolved.

3.2.2. *Paleogene deposits of the Southeast Pyrenean Foreland Basin*

Unlike the Aquitaine foreland, where the sea withdrew rapidly from the Corbières westward to the Béarn in Ypresian time (~46 Ma), the Iberian foreland remained a marine environment until the early Priabonian (~36 Ma) (Sanjuan et al., 2012; Costa et al., 2013). Below we

present the palaeogeography of the Southeast Pyrenean Foreland Basin in two longitudinal segments from east to west, with emphasis on the clastic output generated by the rising Pyrenees, on evidence of clast provenance, and on the diachronous chronostratigraphy of the basin fill.

3.2.2.1. From the Empordà Basin to the Ripoll syncline

The southward displacement of the Eocene foredeep has been well constrained from a sequence stratigraphy perspective from the Empordà Basin to the Ripoll syncline (Puigdefábregas et al., 1986; Burbank et al., 1992b; Vergés and Burbank, 1996; Costa et al., 1996; Tosquella and Samso, 1996; Barnolas and Gil Peña, 2001; Serra-Kiel et al., 2003; Barnolas et al., 2019). Nine depositional sequences (I to IX) were initially identified in this eastern segment of the foredeep: eight within the Eocene and one defining the base of the Oligocene. Their names are directly adopted from the regional lithostratigraphic unit names, hence some ambiguity in the literature between the two schemes — particularly in the case of Bellmunt (unit VI) and Milany (unit VII) and the respective boundaries of these units in each scenario. Units I–III (Ypresian) to IV (Lutetian) testify to thrust sheet emplacement below sea level, with olistoliths, turbidites, and deltaic facies. However, vestigial outcrops of proximal conglomerate beds of Ypresian and Lutetian age occur at several locations in the far east (mapped on the geological sheet of Figueres: Fleta et al., 1994; Pujadas et al., 1989), and occur likewise in the South Pyrenean Foreland Basin (see next Section). The younger depositional units (VI, VII, IX) exhibit thick conglomerate units, including the fan-deltas of the Lutetian Bellmunt (46–41 Ma) and Bartonian Milany (41–37 Ma) formations, which are themselves overlain by the Berga conglomerate sequence (Priabonian–Rupelian boundary, i.e., ~34 Ma). Units V (Beuda: gypsum) and VIII (Cardona: salt beds) consist of evaporites and document the growing confinement of the Ebro Basin and the definitive termination of the marine environment, respectively. Guided by a new calibration of Lower Lutetian biozone SBZ 13 (large foraminifera of the shallow benthic zone) Garcés et al. (2020; compare Figures 2 and 6 therein) have offered a divergent interpretation of the Ripoll syncline based on a revision of the middle (clastic) sequences. In this new framework, the Bellmunt and Milany units are fully reallocated to the Lutetian and the Beuda unit to the Ypresian–Lutetian

boundary — thus suggesting that these formations are substantially older than previously established (e.g., Berástegui et al., 2002).

In the Empordà Basin, the Bellmunt Formation is 2 to 3 km thick and devoid of fossil remains. The top of the conglomerate sequence is covered by the Figueres nappe and in some publications attributed to the Priabonian (Fleta et al., 1994). The base of the Bellmunt Formation in the SW rests conformably on Lower Lutetian marine beds (48–45 Ma), but towards the NE the 1:50,000 scale geological map of Figueres (Fleta et al., 1994) indicates progradation of the conglomerates over Upper Ilerdian–Cuisian marine beds, beneath the Biure nappe (Pujadas et al., 1989). The Bellmunt conglomerates near Figueres are alluvial fan deposits containing a majority of limestone and sandstone pebbles from the Mesozoic and early Cenozoic cover sequences of the Pyrenees, but also containing some debris supplied by basement outcrops. The latter are initially uncommon (5–10%), but their abundance increases in the middle and upper units of the sequence, where they display schist (including a facies reminiscent of the Paleozoic Jujols Series), quartz, quartzite, black chert, various granites (sometimes exclusive in certain beds, with some cobbles up to 40 cm in diameter). However, the total absence of gneiss (particularly augengneiss), which forms substantial outcrops in the Roc de France and Albères massifs today, suggests that this eastern segment of the Axial Zone was not sufficiently deeply eroded at the time to expose this gneiss core.

In the Ripoll syncline, the Milany Formation laps onto the edge of the Pedraforca nappe and is reported to contain granite clasts (Burbank et al., 1992b), but has (confusingly) been named Bellmunt instead of Milany by other authors (Busquets et al., 1992). No gneiss clasts are reported, suggesting that the Carançà gneiss outcrops in the Axial Zone were not yet exposed at the time. The fine-textured fluvial and palustrine basal beds contain the rich mammalian assemblages of Sant Jaume de Frontanyà (SJF) 1 (MP 15: ~40.5 Ma, Lower Bartonian) and (200–270 m lower down the sequence) SJF 2 and SJF 3 (MP14: ~42 Ma, Upper Lutetian) (Busquets et al., 1992; Badiola et al., 2009; Bonilla-Salomon et al., 2016). The outcrops of marine and deltaic facies occur 500 m further down in the stratigraphy (Coubet/Can Bernat Fm., Busquets et al., 1992); they are attributed to marine biozone SBZ13 (Garcés et al., 2020) and are thus clearly Lower Lutetian.

The ELMA-based chronological framework defined by the mammalian fossil sites has been challenged by recent reinterpretations of previous magnetostratigraphic data (Garcés et al., 2020). The three studies available in the literature for this area (Burbank et al., 1992b;

Vergés et al., 1998; Garcés et al., 2020) differ nonetheless substantially; the most detailed (Burbank et al., 1992b, Figs. 9, 15 and 16 therein) spans chrons 21 to 18 or 17, and clearly exposes correlation uncertainties and options. The most recent (Garcés et al., 2020, Fig. 6 therein) restricts the entire lithostratigraphic interval to Chron 21, but without explaining why the other options have been ruled out. Existing geological maps, and particularly the IGME sheet for La Pobla de Lillet (Vergés et al., 1994) and the IGC 1:25,000 scale sheet bearing the same name (Martínez et al., 2013), each also indicate divergent ages for the top of the conglomerate sequence, i.e., Priabonian and Bartonian, respectively. Birot (1937) had previously reported among these upper beds the presence of huge boulders of granite (in the upper levels, granite clasts dominate almost exclusively and the largest boulders are 3 m in diameter), probably supplied by the Mont-Louis batholith, whose nearest outcrops currently lie 30 km to the north, i.e., beyond the currently elevated massifs in Devonian limestone (Tossa d'Alp massif, at the southern edge of the Cerdagne Basin). This evidence suggests a presence at the time of small, steep catchments with high-energy streams capable of delivering large debris — and thus a granitic mountain front nearby (~30 km to the closest modern granite outcrop) and very different from the current landscape. Overall, given the 1400-m-thick sediment pile that separates the Sant Jaume de Frontanyà fossil deposit from the top of the series, and given further the sedimentation rates that can be inferred between the two palaeontological sites SJF 1 and SJF 2–3 (separated by 270 m of sediment accumulation), it cannot be ruled out that the top of the depositional sequence is Priabonian. More data are needed from that region to reach a robust conclusion.

3.2.2.2. From the Llobregat to west of the Segre River

In this western part of the Southeast Pyrenean Foreland Basin, the Bellmunt and Milany sequences have been deformed by Pyrenean tectonics and partly incorporated into the Pedraforca nappe (Figs. 2, 3). South of this tectonic unit lie the well-documented Berga and Oliana conglomerate sequences, which are 2500 m thick and have been subdivided into three units based on conspicuous boundaries within the fanning dip structure (Riba, 1973, 1976). The clast compositions are lithologically fairly uniform, with debris from the Axial Zone (granites included) rather unevenly distributed through the sequence. Axial Zone lithologies are thus sporadically abundant, such as in the lower Cardener conglomerate beds

or at the top of the sequence near the town of Oliana, but are also at times rare or absent. Granite cobbles may attain diameters of 40–50 cm, with upward coarsening through the stratigraphy (limestone boulders ~1 m in diameter). The base of the Berga sequence lies conformably over the Lower Priabonian marine shales and is thus most likely also of Priabonian and Rupelian age (~36 to ~31 Ma; Carrigan et al., 2016), but the top of the sequence is undated. A revised magnetostratigraphy by Costa et al. (2010) of the results published by Burbank et al. (1992a) and Vergés and Burbank (1996) has confirmed the Priabonian age of the basal marine beds, and it additionally shows that the base of Oliana Unit 4 is part of the Rupelian (~30.5 Ma). This marker horizon, however, is still overlain by at least 500–700 m of conglomerate and sandstone beds, which — by linear extrapolation of the earlier sedimentation rates — should place the top of the Oliana–Berga conglomerate sequence in the late Oligocene (Chattian: 27–28 Ma). Farther out into the Ebro Basin, the conglomerate formations change to more distal molasse facies such as the yellow Solsona and red Artés sandstone sequences, and further still to shale and lacustrine limestones. These distal sequences contain a dozen mammalian fossil sites spanning Priabonian biozones MP 19–20 (or perhaps MP 18) at Cardona, Sant Cugat de Gavadons, and Roquefort de Queralt; upward to to MP 21 (Santpedor), MP 22 (Calaf), MP 23 (Tàrrega), and MP 23/24 (Vinaixa) which, at ~30 Ma, all document the Rupelian Stage (Barberá et al., 2001; Costa et al., 2011).

West of the Segre River, near Artesa de Segre, a magnetostratigraphic study covering an 1800-m-thick molasse sequence consisting predominantly of clay and sandstone has yielded a Priabonian base (35 Ma) and a Chattian top (25 Ma) (Meigs et al., 1996). This molasse sequence transitions northward to a much coarser sequence of conglomerate beds consisting almost exclusively of Mesozoic limestone pebbles. These have buried portions of the SPCU thrust-front scarps between the Montsec and Oliana, for example around the Col de Comiols near Benavent. Five depositional sequences have been identified and correlated with those reported around Oliana (Maestro-Maideu and Serra-Roig, 1996). The chronology provided by Meigs et al. (1996), however, remains uncertain given the occurrence of interruptions in the stratigraphy and the absence (thus far) of independently corroborating geochronological evidence in this area.

3.2.3. Paleogene deposits of the South Pyrenean Foreland Basin

Still farther west along the strike of the orogen, roughly between the town of Tremp and the city of Pamplona, the Paleogene clastic sequences accumulated in a continuous depositional zone known as the South Pyrenean Foreland Basin (Barnolas et al., 2019), also commonly dubbed Jaca–Tremp Basin. This depositional area, however, is not easy to reconstruct, (i) partly because the Paleogene deposits have been concealed by younger Neogene sequences at the margins of the Ebro Basin, but also (ii) because the Montsec Thrust and the South Pyrenean Frontal Thrust (Fig. 2) detached and carried the Jaca–Tremp Basin piggyback southward in several stages during the middle and late Eocene to early Miocene — thus imparting tectonic deformations to all of the fill sequences. As a result, despite the fact that structural geologists consider the SPFT as the limit between the Pyrenean crustal wedge and the Ebro Basin, in terms of stratigraphy this limit is not adequate because parts of the South Pyrenean Foreland Basin were situated in the thrust-displaced, and others in the undisplaced, foreland area during the same period of the past. It is thus useful to bear in mind that synorogenic sedimentation in the south-Pyrenean foreland occurred in two contrasting environments separated by the Sierras Exteriores: the elongated piggyback Jaca–Tremp Basin situated north of the Sierras Exteriores, and the less intensely deformed outer Ebro foreland basin located south of them (Fig. 2).

In the Sierras Exteriores west of the Noguera Ribagorçana River, the Peralta de la Sal Basin displays a very similar chronostratigraphic model to that of the Artesa area mentioned above (Meigs, 1997). In the Ebro foreland, the history of denudation in the orogen is recorded by the mudstone and sandstone sequences that overlie the Priabonian evaporites (Balaguer and Barbastro gypsum deposits, Fig. 5, E-Aragón transect), and that have been deformed into a fairly continuous frontal anticline. Extensive outcrops of the 1000-m-thick Peraltilla Formation (Fig. 5, E-Aragón transect), which consists of red mudstone floodbasin deposits interbedded with shoestring sandstones, can be observed west of the Cinca River. The bottom of the sequence (marl and lacustrine limestones) has been ascribed to the early Oligocene based on a flora of charophytes (Reille, 1967, 1971) and on a micromammalian fossil assemblage (locality: Peraltilla) assigned to MP 23, i.e., ~31 Ma (Alvarez-Sierra et al., 1990; Cuenca et al., 1992). The sequence has been folded and is unconformably covered by an Aquitanian terrigenous sequence. The fine-textured sedimentological features of the Peraltilla sequence (Fig. 5), with just a few gravel-bearing beds containing predominantly

small quartz clasts,would suggest a relatively low-energy environment at the front of the outer sierras at the time, even though clast provenance analysis also documents some sediment transfer from the Axial Zone (Yuste et al., 2004). Overall, the age of the conglomerate beds in the region around Barbastro and Graus remains unclear, with some authors postulating continuous aggradation of the Huesca megafan from the early Oligocene to the Miocene (Hirst and Nichols, 1986; Luzon, 2005).

The repository for the coarser, high-energy Paleogene clastic output from the Pyrenean orogen was the Jaca–Tremp Basin (Fig. 5, Aragón transects) situated to the north of the Sierras Exteriores, confirming that high relief was present in at least parts of the hinterland at the time. The Jaca–Tremp Basin began to form and accumulate deposits quite early in the Iberia–Europe convergence history. In the east, it received a 1000 m-thick discharge of the Garumnian series, which lies conformably over the late-Cretaceous marine and Maastrichtian littoral sandstone beds (Aren Formation). The leading edge of the upper Pedraforca–Bóixols upper nappe unit terminates in this sequence. An extensive Ilerdian carbonate platform documents a distinctive but brief respite in the tempo of clastic output from the rising orogen. Accordingly, these well-defined marine episodes (the Ilerdian Stage, i.e., Lower Ypresian, received its credentials as an international stratotype in the Tremp Basin: see Pujalte et al., 2009) were soon overprinted by an Upper Ypresian to Lutetian depositional system of piedmont, alluvial plain, deltaic and shelf-sea lithofacies. This succession of thick sandstone and conglomerate beds progrades from east to west (Nijman, 1998), parallel to the strike of the orogen.

The conglomerate units of the Tremp Basin were being supplied by topography situated to the northeast of the depositional area, i.e., where the Proto-Pyrenees had formed and were presently expanding westward to form the Ancestral Pyrenees. The source rocks were mainly sedimentary cover sequences, with nonetheless arkose deposits and a minority presence of basement clasts from the Axial Zone. The pebbles are well rounded, with median sizes ranging from 10–20 cm to 40–50 cm in the more massive Campanue Formation (500–1000 m thick), the top of which could be of early Lutetian age (~45 Ma; Fig. 5, E-Aragón transect). The fluvial facies exposures contain a large number of mammalian fossil sites, all rather limited in taxonomic diversity (Crusafont et al., 1956; Crusafont et al., 1973; Antunes et al., 1997; Badiola et al., 2009). In the Ager sub-basin (16 sites), the clastic sequence appears quite old (3 sites: MP 8–MP 9, i.e., ~52 Ma), with the remainder labelled as MP 10

(~50 Ma). In the larger Graus–Tremp sub-basin (Montllobar: 6 sites; Pont de Montanyana: 10 sites; Isabena: 11 sites), all of the fossil assemblages are now ascribed to biozone MP 10, i.e., to the Upper Ypresian (Antunes et al., 1997; Badiola et al., 2009) instead of the Lutetian (Crusafont et al., 1956; Sudre et al., 1992).

The Capella Formation (Fig. 5, E-Aragón transect), which is 600 m thick and of fluvial origin, records the tipping moment when its sedimentary sequences (which are exposed in the Isábena River valley) became lastingly cut off from marine influence. The Capella Formation is reported to connect laterally to the upper section of the Campanue Formation, but its age is poorly constrained: its base contains an MP 10 assemblage (at Torrelabad); and two sites from the middle part of the stratigraphy (Barranc de Estaran, Casa Ramon) are labelled as MP 11–MP 12, i.e., ~46–48 Ma (Antunes et al., 1997; Badiola et al., 2009). However, the Barranc site has been revised as MP 13, i.e., ~44 Ma, by Teixell et al. (2016), whereas the Graus occurrence (MP 14, i.e., Upper Lutetian) has not been precisely located in consulted publications although it appears to lie within the Capella Formation.

The continental character of the basin environment was accentuated at the time of the Escanilla Formation (Fig. 5, E-Aragón transect), which on geological maps displays a slight unconformity over the underlying Capella and Campanue formations in the south and southwest, but forms a much more accentuated angular unconformity over the Triassic and Cretaceous outcrops of the Mediano anticline. The Escanilla Formation consists of 500 to 1000 m of red- and ochre-coloured mudstone, and of grey conglomerates containing some pebbles from the Axial Zone. This formation also displays two levels of limestone and lignite containing the two taxonomically diverse fossil sites of Capella (MP 14, ~42 Ma, not to be confused with the name of the underlying formation) and Laguarres (200 m further up-sequence: MP 15, i.e., ~40.5 Ma according to Sudre et al., 1992; but MP 16, i.e., ~39 Ma according to Antunes et al., 1997 and Badiola et al., 2009). The age of the Escanilla sequence thus spans the Upper Lutetian and entire Bartonian. The top of the sequence, which has not been preserved, could thus potentially be extrapolated into the Priabonian, and perhaps even the early Oligocene. This biochronology is corroborated by magnetostratigraphic data from the same area (Bentham and Burbank, 1996; Vinyoles et al., 2020).

West of the Graus meridian, the siliciclastic sequence of the Jaca–Tremp Basin forms a transition with the Ypresian and Lutetian flysch-filled Ainsa foredeep and the Hecho submarine fan system (4400 m thick; Labaume et al., 1985). It contains limestone

olistostromes initially considered to have been supplied from a northern source area (Labaume et al., 1985), but more probably related to a destabilisation of the Guara carbonate platform located at the southern border of the flysch basin (Barnolas and Teixell, 1994; Barnolas and Gil-Peña, 2001). To the north, the flysch sequence covered the region corresponding to the high Pyrenean range of today (Teixell, 1998), connecting with the Aquitaine foredeep in the vicinity of the modern Pic d'Anie. The meridian line passing through the Pic d'Anie consequently locates the point where the Ancestral Pyrenees terminated as an emerged mountain range during middle Eocene time.

No Lutetian deltas or alluvial fans are documented west of the Campanue palaeofan. The default hypothesis is that none ever formed given the absence of a mountain range at these longitudes at that time. In Bartonian time, the pro-wedge foredeep rolled southward under the effect of increased crustal loading, and became until the early Priabonian a depocentre for 1700 m of marine shale (Pamplona Series). Compared to the earlier flysch episode, the depositional environments were shallower and included deltaic and continental facies indicative of rising uplands to the north and an active tectonic front probably located at the Oturia thrust front (Fig. 2). From base to top, and prograding to the SW over marine shales, the clastic sequence (Fig. 5, W-Aragón transect) consists of the Sabiñanigo Formation (Bartonian sandstone), the deltaic sandstone facies of Belsue–Atarés, and lastly the massive conglomerate and red mudstone beds of Santa Orosia, commonly tied to the Priabonian (Puigdefàbregas, 1975; Roigé et al., 2016, 2017; Garcés, 2020, Fig. 3 therein) but recently reassigned to the Upper Bartonian (Vinyoles et al., 2020). The clastic influx continues up-sequences with the Cancias conglomerates, which are Priabonian to Rupelian and transition laterally to the fluvial beds of the Campodarbe Fm. The extensive outcrops of Santa Orosia–Cancias conglomerates (500–900 m thick) between the modern Cinca and Gállego rivers contain boulders up to 60 cm in diameter consisting mainly of sandstone from Eocene flysch and (in lesser proportions) of limestone, with nonetheless rare evidence of debris transported from the Axial Zone (which was already exposed farther east: Roigé et al., 2016) and perhaps from the North-Pyrenean Zone (Roigé et al., 2017). This strongly suggests that the basement had not yet been exposed by denudation in this (nonetheless emergent) western segment of the Pyrenean orogen.

The continental Campodarbe Formation, a western equivalent of the Escanilla Formation (Fig. 5, W-Aragón transect), conformably overlies the last deltaic and evaporitic deposits of

Priabonian age and is ubiquitous from the Jaca syncline westwards to the Pamplona syncline and southwards to the south of the Sierras Exteriores, where the Peraltilla Formation is its stratigraphic equivalent (Fig. 5, E-Aragón transect). The Campodarbe Formation was studied in detail by Puigdefábregas (1975) and shown to attain maximum thicknesses of 3000 m at Guarga (east of the Gállego River), 4000 to 5000 m at Onsella (50 km to the west), and perhaps 7000 m near the border with the modern province of Navarra (i.e., another 50 km farther west; note that this maximum thickness includes the Miocene cover sequence). The Campodarbe Formation consists of fluvial sandstone and shale deposited by rivers flowing WNW, i.e., parallel to the strike of the orogen. The palaeochannels contain quartz pebbles. On its northern and northeastern edge, the formation is overtopped by thick, prograding synorogenic alluvial deposits produced by the eroding Ancestral Pyrenees, such as the Santa Orosia–Cancias palaeofans, which possibly continued to aggrade during the lower Oligocene, and the Peña de Oroel and San Juan de la Peña palaeofans near the city of Jaca. Stratigraphically, these two conglomerate sequences belong to the top of the Campodarbe Formation and exhibit onlapping synsedimentary unconformities. Their clast content predominantly consists of Eocene sandstone and limestone from the aforementioned olistostromes of the flysch-filled Ainsa–Jaca trough, implying once again that the basement rocks of the Axial Zone were not yet exposed at that time.

The age of the Campodarbe Formation is imprecise (Priabonian to late Oligocene) and based on charophyte remains. Magnetostratigraphic evidence (Hogan and Burbank, 1996) has provided a Priabonian age for the lower 1500 m (base at Chron 16rn, ~36 Ma, Costa et al., 2010) and a Rupelian age for the overlying 2300 m at the Salinas section, terminating at Chron 10r (~29 Ma). However, the Salinas section lacks the syntectonic upper conglomerate beds of the Peña de Oroel and San Juan palaeofans, which were ascribed to the late Chattian and even to the earliest Miocene by Reille (1971) and Puigdefábregas (1975). More recently, Oliva-Urcia et al. (2016) found that the top of the fluvial Campodarbe Formation in the foreland zone of the Sierras Exteriores coincided with Chron 7r (i.e., 24.5 Ma, latest Chattian); in the Jaca syncline, which at that time was still undergoing tectonic deformation, the top of the fluvial units of the Campodarbe Fm. (i.e., beneath the Peña de Oroel and San Juan conglomerates) is reported as no younger than 31 Ma. In this subregion, the Rupelian–Chattian deposits are thus understood to have been folded and eroded, thereby cannibalizing the Campodarbe Fm. and younger conglomerates of the deforming Jaca

syncline, and supplying from this source-material the late Oligocene and Aquitanian Sariñena and Uncastillo formations (which make up the Luna Fan situated south of the Sierras Exteriores; Oliva-Urcia et al., 2019; Fig. 5, W-Aragón transect) (see Section 3.2.5 on Neogene deposits). Still more recent dating of volcanic zircon crystals contained in the San Juan de la Peña and Peña de Oroel conglomerate beds, however, has challenged this chronostratigraphic model and indicates instead that these conglomerate deposits of the Jaca Basin are as young as 24–22 Ma (i.e., Aquitanian) (Roigé et al., 2019). This would imply that sequences in the Luna Fan's source area are the same age as the Luna Fan itself, in which case the Sariñena and Uncastillo conglomerate sequences cannot be merely re-eroded derivatives of the folded Jaca Basin conglomerates. Note that these very young ages remain unreported in the most recent synthesis on the region (Garcés et al., 2020, Fig. 3), according to which no conglomerate units are younger than Chattian, and which assigns Peña de Oroel to the Priabonian–Rupelian boundary and San Juan de la Peña fully to the Rupelian. In this region, where sequences suitable for magnetostratigraphy are scarce and where no terrestrial fossils have so far been reported from the San Juan and Peña conglomerate units, further field research is probably necessary as such occurrences may exist.

3.2.4. Two geological enigmas in the Graus–Tremp Basin

1.2.4.1. Unexplained offsets between the Southeast and South foreland sequences

Roughly between the towns of Graus and Tremp, the South-Pyrenean Central Unit (SPCU) consists of thrust units and a series of piggyback basins (Fig. 2), with the larger basin (Tremp–Graus) situated on the back of the Montsec Thrust Sheet, and the smaller (Ager) basin (south of the Montsec thrust front) riding on the Montroig Thrust Sheet which comes out at the base of the Serres Marginals (see Fig. 2; Turner, 1990; Teixell and Muñoz, 2000; Muñoz et al., 2018). This part of the SPCU is also known to geographers as the Conca de Graus–Tremp.

The geometry and palaeogeography of the SPCU have raised a number of unresolved issues, summarised here. The clastic sequences of the piggyback basin were predominantly supplied by the high ranges of the Pyrenees, but secondarily also by the SPCU fold systems and by the

Ebro massif to the south (which until at least the Paleocene was still above sea level: Puigdefábregas, 1975; Gómez-Gras et al., 2016; Thomson et al., 2017). Throughout the South Pyrenean Foreland Basin, the fill sequence gets younger from east to west and sedimentation was continuous from 66 to 28 Ma according to Garcés et al. (2020), and even until 25–23 Ma according to Roigé et al. (2019). It thus forms an uninterrupted, time-transgressive lateral progression along the Iberian foreland as far as the Jaca–Pamplona marine foredeep, which received a thick flysch sequence of early and middle Eocene age almost identical to the eastern sequence in the Ripoll Basin. The outstanding paradox of this regional succession is that the Catalonian flysch deposits of the Southeast Pyrenean Foreland Basin are mapped as overridden by the Pedraforca nappe on the east side of the SPCU, whereas the Aragonian flysch deposits appear to lie over the SPCU and the westward continuation of the South Pyrenean Zone in the Ainsa area (Fig. 2), riding piggyback on the SPCU and displaying their own endemic thrust sequence (e.g., Chanvry et al., 2018). Confusingly, therefore, what appears (at least in terms of lithostratigraphy and facies) to be the same Paleogene sequence either overlies or underlies the SPCU thrust units. This anomaly in the apparent architecture of the pro-wedge basins has often been sidestepped, but Nijman (1989) addressed it and offered three plausible explanations for this configuration. They are all underpinned by the logical inference that the Iberian foreland was made up in the early Paleogene of two marine foredeeps, one beneath the SPCU and overridden by it, and the other above it, with the two depositional sequences eventually merging in the west.

Maps and reconstructions by Payros et al. (2009), Martinius (2012) and Thomson et al. (2017; Fig. 11 therein) suggest that a marine connection between the Ripoll and Ainsa basins could have occurred as a narrow corridor in the region of the Ager Basin at the time of deposition of the Ager Group, ~55–51 Ma, but that it is now either concealed beneath the advancing Montsec thrust, or lay over it but has since then been eroded (Muñoz et al., 2013). The very rapid southward advance of the SPCU by at least 40–45 km in just 4 Ma during the late Lutetian (44–41 Ma) emphasizes the importance of the Triassic evaporites as a lubricant on the thrust sole and is probably key to understanding the elusive palaeogeography of that period. Subsequent to the rapid thrust propagation, Thomson et al. (2017) suggest the South Pyrenean Foreland Basin became separated from the Southeast Pyrenean Foreland Basin as a result of topographic damming along the Segre oblique ramp

fault zone (Fig. 2). No definitive solution has been put forward until now to adjudicate between these alternative palaeogeographic scenarios (Barnolas et al., 2019). A possible solution to the enigma would nonetheless be the coexistence of two distinct, strike-parallel marine foredeeps. The eastern foredeep, initially offset to the south of the western foredeep, opened out on the Tethys (see palaeogeographic maps in Plate I); it perhaps also, at least initially, communicated with its western counterpart through shallow straits not yet identified (discussion in Garcés et al., 2020).

3.2.4.2. The 'Nogueres conglomerates' anomaly

The unconformable 'Nogueres conglomerate units' (named collectively thus in this review, but more commonly named from just one of their four outcrops: the conglomerates of La Pobla de Segur) have long been singled out as unique and enigmatic within the Pyrenean orogenic environment (Ashauer, 1934; Birot, 1937; Crusafont et al., 1956; De Sitter, 1961; Rosell and Riba, 1966; Rosell, 1967; Reille, 1971; Mellere and Marzo, 1992; Coney et al., 1996; Vincent and Elliot, 1996; Vincent, 2001; Beamud et al., 2003, 2011). They occur in the Jaca–Tremp Basin between the modern Isábena and Segre rivers, and are mostly coaxial with the modern Noguera Ribagorçana and Noguera Pallaresa rivers — hence the 'Nogueres' appellation proposed here. Compared to other conglomerate sequences further east or west, their main characteristic is that they are recessed in a more northern position of the pro-wedge. A few residual outliers have also been mapped on the Pedraforca tectonic unit east of the Segre, but this Nogueres sequence mainly occurs as four geographically distinct outcrops, from west to east: Serra de Sis, Sierra de Gurp, La Pobla de Segur; and, offset to the north: the Senterada outcrop. Cumulative thicknesses attain 3500 m, subdivided into 5 allostratigraphic units altogether forming a stack of 20 alluvial fans as well as an onlapping backfill sequence all the way up to the Axial Zone (Mellere and Marzo, 1992; Beamud et al., 2003, 2011). The size of the time gap recorded by the basal unconformity decreases from north to south, with the conglomerate beds resting successively on the Hercynian basement, on the folded Cretaceous cover sequence of the SPCU (Figs. 1, 3, 5), and on the Paleocene and Lower Eocene deposits of the Jaca–Tremp Basin (e.g., the upper Ypresian in the Sierra de Sis; MP 10 biozone near Cajigar, Isábena area, Badiola et al., 2009). Then, just a few

kilometres to the SW, they connect to the Escanilla Formation, which itself rests disconformably on the underlying Lower Lutetian units (Beamud et al., 2003).

The Nogueres conglomerate sequence can thus be considered to represent the proximal eastern tracts of the fluvial systems that supplied the Campodarbe Formation to the Jaca Basin (Michael et al., 2014). Their age at La Pobla de Segur has been constrained by 3 mammalian fossil sites (Sosis, Roc de Santa, Claverol), which rank taxonomically among the most diverse of the Pyrenean Eocene. They are situated within the lacustrine facies of allostratigraphic Unit 2, to which may be added the slightly more elevated site of Casa Gramuntil at the base of allostratigraphic Unit 3 (López-Martínez, 1998). All of these assemblages are attributed to the base of the Priabonian, i.e., MP 17a (Crusafont et al., 1963; Crusafont and Golpe, 1973; Sudre et al., 1992; Antunes et al., 1997; Sigé, 1997; López-Martínez et al., 1998; Badiola et al., 2009). The lower allostratigraphic unit of La Pessonada (~1000 m thick) is then plausibly of Bartonian age. Magnetostratigraphic data place the top of allostratigraphic Unit 5 within the Chattian, i.e., 27 Ma (Beamud et al., 2011). Such an age is plausible, but in that case the magnetostratigraphy requires MP 17a to be pushed down the chronostratigraphic scale (by ~5 Ma) to the Upper Lutetian (Beamud et al., 2003). The proposition to recalibrate substantial portions of the ELMA scale on the basis of one local magnetostratigraphic study (see Fig. 6 in Beamud et al., 2003, which assigns biozones MP14 to MP17a to the time bracket initially restricted to MP14) has so far not, however, been endorsed by more recent updates of the ELMA scale, which still appear to maintain MP 17a within the Priabonian (Badiola et al., 2009; Vandenberghe et al., 2012). The local magnetostratigraphic study of the Nogueres conglomerate beds thus lacks solid geochronological moorings, with currently little more than a long-distance correlation with the marine beds of the Ainsa foredeep. Moreover, biozone MP 17a was very short-lived (~0.4 Ma) and unfortunately falls entirely within a single, normal magnetic chron (C17n). In contrast, the > 200-m-thick Nogueres fossil-bearing sequence, despite mostly displaying a reverse polarity signal, is reported as spanning three polarity inversions, with some erratic results at the top of the sequence. The main fossil-bearing sites (Sossis, Claverol, Roc de Santa), which all occur within the same lacustrine carbonate unit (30–35 m thick; López Martínez, 1998), nonetheless all appear to correlate with a well-defined normal polarity interval (Beamud et al., 2003, Fig. 3 therein).

The Nogueres conglomerates episode raises several questions in terms of orogen dynamics during the Paleogene. Firstly, the unconformable Nogueres clastic sequence has drowned a mountainous palaeolandscape in which continental erosion had produced a diverse gallery of high-amplitude structural landforms such as hogbacks, razorbacks and anticlinal or monoclinal valleys out of the folded Mesozoic cover sequence (Birot, 1937; Reille, 1971). Crustal deformation and differential erosion thus occurred simultaneously, but this first episode was followed, during and after Bartonian time (~37 Ma), by subsidence and burial. The subsidence migrated northward towards the orogen's axis, which is the reverse of what was happening at the same time in the Jaca–Tremp furrow (southward rollover of the depocentre). Clast provenance analysis of the Nogueres sequence indicates exclusive input from the local Mesozoic limestone outcrops near the base of the sequence, but with an increasingly high proportion of Hercynian basement lithologies towards the top. The source rocks, however, are fairly near-field outcrops belonging to the leading edge of the Nogueres basement nappe, and involve abundant Devonian limestone, Carboniferous sandstone, Silurian rocks, ophites, and Permo-Triassic sandstone and conglomerate. These features are equally true for the Pobla de Segur and Senterada outcrops. In the latter case, an increase in granite cobble frequency is only substantial in the uppermost beds, where metre-sized granite boulders associated with Devonian and Permo-Triassic boulders several metres in diameter suggest a proximal facies supplied by steep catchments on a steep mountain front (see Section 4.1.3.3 for links with the geomorphological evolution of this area). The granite outcrops geographically nearest to the Senterada sequence lie 12 to 15 km to the north of the current edge of the Axial Zone, where the highest summits today are made up of Paleozoic sedimentary rocks. It can be inferred from this evidence that the proximal facies of the upper Senterada sequence testifies to a topographic configuration of the Pyrenees in the late Paleogene very different from the Pyrenean mountain landscape of today — evidence already emphasized farther east in the Pedraforca–Ripoll area (late Priabonian beds of Catllaras–Serrat Negre). Vincent (2001) had reached a similar conclusion in the context of the Sierra de Sis. He noted, after Reille (1971), that the tourmaline-bearing petrographic fingerprint of certain granite clasts indicated a far-field provenance, potentially from outcrops in the massifs of Tramesaygues and Aiguestortes, which are situated in the upper valley of the Neste de Louron — i.e., 40 km to the NNW and 5 km to the north of the modern-day boundary between France and Spain (Reille, 1971; Michael et al., 2014). From

this we can infer that, during the late Paleogene, the Ancestral Pyrenean mountain range was even more asymmetrical than its modern successor, with a continental drainage divide situated just 20 km to the south of the North Pyrenean Fault, and perhaps even (based on clast provenance studies) within the North-Pyrenean Zone at locations farther west (Roigé et al., 2017).

3.2.5. Early to middle Miocene sedimentation

3.2.5.1. General chronostratigraphy of the Miocene clastic deposits

Like their Oligocene predecessors (Campodarbe Fm., etc.), the Neogene sediments of the Ebro Basin (Figs. 1, 5) were initially entirely contained within an enclosed, internally drained basin, and as a result are much thicker than in the Aquitaine Basin, which remained connected to the Atlantic Ocean. The five tectono-sedimentary units (TSU 4 to TSU 8) reported in Iberian literature reach a total thickness of ~1000 m, and TSU 4 straddles the Oligocene and the Miocene. Between the Alcanadre River and the summit of the Sierra d'Alcubierre, the series spans an age band from 23 to 13.5 Ma and is 636 m thick. Magnetostratigraphy and mammalian fossil sites have provided constraints on the fill-sequence chronology, with TSU 5 falling between 21.5 and ~16 Ma (MN 2, MN 3, MN 4), TSU 6 between ~16 and 14.4 Ma (MN 5), and TSU 7 between 14 and 12 Ma (top of MN 5, MN 6, MN 7–MN 8). The age of TSU 8, which is preserved only on the southern edge of the Ebro Basin, is uncertain (Pérez-Rivarés et al., 2002, 2004, 2018; Larrasoaña et al., 2006; Agustí et al., 2011; Vázquez-Urbez et al., 2016). The Neogene outcrops of the Iberian foreland are organised in concentric belts with, starting from the centre and moving north towards the mountains, gypsum-rich evaporites (Zaragoza Fm.), then lacustrine carbonates (Alcubierre Fm.), followed by distal fluvial systems (ochre mudstone with shoestring sandstone channel fills), and lastly a discontinuous belt of proximal syntectonic conglomerates. The latter two sequences have been named Uncastillo Formation in the NW, and Sariñena Formation in the NE (Quirantes and Riba, 1973; Arenas, 1993; Arenas and Pardo, 1999; Arenas et al., 2001; Luzón, 2005) (Fig. 5, E- and W-Aragón transects).

Clastic output from the Pyrenees during the Neogene was conveyed by two major river systems which were now perpendicular to the earlier Paleogene sediment routing systems

of the Campodarbe Formation: one with its mountain hinterland in the central Pyrenees (which produced the Huesca megafan/Sariñena Formation) and coaxial with the Cinca palaeostream; the other with its hinterland in the western Pyrenees (Luna megafan/Uncastillo Formation) and coaxial with the Gállego catchment (Hirst and Nichols, 1986; Jones, 2004; Nichols, 2005, 2018). These Ebro Basin megafans, with their apices situated along the front of the Sierras Exteriores, are associations of channel and overbank deposits tens of kilometres in radius. The Miocene outcrops do not extend eastward beyond the Cinca–Segre drainage divide. This interruption is most likely an erosional boundary, but whether a megafan the size of the Huesca fan ever existed to the east of the Segre River remains a matter of speculation. It is intriguing to note that the eastern limit of Neogene outcrops in the Ebro Basin occurs almost exactly at the same distance from the Mediterranean coastline (~100–120 km) as its counterpart in the Aquitaine Basin (Fig. 1) — thus reflecting perhaps a response to Mediterranean rifting farther east and to the ensuing regional uplift, which most likely resulted in displacing both the foreland and retro-foreland depocentres towards the west (Gaspar-Escribano et al., 2001).

Denudation of the Ebro Basin during the late Neogene, after its connection with the Mediterranean base level, has resulted in a preservation of the harder lithologies such as the central carbonate and peripheral conglomerate masses, but has stripped a large proportion of the softer marl outcrops that formed the distal alluvial facies of the depositional fan systems. Added to the relative scarcity of continental fossil remains among the Cenozoic rocks along the southern fringe of the pro-wedge, stratigraphic correlations between (i) distal and proximal alluvial deposits as well as between (ii) proximal deposits along the strike of the orogen have been difficult to establish and thus require caution. As a result, variations through time in the intensity of sediment delivery by the Ancestral Pyrenees remain difficult to reconstruct regionally, but an attempt is made below to unravel these issues based on a critical review of the literature.

3.2.5.2. Range-front conglomerate sequences south of the Sierras Exteriores

The thickness of Neogene mountain-front conglomerate sequences in the Ebro Basin is usually several hundreds of metres, but along the base of the western Sierras Exteriores, e.g., near Luesia, the Miocene accumulation is reported to attain a thickness of 1600 m

(Arenas et al., 2001). Its age has been difficult to establish directly, and mostly relies on far-field correlations with dated deposits lying at the centre of the Ebro Basin. The most significant fossil assemblage is from within the Sariñena Formation at Santa Cilia, and was obtained from a stratified fluvial sequence within the conglomerate beds situated at foot of the Sierra de Guara. The sequence has been tectonically deformed and rests unconformably on the Oligocene Peraltilla Formation. Taking account of dip angles, the fossil site seems to occur ca. 500 m above the unconformity, with an additional ~400 m thickness of the conglomerate sequence is stacked above it. The Santa Cilia age is earliest Aquitanian, biozone MN 1 (local zone X; Crusafont et al., 1966; Alvarez-Sierra et al., 1990; Cuenca et al., 1992). A second mammalian fossil site at Ayerbe has been deemed coeval with Santa Cilia because of its fossil mammalian contents, which are indicative of Aquitanian taxa at two separate locations (Crusafont and Pons, 1969). In a more distal position, the sites of San Juan and La Galocha were sampled over a vertical stratigraphic thickness of ~80 m. The base of San Juan is ascribed to biozone MN 2b, i.e., late Aquitanian or early Burdigalian (local zone Y2), whereas La Galocha 5, at the top of the section, corresponds to the base of MN 3, i.e., early to middle Burdigalian (zone Z; Alvarez-Sierra et al., 1990). The magnetostratigraphic research has produced results of increasing quality and accuracy through time. The earlier work (Hogan and Burbank, 1996), which focused on the Priabonian marine beds and on the Ayerbe fossil site, reports from Campodarbe four pulses of syntectonic conglomerates separated by synsedimentary unconformities. The first three pulses occurred between 29.5 and 24 Ma (i.e., Oligocene), with only the fourth established as Aquitanian. Focusing on existing sequences around Huesca, other workers (Arenas, 1993; Arenas et al., 2001; Oliva-Urcia et al., 2016) identified three stratigraphic units (named U1 to U3), in which U3 correlates with TSU 5 in the central part of the Ebro basin (21.5–16 Ma). These same authors have cast doubt on the significance of the Ayerbe assemblages, emphasizing instead the importance of erosion-related intraformational lacunae in the section studied by Hogan and Burbank (1996). The new magnetostratigraphic record at Luesia, which is reportedly more continuous, places the top of the Campodarbe Formation at 24.5 Ma. The age of the three youngest conglomerate sequences overlying the Campodarbe Fm. ranges between 24.5 and 22.5 Ma (equivalent to units U1 and U2), and the fourth conglomerate sequence belongs to U3. Oliva-Urcia et al. (2019) have since proposed alternative magnetostratigraphic correlations for U3, wich seems only the equivalent of the base of TSU 5. These authors now

place the top of U3-2, which contains the entire Riglos conglomerate sequence (i.e., the fourth sequence) in the Aquitanian, ca. 21 Ma. No age is currently provided for U3-3. A fifth, quite thick and isolated conglomerate sequence known as Peña del Sol also occurs near Ayerbe (NW of Huesca). Its outcrop rises to ~1300 m and rests unconformably on the Sierras Exteriores. Although reported in the literature (Alastrué et al., 1957), its age is currently unknown but possibly Burdigalian.

The Neogene chronostratigraphy is difficult to untwine because different authors have crafted different nomenclatures: Pérez-Rivarés et al. (2018), working on the Paleogene as well as the Neogene, have favoured the TSU idiom (which is calibrated on mammalian biozones and magnetostratigraphic criteria); but others (e.g., Arenas, 1993 and later), who focus chiefly on the Neogene and rely on the methods of sequence stratigraphy underpinned by magnetostratigraphy, have opted for the U (but also sometimes N) notation. It consists in subdividing the TSU units.

In summary, based on the best quality fossil-bearing sites (chiefly Santa Cilia and La Galocha 5), the Neogene conglomerate belt along the northern edge of the Ebro Basin south of the Sierras Exteriores contains debris supplied to it from the late Chattian to possibly the earliest Burdigalian. It cannot be ruled out that delivery by Pyrenean rivers of coarse gravel deposits continued into the middle Miocene given the occurrence, for example, of sandstone beds in TSU 7 at the centre of the Ebro Basin (i.e., in distal positions: San Caprasio, Sierra de Alcubierre). However, the great thickness (~500 m) of lacustrine limestone and evaporites in TSU 5 and TSU 6, which both appear to lap northward over the sandstone deposits of the Sariñena Formation (Pérez-Rivarés et al., 2002, 2018, see cross-sections therein), remains a robust indication that clastic output from the Pyrenean range had declined substantially after ~20 Ma. Further to the NW, the Bardenas Reales recorded a similar evolution, with a decline in clastic input from the Pyrenees (red sandstone and siltstone) giving way to lacustrine limestones near the boundary between TSU 5 and TSU 6, i.e., 16.1–16.05 Ma (Larena et al., 2020). A decline in tectonic activity is thus documented by the sedimentary petrology of the stratigraphic sequence from at least TSU 6 onwards, thereafter allowing a stronger expression of climatic signals in the region as recorded by fluctuations in palaeolake shoreline boundaries (Arenas, 1993; Larena et al., 2020). From this it can be inferred that topographic relief in the orogenic belt was becoming progressively more subdued during and after Burdigalian time.

The Neogene conglomerate belt along the northern border of the Ebro Basin is clearly of syntectonic origin. This interpretation is supported by the thickness of the sequences, their synsedimentary intraformational unconformities, and their geographical and structural links with the outer Pyrenean frontal thrusts (Puigdefábregas and Soler, 1973; Puigdefábregas, 1975; Hogan and Burbank, 1996; Arenas et al., 2001). The two earlier conglomerate pulses buried the Sierras Exteriores thrust front (e.g., west of the Gállego River: Ayerbe, Aguëro, San Felices areas). The Guarga thrust sheet was itself folded and sheared internally into finer thrust units, thereby giving rise, among the various structures, to the Santo Domingo anticline. This large, plunging anticline propagated westward at the time when the Uncastillo Formation was being deposited. In its eastern part, clastic pulses 4 and 5 (generating the conglomerate sequences observed at Riglos, and in the Linás palaeofan and the Peña del Sol) are only slightly folded in the vicinity of the thrust front (Nichols, 2018). As such, they record the last moments of tectonic deformation in the Sierras Exteriores (i.e., Aquitanian to early Burdigalian; Oliva-Urcia et al., 2019).

In terms of size and clast provenance, two classes of early Neogene alluvial fan coexisted in the Ebro foreland. Numerous small alluvial fans form aprons along the fronts of the Sierras Exteriores. They contain boulders up to 3 m in diameter and consist of weakly rounded limestone pebbles. These sequences typically bury steep structural scarps and landforms (Reille, 1971). Much larger fans, chiefly the Huesca and Luna megafans but also the Peña del Sol, contain debris from much more distant sources. Palaeochannel fills in the Luna megafan display an abundance of pebbles of Eocene brown sandstone (70–95%) alongside greyish-blue limestone (5–30%) and very rarely quartz, quartzite and chert (Arenas, 1993). These debris assemblages may in some cases originate directly from the Eocene flysch outcrops of the west-central Pyrenees, but most of the time they are reworked debris from the Jaca syncline and its Campodarbe Formation (see Section 3.2.2), which at the time was undergoing intense folding and incorporation into the outward-growing pro-wedge (Hirst and Nichols, 1986; Arenas et al., 2001).

The Huesca megafan contains biotite-rich arkose and sandstone suggestive of inputs from the Axial Zone (Hirst and Nichols, 1986), although proportions of these constituent lithologies are less than in the older Peraltilla Formation (Yuste et al., 2004). Provenance from the basement outcrops at places such as Alquezar and Bierge-Rodellar is nonetheless conspicuous, with an abundance of dark quartzite, quartz, Permo-Triassic conglomerate,

some schist and granitoid pebbles. In the Cinca River saddle, between the Sierra de Guara and Sierra de Montsec, the Miocene Graus Formation (sandstone and conglomerate) laps extensively onto the Sierras Exteriores and fills up the Peralta de la Sal and Benabarre sub-basins. The Graus Formation also laps northward unconformably onto the Eocene Escanilla and Capella sequences. Its conglomeratic proximal and molassic distal facies are identical to those of the palaeontologically-dated Miocene deposits west of the Cinca valley.

For the benefit of future investigations, it must be emphasized overall that geologists are undecided about where to locate the stratigraphic boundary between the Oligocene and Miocene conglomerate units east of the Cinca valley, i.e., along half the length of the mountain range. This is mostly ascribable to the scarcity of fossil-bearing sites. Depending on the publication date of the geological sheets, the gravel sequences covering the Paleogene fold structures (particularly the Graus Formation) are thus either labelled as Paleogene or Neogene. This also varies depending on whether focus is on Catalonia, where Paleogene conglomerate sequences are omnipresent, or on the west-central foreland zone around Huesca, where then Neogene age of the gravel beds is well constrained by their fossil content. For example in the Peralta Basin, a magnetostratigraphic sequence (Meigs, 1997) has revealed the existence of three syntectonic units, namely Priabonian–Rupelian, basal Chattian (Peraltilla Formation), and Upper Chattian. The latter unit appears to be an equivalent of the Sariñena–Graus units, which seal the youngest crustal-shortening-related fold structures and consist of clasts supplied by outcrops in the Axial Zone. It is likely that these unconformable conglomerate sequences have at times been bundled (or confused) with the unconformable Nogueres conglomerate units (described in Section 3.2.4.2), which, however, are of Paleogene age. Some authors have indeed suggested that the aggradation of the Nogueres sequence continued into the Miocene or at least the late Oligocene (Vincent and Elliott, 1996; Vincent, 2001; Jones, 2004), evidence for which is nonetheless debatable given the absence of direct, in situ biostratigraphic clues.

In conclusion, establishing the age of conglomerate sequences is essential to the interpretation of mountain ranges, but dating conglomerate beds remains difficult. The interpretation advocated by Oliva-Urcia et al. (2019) for the Jaca Basin and the Luna Fan is currently the most coherent at the scale of the western Pyrenees, and more consistent with the Ayerbe and Santa Cilia ELMA ages than some previous palaeomagnetic studies. The endemic tectonic deformation recorded in the Jaca Basin also explains the absence of coeval

conglomerate sequences of a similar nature to the Luna and Huesca fans in the Aquitaine Basin at those longitudes. On a more restricted scale, discrepancies between ages obtained for the fans of the Jaca Basin (San Juan de la Peña, and Oroel), which are early Neogene according to Roigé et al. (2019) on the basis of U–Pb and (U–Th)/He double dating, but 10 to 12 m.y. older than that according to magnetostratigraphic reconstructions (Garcés et al., 2020), will require further clarification.

3.2.6. Sharp regime change during the late Miocene

The youngest generations of Cenozoic sedimentary deposits in the Ebro Basin are tectonically disturbed (gentle undulations illustrated by Pérez-Rivarés et al., 2018, Fig. 4 therein) and imprecisely dated by palaeontological evidence. The most elevated palaeontological site of San Caprasio (812 m; Fig. 5, E-Aragón transect), which lies at the heart of the basin in the Sierra d'Alcubierre, had initially been dated to the Astaracian (i.e., Aragonian–Vallesian boundary, biozones MN 7–MN 8; Agustí et al., 1994). However, this biochronological age was established from just three micromammalian taxa, and later magnetostratigraphic investigations within the carbonate rocks of TSU 7 reassigned the site to chron C5AC; this corresponds to the base of MN 6, i.e., 13.8 Ma (Pérez-Rivarés et al., 2002). This revised age has been validated by palaeontologists (Agustí et al., 2011). The most recent fossil-bearing sites are located in the SW part of the Ebro Basin near Tarrazona, but they occur in the topmost sections of TSU 7 (Villena et al., 1992; Cuenca et al., 1992; Murelaga et al., 2008) such as at El Buste (MN 7–MN 8, ~12.6 Ma) and La Ciesma (MN 7–MN 8, ~12.1 Ma); the top of TSU 7 has not provided robust magnetostratigraphic constraints (Pérez-Rivarés et al., 2018; Fig. 7 therein). No fossil assemblages have been detected in TSU 8, which corresponds to the tilted lacustrine limestone plateau of Muela de Borja (804–724 m). In this area, the top of TSU 7 has been estimated as slightly younger than 12 Ma; accordingly, TSU 8, which is at most 60 m thick, should be younger still (Vasquez-Urbez et al., 2013). Early field geologists reported a site in that area known as Monteagudo 'vallesiense', which contained large mammalian fossils such as *Hipparion*, but it seems no archive has been kept of its precise location (mentioned in Cuenca et al., 1992).

Despite these lacunae in the Miocene chronostratigraphy (i.e., TSU 8), it can be inferred that the termination of internal drainage in the Ebro Basin occurred at some time after 12–11

Ma. Speculation over the exact timing of this major geodynamic change has nonetheless been intense, particularly in relation to the possible impact of the Messinian salinity crisis in reconnecting the Ebro Basin with the Mediterranean Sea (Coney et al., 1996). A late Cenozoic transition from internal to external drainage was actually a general feature across the Iberian Meseta, whether or not the rivers join up with the Mediterranean. Given that such was the case for the Tagus and the Duero, which connect to the Atlantic, there should thus be no reason for the short-lived Messinian base-level fall to have driven the process. Accordingly, some authors have ruled out the role of the Messinian sea-level fall and advocated instead a progressive rather than abrupt reconnection of the Ebro Basin, beginning only in the Pliocene. Babault et al. (2006) persuasively ruled out any major impact from the Messinian Salinity Crisis by showing that the Ebro Basin should in that case display a 300-km-long pre-Pliocene canyon, cut during the Messinian lowstand and similar to that of the Rhône River in France. This is clearly not the case.

A consensus has progressively emerged in favour of a much earlier reconnection of the Ebro to the Mediterranean rather than an abrupt, short-lived event triggered by the Messinian salinity crisis (review in Garcés et al., 2020). Inferences in favour of this scenario are provided by numerical models rather than by field constraints, but consistently generate a best estimate falling between 13 and 8.5 Ma (García-Castellanos et al., 2003) or between 12 and 7.5 Ma (García-Castellanos and Larrasoaña, 2015). This time window (late Serravalian–Tortonian) coincides with a strong influx of sediment into the Valencia Basin (Castellón Group) (Urgeles et al., 2011; Cameselle et al., 2014), and seems compatible with thermochronological data that have been produced for the Nogueres conglomerate beds, into which fluvial incision began ca. 9.5 Ma (Fillon and van der Beek, 2012; Fillon et al., 2013). Note that these studies postulate palaeoelevations of either ~1000 m (García-Castellanos et al., 2003; Babault et al., 2006) or 530–750 m (García-Castellanos and Larrasoaña, 2015) for the top of the Ebro Basin fill prior to marine base-level reconnection. In both cases these are substantial elevations above sea level, but they do not allow for the (highly likely) possibility that the Ebro Basin has itself undergone regional dynamic uplift in the last 12 m.y., with widespread evidence of elevation change and rock deformation (e.g., Soto et al., 2016; Pérez-Rivarés et al., 2018; Conway-Jones et al., 2019).

The onset of fluvial incision in the Ebro Basin coincided with (i) the major episode of incision also recorded in the Aquitaine Basin, i.e., the ravinement surface beneath the Vallesian (i.e.,

middle Tortonian) ‘Clay-with-pebbles’ formation previously presented (Fig. 5, Ariège and Béarn transects); and with (ii) the growth of the Lannemezan megafan. Such symmetry and synchroneity in the response of the two foreland basins to fluvial incision strongly suggests a regional episode of crustal uplift occurring not just in the Pyrenees but also more widely in Iberia and the Massif Central (Boschi et al., 2010) — much rather than a contingent event such as drainage piracy restricted to the Ebro River. A regional, sub-crustal driving process among those examined in Section 2.4 would be a good candidate for explaining this situation. The hypothesis of mantle-supported dynamic topography (Casas-Sainz and de Vicente, 2009; Gunnell et al., 2008, 2009; Boschi et al., 2010; Calvet et al., 2015a) contributing to re-energise not just the Pyrenean mountain belt during the Neogene and Quaternary period, but also the pro- and retro-foreland basins themselves, substantially alters the conventional view that the Pyrenees arose purely out of crustal thickening at the plate margins during the late Cretaceous and Paleogene, and that its topographic mass has stood in dynamic steady state for 25 million years (Curry et al., 2019). Instead, the Pyrenees is a transient orogen which has undergone a complex history of topographic uplift, decay, and resurgence. This alternative scenario for the modern Pyrenees as a youthful Neogene mountain range successor to an older Paleogene ancestor is also better suited to explaining the 25 million years of internal drainage of the Ebro Basin. The Catalan Ranges that close the Ebro Basin to the east are merely a few tens of kilometres wide, and they have additionally been extensively fragmented since the early Miocene by coast-oblique extensional grabens through which streams would have easily made inroads to keep the Ebro Basin connected to sea-level.

Contrary to the Aquitaine Basin, fluvial incision of the Ebro Basin after ~10 Ma was interrupted by only very few quiescent moments of alluvial aggradation and terrace formation, which explains why the Ebro Basin displays few late Neogene and Quaternary aggradational terraces compared to the Aquitaine Basin. The Ebro Basin likewise displays no analogues of the Lannemezan Formation and its multiple late Neogene megafans, which at one time buried considerable portions of the retro-wedge (see Section 3.1.5). This contrast is likely explained by regional dynamic (Conway-Jones et al., 2019), but also partly isostatic, uplift in excess of 800 m a.s.l. of the Ebro Basin itself during the last 10–12 m.y., following a different style and greater magnitude than the simple basinward tilt motion recorded in Aquitaine, where the piedmont grades much more progressively to its marine base level.

3.3. The sedimentary record of extensional basins in the eastern Pyrenees

The Gulf of Lion became established as a new marine base level for the Pyrenees towards the end of the Oligocene (Bache et al., 2010), i.e., at a time when the Ebro Basin was internally drained and the shores of the Aquitaine Basin lay far to the west. The first stages of crustal thinning occurred above sea level or in a very shallow sea. After ~23 Ma the entire system became rapidly submerged as a result of accelerated subsidence, resulting in today's hyperextended Gulf of Lion (Jolivet et al., 2020). The Mediterranean has controlled the geomorphological evolution of the eastern Pyrenees from Aquitanian time to the present in a context of increasing tectonic fragmentation of the Paleogene mountain range by Neogene extensional faulting.

3.3.1. Oligocene to Miocene basin fills: proxies of surface dynamics in the Ancestral Pyrenees

The extensional faulting has produced a population of half-grabens that strike NE–SW and NNE–SSW. The Oligocene basins onshore are relatively small, and their fill sequences were supplied by their eroding footwalls rather than by denudation occurring further afield in the Pyrenean hinterland. More information would be provided by the graben systems buried beneath the continental-shelf sediments, e.g., the Catalan, Cathare and Central grabens (the latter an extension of the onshore Roussillon Basin), but boreholes have until now barely reached those depths (Cravatte et al., 1974; Arthaud et al., 1981; Guennoc et al., 2000; Mauffret et al., 2001; Bache et al., 2010). The syn-rift sequence of these offshore basins contains conglomerate deposits made up of limestone and other Paleozoic clasts, anhydrite-rich red clay, and a cap of early Aquitanian marine limestone. The late Chattian marine beds have also been detected off- as well as onshore in western Provence, beneath the Aquitanian coastal parastratotype at Carry-le-Rouet (Oudet et al., 2010; Demory et al., 2011). The Catalan divergent margin and the Valencia Trough share a tectonic and sedimentary history similar to that of the Gulf of Lion. Extension in the south has even inverted some Oligocene piggyback basins that were previously linked to convergent tectonics in the Catalan Ranges (Roca, 1996; Roca et al., 1999).

The Aquitanian sea-level rise approaching from the east did not initially reach past the longitude of Montpellier. The Narbonne–Sigean Basin at that time was receiving slope breccia, small matrix-supported (red clay) debris fans, well-rounded alluvial gravels comprising quartzite from as far away as the Mouthoumet Massif, but mostly shale and quite thick, white lacustrine limestone deposits — all suggesting low-energy topography in the Corbières hinterland (Calvet, 1996). The total thickness of the Narbonne fill sequence is ~1 km, and consists of two units (Aguilar, 1977; Aguilar and Michaux, 1977): the first is Oligocene (MP 28, ~26 Ma), and the other starts during the late Oligocene (MP 30, ~24 Ma) but consists mostly of an Aquitanian biozone (two MN 1 micromammalian assemblages among the lower beds). Aquitanian gypsum deposits are indicative of a paralic environment (Rosset, 1964), and thus of proximity to a coastline. Farther west on the mainland, the Tuchan–Paziols Basin only contains fluvial sequences (thickness: ~500 m) comprising quartzite-bearing basal conglomerate (Mouthoumet provenance), followed by a thick sequence of marl and pebbles of local limestone containing in its uppermost levels a late Oligocene faunal assemblage (perhaps MP 28; Calvet et al., 1991). To the south of the Ancestral Pyrenees, the small Campins Basin, in the Vallès, contains 700 m of clay, lignite, lacustrine limestone, arkose, and locally-sourced conglomerate containing basement clasts. The fossil faunal assemblages of Campins and Can Quarante both belong to biozone MP 25 (~29 Ma) (Anadon and Villalta, 1975; Anadón, 1986; Aguilar et al., 1997).

As most classic ‘steer’s head’ rift basins, these Oligocene to Aquitanian basins were eventually flooded and overtopped by a more widespread marine transgression. This occurred during the Miocene, promoting the deposition of a relatively thin mudstone and sandstone sequence (i.e., molasse) which rests unconformably over the tectonically deformed earlier sequences of, for example, the Narbonne–Sigean Basin. This Miocene sequence progressed landward onto the folded Mesozoic cover rocks of the Corbières and La Clape, and likewise farther east in Languedoc. The facies are characteristically littoral, but ages are poorly constrained. Bivalve fossils suggest Burdigalian (*Pecten tournali*) and Langhian to Serravallian ages (*Ostrea crassissima*); foraminifera have suggested biozone N 8, i.e., Langhian (Magné, 1978). Fossil rodent assemblages in the coastal facies deposits have yielded the most precise age brackets so far (Aguilar, 1979, 1980, 1981, 1982; see also revised biozones and updated tables in Aguilar et al., 2010 and Gunnell et al., 2009). Among these, Port-la-Nouvelle is a littoral karstic cavity in the Cretaceous limestone, buried by the

molasse and also containing foraminifera and shark-like teeth. The corresponding biozone age (MN 4) captures the late Burdigalian sea-level rise (~16.4–17.2 Ma). Within the molasse, the assemblages of Luc-sur-Orbieu and 'Leucate butte 1' have yielded ages of ~13.4–14.2 Ma (MN 6), i.e., Langhian. Puisserguier (lower portion of biozones MN 7–MN 8), and La Grenatière (upper portion of biozones MN 7–MN 8) denote a Serravallian age (~11.2–13.4 Ma). La Grenatière is situated in the uppermost levels of the marine component of the sequence, but aggradation continued uninterrupted in the form of some additional 100 m of shale and lacustrine limestone, which contain near the top the flagship biostratigraphic site of Montredon. This Vallesian site contains an extremely rich assortment of smaller and larger mammalian remains — including *Hipparion* — and has been placed within MN 10 (i.e., 8.9–9.9 Ma) (Aguilar et al., 1982; Michaux et al., 1988). These fine-textured lacustrine and palustrine deposits, totally devoid of coarser gravel clasts and situated at the landward tip of the Miocene gulf of Narbonne (today quite close to the mouth of the Aude River), again document a low-energy Pyrenean hinterland at this longitude.

During the middle Miocene transgression, extensional fault activity slackened but did not cease. In the Lapalme Basin, for example, Miocene coastal beds containing mollusc-bored pebbles clearly show evidence of synsedimentary deformation in the immediate vicinity of the boundary fault planes (Calvet, 1996). The twin Thézan and Fabrezan basins record the most westerly ingress of the sea during the middle Miocene, but they also contain nonmarine marl interspersed with gravel-filled palaeochannels of uncertain stratigraphic age —probably early Miocene, and perhaps coeval with their laterally continuous marine beds (Ellenberger et al., 1987).

At the more southerly latitude of the Axial Zone, but also further south in the Catalan Ranges, the extensional faults were active until the middle Miocene. The Roussillon Basin, and its westerly extension the Conflent Basin (for a synthesis: Calvet, 1996; Calvet and Gunnell, 2008), show this very clearly. The floor of the Roussillon Basin is plausibly floored by Oligocene deposits, but no outcrops exist. The only indirect indication of this possibility is provided by apatite fission-track cooling ages of 25–27 Ma (and zircon ages of 30 Ma) obtained from potential source rocks in the adjacent Canigou massif (Maurel et al., 2008). The Roussillon fill sequence is 2 km thick. Its lowest documented stratigraphic units are early Burdigalian (base of MN 3, ~19–19.5 Ma obtained in the Conflent Basin at the biostratigraphic site of Espira: Baudelot and Crouzel, 1974; Aguilar et al., 2003, Fig. 11

2407 therein). Its marine uppermost unit is Langhian (N 8–N 9, i.e., ~15 Ma, obtained from the
2408 Elne and Canet boreholes; Gottis, 1958; Clauzon and Cravatte, 1985; Berger et al., 1989). The
2409 marine molasse deposits are relatively thin (~200 m at Canet); they overlie some much
2410 thicker, variegated grey and reddish fluvial sand and clay deposits with lacustrine limestone
2411 at the base. This entire sequence becomes substantially coarser-textured along the SW
2412 border of the Roussillon and in the Conflent Basin, which in this proximal setting displays
2413 rounded boulders up to several metres in diameter.
2414 Such sedimentological features in the Roussillon–Conflent area clearly testify to a high-
2415 energy mountain environment with steep slope systems, ascribable to a period of rifting-
2416 related crustal uplift in the Axial Zone. This has been confirmed by apatite (U–Th)/He and
2417 fission-track rock-cooling ages (17–22 Ma) in the Canigou massif (Maurel et al., 2008), which
2418 record a continuation of the denudation that had already begun during the Oligocene. Clast
2419 provenance analysis of the fill sequence also documents — in inverse order — the successive
2420 stages of denudation of the stratified Canigou–Roc de France–Albères metamorphic dome,
2421 which at this time began to shed debris from the Canigou–Roc de France augengneiss
2422 envelope and from the Albères migmatites. The very coarse-textured sequences disappear
2423 beneath the outcrops of Langhian molasse and are correlated offshore with the thick
2424 Aquitanian and Burdigalian sequences documented from borehole evidence (Cravatte et al.,
2425 1974). Onshore, incision and denudation in the eastern reaches of the Roussillon Basin have
2426 stripped the top of the Neogene sequence down to its Langhian levels in response to the
2427 abrupt Messinian sea-level fall. Offshore, however, boreholes and seismic profiles reveal
2428 that thick Tortonian beds have been preserved on the continental shelf (almost 700 m of
2429 paralic and coastal facies documented by the Tramontane borehole), inclusive of early
2430 Messinian deposits emplaced prior to the salinity crisis.
2431 In Catalonia, the inner graben of the Vallés-Penedés Basin contains a sequence almost
2432 identical to that of the Roussillon (Magné, 1978; Agustí et al., 1990; Cabrera and Calvet,
2433 1996), with the difference that the Tortonian marine transgression in this area has long been
2434 recognised onshore in the coastal zone, e.g., at Barcelona, where rocks from at least the
2435 bottom half of this Stage has been reported (Magné, 1978).
2436
2437 ***3.3.2. Miocene to Pliocene basin fills: proxies of surface dynamics in the Modern Pyrenees***
2438

A second stage of active rifting began during the late Miocene, simultaneously reactivating the older grabens near the coast but also opening entirely new intermontane grabens far into the west of the Axial Zone. Another novelty was the onset of protracted episodes of intraplate volcanism. Although eruptions did not occur in the mountain range itself, a trail of volcanic outcrops occurs from the Massif Central to the Languedoc coastline (Gillot, 1974), with a possible continuation on the continental shelf. The youngest alignment of volcanoes, from the Escandorgue to the coastal town of Agde, ranges from 2 to 0.5 Ma (Dautria et al., 2010). It is inferred to have been generated by lithospheric sources. Traces of volcanic activity reappear in the Iberian part of the Pyrenean crustal wedge, in the Selva and Empordà basins. Age data reach back to at least ~10 Ma and extend to the late Pleistocene (Donville, 1973a, b, c, d; Araña et al., 1983; López Ruiz and Rodríguez Badiola, 1985; Martí et al., 1992; Martí, 2004). The origin of this volcanic activity has been debated: it could be ascribed to partial melting of mantle rocks sourced at 50–60 km depths beneath the Valencia Trough (Martí et al., 1992); to lithospheric thinning beneath the Mediterranean margin of Iberia (Vergés and Fernàndez, 2006); to heating of the base of the crust as a result of lithospheric mantle delamination beneath the Pyrenees (Vanderhaeghe and Grabkowiak, 2014; Chevrot et al., 2018; Dufréchou et al., 2018); to a southward deflection of the Massif Central 'finger' of rising hot asthenosphere (Barruol and Granet, 2002; Barruol et al., 2004; Gunnell et al., 2008); or even to an endemic 'hot finger' of asthenospheric mantle similar to others detected beneath continental Europe and the Mediterranean (Lustrino and Wilson, 2007; Jolivet et al., 2020).

Whereas, in Languedoc, Pliocene marine and continental sedimentation occupies drowned valleys that were cut at the time of the Messinian salinity crisis (Ambert, 1994; Clauzon et al., 1990), in Roussillon the Pliocene depocentre overlies its Miocene predecessor and the ravinement surface between the two sequences is largely concealed. The Pliocene sequence attains a thickness of 800 m at Canet (Clauzon and Cravatte, 1985; Clauzon et al., 1987; Duvail et al., 2000). The proximal facies consist of thick debris cones containing metre-sized boulders at the mouths of the Têt and Tech rivers, and likewise at the base of the south-facing Albères mountain front (Calvet, 1986, 1996; Calvet et al., 2015b; Donzeau-Wiazemski et al., 2010–2015: map and handbook). On the continental shelf, the Pliocene sequence consists of a series of prograding units topped by a distinctly more aggradational Gelasian to Pleistocene depositional wedge. This change of regime indicates a resumption of active

tectonic subsidence of the margin after 2.6 Ma, thus increasing the accommodation space and permitting the aggradation (Lofi et al., 2003, 2005; Duvail et al., 2005). Each depositional sequence is roughly 1 km thick, but it remains difficult to distinguish the Pyrenean inputs from those from the Cévennes and from the Alps via the Rhône.

In the Vallés Basin (Agustí et al., 1990; Cabrera and Calvet, 1996), the marine Langhian beds transition laterally to, but are also apparently conformably overlain by, a 1500 m-thick continental series of clastic beds rich in micromammalian assemblages. This series is very coarse-textured along the NW faulted boundary, and it filled the graben continuously during the late Miocene. The stratigraphy contains the eponymous continental stratotype known as the Vallesian (27 localities yielding assemblages ascribable to biozones MN 9 and MN 10) and ascends into the Turolian (only one locality, Piera: MN 11) (Villalta and Crusafont, 1943; Agustí et al., 1997; Casanovas-Villar et al., 2014). However, the drowned Llobregat valley, which contains a marine and continental Pliocene fill sequence, strikes orthogonally across the graben in a configuration similar to the pattern observed along the Languedoc coastal belt and in the lower reaches of the Ebro River in the Tortosa Basin. The continental shelf hosts a vast clastic sedimentary body known as the Pliocene and Quaternary Ebro Group, which rests disconformably on the older Castellon Group as a result of Messinian incision (Martínez del Olmo, 1996; Cameselle et al., 2014).

New grabens formed along the Mediterranean seaboard in the transitional area between the Pyrenees and the Catalan Ranges, and they occur precisely in the main area that was impacted by late Neogene volcanism. These basins are the Empordà and the Selva grabens. Their boundary faults strike NW–SE, which is identical to the strike of the North Balearic Transfer Zone that controlled the opening of the western Mediterranean back-arc basin and separated it from the Valencia Basin. The Empordà Basin contains a number of internal compartments and secondary depocentres. It has been a receptacle for a series of highly contrasting clastic sequences (synthesis in Calvet, 1996; Saula et al., 1994). At the centre of the basin, around Figueres, a deep borehole has struck a Tortonian sequence comprising marine strata at its base, followed by paralic and coastal facies rocks at depths of 1000 m below the surface. These contain interlayered lava flows (Fleta et al., 1994). In the southern part of the Empordà Basin, the Vallesian (MN 9 at La Bisbal) is exclusively of detrital origin and grades westward to coarse-textured Turolian fluvial units (MN 11 to MN 13, i.e., ~8.9–5.3 Ma, at Olivas, Camallera and Bascara; Crusafont, 1961; Gibert et al., 1979, 1980; Agustí

et al., 1990). The Turolian sequence is at least 350 m thick, and its content of limestone and sandstone pebbles records the denudation of the outer Pyrenean folds of La Garrotxa and of footwall blocks of the extensional Transverse Ranges (Saula et al., 1994). The sequence also contains a siliciclastic contribution from the southern basement outcrops, likely conveyed by an ancestral Ter River. The Pliocene sequence of Empordà is thinner than in the Roussillon Basin and is exclusively of Zanclean age. The Pliocene marine wedge occupies the position of a drowned valley on the Fluvia River, but nothing similar has been observed in the case of the Ter. The Pliocene continental wedge is quite extensive in the northern part of the Empordà Basin, where it was supplied with debris from the Axial Zone as well as from the outer Pyrenean fold belt.

The Selva Basin is vast but its fill rather shallow (maximum 300 m; Pous et al., 1990), and contains late Miocene and Pliocene continental deposits (arkose, palustrine shale, and gravel fans along the western border of the basin). The stratigraphic architecture of these two sequences is poorly known, but their entire depositional history was punctuated by volcanic eruptions, for example at 7.7 and 5.1 Ma (Donville, 1973d, 1976). Pliocene mollusc assemblages are reported (Marcet Riba and Solé Sabaris, 1949; Marcet Riba, 1956), as well as some Miocene mammalian remains (Villalta and Palli, 1973). The lacustrine sediments contained in a maar near Caldes de Malavella (SE edge of the basin) contain a diverse assemblage of late Pliocene vertebrate fauna (MN 16–MN 17; Gomez de Soler et al., 2012).

Simultaneously to the formation of the Empordà and Selva basins, other basins resulting from wrench-fault tectonics were breaking up the Axial Zone and forming as far as 200 km to the west of the Mediterranean shores. Among these, the Cerdagne and Seu d'Urgell half-grabens are aligned along a NE–SW tectonic lineament known as the Têt Fault. They contain up to 1 km of clastic fill, partly as coarse-textured alluvial fans and partly as fluvial and lacustrine beds (Chevalier, 1909; Pous et al., 1986; Cabrera et al., 1988; Roca, 1996). Biochronological constraints on the stratigraphy have been obtained from a large number of Vallesian mammalian assemblages (MN 9–MN 10)(Golpe Posse, 1981; Agustí et al., 1981; Agustí and Roca, 1987), with a Turolian age (MN 13: ~6.7–6 Ma) for the uppermost levels (Agustí et al., 2006). No Pliocene sequence has been detected. The clastic facies indicate growing relief in the surrounding basement-cored uplands, particularly in Turolian time when thick alluvial-fan deposits containing huge boulders suggest tectonic activity along the southern master fault of the Cerdagne Basin (Calvet, 1996; Calvet and Gunnell, 2008). The

presence of warmth-loving plant remains in the sediment record (Menendez-Amor, 1955; Suc and Fauquette, 2012) and $\delta^{18}O$ measurements on fossil mammalian teeth (Huyghe et al., 2020) document a regional uplift of not just the mountain footwalls but also of the basins themselves since Messinian time. Estimated uplift of the Cerdagne Basin over the last 10 m.y. is ~900 m (other estimates suggest this may have even been achieved just in the last 6.5 Ma: Suc and Fauquette, 2012, Fig. 8 therein), or ~500 m over the last 6.5 Ma according to the $\delta^{18}O$ constraints. Unlike the Cerdagne and Seu d'Urgell basins, the Capcir Basin strikes N–S and is unique in that respect. It could be even younger than the other two, perhaps having formed in response to a new regional stress regime (N–S compression and E–W extension), but unfortunately its clastic fill has until now never been dated.

Still further to the west, in the Val d'Aran, the Pruëdo Basin was noted by de Sitter (1954) and interpreted as a valley fill sequence of late Miocene age based on its pollen content. It was later mistaken for a Quaternary ice-marginal or interglacial aggradational deposit, but has more recently been dated as Vallesian based on a revision of its botanical remains (Ortuño et al., 2013). Its bounding master fault is the E–W Maladeta Fault. The Pruëdo Basin has been substantially disfigured by denudation and by Pliocene to Quaternary valley incision so that only very small, dispersed vestiges remain to be pieced together. It cannot be ruled out that other hard-to-find, late Neogene tectonic basins may exist in the Pyrenees. Possible candidates could be the topographic basin of Ossès in the Basque Country, which is aligned on a SW–NE fault (Viers, 1960); and likewise some small grabens across the Arres d'Anie, reported as neotectonic by Viers (1960) and Hervouët (1997). Extending the effects of Mediterranean rift and wrench tectonics to such westerly locations clearly calls for extreme caution, as they could more likely result from endemic gravitational forces being exerted on the west-Pyrenean crust since the relaxation of the compressive regime that endured until at least the middle Miocene, or from outer-arch extension in the crest of the Axial Zone antiform in the Anie–Larra context (e.g., Arlas graben).

4. A view from the mountains: tracking relief evolution from landform assemblages and the rock cooling record

The broad sketch of Pyrenean palaeogeography viewed from the basins gains further detail and finer resolution from (i) documentation by thermochronological methods of rock-cooling patterns within the mountains and valleys of the modern range; and (ii) the geomorphological information encoded in various suites of mountain and piedmont landforms.

Orogens in numerical models have been described as dynamic systems that tend towards equilibrium. This state of equilibrium of the critical taper thus formed is expressed by a topographic steady state, in which the creation of topography by crustal thickening is balanced by its destruction by surface denudation (e.g., Willett and Brandon, 2002). Once the upward- and outward-growing orogen has attained the steady state, the orogen is said to be mature. In order to test this model, we should be able to distinguish the successive growth and steady-state phases in the geological record. In the case of the Ancestral Pyrenees, however, the record so far has revealed a permanent state of transience, in which rates of crustal deformation and crustal denudation during the Paleogene were neither steady through time at any given location nor spatially uniform. Signs of the orogen ever having attained a recognizable state of maturity are difficult to pin down (see also Rahl et al., 2011; Whitchurch et al., 2011; Parsons et al., 2012; Ford et al., 2016).

Given these persistent signatures of transience in the sediment record, it is reasonable to expect that a record of unsteady or transient landscape evolution (Allen, 2008) should also be encoded in landform assemblages within the mountain range, whether in the Axial Zone or the outer fold belts. It is thus expected that slope systems, interfluve summits, and perhaps valleys at times responded in characteristic ways to relative respites in the history of crustal deformation, and/or were at certain places buffered from base-level changes. A rapid overview of the mountain landscape would tend to confirm this working hypothesis, with its (i) mosaic of mountain-top, low-gradient surfaces of varying sizes and states of conservation, always in abrupt juxtaposition with (ii) a population of younger incisional landforms, themselves displaying evidence of successive stages of downcutting and drainage reorganisation such as dry valleys, wind gaps, mountain-flank pediments and rock benches, and all situated above (iii) the usual staircases of Quaternary alluvial terraces, fans and debris cones. In Section 4 we focus on the suites of older, pre-Quaternary erosional landforms, and address the Quaternary landforms in Section 5.

4.1. Diagnostic landforms: the Pyrenean erosion surfaces

An intriguing collection of elevated, low-gradient land surfaces populates a number of summit areas of the Pyrenees, whether in the elevated Axial Zone or the outer tectonic belts, and whether the massifs have undergone glaciation or not (Fig. 6). Most are invisible to road travellers, but hillwalking geomorphologists have been reporting them from various parts of the mountain range for over 100 years (de Martonne, 1910; Blanchard, 1914; Sorre, 1913; Nussbaum, 1930, 1931; Boissevain, 1934; Pannekoek, 1935; Birot, 1937; Goron, 1941a; Sermet, 1950; De Sitter, 1952; Zandvliet, 1960; Calvet, 1996). The presence of such low-energy geomorphological archives in a high-energy mountain landscape has never been fully explained, but generates at least five threads of inquiry:

- the spatial distribution of these low-gradient surfaces (are they ubiquitous or confined to certain areas? do they occur at uniform altitudes?);
- the age of the erosion surfaces with respect to the Proto-, Ancestral and Modern Pyrenees, respectively;
- the relative ages of the different surfaces (i.e., is there just one generation, which perhaps underwent subsequent tectonic offsets? or are there several distinguishable generations?);
- the geodynamic conditions (pre-, syn-, or post-shortening evolution of the orogenic belt) under which the low-energy topographic end-state that they document could be attained;
- the elevation at which the erosion surfaces were formed: did the Ancestral Pyrenees undergo some widespread form of summit levelling at high altitude (i.e., 'altiplanation')? Or did the transition from the synorogenic Ancestral to the postorogenic Modern Pyrenees involve some form of transient peneplanation prior to regional uplift and deep re-incision by rivers and glaciers?

4.1.1. Mapping low-gradient montane surfaces: a note of caution

Low-gradient summit surfaces require authentication by systematic field observation, particularly to make sure that the flat topography is erosional (e.g., truncates upturned

geological strata, faults or rock fabrics) rather than depositional or structural. Given also that very small relics (0.1 to 1 km²), which may evade detection by digital elevation models, may provide crucial clues, field inspection is invaluable (Fig. 6).

A number of DEM- and GIS-based automated mapping exercises have been attempted for various segments of the mountain range on the basis of user-defined topographic criteria. No single method is entirely unequivocal, thereby emphasizing the difficulty of producing a complete, unbiased database. For example, early work by Babault et al. (2005b) used a DEM with a ground resolution of 90 m, and inferred erosion surfaces from a comparison between local relief as defined within a 5 km moving window and mean relief as defined within a 30 km window. The algorithm resulted in extracting a population of land surfaces displaying slope angles ≤ 11° and local relief ≤ 750 ± 250 m, but this ended up including many of the Quaternary glacial cirque floors of the Axial Zone. Using the same DEM data source, Calvet and Gunnell (2008) produced instead a slope map. Retaining a mask with slope-angle values ≤ 8°, the authors then proceeded to manually eliminate all Quaternary landforms and structural and depositional surfaces based on independent knowledge. Bosch et al. (2016a) elaborated a strategy for eliminating glacial landforms by using a 25x25 m resolution DEM, and by retaining land surfaces that simultaneously obeyed a set of rules such as local relief ≤ 300 m and slope angle ≤ 20°. The claimed (and somewhat surprising) size detection threshold was 500 m². The resulting regional map is paradoxical in that it turns out to be very accurate in the light of independent field knowledge, but somehow misses the well documented population of erosion surfaces situated in the Sub-Pyrenean fold belts, as well as most surfaces that occur below 1000 m generally. Automatically excluding glacial landforms also runs the risk of under-representing the population of erosion surfaces because glaciers in the Pyrenees have often just barely retouched some of these erosional land surfaces, for example in the case of anomalously wide glacial cirque floors in granite outcrops of the eastern Pyrenees (Delmas et al., 2014, 2015; Crest et al., 2017). More recently still, Ortuño and Viaplana-Muzas (2018) used a 0.5x0.5 km moving window on a 60 m ground-resolution DEM to produce a mask of land surfaces where slope angles were ≤ 20° and local relief ≤ 350 m, while also using independent knowledge as a control. Unlike previous outputs, the resulting map reveals a population of surfaces among the outermost Pyrenean fold belts, but occurrences at elevations below 1100 m remained undetected. In

summary, despite the useful reconnaissance work achieved by these desktop methods, field inspection remains an essential tool in the chain of evidence.

4.1.2. Geographical distribution of the erosion surfaces

4.1.2.1. Principal occurrences (Axial Zone and adjacent structures)

The spatial pattern and morphology of erosion surfaces is well established in the east of the Modern Pyrenees (Fig. 7), where the total surface area of orogenic wedge concerned by the gentle topography is ~15% (Calvet, 1996; Calvet and Gunnell, 2008). Two distinct generations can be mapped in some massifs (e.g., eastern Corbières, Carlit), and this bimodal feature is extendable to southern Andorra, the Aston and the Madrès. The upper, mountain-top surface (noted S_0 in Calvet, 1996, and relabelled S in Calvet and Gunnell, 2008 and in subsequent publications) initially was either an undulating peneplain or a true pediplain: there are no discriminating criteria other than the occasional presence of monadnocks such as the Pic Carlit itself (2921 m), rising like an inselberg above an almost perfectly smooth erosional platform (Fig. 7E, F). These residual summit surfaces have been embayed at lower elevations by a population of mountain-flank surfaces, or pediments, some of which are quite extensive (noted S1 in Calvet, 1996; but P1 in Calvet and Gunnell, 2008 and publications thereafter). The elevation difference between S and P1 is typically 300 to 500 m, regardless of whether they occur in the limestone thrust-and-fold belt of the eastern Corbières, or the plutonic Carlit or gneissic Aston massifs of the Axial Zone (Fig. 7E, F, G). In any given massif, S is always in a ridge-top position — whether at 600–900 m in the Corbières or at 2400 m in the Madrès, ~2800 m in the Carlit massif, and likewise around Andorra (Hartevelt, 1970).

These widespread relics of low-gradient, low-energy topography are the legacy of some advanced state of orogenic downwearing of the Ancestral Pyrenees in at least the eastern third of the modern mountain range. Surface P1 occurs ca. 100–200 m a.s.l. at the Mediterranean seaboard, for example cross-cutting fold structures of the eastern Corbières orocline (Fig. 7A), of the Figueres-Montgri thrust sheet, and likewise basement structures in the Albères. From the Mediterranean seaboard, the elevation of P1 rises rapidly westward to 400–600 m (Fig. 7D). Around the Madrès massif, low-gradient plateaus of P1 affinity occur

between 1300 and 2000 m. Around the Carlit massif, a very extensive occurrence of P1 (Plateau des Lacs) slopes from 2400 to 1600 m to the Cerdagne graben (Fig. 7E). In the Aston massif, P1 rises from 1400 to 2200 m (Fig. 7H) (see also Monod et al., 2016). The Canigou–Carançà–Puigmal horst appears to be the only massif of the eastern Pyrenees where P1 is not paired with a residual of S at some altitude above it. Here, P1 on the western flank of the Puigmal slopes gently westward from 2600 to 1800 m (Calvet, 1996); a more elevated, S-generation surface was either never completed or was destroyed by subsequent denudation — in either case because the Canigou–Puigmal was tectonically one of the most active massifs of the eastern Pyrenees during the late Oligocene and early Miocene (Calvet and Gunnell, 2008).

West of Andorra and as far as the Pic du Balaïtous, the Axial Zone lacks detectable remains of a summit surface. Early observers had reached the same conclusion (Birot, 1952), apart from the illusion of a possible *Gipfelflur* underpinned by the occasional blunt ridge top, or the few hectares of a steeply inclined topographic ramp here or there (e.g., the top of Montcalm: 3080 m, 3 ha; the Pic de Fonguera, on the eastern boundary of the Encantats massif: 2883–2764 m, 20 ha; Martí Bono and Puigdefábregas, 1968). In contrast to these tenuous vestiges of S, some lower surfaces corresponding to P1 are relatively widespread in the surroundings of the higher massifs. The most striking examples occur between the Noguera de Vallferrera and Noguera de Cardós rivers (Zandvliet, 1960), with the Plaus de Boldís (150 ha, rising from 2450 to 2591 m) and the flat ridgetop of Roca Cigalera (35 ha, 2542–2667 m). From the vantage point of these erosion surfaces, the Pica d'Estats–Montcalm (summit elevation: 3152 m) stand as large residual massif of the ancestral Pyrenees, perhaps never eroded for reasons of positional remoteness within the watershed systems rather than of intrinsic rock hardness. Zandvliet (1960) mapped at least two generations of paleoplains in that area, at 2600–2400 m and 2300–1800 m — the latter highly undulating. Similar low-gradient land surfaces of P1 affinity occur around 2000–2200 m in the Val d'Aran, below the Encantats massif (Montanha de Porera, Pruëdo, Roquetes Blanques) (de Sitter, 1954; Kleinsmiede, 1960; Ortuño et al., 2008, 2013, 2018); and likewise between the Pique and Neste rivers in the Oueil massif, where flat-topped interfluve strips (2000–1800 m) extend out from the residual summit of Mt. Né (2147 m). West of the Neste River, similar interfluve strips occur around 2000 m and form a pattern of low-gradient chutes extending straight out of the vast, flat-floored granite cirques that ornate the

northern front of the Néouvielle massif around 2200 m a.s.l. Barrère (1952) had previously emphasized the anomalously wide floors of these cirques and speculated that these prima facie glacial landforms were really preglacial etchbasins in the granite. Along the southern edge of the Axial Zone, a few conspicuous mountain-top surfaces occur between 2200 and 2500 m to the south of the Aneto massif (Tuca Royero, 2548 m, 41 ha) and between the Cinca and Cinqueta rivers (e.g., the Tozal d'Escubillons: 2427 m, 20 ha).

A gap appears to exist between the localities mentioned above and the westernmost Pyrenees of the Basque Country, where summit surfaces reappear (Viers, 1960). These summit surfaces belong to generation P1 rather than S because of the masses of residual relief that rise above them at many places. The land surfaces cut across folded Cretaceous limestones of the Axial Zone cover sequence, such as where the Lakora nappe (Devonian and Silurian rocks) overrides the Arres d'Anie (Fig. 8I). The Larra–Arres d'Anie is a vast karstic plateau sloping westward (2150–1600 m) away from the residual pyramidal peaks of Anie (2504 m), Soum Couy (2315 m), and Arlas (2044 m) (e.g., Uzel et al., 2020). At elevations below the upstanding residual Pic d'Orhy (2017 m), these erosion surfaces continue westward as the Pelluségagne (1600 m) and Okabe (1466 m) plateaus, which truncate the Devonian rocks of the Iraty massif as well as its folded Cretaceous and Eocene cover sequence further south (Fig. 8H). Lastly, all the ridge tops of the Pays des Nives are flat around 1400–1200 m, cutting across the Hercynian basement of the Aludes massif as well as across its envelope of overthrust cover rocks.

4.1.2.2. Occurrences in the outer fold-and-thrust belts

The previously mentioned erosion surfaces of the Corbières continue along much of the North- and Sub-Pyrenean zones. The S/P1 pair is mappable as far west as the Pays de Sault. Where it occurs on massive Jurassic and Lower Cretaceous limestone, surface S forms elevated plateaus which typically rise towards the SW and exhibit a rich gallery of mesoscale exo- and endokarstic features: Roc Paradet (900 m) (Fig. 7C), Fanges (1000 m), Bac d'Estable (1450 m), Forêt de la Serre (1330 m), etc. Erosional corridors ascribable to P1 present themselves more as wind gaps and dry valleys between these massifs, i.e., more as fluvial straths than as pediments. They are usually lined with quartz gravel trains and associated with horizontal endokarstric galleries and conduits, which are sometimes filled with deeply

weathered allochtonous gravels supplied by the Axial Zone (e.g., Clat cave, in the Clat palaeovalley, 1130 m). From here westwards, however, any clear distinction between S and P1 becomes impossible. The only evidence is a generally bevelled appearance of massif summits, but at an apparently random range of mean elevations suggesting either the existence of several generations of surfaces, or differentiated magnitudes of neotectonic movements responsible for offsetting a single original surface (see Goron, 1931, 1937, 1941a for a descriptive inventory; chronological interpretations therein, however, are obsolete). Mountain-flank erosional benches are also noted in some basement massifs such as the Tabe, Arize (Le Planel, 1067 m; Plaine d'Uscla, 1274), and Bouirex. They are nonetheless best preserved on massive limestone such as, from east to west: La Frau (1650 m, which contains a very ancient network of horizontal endokarstic galleries at la Caunha de Montségur); the Pech de Foix (700–1000 m); the Sourroque (1200 m) and Paloumère massifs (1200–1600 m) in the Salat catchment; a sequence of very smooth ridgetop flats around 1200 m between the Garonne, Neste and Adour rivers; the Ourdinse plateau (1500 m) and the residual plateau of Mailh Massibé–Montagnon (1973 m), both situated between the Gave d'Ossau and Gave d'Aspe (Uzel et al., 2020); and lastly the Arbailles massif, deeply corroded by karstic processes but where upturned and folded geological structures appear truncated at an elevation of 1000–1200 m by an erosion surface ornamented by small erosional hills. The erosional nature of the plateau surface is further testified by a number of truncated karstic cavities now exposing speleothems to the open air (Viers, 1960; Vanara et al., 1997; Vanara, 2000).

On the Iberian side of the orogen, erosional bevels in the Pedraforca nappes have been documented (Calvet, 1996). East of the Segre valley, two generations of erosion surfaces have been identified on that basis: the summit surface, which has been tectonically deformed, cross-cuts the Odèn–Port de Comte fold structures (1800–2300 m) (Fig. 8A), bevels the top of El Verd (2282 m), probably also the Rasos de Peguera (2077 m) and Raso d'Ensija (2200–2298 m), and likewise the south-facing dipslope of the Serra del Cadí (2400–2600 m). Meanwhile, the lower surface, which is less conspicuous, forms a bench in the Pedraforca nappe around 1800 m (Roca de Santaló, Pla de Prat). West of the Segre (see detailed map by Peña, 1984), the vestiges of low-gradient topography descend from Boumort (2077 m) southward towards the Serra de Careu (1760 m); and also northward towards the Serra de Prada (1800–1600 m), where the surface cross-cuts not just the

massive Upper and Lower Cretaceous limestones but also the unconformable cover of Paleogene conglomerates dipping NNW (Fig. 9B, C, G, H; Peña, 1984, with detailed maps). Farther north, the same generation of erosion surfaces can be observed at the top of the Serra de Tahús and as far as the Col de Cantó (1900–1750 m). They cut across the complicated geological structure at the leading edge of the Nogueres thrust sheet.

The fold belt of the Sierras Interiores, between the Noguera Ribagorçana and Noguera Pallaresa as well as towards the Isábena River, are likewise truncated by summit surfaces. The truncated beds include the unconformable and tectonically deformed conglomerate sequences such as at Sis, where the upper units of the Collegats Fm. form an anticline, then dip 15 to 30° to the NNE, and are finally upturned near Bonansa (dips of 42°S; Vincent, 2001, Figs. 2, 5 and 10a therein; see also geological sheet 'Pont de Suert' by García Senz et al., 2009). The low-gradient topographic surface of the Serra de Sis (1700–1780 m a.s.l.) cross-cuts all of these structures, indicating that the erosion surface is younger than the observed tectonic deformations of the conglomerate beds. Conspicuous vestiges of summit erosion surfaces affecting the folded Mesozoic structures of the area likewise occur at similar elevations at Cruz de Bonansa (1800 m), Sant Gervàs–Muntanya d'Adons (1850–1750 m, 60 ha) and Serra de Comillini (1550 m), where the surface even slopes very slightly towards the Axial Zone and suggests a component of tectonic tilting in the opposite direction to their initial slope (Fig. 9F). Other conspicuous summit surfaces occur on the Sierra de Ballabriga (2000 m, 20 ha), the Turbón anticline (2370–2250 m, 82 ha, Fig. 8G), the Cotiella massif (where residual relief subsists above the floor of the erosion surface), Punta Llerga (2240 m, 38 ha), and the Entremon plateau (2300 m, 250 ha). South of the Graus–Tremp Basin, the Montsec range clearly displays a pair of tiered surfaces: the upper level (Fig. 8C), which was mapped by Peña (1984), has been deformed but bevels the northern dipslope of the thrust sheet between 1650 and 1500 m; the second, more extensive surface is subhorizontal and extends at the lower elevation of 1150 m around the Col de Comiols (Fig. 8B, D). Peña (1984) had also reported this lower surface but interpreted it as an older surface partly exhumed from beneath the conglomerate beds. Reinspection of the Comiols area shows that the massive Cretaceous limestone and its unconformable cover of SE-dipping Paleogene conglomerate beds are both bevelled by the lower topographic surface, which can thus be subsumed under generation P1. P1 also displays benches cut into the southern flank of the Montsec, and locally at the NE termination of the sierra. Although some of these benches

2819 locally appear structural at some locations, their erosional nature is not in doubt. The
2820 surface is also observed at the NW edge of the Montsec range, where it grades to the top of
2821 the (unconformable) Graus conglomerate and finer molasse sequence — which is presumed
2822 of Miocene age. East (Peña, 1984) and west of the Noguera Ribagorçana, the Sierras
2823 Exteriores also bear erosion surfaces (Sant Mamet, 1300 m, Fig. 8B; Serra de Milla, 900–1000
2824 m; Sierra de Carrodilla, 900–1000 m, etc.).
2825 West of the Cinca River, in the Sierras Interiores, Monte Perdido displays structural summit
2826 surfaces coinciding with the top of recumbent folds (Birot, 1937). Likewise, the sierras of
2827 Tendeñera, Collarada and Visaurin exhibit an assemblage of structural and glacial landforms,
2828 but no erosion surfaces. An exception is noted at the border between Aragón and Navarra,
2829 where in the Sierra de Leire (1300 m; Barrère, 1981) the folded structures in limestone
2830 (Campanian, Paleocene and Ilerdian sequence) rising above the flysch have been bevelled by
2831 erosion. Plateau areas in soft flysch, such as the Llano de la Sierra (1100 m) and the Plana de
2832 Sassi (1000 m) in Navarra (Barrère, 1962), may represent partial planation landforms of a
2833 younger generation than P1. The Sierra de Guara displays up to 3 erosional bench levels
2834 (Barrère, 1952; Rodríguez-Vidal, 1986). The most conspicuous level is tilted from west to
2835 east, dipping from 1700 m near the centre (Fig. 8F) to ~1200 m at Sierra de Sevil (Fig. 8E).
2836 Throughout the area, a number of ~300 m-tall residual rock masses nonetheless rise above
2837 it. The surface truncates the tight folds in Upper Cretaceous to Lutetian limestone, but also
2838 (farther north) the succession of accordant homoclinal ridges in the Paleogene Campodarbe
2839 sandstone. This extensive erosional level possibly grades to the top of the Peña del Sol
2840 conglomerate beds, suggesting a chronostratigraphic link between the two. More recent
2841 partial planation benches form mountain-flank notches into the south and east sides of the
2842 Sierra de Guara, where they also appear to cut across the dipping conglomerate beds of the
2843 Sariñena and Uncastillo formations (e.g., at El Ciano, 1100 m, and at the Santa Cilia
2844 belvedere, 900–1000 m).
2845
2846 ***4.1.3. Age and origin of the erosion surfaces***
2847
2848 The major items of evidence arising from the inventory of erosion surfaces in the Pyrenean
2849 orogenic wedge are (i) the near-systematic occurrence of a pair of surfaces — a mountain-
2850 top and a mountain-flank surface — throughout the eastern third of the Pyrenees; (ii) the

regional extent of the mountain-top surface within this eastern segment of the mountain range; (iii) the absence of a well-defined mountain-top surface in the elevated Axial Zone massifs of the central Pyrenees, i.e., over a distance of 160 km from the Encantats westward to the Pic d'Anie; and (iv) the occurrence, often very clear but sometimes more hypothetical, of erosion surfaces (sometimes several generations) throughout the fold-and-thrust belts of the pro- and retro-wedges, as well as in the ranges standing along the continental drainage divide in the western Pyrenees (Basque Country). Age constraints on all of these features have been provided.

4.1.3.1. Transient legacies of a low-energy environment: evidence from thermochronology

None of the erosion surfaces in the inventory above are pre-orogenic, i.e., none were formed before the Proto- or the Ancestral Pyrenees. Such a view was once held on the basis of a small vestige of marine Cretaceous caprock at the top of the Pic de Balaïtous (García Sainz, 1940), i.e., precisely in the segment of the Pyrenees where no other vestigial summit surface occurs. It is now clear, however, that the isolated character of this outlier confirms on the contrary that all other potential vestiges of this sub-Cretaceous unconformity have been destroyed by vigorous syntectonic denudation (Upper Cretaceous beds occur farther east, but are buried beneath the Gavarnie Thrust; they can be followed for ~40 km but cannot be used as geomorphological markers). Abundant apatite fission-track (AFT) and apatite helium (U–Th/He, or AHe) data exist for the central and western Pyrenees (Yelland, 1990, 1991; Fitzgerald et al., 1999; Morris et al., 1998; Sinclair et al., 2005; Gibson et al., 2007; Metcalf et al., 2009; Jolivet et al., 2007; Meresse, 2010; Filleaudeau et al., 2011; Beamud et al., 2011; Rahl et al., 2011; Fillon et al., 2013; Michael et al., 2014; Vacherat et al., 2014, 2016; Bosch et al., 2016; Labaume et al., 2016b; DeFelipe et al., 2019). Somewhat fewer have been produced for the eastern Pyrenees (Garwin, 1985; Yelland, 1990, 1991; Sère, 1993; Morris et al., 1998; Maurel, 2003; Maurel et al., 2002, 2008; Gunnell et al., 2009; Rushlow et al., 2013) and Catalan Ranges (Juez-Larré and Andriessen, 2006). These rock-cooling studies show that Paleogene denudation depths were much too large (at least 6–10 km) for any pre-tectonic erosion surfaces to have survived the orogeny of the Ancestral Pyrenees. The data mostly document the pre- and synorogenic histories, particularly the Paleogene denudation maximum, and also reveal a north-to-south time lag in the timing of

peak denudation. They subsidiarily detect some effects of Oligocene to Miocene crustal extension in the east, and locally pick up recent valley incision in the Central Pyrenees (out of 250 AFT central ages, 11 lie between 10 and 20 Ma, with 2 ages at 11 and 12 Ma at Bielsa and in the Ossau massif; among 150 published AHe ages, 22 lie between 10 and 20 Ma, and 8 are younger than 10 Ma).

Gunnell et al. (2009; Fig. 10) produced a series of AFT and AHe data exclusively focused on samples collected from relict surfaces in the eastern Pyrenees. They show that denudation rates at those locations declined after the Paleogene tectonic paroxysm. By late Oligocene to early Miocene time, rock-cooling histories at each sampling site across the region had attained a low-temperature plateau indicative of a terminal decline in denudation intensity (Fig. 10C). Because of sensitivity limitations, the thermochronology cannot confidently discriminate between different generations of erosion surface such as S and P1, which in the landscape are nonetheless clearly distinct and typically offset by elevation differences of 0.5 km or less. Regardless of this minor caveat, however, a plateau in the rock cooling curves of a low-relief landform in a high-energy mountain range is nonetheless a clear signal of post-shortening topography having reached a state of low erosional energy and, by reasonable inference, of low relief. As evident in the landscape, the low-gradient topography has endured from ~25 Ma to this day (Fig. 10C). Such patterns have been observed in many mountain ranges around the world (for a review: Calvet et al., 2015a), and in the Pyrenees they are fully consistent with the fact that the erosion surfaces cross-cut the many syntectonic structures of the orogenic wedge such as thrust sheets, nappes and folds — whether in the Axial Zone or among the crumple belts of the pro- and retro-wedge.

Diagnostic but understated rock-cooling plateaus such as illustrated in Fig. 10 have been obtained independently in most other studies of Pyrenean thermochronology, whether based on the interpretation of vertical profile sampling or on single-sample modelling of fission-track lengths. For example, in the Maladeta massif three cooling models have detected a slackening of denudation rates (Gibson et al., 2007), with a succession of moderate denudation rates between 50 and 30 Ma (300 m/Ma), followed by a sharp but brief acceleration around 30 Ma (1.5 km/Ma), then followed by a comparatively quiescent and definitive phase of very slow cooling after 30 Ma (30 m/Ma) (Fig. 10D). Again in the Maladeta massif, an independent study using the vertical profile method has evidenced a long stagnation of the samples in the apatite fission-track Partial Annealing Zone between 30

and 5–10 Ma subsequent to a period of very rapid denudation ca. 35–30 Ma (Fitzgerald et al., 1999). Along the southern edge of the Axial Zone, five samples from another study extending between the Noguera and the Ter watersheds have documented a sharp rock-cooling plateau after ~20 Ma (Rushlow et al., 2013). In the Arize and Trois Seigneurs massifs, three cooling models by Vacherat et al. (2016) likewise reveal a clear thermal plateau after 50 or 35 Ma depending on location. AFT ages obtained from detrital apatite crystals extracted from unconformable Paleogene conglomerate sequences in the pro-foreland have also provided similar thermal signatures, with clear flatlining after either 50 Ma or 30 Ma (depending on the model and location), and thus suggesting a sharp and lasting decline in denudation intensity after Rupelian time at the latest. The exact timing probably depends on the provenance location (latitude, i.e., distance) of the granite pebbles collected for the study, and perhaps also on a moderate component of burial and exhumation of the samples from within the conglomerate (Beamud et al., 2011; Rahl et al., 2011).

Attempts at remodelling the existing data for the central Pyrenean Axial Zone (31 AFT and 17 AHe samples) have confirmed the rock-cooling plateau, which presents itself as a period of extremely low denudation (20m/Ma) between ~30 Ma and the Present and was preceded by an episode of extremely rapid denudation between 37 and 30 Ma (> 2.5 km/Ma) (Fillon and van der Beek, 2012). Thermochronological evidence from the western Pyrenees also shows a thermal plateau after 30 to 15 Ma depending on the location, but cooling models produce a post-Pliocene acceleration involving rapid denudation after ~5 Ma (Jolivet et al., 2007). Given that this acceleration also concerns the high summits of the Néouvielle massif, this could tentatively be an expression of the 'Miocene acceleration' artefact pointed out by Gunnell (2000) and Dempster and Persano (2006), which is related to parameter choices around the fission-track annealing algorithms used in the modelling. Still farther west, the outlines of a thermal plateau after 20–10 Ma are apparent in profile models of the Pic de Balaïtous, as likewise in the Lakhoura profile after 30–20 Ma, on a longitudinal traverse close to the Pic d'Anie (Bosch et al., 2016).

4.1.3.2. Refined age constraints on the two generations of erosion surface

In the eastern Pyrenees, rifting during the early Miocene was largely responsible for the tectonic regime which generated the pairs of S–P1 surfaces. Rifting generated substantial

local relief in certain areas such as Mt. Canigou, but this was an exception. Other morphotectonic units (Carlit, Campcardos, Aston, Madrès, Corbières...) were not affected by such large vertical fault offsets. Rifting initiated a cycle of topographic rejuvenation in response to the newly forming local marine (Mediterranean) base levels, with generation P1 developing 200 to 500 m below summit surface S.

4.1.3.2.1. The range-top paleoplain (S)

The precise age of the summit surface, S, is poorly constrained but broadly fits into a time window between the late Oligocene and the Aquitanian. The sedimentological inflexion observed during Chattian time in the eastern Aquitaine Basin (see Section 3.1.2), when conglomerate influx was replaced in the stratigraphy by lacustrine limestone, provides a relatively robust palaeoenvironmental indication of declining topographic energy in the Ancestral Pyrenees at the time. Thick lacustrine limestone also occurs in the Upper Oligocene units of the Narbonne Basin and (with interlayers of lignite) in the eastern Ebro Basin at Calaf, Tàrrega (Rupelian), and Mequinenza (Chattian) (Cabrera and Saez, 1987; Gomis et al., 1997). Some climate-driven lake fluctuations relevant to ~1 m.y. cycles nested within this broader pattern have also been detected (Valero et al., 2014).
It is often admitted that these low-energy deposits grade laterally to the Nogueres and Berga conglomerates, and that the latter are thus also of Chattian age (e.g., Vincent and Elliott, 1996; Vincent, 2001; Jones, 2004). No direct palaeontological evidence in the Solsona molasse or in the Berga conglomerates, however, currently supports a Chattian age for the conglomerates; the youngest magnetostratigraphic record is mid-Rupelian (i.e., ~30 Ma; Carrigan et al., 2016; see also discussion in Section 3.2.2.2). As recorded from all three piedmont basins to the north, east and south of the Ancestral Pyrenees, a period of decreasing clastic output from the eastern part of the mountain range thus cannot be ruled out during Chattian time. A low-energy environment is more difficult to infer from lithostratigraphic criteria for the subsequent Aquitanian stage, particularly in the eastern half of the Pyrenees, because the region east of the Segre River has been an area of either nondeposition or complete erosion of whatever Aquitanian record may have existed. An expansion of lacustrine limestone facies has nonetheless been described in the lower Cinca catchment around that time (Valero et al., 2020), thereby suggesting limited coarse-textured

terrigenous influx from the Pyrenees in that area. Aquitanian siltstone and limestone deposits likewise overlie the Pyrenean molasse in the centre of the Aquitaine Basin ('trilogie agenaise') and exist in the eastern basins (Narbonne Basin, and base of the Roussillon Basin fill sequence at depths of –1200 to –1500 m in the Canet borehole; Berger et al., 1988).

The absence of erosion surfaces in the central Pyrenees, i.e., the exclusive presence of mountains with spiky rather than flat tops (Adams, 1985; Calvet et al., 2015a), calls for three alternative scenarios (Fig. 11):

(i) Scenario A: the paired S/P system was ubiquitous throughout the Pyrenees; surface S also existed in this portion of the Ancestral Pyrenees, but it was destroyed by more intense denudation (and, later, by glaciation) than in the eastern Ancestral Pyrenees, and by higher magnitudes of post-shortening uplift (confirmed by the high modern elevations of the central Pyrenean massifs).

(ii) Scenario B (a variant of A): the paired S/P system only existed in the east of the orogen, in direct relation with Mediterranean extensional tectonics. Subdued relief was also generated in the western Pyrenees, but the two erosion surfaces conspicuous in the east here blur into a single phase of downwearing which terminated in the middle Miocene. This single surface was destroyed by subsequent morphotectonic events but is preserved among fold and thrust units on both flanks of the crustal wedge as well as on the continental dividing ranges of the Basque Country.

(iii) Scenario C: surface S never developed in the higher massifs of central Pyrenees because of persistent tectonic activity in this segment of the orogen, where thrust displacement continued until the early Miocene and possibly as late as the middle Miocene (Jolivet et al., 2007; Huyghe et al., 2009). As a result, little more than pediments would have developed on the flanks of the high range, beveling folds in the pro- and retro-wedges and at the western termination of the orogen. These imperfect but mappable erosional landforms would have evolved iteratively from the end of the Paleogene to the middle Miocene, thereby granting them stronger membership ties to generation P1 than to generation S.

4.1.3.2.2. The range-flank pediments (P1)

3009 Age constraints on surface P1 are good in the eastern Pyrenees. Depending on location,
3010 different occurrences of pediment P1 (i) cross-cut uptilted Upper Oligocene and Aquitanian
3011 beds within the Narbonne and Tuchan–Paziols basins; (ii) grade to the top of the middle
3012 Miocene shoreline outcrops of the Mediterranean seaboard (Fig. 7A, B); and (iii) display
3013 across their treads a very large number of fossil micromammalian assemblages preserved in
3014 regolith-filled cracks of the limestone pavements, with ages ranging between 20 and 10 Ma.
3015 The preservation of these fossil assemblages suggests a low-energy geomorphological
3016 environment. In the Canigou massif, P1 formed after the intense period of rifting and deep
3017 unroofing of the Paleozoic gneiss dome, which (based on the inverse stratigraphy and age of
3018 correlated deposits in the adjacent intermontane basins such as the Conflent; see Section
3019 3.3.1) occurred during early Aquitanian to Burdigalian time. In the Corbières and Minervois,
3020 P1 continued to evolve in the late Miocene, coevally with the lacustrine limestone deposits
3021 of Montredon (biozone MN 10, 10–9 Ma) (Calvet, 1992, 1996; Calvet and Gunnell, 2008;
3022 Gunnell et al., 2009). In the Ariège, the upward-fining molasse sequence from the Aquitanian
3023 through to the late Burdigalian, as likewise the onlap of lacustrine limestone beds southward
3024 up to the outermost folds of the Petites Pyrénées, suggest a similar chronology valid for the
3025 planar surfaces of the Aston massif. Hillslope gradients probably reached their lowest energy
3026 state during the middle Miocene.
3027 Along the pro-wedge, the Sierras Interiores and their overlying (unconformable and often
3028 north-dipping) Nogueres conglomerate sequences between the Segre and Esera valleys have
3029 been truncated by a single erosion surface. This population of occurrences is at least post-
3030 Chattian, and perhaps belongs to generation S. Along the margins of the Ebro Basin, the
3031 upper surface at Montsec probably also correlates with generation S. The lower surface,
3032 however, which truncates the conglomerate sequence reputedly of Chattian terminal age,
3033 would correlate with P1. This interpretation is supported by the apparent stratigraphic
3034 correlation between the surface and the conglomerate sequence at the western end of the
3035 Sierra del Montsec, the Sierra Carrodilla, and the Sierra de Guara, where occurrences of P1
3036 grade to the top of the Graus, Sariñena and Uncastillo formations, respectively (Fig. 8).
3037 Attenuation of relief steepness is also indirectly documented by the widespread
3038 progradation of carbonate platforms after 15–16 Ma (see Section 3.2.5.2).
3039
3040 *4.1.3.3. Base-level controls on erosion surface completion*

Compared to continental-scale peneplains, which are generated over time scales compatible with the Wilson cycle, the short geological time to completion of low-gradient surfaces S and P1 in the Pyrenees can be explained by three complementary causes, all of which are particularly relevant to the eastern Pyrenees.

- The narrowness of the Ancestral Pyrenees at the end of the Paleogene is a first factor. Whether in the retro- or the pro-foreland, the Pyrenean fold-and-thrust belts were in large part buried beneath the molasse and conglomerate sequences described in previous sections, so that the Paleogene mountain range was effectively a narrow backbone consisting mainly of the Axial Zone and the NPZ. Whereas the compressionally deformed crust in the central Pyrenees (inclusive of the SPCU) is 160 km and the mountainous relief currently ca. 140 km wide, during the Paleogene the width of mountainous relief at that same longitude would not have exceeded 80 km.
- The interruption of tectonic convergence during the Oligocene in the eastern Pyrenees, and the onset of Mediterranean extension responsible for fragmenting the mountain belt into a collection of basins and footwall uplands, is a second factor. The overall rate at which denudation occurs depends on the ratio of surface-area to volume of rock to be consumed by denudational processes — i.e., the greater the surface area of exposed mountain fronts (e.g., a mosaic of footwall uplands separated by local tectonic base levels, more vulnerable to erosional inroads made by river catchments than a monolithic, e.g. cylindrical, mountain range), the faster the volume as a whole can be consumed by backwearing river systems. Here, extensional fragmentation into discrete tectonic blocks multiplied the total length of mountain fronts vulnerable to erosion by steep catchments, reduced the size of relief units exposed to denudation, and thus conspired to promote conditions of rapid relief decay and erosion-surface completion.
- Possibly also a dense lithospheric root (see Section 2.4) was pulling downward and delaying the full potential for isostatic rebound. Rebound is a function of the elasticity of the underthrust Iberian Plate and of orogen width (assumed to represent a line load). In the case of an orogen narrower and shorter than the Modern Pyrenees, isostatic rebound of the Ancestral Pyrenees was perhaps 15% of what Airy isostasy would otherwise predict (Montgomery, 1994).

These considerations relax the need for assuming that the summit surfaces were formed at palaeoelevations of 2000 m or more, i.e., at their currently observed altitudes of occurrence, just by clipping off the tops of certain massifs of the Ancestral Pyrenees in Oligocene time. This is theoretically feasible under the assumption of substantially raised foreland base levels, for which there is, however, potential evidence only in the anomalous Nogueres area on the Iberian side and none whatsoever on the retro-wedge side. This view is an avatar of the hypothesis formulated ca. 30 years ago that climate rather than tectonics drive mountain building (Molnar and England, 1990), subsequently simulated in sandbox models inspired by the (striking, but atypical) Nogueres pro-foreland setting (Babault et al., 2005a, 2007). Opposite conclusions have since been drawn from global data and levelled at the climate-driven doctrine (Willenbring and von Blackenburg, 2010). Note that in the Pyrenean context, the raised foreland scenario would also imply (i) that the narrow, Ancestral Pyrenees somehow remained altitudinally stationary and unaffected by fluvial dissection during the last ~25 m.y.; and (ii) that the externally drained Aquitaine Basin somehow was also (like parts of it Ebro counterpart) an overfilled basin, with clastic backfill rising up to the Axial Zone. No evidence in favour of such north–south symmetry, however, exists (see also Sinclair et al., 2009).

The scenario of a raised base level caused by an overfilled Ebro basin would imply that the summit erosion surface graded to the top of the pro-foreland Nogueres conglomerate sequence, for which there is no direct evidence comparable with, for example, the clastic depositional ramps (so-called ‘gangplanks’) that today still connect the Colorado Front Range to the Ogallala Formation of the High Plains of Texas, Colorado or Wyoming (see Calvet et al., 2015a, and references therein, for an overview).

Initially formulated by Coney et al. (1996), the scenario portraying the Nogueres conglomerates (sensu Section 3.2.4.2) as a backfill sequence lapping northward onto low-gradient erosion surfaces in the Axial Zone, with the erosion surfaces evolving concomitantly at elevations controlled by this raised clastic base level, has reverberated widely through Pyrenean literature and been simulated in sandbox experiments (Babault et al., 2005b, 2007). This model, however, is unique to the south-central Pyrenees (no similar conformations occur in the eastern Pyrenees, or along the Aquitaine retrofreland, or in the context of the Berga–Serrat Negre conglomerates further east or the Santa Orosia–Cancias

conglomerates further west), and is actually unsupported by field evidence in its own testing ground.

Any notion that the topmost Nogueres conglomerate beds and extant summit erosion surfaces in the Axial Zone are coeval and cogenetic is challenged by a number of underpinning criteria (Fig. 9):

(i) the huge boulder-bed facies of the proximal deposits, requiring a high-energy environment in the Axial Zone (Fig. 9A, B, D, E) rather than low-energy, low-gradient land surfaces (these typically generate finer-textured alluvium more akin to the Ogallala Fm. in the foreland of the Laramide Rockies);

(ii) the attitude of the conglomerate beds, which, far from having conserved the depositional slope typical of clastic ramps between a mountain range and its foreland, are systematically folded and/or tilted northward towards the Axial Zone (Fig. 9F).

(iii) the fact that the conglomerate sequences are themselves cross-cut by low-gradient erosional topography. These land surfaces are thus necessarily younger than the structures they have truncated, and thus younger than the clastic sequences themselves.

To the west of the Nogueres conglomerate outcrops, the Santa Orosia conglomerates (Bartonian to Priabonian) have been warped into the shape of a syncline and offset by the Oturia Thrust. The erosion surfaces at Col de Comiols and Serra de Sis, which were analysed in Section 4.1.2.2 (Fig. 8B, D; Fig. 9), and in the Boumort massif (Fig. 9) call for similar conclusions: the conglomeratic fan deposits have all undergone tectonic deformation and tilting towards the Axial Zone, i.e., towards their source areas (Birot, 1937; Rosell and Riba, 1966; Rosell, 1967; Reille, 1971; Muñoz et al., 2010). The intensity of deformation decreases upsequence but affects the entire stratigraphy, including the topmost 'allogroups' (Senterada and Antist, Fig. 9F), which are inexplicably illustrated as horizontal beds in some publications (Melleres and Marzo, 1992; Beamud et al., 2011, Fig. 2 therein). Overall, the summit surface on all of the structures from the Bóixols anticline to the Serra de Prada cross-cuts not just the homoclinal structures in massive Mesozoic limestone but also the entire Nogueres conglomerate sequence itself, from the Pessonada allogroup in the south to the Pallaresa allogroup in the north (Fig. 9C, G, H).

In the Aquitaine foreland, the homologous Palassou conglomerates are likewise folded and, at many places, upturned vertically and cross-cut by low-gradient erosional surfaces — for example north of the Mouthoumet massif. As on the Iberian side of the orogen, there is thus no robust evidence to support the hypothesis that the Palassou conglomerates and the elevated erosion surfaces on massifs such as Aston, Arize and the Pays de Sault are coeval and cogenetic. As an additional caveat, connecting by imaginary lines vestiges of generation S or P1 at their current altitudes in the Axial Zone to the top units of conglomerate sequences in the Aquitaine or Roussillon basins would require gradients of 4% to account for these putative clastic 'gangplanks'. Unless allowance is made for uplift-related postdepositional tilting, such steep gradients are unrealistically high compared to the natural depositional slopes commonly reported for alluvial megafans of the sizes typically observed along mountain range fronts (Calvet and Gunnell, 2008).

By logical elimination, it thus appears highly likely that the summit surfaces are vestiges of a paleoplain that formed regionally across parts of the Ancestral Pyrenees at lower elevations than the current altitudes of its vestiges would suggest — and that they were later uplifted. A variety of geophysics- and geomorphology-based inferences calibrated against the anomalously high longitudinal gradients of Quaternary alluvial terraces (Delmas et al., 2018), and predicated on realistic depositional slopes observed in modern piedmont zones (i.e., the natural gradients of large piedmont fans: see Miall, 2016; Ventra and Clarke, 2018), have suggested that the initial altitude of this paleoplain — i.e., its mean altitude when the orogen had attained an all-time state of least topography, including in the Axial Zone — would have not exceeded 800 m (Gunnell et al., 2008, 2009). The topography of the eastern Pyrenees was thus neither a sea-level peneplain nor a high-elevation peneplain but a mid-elevation, irregular plateau region displaying a greater proportion of low-gradient erosion surfaces than of steep alpine peaks.

4.2. Late Neogene regrowth of the mountain range: chronology and evidence from landforms

Fundamentally, the altiplanation hypothesis for the Pyrenees postulates that the Modern Pyrenees are just a vertically incised but altitudinally unmodified version of the Ancestral Pyrenees (Curry et al., 2019). It thus downplays the magnitude of the step change required

to explain the transformation of the Ancestral into the Modern Pyrenees, and essentially regards the distinction as unimportant. Much evidence is available, however, to show that the late Neogene, i.e., the last 10–12 million years, was the period of a second rising of the Pyrenees as a continuous and elevated mountain range between Iberia and Europe. The evidence in support of this phenomenon derives primarily from geomorphological clues, now widely recognised (Section 4.1) but commonly misreported (e.g., Curry et al., 2019). It is further corroborated by a number of tectonic and stratigraphic observations and backed up by indications concerning the processes at the lithosphere–asthenosphere boundary (see Section 2.4, and Jolivet et al., 2020).

4.2.1. Evidence of late Neogene uplift throughout the Pyrenees

4.2.1.1. Thermal relaxation and lithospheric thinning since 10 Ma

If we assume that the Pyrenean paleoplain formed at a mean palaeoelevation of less than 1 km (mean or maximum is immaterial in the context of a low-relief erosional plain; Gunnell et al., 2008, 2009; Delmas et al., 2018), it follows that ~60% of the topographic relief we observe today (summits in the eastern Pyrenees: ~2.7 km) was produced during the late Neogene, and in several stages involving regional surface uplift. The inferred mean topographic uplift rate is 0.2 mm/yr, i.e., sufficiently slow to lie within the uncertainty envelope of present-day detection of vertical crustal motion by GPS (0.1 ± 0.2 mm/yr: Nguyen et al., 2016). In the west-central Pyrenees (Aspe valley), Uzel et al. (2020) inferred ca. 1 km of Neogene and Quaternary uplift-driven valley incision, with evidence of greater relative uplift in the Axial Zone than in the NPZ. Assemblages of late Miocene warmth-loving plant remains and $\delta^{18}O$ measurements in fossil teeth in the sedimentary deposits of the Cerdagne Basin (1200 m a.s.l.) confirm the notion of recent regional uplift (Suc and Fauquette, 2012; Huyghe et al., 2020), and even more so in the Val d'Aran (now at ~2000 m; Ortuño et al., 2013; see also section 3.3.2). As argued in Section 2.4, maintaining the buoyancy of the crust to the east of Andorra almost certainly implies a thermal contribution from the asthenospheric mantle, which in turn causes thermal or mechanical thinning of the mantle lithosphere (Gunnell et al., 2008, 2009). The resulting dynamic uplift supports the regional topography of the Modern Pyrenees at least in the east (Chevrot et al., 2018) — a

process also consistent with the situation inferred for the neighbouring Catalan Ranges (Lewis et al., 2000) and with the incidence of late Neogene volcanism, and which has also been adduced to explain the geologically recent uplift of the Moroccan Atlas Mts. (Teixell et al., 2005). The most recent deep tomography based on teleseismic and gravity data has imaged a low-velocity anomaly located between the surface and a depth of 100 km. It coincides with a strong density anomaly interpreted as a mass of eclogite in the deep crust, also consistent with the depth-distribution of seismic activity in the crust (Dufréchou et al., 2018). The conjunction of these independent components of evidence supports the notion of a crustal drip or a delamination process currently occurring beneath the Modern Pyrenees west of Andorra. Meanwhile, the Ancestral Pyrenees to the east of Andorra had lost their crustal root much earlier, most likely during early Neogene (see also Jolivet et al., 2020), thus also explaining the unique geomorphological identity of the eastern Pyrenees.

4.2.1.2. Sedimentological signatures of growing relief amplitude

An increase in clastic output, both in terms of volume of debris and average clast size, since the late Miocene is recorded in piedmont deposits such as the Lannemezan megafan, among the eastern extensional basins such as the Roussillon, Empordà, Cerdagne, and in the Mediterranean and Atlantic offshore clastic wedges (Kieken, 1973; Lofi et al., 2003; Duvail et al., 2005; Bache et al., 2010; Cameselle et al., 2014; Granado et al., 2016; Ortiz et al., 2020; also see sections 3.1.5.2, 3.2.6 and 3.3.2). A climatic cause for accelerated denudation is theoretically possible, but the time period of regional uplift spans palaeoclimatic regimes as diverse as the warm subtropical conditions alternating between super-humid and semi-arid of the Tortonian, Messinian and Pliocene; and the cold, glaciated and temperate oscillations of the Quaternary. Tectonics-driven relief growth and steepening of hillslopes seems a more plausible explanation for terrigenous delivery by the mountain range, and is consistent with the lithospheric and mantle processes mentioned above. Another strong indication of neotectonic activity is the occurrence of well-preserved triangular-faceted spurs, for example along the southern boundary-fault scarp faces of the Roussillon and Cerdagne basins. These are in each case associated with debris-cone sequences several hundred metres thick, of Pliocene and Turolian age, respectively, containing giant boulders supplied by very steep range-front catchments (Calvet, 1996; Calvet and Gunnell, 2008).

4.2.1.3. Late Neogene and Quaternary tectonic deformation

Many Pyrenean deposits of Miocene to Quaternary age exhibit tectonic strain indicators, from tilting to fault-controlled offsets (synthesis in Philip, 2018). The known spatial distribution of these tectonic indicators, however, is quite uneven: in the Roussillon Basin, for example, faults in the Miocene fill sequences are widespread, but faults in the Pliocene wedge-top layers are more uncommon and restricted to a few documented sites. At the scale of the entire Pyrenees, the inventory of tectonically offset Quaternary deposits does not exceed ~20 sites (Fig. 12). The intensity of deformation is variable depending on the sequence: Upper Miocene units are steeply upturned in the Cerdagne, La Seu, and Empordà basins, and fault throws through the graben fills attain ~1 km. Strata in Pliocene sequences exhibit shallower dips, and fault throws do not exceed a few hundred metres. Tectonic offsets through Quaternary deposits are an order of magnitude less. Deformational style is also variable, and includes extensional (widespread in the Mediterranean domain and as far west as the Val d'Aran), strike-slip, and thrust faults (Viers, 1960, 1961a; Ellenberger and Gottis, 1967; Birot, 1969; Mouline et al., 1969; Ambert, 1977; Pous et al., 1986; Cabrera et al., 1988; Briais et al., 1990; Philip et al., 1992; Massana, 1994; Saula et al., 1994; Carbon et al., 1995; Roca, 1996a; Genna et al., 1997; Goula et al., 1999; Calvet, 1996, 1999; Fleta et al., 2001; Baize et al., 2002; Alasset and Meghraoui, 2005; Dubos-Sallée et al., 2007; Ortuño et al., 2008, 2018; Lacan et al., 2012; Lacan and Ortuño, 2012; Philip, 2018). Inside limestone cave systems, endokarstic galleries offset by tectonic throws of up to 10 m have been reported at La Pierre Saint-Martin (Maire, 1990), in the Arbailles massif (Vanara et al., 1997), and in the Villefranche syncline (Coronat massif, Calvet et al., 2015b; Hez et al., 2015); however, the ages and slip directions of these tectonic fractures are difficult to establish. As a result, just as it is proving difficult to determine the fault-plane solutions of modern-day earthquakes in the Pyrenees (see below), the chronology of stress regimes during the late Neogene is difficult to reconstruct. It is likely that it was neither uniform across the orogen nor constant through time at any given site.

During the latest Miocene and Quaternary, N–S convergence resumed but was apparently too weak or too short-lived to contribute measurably to mountain building. Evidence for this is provided by a reverse fault along the southern boundary of the Roussillon Basin, where

the Miocene beds are overthrust but the unconformable Pliocene overburden appears undisturbed by additional tectonic strain (Calvet, 1996, 1999). The Quaternary deposits, however, are in turn reverse-faulted, with similar features also observed elsewhere — whether in the Axial Zone (Cerdagne, Estavar and Martinet reverse faults) or in the outer belts of the orogenic wedge. Most of the faulting occurrences affect middle and younger Pleistocene sequences. Characteristic occurrences in the retro-wedge/retro-foreland zone include reverse faults at Caramany (Agly River valley), in the Montagne Noire near Revel, and cutting through the Horsarrieu and Meilhan anticlines along the Adour River valley; an anticline warping the Würmian alluvial terrace along the Gave d'Aspe at Asasp-Arros; the small fracture swarms in early Pleistocene (or Pliocene?) deposits at Biarritz; and contrasting evidence in Holocene deposits along the Lourdes Fault of a reverse-fault geometry at Arcizac, but a Holocene normal-fault geometry at Capbis. Among occurrences in the pro-wedge, worth mentioning are the reverse faults at Isaba in the Roncal River valley, Canelles along the Noguera Ribagorçana, Balaguer along the Segre, and Serinyà along the Fluvià. Indices of extensional faulting in Quaternary deposits are comparatively scarce anywhere within the orogen: e.g., at Osséja (Cerdagne), at La Seu d'Urgell, and at Graffan–Ferrals (Corbières), where Pleistocene travertine on the Orbieu River exhibit tectonic offsets. Pure strike-slip motion is reported in the early Pleistocene lacustrine limestone beds of the Fluvià watershed. Extensional and strike-slip displacement of the entire Pliocene sequence have been well documented in the Roussillon Basin, with an additional offset of ~10 m (for example at the protected site of special geological interest near Ille-sur-Têt) also affecting the uppermost alluvial terrace deposit of the Têt River.

Present-day tectonic activity is very weak throughout the Pyrenees. The rate of convergence measured by GPS between Africa and Europe is 3–4 mm/yr. The Pyrenees are undergoing extension, today principally in their western segment, at a rate of ~0.5 mm/yr — although only a few of the GPS measurements truly register above the background noise. From this it has been inferred that Iberia and Europe are now locked to one another, thus forming a single tectonic plate (Nocquet and Calais, 2003, 2004; Fernandes et al., 2007; de Vicente et al., 2008; Asensio et al., 2012). The main focus of continental deformation has jumped to the southern boundary of the Iberian Plate in the Betic Ranges. Seismicity in the Pyrenees is moderate (Fig. 13), with 35 events exceeding M_L 5 since 1950 (e.g., St-Paul-de-Fenouillet, 1996, M_L 5.2; Arudy, 1980, M_L 5.1: Rigo and Cushing, 1999), and 12 of a higher intensity (i.e.,

> VIII on the Modified Mercalli scale) since the Middle Ages (Souriau and Pauchet, 1998). Focal mechanisms, however, are poorly constrained: some studies have supported a compressional stress regime (Goula et al., 1999), which is in agreement with geological evidence of Quaternary reverse and strike-slip faulting (Philip et al., 1992; Calvet, 1996, 1999; Carbon et al., 1995; Goula et al., 1999; Fleta et al., 2001; Baize et al., 2002; Alasset and Meghraoui, 2005; Lacan et al., 2012; Lacan and Ortuño, 2012); but recent revisions favour instead an extensional regime (Chevrot et al., 2011). The most recent synthesis (Rigo et al., 2015), however, suggests a more nuanced picture, with emphasis on variation in deformational style and intensity through time, and with a gradient from weak transtension in the west to weak transpression in the east.

Vertical crustal motions have been documented by levelling methods, with debatable values of up to 1 mm/yr at Mt. Canigou and in the Têt valley (cited in Calvet, 1996, after Lenôtre and Fourniguet, unpublished BRGM report from 1987; see also Philip, 2018), and 1–4 mm/yr in NE Catalonia (Gimenez et al., 1996). With very low measured values of 0.1 ± 0.2 mm/yr, GPS measurements of vertical displacement currently remain within the noise of analytical error (Nguyen et al., 2016). This inventory excludes the occurrences of slope tectonics that have been mapped and analysed by Jarman et al. (2014) and Ortuño et al. (2017), and which tend to impact the upper portions of slopes in some massifs. On balance, field evidence weighs in favour of a compressive regime during Quaternary time, thus at odds with focal mechanism data as well as with short-span GPS measurements.

4.2.2. Geomorphological indicators of episodic surface uplift

4.2.2.1. A late Neogene generation of rock pediments (P2)

Late Neogene uplift was not steady. Pauses or relative lulls allowed pediments (i.e., partial planation surfaces) to expand across the edges of the Neogene extensional basins in the east, but also into more interior areas of the Axial Zone in the form of flat-floored erosional corridors, bedrock straths or topographic basins, usually in soft or weatherable rock outcrops such as marl, flysch, deeply weathered granite; but also limestone basins (poljes), which today have become fossil landforms (Figs. 6, 14). The age of these landforms is often

difficult to establish. The oldest occurrences grade to (and thus seem correlative of) the Vallesian deposits of Cerdagne and La Selva.

The pediment generation most indicative of unsteady post-shortening uplift regime is a second generation of rock pediments and palaeovalleys, here labelled generation P2. Its residual occurrences grade to the tops of retro-wedge megafans such as the Lannemezan, and are thus roughly of late Pliocene or earliest Pleistocene estimated age (Goron, 1941a; Delmas et al., 2018). These partial pediments are several kilometres across. They form deep, flat-floored embayments into the mountain topography, typically hanging today 200–400 m above the modern valley floors. Smaller erosional benches of a younger generation (labelled here P3) grade laterally to the oldest Pleistocene alluvial terrace deposits (generation T5, see Section 4.2.2.3 and Section 5), and may thus qualify as bedrock straths. These successive cohorts of planar landforms are relatively ubiquitous and formed prior to the deep vertical valley incision and widespread slope steepening events of the Pleistocene. Quaternary glaciation has often failed to erase these late Neogene features from the landscape. Occurrences of these characteristically low-gradient landforms have been widely mapped in the central Pyrenees, e.g., in the Noguera Pallaresa, Ariège, and Salat watersheds, and even more conspicuously in the Agly and Tech watersheds and around the edges of the eastern Neogene basins such as the Roussillon, Cerdagne, and Empordà. These pediments are particularly extensive among granitic outcrops but also in schist (Goron, 1931, 1937, 1941a; Zandvliet, 1960; Hartevelt, 1970; Lagasquie, 1969, 1984a, b, 1987; Calvet, 1996; Delmas et al., 2018). Around the edges of the Cerdagne Basin, a good example of P2 is the Plateau de la Perche (Fig. 14D), which bevels the basement along the edge of the basin as well as an upturned sequence of Vallesian and Turolian deposits within in. Other landforms belonging to this generation include the Plateau de Sault, the surface of which is smeared with siliciclastic lag deposits displaying identical facies to the constituent depositional units of the Lannemezan megafan. Occurrences of pediment P2 are also observed in the Neste watershed, in the weathered granite outcrops of Bordères (Monod et al., 2016). In the outer relief units of the orogenic wedge, e.g., in the Empordà Basin, the pediment surfaces grade to the top of the Pliocene gravel beds of the Llers–Figueres plateau. Similar configurations are reported on either side of the lower Aude valley, e.g., in the Corbières (at Les Vals) and in the Minervois (Montouliers–Montplo) (Birot, 1969; Ambert, 1994; Larue, 2008). Farther west, from the Ariège to the Gave rivers, the P2 piedmont ramp cuts across almost all of the

Sub-Pyrenean fold sequences — particularly folds in the Cretaceous and Eocene flysch — and is even locally embayed into its regional P1 predecessor (Fig. 14A, B, C).

The Lannemezan gravels and their analogues, which form a debris mantle widely distributed across the P2 topographic surface, are a constant diagnostic feature of P2 (Goron, 1941a; Taillefer, 1951; Lagasquie, 1969, 1984b). Save a few very rare exceptions, this generation of deposits seems absent from the Basque Country, where the watersheds are mostly in limestone and thus could not supply siliciclastic debris to the piedmont. P2 is nonetheless very extensive in the Basque region. Despite the scarcity of diagnostic gravels, the landform is topographically continuous with the Ossau megafan (Fig. 14B), which displays a debris accumulation of the same nature as the lag gravels encountered across, and basinward of, occurrences of P2 farther to the east. The spatial distribution of P2 between the Adour River and the Pyrenean mountain front overall forms a belt of pediments ~20 km wide at elevations ranging between 300 and 180 m (Fig. 14A). The erosional surface cuts mainly across flysch, but equally across vertically upturned beds of massive Cretaceous limestone as well as gneiss and schist. A few large, residual monadnocks in the Garralda quartzite, the Ursuya gneiss, and the Permo-Triassic sandstone of La Rhune have resisted denudation, and these topographic residuals themselves display hillflank benches that are legacies of an older generation of pediments. P2 often extends inward between those massifs, and for example joins up with the interior topographic basins of Ossès and Saint-Jean-Pied-de-Port (Viers, 1960).

On the pro-wedge, similar suites of planar landforms extend across outcrops of Eocene and Cretaceous flysch and shale. In francophone literature, these are known as the ‘mature hanging landforms’ of Navarre (Barrère, 1962) and (in the case of the oldest vestiges of soft-rock wash pediments in that region) have also been named ‘coronas’ (Barrère, 1952, 1975, 1981; Peña, 1984; Stange et al., 2018). The most elevated generation of pediments is capped by very ancient breccia containing large boulders. Occurrences of this caprock are well preserved at the wide col below the village of Merli, 350 m above the Isabena River and 450 m above the Esera River; and likewise at San Victorian–La Mula, at the base of the abrupt Peña Montañesa range (2300 m) — i.e., ~500 m above the Cinca River and 360 m above more local tributaries. The most elevated generations of wash pediments in the Conca de Tremp hang 200–250 m above the Noguera Pallaresa, and farther to the east the Pla de

Lladurs hangs ~400 m above the Cardener River (Fig. 14E). All of these mantled pediments in soft rock belong to the same generation P2.

4.2.2.2. Dry valleys and drainage piracy

Dry valleys in the Pyrenean landscape consist mostly of broad, shallow furrows which document a time of progressive drainage reorganisation during the early rise of the Modern Pyrenees, when the intensity of fluvial incision into the low-relief landscape of the late Ancestral Pyrenees was still moderate. These ancient valleys sometimes display perfectly preserved entrenched meander belts (e.g., the dry valley at Col de Saint Louis, in the Fenouillèdes massif). Different generations of ancient valley floors have been identified. Occurrences at high altitudes are rare and, in that case, correlate with pediment surface P1. They often lie at elevations identical to the upper portion of the pediments. The largest population of dry valleys is coeval with pediment generation P2 and occurs systematically at elevations lower than P1. In the piedmont zones, some of the valleys are Quaternary. Whatever their exact age, they all document a diachronous process of river piracy and progressive drainage reorganisation during post-shortening time. This process and its intricate patterns, however, have never been studied comprehensively or systematically. The most spectacular dry valley is perhaps the Pla de Beret (1870 m), which occurs in the catchment headwaters of a strikingly underfit Noguera Pallaresa in the central Pyrenees (Fig. 14G). This flat-bottomed hanging valley is 500 to 800 m wide and has been only lightly transformed by glacial erosion. Its gentle descent northwards eventually curves eastwards around the granitic Marimanya massif — an obvious adaptation to the local structural geology. Its natural watershed is the Encantats massif to the south, but the retro-foreland Garonne River, which in this area is much closer to its regional base level than the pro-foreland rivers, has beheaded the Noguera watershed. This process was probably assisted by late Neogene tectonic activity along the Maladeta Fault (Ortuño et al., 2008), and as a result of deep incision the Garonne now flows ~600 m below the Pla de Beret. Another major drainage capture along the main divide occurred at the Col de Puymorens in the eastern Pyrenees, also a broad palaeovelley. A river flowing through it used to join up with the Segre and the Mediterranean but now joins the current Ariège drainage network northwards to the Atlantic (Fig. 14F). In the eastern Pyrenees, the Têt River has also lost part of its left bank

watershed to the Aude River as a consequence of tectonic downthrow in the Capcir graben; the shallow cradle of abandoned hanging valleys can still be observed along the skyline of the N–S boundary fault scarp to the east of the graben.

Most of the other dry valleys have been preserved by dint of the drainage becoming subterranean through extensive belts of massive limestone. A series of dry valleys, for example, has been preserved in the retro-wedge Aptian/Barremian outcrops that extend from the Fenouillèdes to the Pays de Sault. The dry valleys document a redirection of drainage towards the Aude (a Mediterranean river), thereby beheading the Hers (an Atlantic river) and also leading to internal drainage reorganisations within the Agly catchment (another Mediterranean river). Similar ancient valleys correlate topographically with karstic landforms such as the large Pays-de-Sault polje, and stratigraphically with gravel deposits of Lannemezan affinity which occur as a well-preserved trail all the way into the youngest and best-preserved dry valley of the area at the Col du Chandelier. All of these ancient valleys currently hang 300–400 m above the modern active valley floors. Similar configurations have been well studied in the Arbailles massif (Vanara et al., 1997; Vanara, 2000), which is cut by the two large dry valleys of Ithé and Eltzarreordokia. The floors of these dry valleys lie more than 400 m above the active Bidouze and Saisons watersheds, and they are the legacy of ancient streams flowing northward through the Arbailles from the Mendibelza massif situated to its south. In the South-Pyrenean massifs of the pro-wedge, the Llinars–Pla de la Llacuna dry valley (see Fig. 8A), which must be very ancient given its relative elevation of 875 m above the Segre River at Oliana, is an important landmark. The eastern termination of the Montsec thrust-front scarp is incised by three ramified dry valleys that have been cut to depths of 100–150 m beneath pediment P1 and currently hang 750 to 650 m above the Noguera Pallaresa river channel (Fig. 8B). These ancient streams used to drain the eastern half of the Conca de Tremp and joined either the Segre or the Noguera Pallaresa after having cut through the Montsec gorges. They were subsequently beheaded and became diverted towards the Noguera Pallaresa upstream of its gorge through the Montsec, thus abandoning their earlier courses.

The retro-foreland basin retains a number of unexplained features deserving future investigation, such as the Aude valley and its watershed, for example. It has been speculated that parts of the Aude headwaters at one time joined up with the Garonne via the Plateau de Sault and the Hers Vif valley; or via Limoux, then the Seuil de Naurouze and the Hers Mort

valley, which contains vestiges of a middle Pleistocene alluvial terrace at Castelnaudary (Gottis et al., 1972). Very little direct evidence supports these views, however, and heavy mineral provenance studies in the alluvial material have proved inconclusive (Larue, 2007). It appears that the Aude has primarily captured left-bank rivers flowing down from the Montagne Noire, such as the Fresquel, which were former tributaries of the Garonne. Several dry valleys in the lower region of the Aude watershed, which are associated with mappable middle Pleistocene alluvial deposits, have been cut into erosional benches consistent with generations P1 and/or P2, and suggest a progressive drift of the Aude drainage network towards the NE through its limestone fold belts until fairly recently. Whether this trend was driven by tectonic (Ellenberger and Gottis, 1967; Genna et al., 1997; Larue, 2001, 2007) or climatic (Ambert, 1976, 1994) causes remains debated.

4.2.2.3. Staircases of alluvial terraces

Vertical successions of alluvial terraces are commonly used as records of crustal uplift (Bridgland, 2000; Kiden and Törnqvist, 1998; Bridgland and Westaway, 2014; Demoulin et al., 2017), particularly when the elevation offset between two given generations of alluvial deposit increases upstream but tends to level off in the vicinity of the coastline and eventually become a stack of conformable stratigraphic units on the continental shelf. In the Pyrenean context, this configuration is valid in the case of the Roussillon Basin (see Section 5), where five generations of Quaternary alluvial deposits fit this scenario (Delmas et al., 2018), and where the steep seaward tilt of the boundary between Pliocene marine and Pliocene continental deposits also confirms a rise of the east-Pyrenean Axial Zone during the last 4–5 Ma (the stratigraphic boundary is detected at –200 m at the coastline in the Canet borehole, and at +280 m in the intermontane Conflent Basin to the west). The hinge zone at the coast remained relatively stationary over that time period, which explains why the Corbières and Albères coastlines fail to display the abundance of uplifted Pleistocene marine terraces that might be expected in other active tectonic settings. The presumed Tyrrhenian Stage (i.e., highstand palaeoshoreline), which is the best preserved among potential candidates in the Roussillon-Languedoc region, occurs at an altitude of +7 m (Barrière, 1966). Alluvial terrace sequences similar to those of the Têt are also recognised along the Orb (Larue, 2008) and Aude rivers in Languedoc, the Fluvià and Ter rivers in Catalonia, and

equally the Garonne, the Gave rivers, and the lower Adour. Alluvial terraces have similarly been used in the Ebro Basin to document regional uplift, with patterns likewise suggesting increasing magnitudes of uplift towards the mountain belt and an acceleration of uplift during the late Neogene (Stange et al., 2013a, 2016; Lewis et al., 2017).

The vertical successions of alluvial terraces also record a number of strike-perpendicular tectonic upwarps that have caused the rivers to migrate laterally across their foreland topography. In the Aquitaine Basin (Enjalbert, 1960; Barrère et al., 2009), the middle segment of the Garonne has steadily drifted eastward by at least 25 km, forming the extensive left-bank staircase of terraces in the Toulouse area and undercutting the upper terrace system of the Tarn River in the process. The lower Ariège River has undergone a similar evolution. The magnitude of retro-foreland tectonic deformation is appreciated by comparing the maximum altitude of the highest terrace of the Garonne in the Forêt de Bouconne (330 m), west of Toulouse, with the heights of interfluve summits in the Lauragais area, which are capped by coeval alluvial gravels from the Montagne Noire and never exceed 280 m between the Ariège and Hers Mort valleys. Likewise, the Comminges area, which is situated between Saint-Gaudens and Tarbes, was in late Serravallian time the last surviving fluvio-lacustrine depocentre of the Aquitaine Basin: as a consequence of uplift, its deposits now hold a commanding position over the piedmont at an altitude of ~450 m, and the lignite-bearing lacustrine Tortonian beds of Orignac lie at 500 m. Further west, a consistent pattern of downwarping is observed, with for example the successive positions of the alluvial belt of the Gave de Pau indicating a progressive westward drift during the middle Pleistocene. The alluvial belts of the lower Adour River between Soustons and Bayonne also tell a story of southward drift between the early Pleistocene and the present, probably driven by the pattern of coastal subsidence during that same period. This evidence does not appear to be included in existing numerical models that aim to simulate the evolution of the region, and which have emphasized instead the influence of autogenic processes instead of tectonic drivers on both the construction and subsequent incision of the Lannemezan megafan (Mouchené et al., 2017a).

4.2.2.4. The groundwater karst record

During periods of crustal stability, the altitude of major drainage conduits in the karst is adjusted to the upper surface of water tables, the position of which is itself dictated by local topographic base levels. Vadose systems (which typically consist of vertical shafts and narrow meandering saw-cuts) develop instead at times of base-level fall, i.e., in response to crustal uplift and valley incision (Audra and Palmer, 2011, 2013). Discontinuous uplift has accordingly been recorded by the groundwater karst system of some Pyrenean limestone massifs, where several levels of horizontal endokarstic galleries have been mapped over vertical heights of 1 km (Maire and Vanara, 2008). As such, and in similar ways to the alluvial terrace systems but over much longer intervals of geological time, dating the alluvial fill contained in successive generations of endokarstic galleries should provide clues to the chronology of Pyrenean uplift. Thus far, occurrences in the Axial Zone and/or the retro-wedge tectonic belts include the Arbailles massif (5 major levels over a vertical distance of 800 m; Vanara et al., 1997, Vanara, 2000), the Pierre St Martin–Arres d'Anie (8 levels between 1950 m and 450 m; Maire, 1990), the Arbas massif (6 major levels over a vertical distance of 900 m; Bakalowicz, 1988), the Tarascon syncline (middle Ariège valley, with 10 levels over a vertical distance of 600 m; Sorriaux et al., 2016–2018), the upper Aude valley (9 levels over a vertical distance of 600 m), and the Villefranche-de-Conflent syncline (10 to 12 levels over a vertical distance of 1100 m; Calvet et al., 2015b; Hez et al., 2015; Calvet et al., 2019). Among the pro-wedge tectonic units, the Cotiella massif records at least 3 main levels (Belmonte, 2014), and probably 5 to 6 levels occurring at elevations between 2300 and 800 m.

When such karstic cavities are entered by allocthonous rivers transporting quartz-rich debris from Hercynian basement outcrops located upstream, the alluvium deposited in the caves can benefit from terrestrial cosmogenic nuclide (TCN) burial dating in order to establish its residence time under ground. The burial age calculation relies on the radioactive decay of the TCN because, once confined to the cave environment, the debris are shielded from exposure to cosmic rays and thus from further nuclide accumulation. This method usually relies on measuring the concentrations of two nuclides with different half-lives, most commonly ^{26}Al and ^{10}Be, and allows residence times typically between 0.2 and 5.5 Ma to be detected (Granger et al., 1997; Granger and Muzikar, 2001). This kind of work in the Pyrenees is still in its infancy, but data from the Villefranche karst have yielded a mean incision rate of 0.06 mm/yr since the beginning of the Pliocene and 0.11 mm/yr since 1 Ma

(Calvet et al., 2015b). The Arbas massif has recorded 0.24 to 0.13 mm/yr of uplift-driven valley incision since 3.7 to 3 Ma; the Flamisell (Pallars province): 0.11 mm/yr since 1.12 Ma; and the Cotiella massif (Cinqueta canyon) a record 0.67 mm/yr since 1.24 Ma (Genti, 2015; Vernant, 2018) —in a part of the Pyrenees that has also yielded the youngest AFT rock-cooling ages of the orogen (11 Ma). An incision rate of 0.4 mm/yr during the last 400 ka through the Arbailles massif was inferred from the U–Th ages of speleothems (Vanara et al., 1997).

Recent attempts at dating much larger numbers of cave-deposit clasts have nonetheless revealed situations of extreme intraformational age dispersal, with the risk of drawing spurious or arbitrary conclusions about valley incision rates on the basis of inconsistent results (Sartégou et al., 2018). The occurrence of large age dispersals within a seemingly horizontal and laterally continuous alluvial deposit emphasizes two potential sources of error: (i) either a situation of postdepositional sediment mixing within the cave system (possible cause: inputs of older deposits from higher cave levels polluting the deposit through vertical shafts); (ii) or an alluvial unit containing clasts with widely divergent and individually complex exposure histories acquired within the watershed prior to their burial in the cave. In such situations, based on the laws of stratigraphy (in the present case: Charles Lyell's Law of Included Fragments, which governs the logic of relative dating in geology and states that rock fragments must be older than the rock formation containing them), the most likely burial age of an alluvial deposit in a cave must, by default, be the age of its youngest dated clast (Calvet et al., 2019).

5. Quaternary geomorphological evolution

The modern landscapes of the Modern Pyrenees and their piedmonts are dominated by fluvial and glacial landforms. Aeolian, periglacial, and karstic environments have left a less impacting or more localised imprint and are not presented in this review.

5.1. Alluvial deposits

Alluvial terrace treads have been mapped in the pro-wedge valleys outward of the Sierras Interiores, and in some more interior areas near the southern edge of the Axial Zone. Occurrences are also widespread in the upper valleys of the Basque Country, where the

Pyrenees are moderately elevated and were only lightly impacted by glaciation; and throughout the eastern Pyrenees, where the alluvial terrace systems of rivers such as the Têt, the Aude and the Segre have met with opportunities for wide floodplain development in the intermontane grabens of Cerdagne, Conflent and Capcir.

5.1.1. Stratigraphic features

Stages of fluvial incision can be reconstructed from five main generations of alluvial terraces in the eastern basins (Cerdagne, Conflent, Roussillon, Aude) and Aquitaine foreland (Ariège, Garonne, Adour, various Gave rivers). This alluvial chronostratigraphy has benefited from several generations of geological studies underpinned by relative dating criteria such as terrace-tread altitude, palaeontological content, embedded archaeological artefacts (Boule, 1894; Depéret, 1923; Chaput, 1927; Denizot, 1928, etc.), weathering indices, soil characteristics, and connections with frontal moraines (Alimen, 1964; Tricart et al., 1966; Icole, 1968, 1969, 1973; Hubschman, 1973, 1975a, b; Calvet, 1981, 1996; Debals, 2000). Relatively robust correlations have been established on that basis between most watersheds (Calvet et al., 2008; Barrère et al., 2009).

Generations of alluvial deposits in the French geomorphological mapping system are numbered T0 to T5, upward from the modern floodplain to the oldest vestige; on 1:50,000 geological sheets, the ranking is similar but with an alphabetical scheme, i.e., Fz (youngest) to Fu (most ancient). In some cases, a single chronostratigraphic generation of alluvial deposit will be distributed among a population of several terrace treads at slightly different altitudes — e.g., up to 4 treads in the case of T3 on the Têt River (Calvet, 1996; Delmas et al., 2018) and 3 on the Ariège (Delmas et al., 2015) —despite exhibiting identical soil profile and clast weathering characteristics. The opposite situation also occurs, e.g., on some of the Garonne alluvial terraces, when very wide terrace treads are considered diachronous despite being topographically continuous (Chaput, 1927).

In Spain, the earlier systematic inventories tended to share the French approach of numbering generations of alluvial deposits from bottom to top (Mensua et al., 1977; Bomer, 1979; Peña, 1984; Rodríguez-Vidal, 1986; Peña and Sancho, 1988), but Iberian studies have operated on strictly watershed-based inventories of terrace treads, and distinctions between terrace generations are restricted to altitudinal criteria and topographic continuity. The

synthesis for the central part of the Ebro Basin, for example, records 6 terrace levels (from T*I*, i.e., the modern floodplain, to T*VI*) spread over an elevation range of 250 m (Mensua et al., 1977). The uppermost level was given a 'Pliocene to Quaternary' age. The overview produced for the Segre River basin by Peña and Sancho (1988) identified up to 11 terrace levels within a vertical elevation bracket of 200 m in the Cinca tributary watershed and, along similar lines: 8 in the Noguera Ribagorçana and 6 along the Segre itself (modern floodplain included). For the Aragón River, Bomer (1979) reported a minimum of 6 levels. More recent investigations have maintained the tradition of catchment-confined inventories but elected to invert the labelling scheme, thereafter numbering alluvial vestiges from the most elevated / oldest vestige down to the floodplain. This has not only upset the task of matching terrace systems among different valleys of the pro-foreland, but increased the difficulty of correlating the incision histories of watersheds on opposite sides of the mountain range. Under this new rationale, 12 levels were identified by Benito et al. (1998, 2010) above the active floodplain of the lower Gállego River, but only 9 by Lewis et al. (2009, 2017) — who also reported 10 in the Cinca watershed (as opposed to the 11 by Peña and Sancho, 1988). A study by Stange et al. (2013a) reports 8 levels for the Segre (noted TQ0 down to TQ7), 8 for the Cinca (noted in that study Qt2 to Qt10), and 7 for the Noguera Ribagorçana (noted T8 to T2 — but numbering for this particular watershed, unlike the others, starts from the bottom). A correlation of the full sequence of terraces was attempted for the Segre catchment by Peña et al. (2011).

Unlike the Aquitaine Basin, soil and alluvium weathering criteria have not been emphasized in Iberian research, except by Bomer (1979) and Lewis et al. (2009). Predicating correlations between the pro- and retro-foreland river systems on the basis of such criteria holds little promise (i) given the overwhelming prevalence of limestone debris in the Iberian Quaternary alluvium; and (ii) given further the aridity of the Ebro Basin, which has promoted the development of calcrete on all terrace levels (even though caprock indurations get substantially thicker and harder among the older generations of alluvial deposits), except in the upper catchment areas where soil eluviation prevails because of higher rainfall. Indurated facies of this kind are entirely absent from the more humid Aquitaine piedmont, and even from the more Mediterranean Roussillon Basin, where soil eluviation and carbonate dissolution are the rule except locally along limestone scarp-foot settings where hydrological conditions can favour the precipitation of calcium carbonate.

The coarse, and often clast-supported gravel texture of all the Quaternary terrace levels indicates a prevalence of braided channel belts forming floodplains sometimes up to 10 km wide. The depositional sequences are relatively thin (mean thicknesses between 5 and 10 m), and tend to thicken upstream towards the mountain front and near the terminal moraines of outlet glaciers. In the Iberian foreland and among the Mediterranean basins in the east, the alluvial deposits almost always grade laterally to wash pediments covered by a thin mantle of colluvium. These low-gradient and typically concave slope systems become laterally quite extensive in soft-rock outcrops such as shale and molasse, where different generations of these pediments form staircase topography and where the valleys become correspondingly very wide (Barrère, 1975, 1981; Bomer, 1979; Peña, 1984; Stange et al., 2018). Such landscapes are typical of the Iberian drylands and the Maghreb. Apart from the Aude valley, no such landscapes exist in the Aquitaine Basin, where hillslope profiles are more typically convexo-concave and where colluvial deposits are thicker and were emplaced by solifluction and cryogenic transfer rather than by hillwash processes. This sharp contrast emphasizes the profound climatic differences between the pro- and retro-foreland environments, as well as the enduring continuity of the climatic differences — still prevalent today —throughout the Quaternary.

5.1.2. Components of an alluvial chronology

Several of the terraces — mainly the lower levels — connect directly with glacial moraines. Terrace T1, whether along the Garonne or the Ariège, contains numerous Pleistocene faunal remains, typically *Mammuthus primigenius* (Pouech, 1873; Harlé, 1893; Astre, 1928; Clot and Duranthon, 1990), a species that became extinct after the Magdalenian period; but also *Mammuthus trogontherii*, which is understood to have become extinct in the early Weichselian (Astre, 1967).

The first radiometric ages produced in the Pyrenees with the aim of obtaining indirect constraints on the glaciation chronology were ^{14}C ages from peat and lake levels adjacent to some terminal moraines. Results delivered an early Würmian age for these landforms as well as for alluvial deposits from generation T1 (Andrieu et al., 1988; Jalut et al., 1992). In the Roussillon Basin, the continuation offshore of these alluvial units also yielded early or middle (≥ 35,000 yr BP) to late Würmian (18,300 ± 750 yr BP) radiocarbon ages (obtained from

intraformational shell specimens; Monaco et al., 1972). Newer studies have, however, provided ages by direct dating of the alluvial materials, whether by Optically Stimulated Luminescence (OSL) (Lewis et al., 2009, 2017; Benito et al., 2010; García-Ruiz et al., 2013), by TCN burial dating (Stange et al., 2013b, 2014; Delmas et al., 2015, 2018; Nivière et al., 2016; Mouchené et al., 2017b) or by Electron Spin Resonance (ESR) (Duval et al., 2015; Sancho et al., 2016; Delmas et al., 2018). Radiocarbon (Lewis et al., 2009) and palaeomagnetic dating (Sancho et al., 2016; Lewis et al., 2017) have also been attempted, but multi-method dating of alluvial terrace systems is otherwise still an all too rare endeavour.

A Pyrenean-scale synthesis of alluvial chronostratigraphy was produced by Delmas et al. (2018). In the Iberian foreland, only the two uppermost levels are older than the Bruhnes–Matuyama boundary, i.e., > 780 ka. The topmost alluvial deposits have been dated by ESR in the Cinca and Têt watersheds as 1.27 Ma and 1.1 Ma, respectively. These depositional ages are consistent with indirect estimates given by palaeobotanical assemblages for stratigraphically coeval deposits such as the Belin and Sadirac formations in the Landes (see Section 3.1.5.2), likewise for the proto-Garonne floodway (Dubreuilh et al., 1995) — and thus also for the upper units of the Lannemezan Formation (noted ‘Fu’ on French geological maps), which are distinguished by the exceptionally large calibre of their boulder beds (Icole, 1968, 1969, 1973). In the extensional basins of the Mediterranean seaboard, T5 is inset in the the continental Pliocene wedge-top alluvial sequence. The 2–3 Ma age for the top of that sequence was determined on the basis of micromammalian assemblages (MN 15 and MN 16) contained in coeval alluvium trapped in karstic cavities among the limestone plateaus situated at identical elevations along the edge of the Roussillon Basin (Delmas et al., 2018).

For the Middle Pleistocene, an ESR age of 817 ± 68 ka was obtained for TQ2 in the Alcanadre River valley (Duval et al., 2015). Existing TCN profiles have mostly provided minimum ages for the alluvial terraces (Delmas et al., 2018). Combined TCN and ESR ages obtained for generation T3 point to an age range between MIS 16 (terminates at 621 ka) and MIS 8 (terminates at 243 ka) for the Têt, Ariège, and Garonne rivers, which is consistent with the abundance of Pebble culture or Acheulian artefacts collected from these terrace treads (Collina-Girard, 1976, 1986; Capdeville et al., 1997; Bruxelles et al., 2003; Martzluff, 2006; Mourre and Collonge, 2007; Hernandez et al., 2012). With a dozen OSL ages, two TCN vertical profiles, and two ESR ages, the most intensively dated generation of terraces in the

Pyrenees are Level 5 of the Iberian foreland and its equivalent T2 ('Fx') on the French side. It has consistently yielded ages compatible with MIS 6 (terminates at 130 ka).

During the recent Pleistocene, terrace sequence geometries ~~i~~n the Ebro Basin contrasted quite strongly with those of the other piedmonts. In Aquitaine, TCN profiles indicate that glacifluvial valley train T1 aggraded continuously until the Last Glacial Maximum (LGM, 26–19 ka), perhaps extending into the Lateglacial. In Iberia, the last glacial cycle generated a sequence of 4 terraces along the left-bank tributaries of the Ebro River, with just the lowermost tread correlating with the LGM. Fluvial incision rates thus appear to have accelerated everywhere during the Middle Pleistocene, but more so in the Iberian foreland than in Aquitaine, probably because of comparatively larger magnitudes of regional crustal uplift in the Iberian foreland and the rest of the Iberian Plate.

5.2. The impacts of glaciation

Despite their southerly position (43–42° N), the Pyrenees were glaciated at every stage of the Pleistocene, and are still residually glaciated today. Contrary to other Mediterranean mountain ranges, where Quaternary glaciation usually produced localised glaciated core areas, the Pyrenean icefield during glacial maxima typically extended uninterrupted for 250 km from the Capcir Basin in the east to the Pic d'Orhy in the west (Fig. 12). The spatial distribution of Pleistocene glaciers is now well established and has been synthesised and updated repeatedly (Penck, 1883, 1894; Taillefer, 1957, 1967, 1969; Hérail et al., 1987; Martí Bono and García Ruiz, 1994; Calvet, 2004; Barrère et al., 2009; Calvet et al., 2011).

The spatial distribution of Quaternary glaciers was dictated by a combination of E–W and N–S climatic gradients. The N–S asymmetry is the sharpest, with the northern mountain front open to Atlantic influence and concentrating 75% of the glaciated surface area. The Pleistocene mean Equilibrium Line Altitude (ELA) lay between 1200 and 1600 m along the outermost mountain front, rising a little into the core of the Axial Zone (reconstruction from cirque-floor elevations). The tips of the largest outlet glaciers reached lowland altitudes of 350 m (Ariège) and 450 m (Garonne), with glacier lengths attaining 43 km along the Gave d'Ossau, 53 km along the Gave de Pau, 79 km for the Garonne, 65 km for the Ariège, with maximum ice thicknesses in each case 0.8–1 km. Limiting factors of ice extent have been the narrowness of the Pyrenees and the dominance of transverse drainage (limited

opportunities for confluent iceways). Transfluence cols between parallel valleys are uncommon (col de Lhers, col du Portillon) because of fairly ubiquitous supraglacial relief channelling ice in underfilled pre-existing valleys. The large ice accumulation on the north side of the range nonetheless contributed to spill over onto the southern side via a number of divide breaches, each situated at increasingly lower elevations from east to west and some of them late Neogene palaeovalleys (see Section 4.2.2.2) (Col de Puymorens: 1917 m; Port de Bonaigua: 2072 m; Pla de Beret: 1870 m; Col du Pourtalet: 1795 m; Col du Somport: 1631 m). The only documented example of a reverse situation occurs around the Pico de Aneto, the highest summit of the Pyrenees, where several glacial diffluences benefited the Garonne.

The Iberian pro-wedge contained comparatively shorter and thinner (400–600 m) valley glaciers, with outlet-glacier ice fronts terminating at elevations between 750 m and 940 m. Glacier lengths rarely exceeded 30 km (Aragón Subordan: 25 km; Aragón: 23 km; Gállego: 42 km; Ara: 32 km; Cinca: 26 km; Pallaresa: 48 km; Esera: 34 km; Ribagorçana: 24 km; Valira: 31 km). The Pallaresa and Valira trunk glaciers may have attained maximum lengths of 58 and 39 km, respectively, probably aided by inputs from tributary valley glaciers feeding into the trunk valley during periods of maximum ice advance (Serrat et al., 1994; Turu et al., 2007; Turu, 2011; Turu et al., 2011, 2017). On the Iberian side, the ELA rises rapidly southward to elevations above 2100–2200 m in the outermost massifs of the Axial Zone and Sierras Interiores, and to even higher altitudes in the case of south-facing slopes.

The E–W climatic gradient along the range is gradual. The icefield was more fragmented in the east as a combined result of diminishing Atlantic moisture advection from the west, and of the increase in aggregate sunshine hours under Mediterranean influence. Among the outlet glaciers along the northern mountain front, only the Gave de Pau at Lourdes and Gave d'Ossau at Arudy formed piedmont glacier lobes. The ELA was particularly low in the Basque Country (1100–1200 m; Viers, 1960), a fact confirmed by small glacial cirques on east- and north-facing summits as low as 1300 and 1500 m (e.g., Autza, 1304 m), and even occasionally on south-facing slopes (e.g., Orzanzurieta, 1570 m). From there, the ELA rose progressively towards the central Pyrenees (Barrère, 1954, 1963), where it maintained itself around 1300–1400 m among the outermost massifs as far east as the Ariège, whether on north-facing or on south-facing slopes (in the latter case by virtue of disproportionate supplies of windblown snow from the NW, as for example in the Arize massif). The ELA

attains 1600 m in the upper catchments of the Hers, Aude and Boulzane (Dourmidou massif), i.e., ~60 km from the Mediterranean coast. In the eastern Pyrenees, (i) greater fragmentation of relief resulting from the Neogene extensional tectonics and (ii) relative aridity of the sheltered intermontane basins have conspired to a confinement of glaciation to the most elevated massifs of the Axial Zone. Here the ELA is situated between 2000 and 2300 m, the valley glaciers were short (among the longest, the Têt: 18 km, and the Querol: 25 km) and never extended below the 1000–1500 m elevation belt. At these easterly longitudes, the icefield was often little more than a population of cirque glaciers.

Quaternary climatic contrasts in the palaeoglaciology of the Pyrenees were merely an exaggerated version of present-day climatic contrasts, also reflected in the pattern of the modern winter snowline. It can thus be safely inferred that average climatic conditions and average atmospheric circulation patterns in the region have remained similar throughout the Quaternary (Barrère, 1954; Taillefer, 1982; Calvet, 1996). These conditions include: (i) permanent air flow from the W to NW, bringing snow but also favouring its local redistribution over ridgetops and thereby supplying east- and even south-facing cirques (e.g., Crest et al., 2017); (ii) the interference of Mediterranean air flow from the southeast, which is also a source of abundant snowfall in present-day conditions in the eastern part of the range; and (iii) the considerably greater dryness and warmth of the southern and eastern Pyrenees — with negative consequences on the thermal budget of glaciers in those areas.

It would be spurious to overstate the geomorphological legacy of Quaternary glaciation on Pyrenean landscapes and slope systems. The glacial imprint is strongest in the cirque belt (Crest et al., 2017), which in some massifs displays characteristic arêtes and a few pyramidal peaks. In the eastern Pyrenees, however, the limited erosive power of the Pleistocene glaciers has, for example, failed to eradicate the erosion surfaces, and indeed even the very deep mantles of saprolite which, at many places, cover these elevated residuals of Neogene topography (Delmas et al., 2009). Farther west, a number of valleys include areas that underwent between 230 and 400 m of glacial overdeepening (e.g., Gave de Pau and Garonne, based on gravimetric surveys; Perrouty et al., 2015), and up to 100 m in the Ariège valley at Ussat (borehole evidence from BRGM–Banque du Sous-Sol). On the pro-wedge, overdeepened valley sections likewise attain ~400 m at Esterri d'Aneu (Noguera Pallaresa), 300 m at Benasque (Ésera valley), 200 m at Bono and 160 m at Barruera (Noguera Ribagorçana; Bordonau, 1992), 80 m in Andorre (Valira valley), and 160 m at Biescas (Gállego

valley; Turu et al., 2007). Overall, however, most of the larger valleys exhibit large bedrock steps, e.g., along the Ariège at Tarascon and Les Cabannes. None of the wider glacial troughs are calibrated to a characteristic U shape, and V-shaped gorge sections are frequent and even include entrenched fluvial meanders (such as between Ax-les-Thermes and Mérens on the Ariège). This relatively light erosional imprint of warm-based glaciers also explains the indecision among scholars as to the true terminal positions of valley glaciers in some V-shaped valleys such as the Noguera Pallaresa, Cinca, Valira, and Salat.

Rare estimates of catchment-wide glacial denudation during the last glacial cycle have been obtained by calculating the density-corrected volume of glacial sediments contained in glacial accumulation zones. For the short Têt glacier (18 km), mean Würmian (Late Pleistocene) denudation depths did not exceed 5 m (mean denudation rate of 0.05 mm/yr) — a low value compatible with the good state of preservation of pre-glacial erosion surfaces and their regolith in that area (Delmas et al., 2009). Based on sediment volumes trapped in valley-floor rock basins along the Gave de Pau and the Garonne (Perrouty et al., 2015), bedrock denudation during the last 30 ka (i.e., since the onset of ice retreat from its terminal positions) can be calculated after density correction and produces rates of ~0.08 mm/yr and ~0.05 mm/yr, respectively. Based on TCN nuclide concentrations contained in glacially polished bedrock-step surfaces among the cirques of three massifs in the Axial Zone (Maladeta, Bassiès, Carlit), Crest et al. (2017) demonstrated that glacial denudation in the cirques was weaker under icefield conditions during the Würm (1–30 mm/kyr, because the ELA was situated much lower down in the valleys) than under residual (but steep and erosive) cirque-glacier conditions in the widely deglaciated environments of the Younger Dryas and the Holocene (tens to hundreds of mm/kyr). TCN data from supraglacial ridges, meanwhile, document erosion rates of 10–30 mm/kyr during the last 15 to 60 ka. Würm-averaged denudation ratios between cirque floors and ridgetops thus suggest that they underwent similar rates of downwearing, but that cirque glaciers during short time windows and under certain specific conditions are far from negligible geomorphic agencies.

6. Synthesis and discussion: issues resolved and unresolved

From the late Cretaceous to the present, the Pyrenees as a mountain range rising between Europe and Iberia went through three successive and definable states: the Proto-Pyrenees, the Ancestral Pyrenees, and the Modern Pyrenees. Throughout this 84 m.y. period, the mountain range changed in length, width, relief and elevation. Clearly, portrayals of those successive incarnations become more precise for recent geological time as a richer catalogue of indicators becomes available to direct field observation, including landforms and superficial deposits. The oldest landforms of value are the erosion surfaces preserved from the late stages of the Ancestral Pyrenees. Uncertainty nonetheless still hangs over a number of issues, which we present and discuss in this synoptic overview which can be followed by inspecting Plate I.

6.1. The Proto-Pyrenees

Folded structures detected as far west as the Basque Country began to develop after ~84 Ma, but at the end of the Cretaceous the resulting mountain range, or Proto-Pyrenees, formed only in the eastern third of today's Pyrenean range and extended farther east into the area now occupied by the Gulf of Lion. The west-central and western Pyrenees did not exist as a mountain range at the time, i.e., rather only as a belt of crustal deformation (Plate I, panel A). The Garumnian continental sequence is a late- to post-tectonic molasse (only a few growth strata indicating mild deformation), and as such is the product of these eroding Proto-Pyrenees but also of eroding topography in the southeast (e.g., Montseny; Gómez-Gras et al., 2016) and potentially in Corsica and Sardinia (Odlum et al., 2019). Outcrops of Garumnian molasse have been preserved north of the Proto-Pyrenees in the Corbières, and south between Tremp and the Llobregat River valley (Plaziat, 1981, 1984; Rosell et al., 2001). High-energy denudation ca. 78 Ma, probably driven by high relief, has been inferred from fission-track evidence in U–Pb-dated detrital zircons in the Iberian foreland sequences (Whitchurch et al., 2011), and likewise between 80 and 68 Ma from AHe ages on detrital zircon crystals (Filleaudeau et al., 2011). This record of rapid denudation has been confirmed by late-Cretaceous to Paleocene zircon FT cooling ages in bedrock in the NE Axial Zone and North-Pyrenean Zone (Yelland, 1991) and ZHe cooling ages (Ternois et al., 2019). Denudation of the Proto-Pyrenees was sufficiently advanced by early Paleogene time that part of the orogen became drowned by sea-level rise and covered by an early Ypresian (i.e., Ilerdian:

~56–52 Ma) carbonate platform and by shale. A fission-track age of 81 Ma, however, was also obtained from the Ursuya Massif (Basque Country) (Yelland, 1991), and is associated with comparatively ancient AHe ages (Vacherat et al., 2014). This evidence could indicate higher topography farther west during the Garumnian episode than previously believed. Continuing research may provide new resolution to the Basque and Catabrian palaeorelief and denudation histories of that period (DeFelipe et al., 2019). The fate of the eastern Proto-Pyrenees remains largely speculative (Jolivet et al., 2020), but the extended period of tectonic quiescence reported in the literature between 68 and 56 Ma, the abundance of lacustrine limestone in the Garumnian molasse, and the Ilerdian marine transgression (Plate I, panel B) over much of the region suggest that the Proto-Pyrenees had by that time attained a residual state of relative low-elevation and low-relief topography.

6.2. The Ancestral Pyrenees

6.2.1. Growth of the mountain range from east to west

The Pyrenees grew westward during the Eocene as a consequence of continuing tectonic inversion from east to west of the Cretaceous and early Eocene flysch-filled pro- and retro-foredeeps (Plate I, panels B, C, D). Still by the end of Lutetian time, the emergent successor mountain range, i.e., the Ancestral Pyrenees, did not extend westward beyond the Pic d'Anie (0°43' W). Denudation of the thickening crust supplied thick range-front megafans. The debris were delivered in a terrestrial environment to the retro-foreland (Palassou sequences) and in a deltaic environment to the pro-foreland (Plate I, panel C). Crustal denudation of the Axial Zone resulted in part from the north- and southward transport of its sedimentary cover nappes, but also from fluvial erosion. The Hercynian basement core of the orogen only gained widespread exposure during the Bartonian, after which time the delivery of granite and gneiss pebbles to the piedmonts occurred regularly, often in periodic pulses, from the basement window. The Ancestral Pyrenees appear to have peaked (peak energy, peak topography) from the Priabonian to the Oligocene, at a time when the Ebro Basin was also entering its ~25 million-year period of internally-drained confinement and when the mountain-front fan systems on both sides of the orogen became ubiquitous (Plate I, panels D, E). The western Basque termination of the orogen is unique in having remained

marine to this day. Low-temperature thermochronology evidence from crystalline basement rocks in the Axial Zone, from its satellite massifs, as well as from the conglomerate sequences of the pro-foreland, provides a consistent picture of accelerated denudation beginning ca. 50 Ma and peaking around 35–30 Ma (e.g., cooling-inferred denudation rates of up to 1–3 km/Ma between ~35 and 30 Ma in the Maladeta massif; Fitzgerald et al., 1999; Sinclair et al., 2005; Gibson et al., 2007). Denudation also appears to have been spatially nonuniform, progressing from east to west but mostly from north to south (Whitchurch et al., 2011).

The classic model of the central Pyrenees as a high-amplitude antiformal duplex structure (Muñoz, 1992; Vergés et al., 1995) — implying ~20 km of crustal denudation in the Axial Zone in order to attain the current outcrop pattern — has been substantially reconsidered here on the basis of new intepretations of Hercynian and Alpine structures and their tectonic geometries (Soler et al., 1998; Laumonier, 2015; Angrand, 2017; Cochelin et al., 2018; Teixell et al., 2018; Espurt et al., 2019; Ternois et al., 2019). The Hercynian structures of the Axial Zone are only weakly offset by the putative décollement of the 'Nogueres' Thrust (see Fig. 3), and the magnitudes and timing of crustal denudation in the Axial Zone to the north (Marimanya–Artiès massif) and south (Maladeta massif) of that crustal discontinuity are identical (see Cochelin et al., 2018, after Fitzgerald et al., 1999, Sinclair et al., 2005, and Gibson et al., 2007). ZFT results also confirm that denudation depths were not as extreme as initially postulated, as shown for example by many zircon grains having retained the signature of Mesozoic extension in the North-Pyrenean (Vacherat et al., 2016) and Axial zones (Yelland, 1991; Sinclair et al., 2005). Detrital zircons from Paleogene molasse sequences in the Ebro Basin convey a similar message, with only 17% of the 842 grain ages reviewed by Whitchurch et al. (2011) recording a ZFT age compatible with the collisional stages of the Pyrenean orogeny. Erosional denudation did thus probably not exceed depths corresponding to the total resetting of the zircon FT clock, e.g., 7–10 km when assuming an average geothermal gradient of 25–30 °C/km (Whitchurch et al., 2011).

The evidence for reconstructing the elevation, relief and morphology of the Ancestral Pyrenees is very limited. The Paleogene mountain range was narrower than its modern successor, and the fold belts of the retro-wedge were mostly buried beneath the debris of the Aquitaine piedmont. The pro-wedge was likewise drowned by unconformable conglomerate sequences, locally backfilling all the way up to the edge of the Axial Zone in

one atypical region (Nogueres) of the south-central pro-wedge. Flexural modelling of the Ebro Basin has produced maximum palaeoaltitude estimates in middle Lutetian time of 2000 ± 460 m for the mountain range (Millán et al., 1995), with mean and maximum palaeotopogaphic values estimated as 1.5 and 3.5 km, respectively, during the Oligocene orogenic climax (Curry et al., 2019). Other work has used oxygen isotope ratios in Eocene oyster shells sampled from the Ebro Basin. By comparing the $\delta^{18}O$ ratios with those measured in a reference set of similar-aged mollusc shells from the Paris Basin, Huyghe et al. (2012) inferred a magnitude of Pyrenean uplift of 2000 ± 500 m between 50 and 41 Ma. The palaeoaltimetric calibration fails to be valid past the late Bartonian.

6.2.2. Correlation between conglomerate sequences of the pro- and retro-forelands

Beyond these first-order similarities between the pro- and retro-wedges in the Ancestral Pyrenees, some uncertainty remains over the finer detail of the foreland and retro-foreland geological records. For example, no correspondence has ever been established between the four generations of Palassou clastic pulses, which were given a uniform name by French geologists and are now correlated with their Jurançon analogues, and the conglomeratic sequences of the Iberian side, which have received a collection of local names in the literature (Fig. 5). From east to west along the strike of the Ebro Basin, we suggest the following chronostratigraphic correlations:

(i) Palassou 1 could be an equivalent of at least part of the Bellmunt formation in the east, the Queralt conglomerates at Berga, and of the Campanue Formation further west;
(ii) Palassou 2 could match the Milany sequence and upper part of the Bellmunt formation in the east, the basal beds of the unconformable Nogueres sequence (Pessonada unit), the lower part of the Escanilla Formation, and still further west the Sabiñanigo deltaic sandstones, whose proximal conglomeratic facies has an unidentified provenance (its source area could be the Escanilla Fm. in the east; if correct, this would confirm that no mountainous relief shedding clastic debris yet existed at that longitude to the north);
(iii) Palassou 3 could correspond to the lower levels of the Berga sequence in the east, to the Serrat Negre–Catllaras conglomerates and middle levels of the Nogueres sequence in the

central pro-foreland, and to the lower part of the Campodarbe Formation further west (Escanilla and Santa Orosia conglomerate beds);

(iv) Palassou 4 could correlate with all of the younger remaining Oligocene conglomerate beds of the pro-wedge mountain front.

These correlations are inevitably tentative because the tectonic regime of the Ancestral Pyrenees was unsteady, spatially nonuniform, and diachronous given the evident polarity of crustal deformation from east to west and asymmetrical vergence from north to south (Fig. 2). The more striking asymmetry between the pro and retro basins lies in the cumulative thickness of the proximal conglomeratic sequences, which turn out to be considerably greater in the Iberian foreland. This imbalance, however, may be more apparent than real for several reasons: (i) the pro-wedge watersheds were larger than their retro-wedge counterparts, thus with more potential for sediment delivery; (ii) in the Aquitaine Basin, the Paleogene rivers were afforded uninterrupted opportunities to export at least their finer clastic loads to the Atlantic, whereas the Ebro Basin was denied opportunities of sediment bypass for 25 m.y. after the Priabonian; (iii) the outward growth of the orogenic wedge during the Paleogene was much more extensive on the south side of the orogen (e.g., producing the SPCU and the Guarga Unit), with the resulting crustal thickening thus promoting greater opportunities for denudation and for peripheral lithospheric flexure to accommodate greater depositional thicknesses; (iv) the northern piedmont has undergone limited uplift and the Paleogene conglomerate sequences accordingly feature few good exposures, whereas the southern piedmont has risen to 1500–2000 m and been deeply incised, thereby affording an exceptionally rich display of outcrops and stratigraphic sections.

Given that the Cenozoic conglomerate sequences are continental, resorting to the ELMA scale is both inevitable and necessary, but progress on the chronostratigraphy of Paleogene and Neogene clastic sequences would gain from continued efforts towards narrowing the gaps and discrepancies sporadically apparent between the ELMA scale (Vandenberghe et al., 2012; Hilgen et al., 2012) and the magnetostratigraphic scale, particularly when uncertainty envelopes surrounding age constraints are not systematically reported. Although not exceedingly large, discrepancies appear most acute in parts of the Ebro Basin, which overall

nonetheless benefits from an unusually continuous magnetostratigraphic record (e.g., Beamud et al., 2003, 2011; Garcés et al., 2020) compared to the other Pyrenean depocentres.

6.2.3. Topographic decline of the Ancestral Pyrenees

Crustal convergence, which intensified from east to west during the Eocene, ceased fairly abruptly in the east in Chattian time, after which back-arc extension began to open the Western Mediterranean (Plate I, panels E, F). AFT and ZFT data from the Canigou–Carançà and Albères massifs record the early Oligocene to Miocene rifting event quite clearly (Maurel, 2003; Maurel et al., 2002, 2008), but it remains difficult elsewhere in the eastern Pyrenees to attribute any of the Oligocene cooling ages unequivocally to rifting rather than to the final stages of collision.

Meanwhile, compressional tectonics continued in the western half of the Ancestral Pyrenees at least until early Burdigalian time, and perhaps as late as Langhian time according to Huyghe et al. (2009). Thermochronological data in the western part of the Axial Zone document this episode of uplift and erosion, particularly on the south side with some AFT ages spanning the Aquitanian to the middle Miocene (Jolivet et al., 2007; Bosch et al., 2016b). The most salient paradox in this part of the orogen is the absence on its north side of an equivalent of the synorogenic, early Miocene Huesca and Luna megafans (Plate I, panel G), at least given that the age of the Jurançon conglomerates has now been revised and assigned to the Paleogene. The cause of the asymmetry lies perhaps in the southward vergence of tectonic deformation during these late stages of crustal convergence. Folding in the Sierras Exteriores, in particular, was promoted by the progression of the youngest and outermost thrust sheets, i.e., the Bielsa and (further south) the Guarga thrusts. Resulting folds in the poorly consolidated sediments of the Jaca Basin display a total structural amplitude of ~2 km (e.g., the Santo Domingo and the Yebra de Basa anticlines). Such high structural relief associated with lithologies that are quite susceptible to erosion is unique to the south side of the orogen, and the resulting erosion has generated a large proportion of the Huesca conglomerate sequences (i.e., the Aquitanian to Burdigalian Uncastillo and Sariñena formations) (Puigdefábregas and Soler, 1973; Teixell and Garcia-Sansegundo, 1995; Jolivet et al., 2007; Huyghe et al., 2009; Bosch et al., 2016b). Meanwhile, clastic output to

4023 the retro-foreland, where tectonic activity was less intense, was comparatively finer-
4024 textured and thus more readily exported to the deep ocean through the Bélus–Saubrigues
4025 palaeocanyon, which was functional at that time.
4026
4027 *6.2.4. The summit erosion surfaces of the Ancestral Pyrenees: resolved and unresolved issues*
4028
4029 The summit erosion surfaces are the most ancient landforms of the present landscape and
4030 record a period of low energy that prevailed at the time of transition between the Ancestral
4031 and the Modern Pyrenees. When compared with a large number of other ranges around the
4032 world, these low-gradient land surfaces are far from unique features (Calvet et al., 2015a),
4033 and the list of arguments concerning their age and origin presented in Section 4.1.3 supports
4034 a parsimonious explanation emphasizing regional base-level controls. The view that these
4035 elevated erosion surfaces in the Axial Zone, and the former depositional surfaces of the
4036 Nogueres or Palassou conglomerates in each of the piedmont zones, at one time formed a
4037 coeval and cogenetic low-gradient continuum is challenged by the fact that deformed
4038 structures in the conglomerate units are themselves cross-cut by low-gradient erosion
4039 surfaces. The erosion surfaces are thus younger than the youngest conglomerate deposits.
4040 The altiplanation theory inspired by sandbox models (Babault et al., 2005b, 2007; Bosch et
4041 al., 2016a) is therefore unsupported by primary field evidence.
4042 Unresolved issues include the multiplicity of erosion surfaces and their possible diachronous
4043 development across the orogen (Fig. 11). This is prima facie the logical consequence of
4044 diachronous tectonic deformation from east to west, with compressional tectonics still
4045 prevalent during the early Miocene in the west whereas rifting had started in mid Oligocene
4046 time in the east. The widespread mountain-top surface, S, was produced in the east
4047 between the late Oligocene and the Aquitanian (Plate I, panel F), a time frame also
4048 consistent with the approximately simultaneous aggradation of abundant carbonate facies
4049 across all three piedmont areas of the Pyrenees. This consistent pattern would suggest low
4050 turbidity levels because of diminished terrigenous influx from a tectonically active orogen
4051 rather than exclusively a palaeoclimatic signal. Partial planation surface P1 spared a number
4052 of large residual massifs and grades very clearly to middle Miocene marine strandlines in the
4053 Corbières and Languedoc (Plate I, panel H), suggesting a simultaneous relative lull in crustal
4054 deformation at the time of the Langhian highstand.

Uncertainty over these scenarios increases farther west. Among the three conceptual models summarised in Fig. 11, scenario A is improbable given that the clastic record in the western pro- and retro-foreland basins contains no evidence of declining energy in the sedimentary systems: supply of coarse-textured synorogenic sequences was uninterrupted from Priabonian to Chattian time included, and even extended into the Aquitanian according to the new ages (22 Ma) obtained by Roigé et al. (2019) for the Campodarbe Group conglomerates of La Peña. Scenario B postulates diachronous peneplanation of the Pyrenees from east to west. Its main weakness is that it implies minimal mountainous relief at a peak time of evaporite accumulation in the Ebro Basin. Although it could explain the development of thick lacustrine limestone in the last stages of internal drainage in the Ebro Basin (see Section 3.2.6; Vásquez Urbez et al., 2013; Pérez Rivarés et al., 2018) and the return to externally-drained conditions after ~10 Ma, it fails to justify how such extreme aridity could prevail at < 100 km from the Atlantic Ocean without shelter from a mountain barrier. By reference, however, to the sharp contrast in mean annual precipitation observed today across the continental dividing ranges of the Basque Country, whose summits do not exceed 1400–1500 m, it would seem nonetheless that an Ancestral Pyrenean mountain range attaining maximum elevations of ~1400 m among its residual massifs would have been sufficient to shelter the Ebro basin from Atlantic humidity — as advocated by scenario C in Figure 11.

Scenario C admits the possibility that the Pyrenees were never substantially levelled other than in the east. Only partial planation surfaces (i.e., pediments) analogous to P1 formed around the edges of the pro- and retro-wedges, as well as as in the Basque Country (compare Plate I panels F, G and H). This scenario is tentatively the most realistic because in keeping with the chronology of tectonic deformation and the chronostratigraphy of the foreland conglomerate sequences. It concurs with the preservation of the crustal root west of Andorra, whose ongoing erosion / removal (by debated processes, see Section 2.4) appears to have only recently begun (Dufréchou et al., 2018). It is also consistent with the necessity for a sharp climatic contrast between the humid north and arid south sides of the mountain range to have been upheld from the Paleogene through to the middle Miocene. The absence of coarse clastic Miocene sequences in the Aquitaine foreland does not, however, militate in favour of a high-relief mountain range in the hinterland at the time. Likewise, although thermochronology is an insufficiently sensitive tool for discriminating

between scenarios A, B and C given that (for example) cooling ages obtained from sampling sites on surfaces S and P1 are usually indistiguishable, the widespread documentation of a thermal plateau in Pyrenean rock cooling curves (Section 4.1.3.1, Fig. 10C) after 30 or 20 Ma does not militate in favour of intense denudation occurring in the Axial Zone during the Miocene. Limited relief still remains the best candidate for explaining this situation, with low-gradient erosion surfaces forming at elevations of ~800 m or less in connection with one or several among the three base levels of the orogen.

6.3. Shaping of the Modern Pyrenees

The multiple and abrupt breaks in the geological record around and after 10 Ma in all three piedmont environments of the orogenic wedge (Aquitaine, Mediterranean, Ebro) turned a definitive page in the history of the Paleogene mountain range, or Ancestral Pyrenees. The orogen thereafter entered the age of the modern mountain range as we observe it today. The characteristics of these successor Pyrenees (i.e., Modern, post-shortening) were heralded by major changes in the geodynamic regime, involving:

(i) a relaxation of Cenozoic crustal convergence intensity;

(ii) a return to external drainage in the Ebro Basin;

(iii) the opening of new extensional basins far into the Axial Zone, i.e., in locations progressively more remote from the Mediterranean back-arc basin;

(iv) the occurrence of volcanic activity in the eastern part of the mountain belt;

(v) a symmetrical interruption in the depositional stratigraphy not just of the Ebro Basin (which became exorheic after ~10 Ma), but also of the Aquitaine Basin (major ravinement surface beneath the Lannemezan megafan and its coeval analogues along the strike of the mountain range: Ger, Salat, etc.);

(vi) the conveyance of increasingly coarser clastic debris to actively subsiding basins (Turolian fill of the Cerdagne, Empordà and Vallés; Pliocene fill of the Roussillon and Empordà; Lannemezan megafan and its analogues); and lastly

(vii) the construction of increasingly voluminous silicilastic wedges on the continental shelves of the Aquitaine, Valencia, and Gulf of Lion marine domains.

The pull-apart tectonics prevalent during the Oligocene and Miocene in the eastern Pyrenees (Plate I, panels E, F, G, I) progressively gave way to regional uplift of the Pyrenees, elevating the surfaces S and P1 to maxima of 2900 m (e.g., in the Campcardos massif); and likewise raising their younger successor population P2, such as the Plateau de la Perche pediment (eastern Pyrenees) or the Pla de Beret palaeovalley (central Pyrenees), to altitudes exceeding 1500 m. This late regional uplift (Plate I, panels J, K) caused extremely rapid incision of V-shaped valleys during the latest Pliocene and Quaternary. At locations where glaciation has failed to alter valley longitudinal profiles, some large fluvial knickpoints have been preserved such as on the Têt River near Mont-Louis, on the Segre River at Martinet, and on the Aude at Escouloubre — thereby preserving some expanses of unrejuvenated, pre-Quaternary landscape upstream of these knickzones (Figs. 6, 14D).

The geologically recent (and successive stages of) post-shortening surface uplift of the Pyrenees by perhaps up to 2 km is documented not just indirectly by the erosion surfaces, which considered on their own could give rise to circular arguments, but additionally by a range of independent clues:

(i) the substantial increase in volume and clast size of terrigenous inputs to the piedmonts and offsore sequences (particularly the Zanclean of the Roussillon and the Turolian of Cerdagne), which occurred prior to the major climatic downturns of the Pleistocene and therefore cannot systematically be attributed to climatic drivers;

(ii) the deformation, tilting, and normal, inverse or strike-slip faulting recorded in all sedimentary sequences of late Miocene to late Quaternary age, thus testifying to crustal instability caused by more than just an isostatic response to erosional unloading (Vernant et al., 2013; Genti, 2015) (given that extensional faulting can also result from gravitational slope tectonics, reverse and strike-slip faulting are deemed comparatively more robust indices of neotectonic activity, but of course do not rule out normal faulting);

(iii) the geometry of successions of Quaternary alluvial terraces, whose relative vertical offsets increase upstream towards the mountain fronts and into the mountain range (Delmas et al., 2018) but converge and merge as they approach their regional base levels where subsidence has persisted;

(iv) the vertical distribution of fossil cave levels on canyon walls and phreatic or epiphreatic galleries (and even water-table rivers) in limestone massifs, which

provide a more robust record of uplift-driven valley incision than fluvial terraces because, under a solution-limited regime, equilibrium profiles in limestone are attained after a very short time and produce very low gradients (Calvet et al., 2015b);

(v) the fossil warmth-loving plant assemblages in the Cerdagne and Pruëdo intermontane basin fills, which imply very low elevations in the Axial Zone during Vallesian and Turolian time and subsequent uplift of those basin floors by 1000 to 1500 m, i.e., to modern elevations now incompatible with the environmental requirements of these taxa (Suc et al., 2012; Ortuño et al., 2013). Other palaeoaltimetric data for the Cerdagne Basin in the eastern Pyrenees also confirm at least 500 m of late Neogene uplift in the Axial Zone (Huyghe et al., 2020).

Transpression or transtension relating to the Africa–Iberia–Europe convergence and to Mediterranean extension appear to have played a subsidiary and progressively declining role in the rise of the Modern Pyrenees. Uplift, which has impacted not just the mountain range but also its foreland basins and perhaps the entire Iberian Plate, and likewise the Massif Central (Macles et al., 2020) is now attributed to subcrustal and sublithospheric processes driven by boundary conditions that are only partly related to the intrinsic metabolism of an orogenic crustal wedge (see Section 2.4 and Section 4.2.1.1; Pous et al., 1995a, 1995b, Lewis et al., 2000; Barruol et al., 2002, 2004; Gunnell et al., 2008, 2009; Boschi et al., 2010; Casas-Sainz et al., 2009; Chevrot et al., 2014, 2015, 2018; Dufréchoux et al., 2018; Wehr et al., 2018; Conway-Jones et al., 2019; Ortiz et al., 2020; Jolivet et al., 2020). Still unexplained is the apparent acceleration of the uplift and its unsteady regime, illustrated for example by the contrast between generation P2 of wide pediments penetrating deep into parts of the orogen, and the abrupt vertical incision of these planar landforms by the deep, often V-shaped, younger valleys.

7. Conclusion and outlook

The Pyrenean orogen is commonly presented in cuts and slices of space or time. This beef-butcher-diagram approach to Earth science is inevitably part of the naming and classification process of naturalistic endeavour. Ramond de Carbonnières (see Introduction) had forecast the Pyrenees to be a fairly simple model of mountain range, and sure enough: in modern

textbooks the Pyrenees have been erected as a reference model of how the subduction of the lower crust and lithospheric mantle of one plate beneath another produces an asymmetric, doubly vergent collisional orogen. Structural style in the Pyrenees was strongly controlled by architectural differences along strike in the early Cretaceous rift and in the Hercynian basement, but the most prominent signature of the orogen has been showcased in the geological literature as its south-vergent duplex structure composed of imbricate thrust sheets of Hercynian basement and forming an almost round-arched antiform (Fig. 3B). As shown in this review, such an interpretation of the south-vergent Pyrenean nappe structure leaves room for an alternative model involving a Supra-Axial Thrust overspanning the Axial Zone and displaying architecturally a much more elliptical intrados, thus rather resembling a three-centered or round-rampant arch (Fig. 3C).

Other narratives have been nurtured in which local features have been extrapolated and held valid for the rest of the orogen: e.g., the implicit view that Ebro Basin overfilling can explain the erosional response of the entire mountain range in the Cenozoic regardless of features and events in the Aquitaine Basin or the Mediterranean; or consideration that the history of the Pyrenees ended with the end of compressional deformation, i.e., in the earliest Miocene, and that the following 25 Ma were essentially a footnote to the orogen's history — the main key event being the reconnection of the Ebro Basin to the Mediterranean and the ensuing downcutting of fluvial valleys in a orogenic edifice (the Ancestral Pyrenees) that was generated during the Paleogene and somehow succeeded in maintaining steady topographic characteristics therafter. Conversely, other issues have been overlooked or sidestepped despite being essential to a full understanding of Pyrenean evolution: for example, what exactly are the architecture and history of the Eocene Iberian foredeep in relation to the SPCU? Why have Miocene continental deposits been abundantly mapped in Aragon but not in Catalonia? The most likely answer is that none were deposited in the Catalonian part of the Ebro Basin, but the eastern boundary of existing deposits of that age between the Cinca and Noguera rivers does not provide consistent information among existing geological maps. Why do the early Miocene conglomerate sequences of the Ebro foreland display no substantial equivalent in the Aquitaine retroforeland? The primary reason is the greater preservation potential of the internally-drained Ebro Basin, whereas a proportion of sediment was exported out of the Aquitaine Basin via the Saubrigues palaeocanyon; but this falls short of explaining the absence of coarse terrigenous deposits of

Miocene age in the Aquitaine retroforeland. Why have chronostratigraphic correlations between the pro- and retroforeland conglomerate sequences never been attempted? Why have the widespread erosion surfaces, some of which were reported or mapped nearly 100 years ago and provide diagnostic clues about mountain evolution and periods of relative base-level stability, been left out of geodynamic scenarios?

This review has provided tentative answers by elimination of the least plausible, but few are currently definitive. It has presented for the first time a joined-up understanding of the Pyrenees, preferring to deal with the mountain range primarily as a topographic entity and using sedimentary rock facies, thermochronology as well as landforms to infer erosional depths, palaeorelief height or steepness, and the orogen's successive rise and decline through time on both sides of the Europe–Iberia boundary. Spanning ~84 Ma of topographic history as a mountain range, reconstructions show that topography was continuously transient, responding to the push of collisional tectonics, but equally to the drawdown of marine base-level changes; to the encroachment of post-shortening extensional tectonics; to the possible vertical pull by a dense crustal root (eclogite) or a lithospheric underthrust of uncertain angle and size; and likely to the buoyancy afforded by asthenospheric processes in a post-shortening context which, since Neogene time, had essentially become an intraplate rather than a plate-boundary setting. As a result, evidence shows that Pyrenean topography has been through a sequence of contrasted states and characteristics, some elevated and mountain-like: e.g., in late Cretaceous time (Proto-Pyrenees), then between the Eocene and late Oligocene (Ancestral Pyrenees), and finally since the late Neogene (Modern Pyrenees); but others less elevated and more plateau-like (including in the form of regional, base-level peneplains): particularly during the late Cretaceous stage of pre-collisional rift inversion west of the Proto-Pyrenees, likewise during the relatively quiescent Paleocene to Ilerdian interval, and most of all later between ~25 and ~9 Ma (Plate I, panels F, G, H, I). Regional uplift in the late Neogene not just rejuvenated the crustal wedge along much of the modern mountain belt, but it also affected the piedmonts, which, whether in the pro-, retro-, or Mediterranean foreland areas, are currently deeply incised by rivers as a result.

Links between asthenospheric, lithospheric, and surface processes are perhaps best illuminated by the suite of diagnostic landforms examined in this review — a long-neglected component of the puzzle. More than 100 years ago, some geomorphologists interpreted certain mountain ranges as 'raised peneplains' (e.g., Davis, 1902), thereby implying recent

uplift (and concomitant valley incision) of older, eroded orogenic structures. Although the driving mechanism was unknown, the Pyrenees were viewed as one of these mountain ranges (de Sitter, 1952); such a two-stage uplift scenario, however, requires attention to landforms and is likely to remain untested by lithospheric-scale numerical models with a low sensitivity to geomorphological constraints (Curry et al., 2019). The counter-intuitive view that elevated mountain ranges may not just be the result of a closed system involving crustal thickening and rock crumpling appears nonetheless to be gaining new relevance globally, partly through the growing awareness that a global intensification of lithospheric and sublithospheric processes with strong impacts on the Earth's surface relief has been occurring since the late Neogene (e.g., Potter and Szatmari, 2009; Baran et al., 2014; Calvet et al., 2015a; Leroux et al., 2017; Kästle et al., 2019). In the case of the Pyrenees, it is now being recognised that the mountain range stands above a large-scale flow of asthenosphere (Gunnell et al., 2008) that does not result from Pyrenean deformation and yet is strongly affecting the behaviour of the lithosphere and crust of the orogenic belt (Jolivet et al., 2020). It is also affecting the geomorphic response of topography within the mountain range as well as across its flanking sedimentary basins. As shown here, observation-based geomorphology can provide clues about the underlying crustal, lithospheric and sub-lithospheric factors that drive long-term landscape evolution, and can thus potentially be used as a calibration tool when tackling orogen-scale evolution as an inverse problem.

Acknowledgements. This review benefited from thorough and valuable comments by Antonio Teixell and Miguel Garcés. BL thanks Mary Ford and Pierre Labaume for fruitful discussions around the Alpine tectonics of the Pyrenees.

References

Adams, J.E., 1985. Large-scale tectonic geomorphology of the Southern Alps, New Zealand. In: Morisawa, M., Hack, J.T. (eds), Tectonic geomorphology. Allen & Unwin, Boston, pp. 105–128.

Addé-Lacomme, J., 1935. Étude de l'Aceratherium de Bézac (Ariège). Bull. Soc. Hist. Nat. Toulouse 65, 76–10.

Aguilar, J.P., 1977. Données nouvelles sur l'âge des formations lacustres des bassins de Narbonne-Sigean et de Leucate (Aude) à l'aide des micromammifères. Geobios 10, 643–645.

Aguilar, J.P., Michaux, J., 1977. Remarques sur la stratigraphie des terrains tertiaires des bassins de Narbonne-Sigean et de Leucate (Aude). Geobios 10, 647–649.

4276 Aguilar, J.P., 1979. Principaux résultats biostratigraphiques de l'étude des rongeurs miocènes du Languedoc.
4277 C.R. Acad. Sci. Paris D 288, 473–476.
4278 Aguilar, J.P., 1980. Rongeurs du Miocène inférieur et moyen en Languedoc. Leur apport pour les corrélations
4279 marin–continental et la stratigraphie. Palaeovertebrata (Montpellier) 9, 155–203.
4280 Aguilar, J.P., 1981. Évolution des rongeurs miocènes et paléogéographie de la Méditerranée occidentale. Thèse
4281 doct. Etat Sci., USTL Montpellier, 203 p.
4282 Aguilar, J.P., 1982. Biozonation du Miocène d'Europe occidentale à l'aide des rongeurs et corrélations avec
4283 l'échelle stratigraphique marine. C. R. Acad. Sci. Paris sér. II 294, 49–54.
4284 Aguilar, J.P., 2002. Les Sciuridés des gisements karstiques du Miocène inférieur à moyen du sud de la France :
4285 nouvelles espèces, phylogénie, paléoenvironnement. Geobios 35, 375–394.
4286 Aguilar, J.P., Crochet, J.Y., Green, M., Sigé, B., 1982. Contributions à l'étude des micromammifères du gisement
4287 miocène supérieur de Montredon (Hérault). Palaeovertebrata (Montpellier) 12, 75–140.
4288 Aguilar, J.P., Calvet, M., Crochet, J.Y., Legendre, S., Michaux, J., Sigé, B., 1986a. Première occurence d'un
4289 mégachiroptère pteropodidé dans le Miocène moyen d'Europe (gisement de Lo Fournas 2, Pyrénées
4290 orientales, France). Palaeovertebrata (Montpellier) 16, 173–184.
4291 Aguilar, J.P., Calvet, M., Michaux, J., 1986b. Découvertes de faunes de micromammifères dans les Pyrénées-
4292 Orientales (France) de l'Oligocène supérieur au Miocène supérieur ; espèces nouvelles et réflexions sur
4293 l'étalonnage des échelles continentales et marines. C. R. Acad. Sci. Paris sér. II 303, 755–760.
4294 Aguilar, J.P., Michaux, J., 1987. Essai d'estimation du pouvoir séparateur de la méthode biostratigraphique des
4295 lignées évolutives chez les rongeurs néogènes. Bull. Soc. Géol. Fr. 8, 1113–1124.
4296 Aguilar, J.P., Michaux, J., 1990. A paleoenvironmental and paleoclimatic interpretation of a Miocene rodent
4297 faunal succession in Southern France. Critical evaluation of the use of rodents in paleoecology.
4298 Paléobiologie continentale (Montpellier) 16, 311–327.
4299 Aguilar, J.P., Michaux, J., Bachelet, B., Calvet, M., Faillat, J.P., 1991. Les nouvelles faunes de rongeurs proches
4300 de la limite mio-pliocène en Roussillon. Implications biostratigraphiques et biogéographiques.
4301 Palaeovertebrata (Montpellier) 20, 147–174.
4302 Aguilar, J.P., Legendre, S., Michaux, J., 1997. Synthèses et tableaux de corrélations. In: Aguilar, J.P., Legendre,
4303 S., Michaux J. (eds.), Actes du Congrès BiochronM'97. Mém. Trav. EPHE (Montpellier) 21, pp. 769–805.
4304 Aguilar, J.P., Michaux, J., 1997. Les faunes karstiques néogènes du Sud de la France et la question de leur
4305 homogénéité chronologique. In: Aguilar, J.P., Legendre, S., Michaux J. (eds.), Actes du Congrès
4306 BiochronM'97. Mém. Trav. EPHE (Montpellier) 21, pp. 33–38.
4307 Aguilar, J.P., Escarguel, G., Michaux, J., 1999. A succession of Miocene rodent assemblages from fissure fillings
4308 in southern France: palaeoenvironmental interpretation and comparison with Spain. Palaogeogr.
4309 Palaeoclim., Palaeocol. 145, 215–230.
4310 Aguilar, J.P., Antoine, P.O., Crochet, J.Y., López-Martínez, N., Métais, G., Michaux, J., Welcomme, J.L., 2003. Les
4311 mammifères du Miocène inférieur de Beaulieu (Bouches-du-Rhône, France), comparaison avec Wintershof-
4312 West et le problème de la limite MN3/MN4. Coloquios de Paleontología, Univ. Complutense de Madrid, Vol.
4313 Ext. 1, 1–24.

4314 Aguilar, J.P., Lazzari, V., Michaux, J., Sabatier, M., Calvet, M., 2007. Lo Fournas 16-M (Miocène supérieur) et Lo
4315 Fournas 16-P (Pliocène moyen), nouvelles localités karstiques à Baixas, Sud de la France) : Partie I-
4316 Description et implications géodynamiques. Géologie de la France 1, 55–62.
4317 Aguilar, J.P., Michaux, J., Aunay, B., Calvet, M., Lazzari, V., (2010. Compléments à l'étude des rongeurs
4318 (Cricetidae, Eomyidae, Sciuridae) du gisement karstique de Blanquatère 1 (Miocène moyen, Sud de la
4319 France). Geodiversitas 32, 515–533.
4320 Agustí, J., Roca, E., 1987. Síntesis bioestratigráfica de la fosa de la Cerdanya (Pirineos orientales). Estud. Geol.
4321 (Madrid) 43, 521–529.
4322 Agustí, J., Gibert, J., Moya, S., Cabrera, L., 1981. Roedores insectivores del Mioceno superior de La Seu d'Urgell.
4323 Acta Geol. Hispanica ("Homenatge a Lluis Solé Sabaris") 14, 36–369.
4324 Agustí, J., Domènech, R., Julià, R., Martinell, J., 1990. Evolution of the Neogene basin of Emporda (NE Spain),
4325 Field Guidebook. In: Agustí, J., Domènech, R., Julià, R., Martinell, J. (eds), Iberian Neogene basins. Paleontol.
4326 Evol. (Sabadell), Spec. Publ. 2, pp. 251–267.
4327 Agustí, J., Cabrera, L., Domènech, R., Martinell, J., Moyà-Solà, S., Ortí, F., de Porta, J., 1990. Neogene of
4328 Penedes area (Prelittoral Catalan Depression, NE Spain), Field Guidebook. In: Agustí, J., Domènech, R., Julià,
4329 R., Martinell, J. (eds), Iberian Neogene basins. Paleontol. Evol. (Sabadell), Spec. Publ. 2, pp. 187–207.
4330 Agustí, J., Arenas, C., Cabrera, L., Pardo, G., 1994. Characterisation of the latest Aragonian–Early Vallesian (Late
4331 Miocene) in the Central Ebro Basin (NE Spain). Scripta Geol. (Leiden) 106, 1–10.
4332 Agustí, J., Cabrera, L., Garcés, M., Parés, J.M., 1997. The Vallesian mammal succession in the Vallès-Penedès
4333 basin (northeast Spain): paleomagnetic calibration and correlation with global events. Palaogeogr.
4334 Palaeoclim., Palaeocol. 133, 149–180.
4335 Agustí, J., Oms, O., Furió, M., Pérez-Vila, M.J., Roca, E., 2006. The Messinian terrestrial record in the Pyrenees:
4336 the case of Can Vilella (Cerdanya Basin). Palaogeogr. Palaeoclim., Palaeocol. 238, 179–189.
4337 Agustí, J., Cabrera, L., Garcés, M., Krijgsman, W., Oms, O., Parés, J.M., 2001. A calibrated mammal scale for the
4338 Neogene of Western Europe. State of the art. Earth-Sci. Rev. 52, 247–260.
4339 Agustí, J., Pérez-Rivarés, F.J., Cabrera, L., Garcés, M., Pardo, G., Arenas, C., 2011. The Ramblian–Aragonian
4340 boundary and its significance for the European Neogene continental chronology. Contributions from the
4341 Ebro Basin record (NE Spain). Geobios 44, 121–134.
4342 Alasset, J.P., Meghraoui, M., 2005. Active faulting in the western Pyrenees (France): Paleoseismic evidence for
4343 late Holocene ruptures. Tectonophysics 409, 39–54.
4344 Alastrué, B., Almela, A., Ríos, J.M., 1957. Explicación al mapa geológico de la provincia de Huesca. Escala
4345 1:200.000. Inst. Geol. y Min. de España, Madrid, 253 p.
4346 Alimen, H., 1964. Le Quaternaire des Pyrénées de Bigorre. Mémoire du Service de la Carte Géologique, Paris,
4347 394 p.
4348 Allen, P.A., 2008. Time scales of tectonic landscapes and their sediment routing systems. In: Gallagher, K.,
4349 Jones, S.J., Wainwright, J. (eds), Landscape evolution: denudation, climate and tectonics over different time
4350 and space scales. Geological Society, London, Spec. Publ. 296, pp. 7–28.
4351 Allen, P.A., Allen, J.R. 2013. Basin analysis (3rd edn). Blackwell, London, 619 p.

Alvarez-Sierra, M., Daams, R., Lacomba, J.I., López-Martínez, N., Meulen, A. van der, Sesé, C., de Visser, J., 1990. Paleontology and biostratigraphy (micromammals) of the continental Oligocene–Miocene deposits of the north-central Ebro Basin (Huesca, Spain). Scripta Geol. (Leiden) 94, 1–77.

Ambert, P., 1976. Les pertuis de l'Aude Minervoise. Rev. Géogr. Pyrén. Sud-Ouest 47, 275–288.

Ambert, P., 1977. Déformation tectonique d'une terrasse quaternaire de la Cesse à Bize (Aude). Bull. Soc. Hist. Nat. Toulouse 113, 147–151.

Ambert, P., 1994. L'évolution géomorphologique du Languedoc central depuis le Néogène (Grands Causses méridionaux–Piémont languedocien). Doc. BRGM 231, Orléans, 210 p.

Anadón, P., Villalta, J.F., 1975. Caracterización de terrenos de edad estampiense en Campins (Vallés oriental). Acta Geol. Hispánica 10, 6–9.

Anadón, P., 1986. Las facies lacustres del Oligoceno de Campins (Valles Oriental, Provincia de Barcelona). Cuad. Geol. Ibérica 10, 271–294.

Andeweg, V., 2002. Cenozoic tectonic evolution of the Iberian Peninsula, causes and effects of changing stress fields. PhD Thesis, Vrije Universiteit, Amsterdam, 178 p.

Andrieu, V., Hubschman, J., Jalut, G., Hérail, G., 1988. Chronologie de la déglaciation des Pyrénées françaises. Bulletin de l'Assoc. Fr. Étude Quat. (Paris) 34–35, 55–67.

Angrand P. 2017. Évolution 3D d'un rétro-bassin d'avant-pays : le Bassin d'Aquitaine, France. PhD thesis, Univ. de Lorraine, 170 p.

Angrand, P., Ford, M., Watts, A.B., 2018. Lateral variations in foreland flexure of a rifted continental margin: the Aquitaine Basin (SW France). Tectonics 37, 430–449.

Anguy, Y., Damotte, B., Roure, F. 1991. Tirs sismiques latéraux complémentaires au profil ECORS-Pyrénées: apports à la connaissance de l'architecture profonde de la chaîne. C. R. Acad. Sci. Paris sér. II 313, 677–684.

Antoine, P.O., Duranthon, F., Tassy, P., 1997. L'apport des grands mammifères (Rhinocerotidés, Suoïdés, Proboscidiens) à la connaissance des gisements du Miocène d'Aquitaine (France). In: Aguilar, J.P., Legendre, S., Michaux J. (eds.), Actes du Congrès BiochronM'97. Mém. Trav. EPHE (Montpellier) 21, pp. 581–590.

Antoine, P.O., Duranthon, F., Hervet, S., Fleury, G., 2006. Vertébrés de l'Oligocène terminal (MP30) et du Miocène basal (MN1) du métro de Toulouse (Sud-Ouest de la France). C. R. Palevol, 5, 874–884.

Antoine, P.O., Métais, G., Orliac, M.J., Peigné, S., Rafaÿ, S., Solé, F., Vianey-Liaud, M., 2011. A new late Early Oligocene vertebrate fauna from Moissac, South-West France. C. R. Palevol 10, 239–250.

Antunes, M.T., Casanovas, M.L., Cuesta, M.A., Checa L., Santafé, J.V., Agustí, J., 1997. Eocene mammals from Iberian Peninsula. In: Aguilar, J.P., Legendre, S., Michaux, J. (eds.), Actes du Congrès BiochroM'97. Mem. Trav. E.P.H.E. (Inst. Montpellier) 21, 337–352.

Araña, V., Aparicio, A., Martín-Escorza, C., García-Cacho, L., Ortiz, R., Vaquer, R., Barberi, F., Ferrara, G., Albert, J., Gassiot, X., 1983. El volcanismo neógeno-cuaternario de Catalunya: caracteres estructurales, petrológicos y geodinámicos. Acta Geol. Hispanica 18, 1–17.

Arenas, C., 1993. Sedimentología y paleogeografía del Terciario del margen pirenaico y sector central de la cuenca del Ebro (zona aragonesa occidental). Tesis, Universidad de Zaragoza, 858 p.

Arenas, C., Pardo, G., 1999. Latest Oligocene–late Miocene lacustrine systems of the north-central part of the Ebro Basin (Spain): sedimentary facies models and palaeogeographic synthesis. Palaeogeogr. Palaeoclim. Palaeoecol. 151, 127–148.

Arenas, C., Millán, H., Pardo, G., Pocoví, A., 2001. Ebro Basin continental sedimentation associated with late compressional Pyrenean tectonics (north-eastern Iberia): controls on basin margin fans and fluvial systems. Basin Res. 13, 65–89.

Arthaud, F., Ogier, M., Séguret, M., 1980–81. Géologie et géophysique du golfe du Lion et de sa bordure nord. Bull. BRGM I, 175–193.

Asensio, E., Khazaradze, G., Echeverria, A., King, R.W., Vilajosana, I., 2012. GPS studies of active deformation in the Pyrenees, Geophys. J. Int. 190, 913–921.

Ashauer, H., 1934. Die östliche Endigung der Pyrenäen. Abh. Ges. Wiss. Göttingen, Math.-Phys. Kl. 10, 2–115.

Astre, G., 1926. Répartition stratigraphique des deux types de Mammouths. Bulletin Soc. Hist. Nat. Toulouse, 183–188.

Astre, G., 1932. Mammifères des lignites pontiens d'Orignac. Bull. Soc. Hist. Nat. Toulouse 64, 581–584.

Astre, G., 1933. Sur quelques mammifères oligocènes de la vallée de l'Ariège. Bull. Soc. Hist. Nat. Toulouse 65, 120–126.

Astre, G., 1937. Nummulites remaniés dans le Pliocène de Néfiach en Roussillon. C. R. Somm. Soc. Géol. Fr., 347–351.

Astre, G., 1953. Mastodonte de Bourg-Saint-Bernard et érosions miocènes dans le bassin sous-pyrénéen. Bull. Soc. Géol. Fr. 5, 253–259.

Astre, G., 1959. Terrains stampiens du Lauragais et du Tolosan. Bull. Soc. Hist. Nat. Toulouse 94, 8–168.

Astre, G., 1964. Le problème des aires d'affleurement du Stampien terminal au sommet des marno-molasses Tolosanes. Bull. Soc. Hist. Nat. Toulouse 99, 229–234.

Astre, G., 1967. Elephas trogontherii dans des graviers de Palaminy. Bull. Soc. Hist. Nat. Toulouse 103, 19–29.

Astruc, J.G., Hugueney, M., Escarguel, G., Legendre, S., Rage, J.C., Simon-Coiçon, R., Sudre, J., Sigé, B., 2003. Puycelci, nouveau site à vertébrés de la série molassique d'Aquitaine. Densité et continuité biochronologique dans la zone Quercy et bassins périphériques au Paléogène. Geobios 36, 629–648.

Audra, P., Palmer, A.N., 2011. The pattern of caves: controls of epigenic speleogenesis. Géomorphologie: Relief Process. Environ. 4, 359–378.

Audra, P., Palmer A.N., 2013. The vertical dimension of karst: controls of vertical cave pattern. In: Shroder, J.F. (Ed.-in-chief), Frumkin, A. (Volume Ed.), Treatise on Geomorphology, vol. 6, Karst Geomorphology. Academic Press, San Diego, pp. 186–206.

Babault, J., Bonnet, S., Crave, A., van den Driessche, J., 2005a. Influence of piedmont sedimentation on erosion dynamics of an uplifting landscape: an experimental approach. Geology, 33, 301–304.

Babault, J., Van den Driessche, J., Bonnet, S., Castelltort, S., Crave, A., 2005b. Origin of the highly elevated Pyrenean peneplain. Tectonics, 24, TC2010, doi: 10.1029 /2004TC001697.

Babault, J., Loget, N., van den Driessche, J., Castelltort, S., Bonnet, S. and Davy, P., 2006. Did the Ebro Basin connect to the Mediterranean before the Messinian salinity crisis. Geomorphology 81, 155–165.

Babault, J., Bonnet, S., van den Driessche, J., Crave, A., 2007. High elevation of low-relief surfaces in mountain belts: does it equate to post-orogenic surface uplift? Terra Nova 19, 272–277.

Bache, F., 2008. Évolution Oligo-Miocène des marges du micro-océan Liguro-Provençal. PhD thesis, Univ. de Bretagne occidentale, 338 p.

Bache, F., Olivet, J.L., Gorini, C., Aslanian, D., Labails, C., Rabineau, M., 2010. Evolution of rifted continental margins: the case of the Gulf of Lions (Western Mediterranean Basin). Earth Planet. Sci. Lett. 292, 345–356.

Badiola, A., Checa, L., Cuesta, M.A., Quer, R., Hooker, J.J., Astibia, H., 2009. The role of new Iberian finds in understanding European Eocene mammalian paleobiogeography. Geol. Acta 7, 243–258.

Bakalowicz, M., 1988. L'évolution paléohydrologique et morphologique des Pyrénées centrales : l'exemple du massif karstique d'Arbas (Pyrénées garonnaises). Actes des Journées F. Trombe, 8–10 mai 1987, Moulis, CNRS, pp. 43–57.

Baize, S., Cushing, M., Lemeille, T., Granier, B., Grellet, B., Carbon, D., Combes, C., Hibsch, C., 2002. Inventaire des indices de rupture affectant le Quaternaire, en relation avec les grandes structures connues en France métropolitaine et dans les régions limitrophes. Mém. Hors Série Soc. Géol. France 175, 142 p.

Bandet, Y., 1975. Les terrains néogènes du Conflent et du Roussillon nord-occidental. PhD Thesis, Univ. Paul-Sabatier, Toulouse.

Baran, R., Friedrich, A.M., Schlunegger, F., 2014. The late Miocene to Holocene erosion pattern of the Alpine foreland basin reflects Eurasian slab unloading beneath the western Alps rather than global climate change. Lithosphere 6, 124–131.

Barbera, X., Cabrera, L., Marzo, M., Parés, J.M., Agustí, J., 2001. A complete terrestrial Oligocene magnetobiostratigraphy from the Ebro Basin, Spain. Earth Planet. Sci. Lett. 187, 1–16.

Barca, S., Costamagna, L.G., 2010. New stratigraphic and sedimentological invertigations on the Middle Eocene–Early Miocene continental successions in southwestern Sardinia (Italy): paleogeographic and geodynamic implications. C. R. Geoscience 342, 116–125.

Barnolas, A., Teixell, A., 1994. Platform sedimentation and collapse in a carbonate-dominated margin of a foreland basin (Jaca Basin, Eocene, southern Pyrenees). Geology 22, 1107–1110.

Barnolas, A., Chiron, J.C. (eds), 1996. Synthèse géologique et géophysique des Pyrénées. Volume 1: introduction, géophysique, cycle hercynien. BRGM and ITGE, 729 p.

Barnolas, A., Chiron, J.C. (eds), 2018 (2002). Synthèse géologique et géophysique des Pyrénées. Volumes 2 and 3: Cycle alpin, stratigraphie et phénomènes alpins. AGSO and BRGM, 1353 p.

Barnolas, A., Gil-Peña, I., 2001. Ejemplos de relleno sedimentario multiepisódico en una cuenca de antepaís fragmentada: la Cuenca Surpirenaica. Bol. Geol. Min. 112, 17–38.

Barnolas, A., Larrasoaña, J.C., Pujalte, V., Schmitz, B., Sierro, F.J., María P. Mata, M.P., van den Berg, B.C.J., Pérez-Asensio, J.N., Salazar, Á., Salvany, J.M., Ledesma, S., García-Castellanos, D., Civis, J., Cunha, P.P., 2019. Alpine foreland basins. In: South Pyrenean Foreland and Basque–Cantabrian Paleogene Basins. In: Quesada C., Oliveira J.T. (eds), The geology of Iberia: a geodynamic approach, vol. 4: Cenozoic basins. Springer, pp. 7–59.

Barrère, P., 1952a. Le relief des massifs granitiques de Néouvielle, de Cauterets et de Panticosa. Rev. Géogr. Pyrén. Sud-Ouest 23, 69–98.

Barrère, P., 1952b. La morphologie des Sierras Oscences. Actas del Primer Congreso de Estudios Pirenaicos, San Sebastian, 1950, V, Geografia, 51–79.

Barrère, P., 1954. Equilibre glaciaire actuel et quaternaire dans l'Ouest des Pyrénées centrales. Rev. Géogr. Pyrén. Sud-Ouest 24, 116–134.

Barrère, P., 1962. Reliefs mûrs perchés de la Navarre orientale. Rev. Géogr. Pyrén. Sud-Ouest 33, 309–323.

Barrère, P., 1963. La période glaciaire dans l'Ouest des Pyrénées centrales franco-espagnoles. Bull. Soc. Géol. Fr. 7, 516–526.

Barrère, P., 1975. Terrasses et glacis d'érosion en roches tendres dans les montagnes du Haut-Aragon. In: Etudes géographiques, Mélanges offerts à G. Viers. Presses Univ. de Toulouse-le-Mirail, 2 vols., pp. 29–43.

Barrère, P., 1981. Le bassin de Sanguesa, articulation majeure du versant sud des Pyrénées. In: Estudios de Geografía, Homenaje a Alfredo Floristan, Instituto Principe de Viana, 31–39.

Barrère, P., Calvet, M., Courbouleix, S., Gil Peña, I., Martin Alfageme, S., 2009. In: Courbouleix, S., Barnolas, A., eds), Carte géologique du Quaternaire des Pyrénées, 1:400,000 scale. BRGM and ITGM.

Barrière, J., 1966. Le rivage tyrrhénien de l'étang de Bages et de Sigean (Aude). Bull. Assoc. Fr. Etude Quat. 3, 251–283.

Barruol, G., Granet, M., 2002. A Tertiary asthenospheric flow beneath the southern Massif Central indicated by upper mantle seismic anisotropy and related to the west Mediterranean extension. Earth Planet. Sci. Lett. 202, 31–47.

Barruol, G., Deschamps, A., Coutant, O., 2004. Mapping upper mantle anisotropy beneath SE France by SKS splitting indicates Neogene asthenospheric flow induced by Apenninic slab roll-back and deflected by the deep Alpine roots. Tectonophysics 394, 125–138.

Baudelot, S., Crouzel, F., 1974 La faune burdigalienne des gisements d'Espira de Conflent. Bull. Soc. Hist. Nat. Toulouse 110, 311–326.

Baudelot, S., Olivier, P., 1978. Les rongeurs (mammalia, Rodentia) de l'Oligocène terminal de Dieupentale, Sud-Ouest de la France : Tarn et Garonne). Geobios 11, 5–19.

Baulig, H., 1928. Le Plateau Central de la France et sa bordure méditerranéenne – Etude morphologique. A. Colin, Paris, 591 p.

Beamud, E., Garcés, M., Cabrera, L., Muñoz, J.A., Almar, Y., 2003. A new middle to late Eocene continental chronostratigraphy from NE Spain. Earth Planet. Sci. Lett. 216, 501–514.

Beamud, E., Muñoz, J.A., Fitzgerald, P.J., Baldwin, S.L., Garcés, M., Cabrera, L., Metcalf, J.R., 2011. Magnetostratigraphy and detrital apatite fission track thermochronology in syntectonic conglomerates: constraints on the exhumation of the South-Central Pyrenees. Basin Res. 23, 309–331.

Beaumont, C., Muñoz, J.A., Hamilton, J., Fullsack, P., 2000. Factors controlling the Alpine evolution of the central Pyrenees inferred from a comparison of observations and geodynamical models. J. Geophys. Res. 105, 8121–8145.

Bellec, V., 2003. Évolution morphostructurale et morphosédimentaire de la plate-forme aquitaine depuis le Néogène. PhD thesis (unpubl.), Univ. of Bordeaux, 268 p.

Bellec, V., Cirac, P., Faugères, J.C., 2009. Formation and evolution of paleo-valleys linked to a subsiding canyon, North Aquitaine shelf (France). C.R. Geosciences 341, 36–48.

Belmonte, A., 2014. Geomorfología del macizo de Cotiella (Pirineo oscense): cartografía, evolución paleoambiental y dinámica actual. PhD thesis, Universidad de Zaragoza, 581 p.

Benito, G., Pérez-González, A., Gutiérrez, F., Machado, M.J., 1998. River response to Quaternary large-scale subsidence due to evaporite solution (Gállego River, Ebro Basin, Spain). Geomorphology 22, 243–263.

Benito, G., Sancho, C., Peña, J.L., Machado, M.J., Rhodes, E.J., 2010. Large-scale karst subsidence and accelerated fluvial aggradation during MIS6 in NE Spain: climatic and paleohydrological implications. Quat. Sci. Rev. 29, 2694–2704.

Bentham P., Burbank D.W., 1996. Chronology of Eocene foreland basin evolution along the western oblique margin of the South-Central Pyrenees. In: Friend, P.F. Dabrio, C.J. (eds), Tertiary basins of Spain, the stratigraphic record of crustal kinematics. Cambridge University Press, Cambridge, pp. 144–152.

Berástegui, X., García-Senz, M., Losantos, M., 1990. Tecto-sedimentary evolution of the Organyà extensional basin (central south Pyrenean unit, Spain) during the Lower Cretaceous. Bull. Soc. Géol. Fr. 8, 251–264.

Berástegui, X., Caus, E., Puig, C., Serra-Kiel, J., 2002. Le Paléogène du secteur oriental du bassin sud-pyrénéen, livret guide. IUGS–UNESCO–IGCP, AGSO, GEP, 77 p.

Berger, G., Clauzon, G., Michaux, J., Suc, J.P., Aloïsi, J.C., Monaco, A., Got, H., Augris, C., Gadel, F., Buscail, R., 1988. Carte géologique de la France, 1:50,000 scale, sheet Perpignan (1091), Orléans, BRGM. Handbook by Clauzon, G., Berger, G., Aloïsi, J.C., Got, H., Monaco, A., Buscail, R., Gadel, F., Augris, C., Marchal, J.P., Michaux, J., Suc, J.P. (1989), 40 p.

Bergounioux, F.M., Crouzel, F., 1960. Mastodontes du Miocène du Bassin d'Aquitaine. Bull Soc. Hist. Nat. Toulouse 48, 232–286.

Bergounioux, F.M., Crouzel, F., 1971. Un gisement fossilifère Oligocène à Saverdun (Ariège). Bull Soc. Hist. Nat. Toulouse 107, 89–92.

Besson, F., 2000. Le paysage pyrénéen dans la littérature de voyage et l'iconographie britannique du dix-neuvième siècle. L'Harmattan, Paris 463 p.

Bestani, L., Espurt, N., Lamarche, J., Bellier, O., Hollender, F., 2016. Reconstruction of the Provence Chain evolution, southeastern France. Tectonics 35, 1506–1525.

Bilotte, M., Peybernès, B., Souquet, P., 1979. Les Pyrénées catalanes dans la région de l'Empordà. Relations entre zones isopiques crétacées et unités structurales. Acta Geol. Hisp., 14, 280–288.

Birot, P., 1937. Recherches sur la morphologie des Pyrénées orientales franco-espagnoles. Baillière édit., Paris, 318 p.

Birot, P., 1952. Sur quelques contrastes fondamentaux dans la structure et la morphologie des Pyrénées. Actas del Primer Congreso de Estudios Pirenaicos, San Sebastian, 1950. Geografia 5, 17–21.

Birot, P., 1969. Le Quaternaire de la basse vallée de l'Orbieu. Livret guide excursion A6, Pyrénées orientales et centrales, Roussillon, Languedoc occidental, VIIIe Congrès INQUA, Paris, 101–105.

Blanchard, R., 1914. La morphologie des Pyrénées françaises. Ann. Géogr. 23, 303–324.

Blockley, S.P.E., Lane ,C.S, Hardiman, M., Rasmussen, S.O., Seierstad, I.K, Steffensen, J.P., Svensson, A., Lotter, A.F., Turney, C.S.M., Ramsey, C.B, 2012 Synchronisation of palaeoenvironmental records over the last 60,000 years and an extended INTIMATE event stratigraphy to 48,000 b2k. Quat. Sci. Rev. 36, 2–10.

Boillot, G., Capdevila, R., 1977. The Pyrenees: subduction and collision? Earth Planet. Sci. Lett. 35, 151–160.

Boillot, G., Capdevila, R., Hennequin-Marchand, I., Lamboy, M., Leprêtre, J.-P., 1973. La zone nord-pyrénéenne, ses prolongements sur la marge continentale nord-espagnole et sa signification structurale. C. R. Acad. Sci. Paris D 277, 2629–2632.

Boissevain, H., 1934. Étude géologique et géomorphologique d'une partie de la vallée de la haute Sègre (Pyrénées Catalanes). Bull Soc. Hist. Nat. Toulouse 66, 33–170.

Bomer, B., 1979. Les piedmonts du Bassin de l'Ebre (Espagne). Méditerranée 36, 19–25.

Bond, R.M.G., McClay, K.R., 1995. Inversion of a Lower Cretaceous extensional basin, south central Pyrenees, Spain. In: Buchanan, J.G., Buchanan, P.G. (eds), Basin Inversion. Geological Society, London, Spec. Publ. 88, pp. 415–431.

Bonilla-Salomon, I., Minwer-Barakat, R., Vianey-Liaud, M., Moya-Sola, S., 2016. Middle Eocene rodents from Sant Jaume de Frontanya (eastern Pyrenees, northern Spain) and biochronological implications. J. Vertebr. Paleontol. 36, e1121149-2.

Bordonau, J., 1992. Els Complexos glacio-lacustres relacionats amb el darrer cicle glacial als Pirineus. Geoforma edit., Logroño, 251 p.

Bosch, G.V., van den Driessche, J., Babault, J., Robert, A., Carballo, A., Le Carlier, C., Loget, N., Prognon, C., Wyns, R., Baudin, T., 2016a. Peneplanation and lithosphere dynamics in the Pyrenees. C. R. Géoscience 348, 194–202.

Bosch, G.V., Teixell, A., Jolivet, M., Labaume, P., Stockli, D., Doménech, M., Monié, P., 2016b. Timing of Eocene–Miocene thrust activity in the western Axial Zone and Chaînons Béarnais (west-central Pyrenees) revealed by multi-method thermochronology. C. R. Geoscience 348, 246–256.

Boschi, L., Faccena, C., Becker, T.W., 2010. Mantle struture and dynamic topography in the Mediterranean. Geophys. Res. Lett., 37, L20303, doi:10.1029/2010GL045001.

Bosq, M., Bertran, P., Beauval, C., Kreutzer, S., Duval, M., Bartz, M., Mercier, N., Sitzia, L., Stéphan, P., 2019. Stratigraphy and chronology of Pleistocene coastal deposits in northern Aquitaine, France; a reinvestigation. Quaternaire 30, 5–20.

Boulanger, D., Poignant, A., 1970. A propos de l'âge de la base des poudingues de Jurançon. C.R. Somm. Soc. Géol. France, 2, 35–36.

Boule, M., 1894. Le plateau de Lannemezan et les alluvions anciennes des hautes vallées de la Garonne et de la Neste. Bull. Serv. Carte Géol. France 43, 447–469.

Bourcart, J., 1947. Étude des sédiments pliocènes et quaternaires du Roussillon. Bull. Serv. Carte Géol. France 218, 395–476.

Briais, A., Armijo, R., Winter, T., Tapponnier, P., Herbecq, A., 1990. Morphological evidence for Quaternary normal faulting and seismic hazard in the Eastern Pyrenees. Ann. Tectonicae 4, 19–42.

Bridgland, D.R., 2000. River terrace systems in north-west Europe: an archive of environmental change, uplift and early human occupation. Quat. Sci. Rev. 19, 1293–1303.

Bridgland, D.R., Westaway, R., 2014. Quaternary fluvial archives and landscape evolution: a global synthesis. Proc. Geol. Assoc. 125, 600–629.

Briffaut, S., 1994. Naissance d'un paysage. La montagne pyrénéenne à la croisée des regards, XVIe–XIXe siècle. Sources et Travaux d'Histoire Haut-Pyrénéenne (Association Guillaume Mauran), vol. 8, 622 p.

Bruxelles, L., Berthet, A.L., Chalard, P., Colonge, D., Delfour, G., Jarry, M., Lelouvier, L.A., Arnoux, T., Onézime, O., 2003. Le paléolithique inférieur et moyen en Midi toulousain : nouvelles données et perspectives de l'archéologie préventive. Paleo (Les Eyzies) 15, 7–28.

Bugnicourt, D., Claracq, P., Dupéron, J., Privé-Gil, C., Sauvage, J., 1988. Sédimentologie, bois fossils et palynology d'une couche à lignites de Capvern, plateau de Lannemezan (Hautes-Pyrénées). Bull. Centre Rech. Explor. Prod. Elf Aquitaine (Pau) 12, 739–757.

Burbank, D.W., Verges, J., Muñoz, J.A., Bentham, P., 1992a. Coeval hindward- and forward-imbricating thrusting in the south-central Pyrenees, Spain: timing and rates of shortening and deposition. Geol. Soc. Am. Bull. 104, 3–17.

Burbank, D.W., Puigdefabregas, C., Muñoz, J.A., 1992b. The chronology of the Eocene tectonic and stratigraphic development of the eastern Pyrenean foreland basin, northeast Spain. Geol. Soc. Am. Bull. 104, 1101–1120.

Busquets, P., Ramos-Guerrero, E., Moyà-Solà, S., Agustí, J., Colombo, F., Checa, L., Khöler, M., 1992. La Formación de Bellmunt (Unidad del Cadí, Pirineo oriental): aportaciones bioestratigraficas de los sistemas lacustres y palustres asociados. Acta Geol. Hisp. 25, 109–116.

Cabrera, L., Roca, E., Santanach, P., 1988. Basin formation at the end of a strike-slip fault: the Cerdanya basin (Eastern Pyrenees). J. Geol. Soc. (London) 145, 261–268.

Cabrera, L., Saez, A., 1987. Coal deposition in carbonate-rich shallow lacustrine systems: the Calaf and Mequinenza sequences (Oligocene, eastern Ebro Basin, NE Spain). J. Geol. Soc. (London) 144, 451–461.

Cabrera, L., Calvet, F., 1996. Onshore Neogene record in NE Spain: Vallés-Penedés and El Camp half-grabens (NW Mediterranean). In: Friend, P.F., Dabrio, C.J. (eds), Tertiary basins of Spain, the stratigraphic record of crustal kinematics. Cambridge University Press, Cambridge, pp. 97–105.

Cahuzac, B., Janin, M.C., Steurbaut, E., 1995. Biostratigraphie de l'Oligo-Miocène du bassin d'Aquitaine fondée sur les nannofossiles calcaires. Implications paléogéographiques. Géologie de la France 2, 57–82.

Cahuzac, B., Poignant, A., 1996. Foraminifères benthiques et Microproblematica du Serravallien d'Aquitaine. Géologie de la France 3, 35–55.

Cahuzac, B., Turpin, L., 1999. Stratigraphie isotopique du Strontium dans le Miocène marin du Bassin d'Aquitaine (SW France). Rev. Soc. Geol. Esp. 12, 37–56.

Cahuzac, B., Poignant, A., 2004. Les foraminifères du Burdigalien moyen à supérieur de la région sud-aquitaine, golfe de Saubrigues, SW France). Rev. Micropaléontol. 47, 153–192.

Cahuzac, B., Janssen, A.W., 2010. Eocene to Miocene holoplanktonic Mollusca (Gastropoda) of the Aquitaine Basin, southwest France. Scripta Geologica 141, 1–193.

Calvet, M., 1986. La stratigraphie du Néogène du Roussillon et le problème des séries détritiques de bordure. Essai de mise au point. Géologie de la France 2, 205–220.

Calvet, M., 1981. Nappes alluviales et niveaux quaternaires du bas-Vallespir. Implications néotectoniques et paléoclimatiques. Rev. Géogr. Pyrén. Sud-Ouest 52, 125–159.

Calvet, M., 1992. Aplanissements sur calcaire et gîtes fossilifères karstiques. L'exemple des Corbières orientales. Tübinger Geogr. Stud. 109, pp. 37–43.

Calvet, M., 1996. Morphogenèse d'une montagne méditerranéenne : les Pyrénées orientales. Doc. BRGM 255, 3 vols. BRGM, Orléans, 1177 p.

Calvet, M., 1999. Régime des contraintes et volumes de relief dans l'Est des Pyrénées. Géomorphologie : Rel., Proc., Environ. 3, 253–278.

Calvet, M., Lemartinel B., 2002. Précipitations exceptionnelles et crues éclair dans l'aire pyrénéo-méditerranéenne. Géomorphologie : Rel., Proc., Environ. 1, 35–50.

Calvet, M., 2004. The Quaternary glaciation of the Pyrenees. In: Ehlers, J., Gibbard, P. (eds), Quaternary glaciations — extent and chronology; part I: Europe. Elsevier, Amsterdam, pp. 119–128.

Calvet, M., Aguilar, J.P., Crochet, J.Y., Dubar, M., Michaux, J., 1991. Première découverte de mammifères oligocènes et burdigaliens dans les bassins de Paziols–Tautavel–Estagel (Aude et Pyrénées-Orientales), implications géodynamiques. Géologie de la France 1, 33–44.

Calvet, M., Gunnell, Y., Delmas, M., 2008. Géomorphogenèse des Pyrénées. In: Canérot, J., Colin, J.P., Platel, J.P., Bilotte, M. (eds), Pyrénées d'hier et d'aujourd'hui. Atlantica and BRGM, Biarritz–Orléans, pp. 129–143.

Calvet, M., Gunnell, Y., 2008. Planar landforms as markers of denudation chronology: an inversion of East Pyrenean tectonics based on landscape and sedimentary basin analysis. In: Gallagher, K., Jones, S.J., Wainwright, J. (eds), Landscape Evolution: Denudation, Climate and Tectonics Over Different Time and Space Scales, Geological Society, London, Spec. Publ. 296, pp. 147–166.

Calvet, M., Delmas, M., Gunnell, Y., Braucher, R., Bourlès, D., 2011. Recent advances in research on Quaternary glaciations in the Pyrenees. In: J. Ehlers, Gibbard, P.L. (eds), Quaternary glaciations, extent and chronology, a closer look; Part IV. Developments in Quaternary Science 15, Elsevier, pp. 127–139.

Calvet, M., Gunnell, Y., Farines, B., 2015a. Flat-topped mountain ranges: their global distribution and value for understanding the evolution of mountain topography. Geomorphology, 241, 255–291

Calvet, M., Gunnell, Y., Braucher, R., Hez, G., Bourlès, D., Guillou, V., Delmas, M., Aster Team, 2015b. Cave levels as proxies for measuring post-orogenic uplift: evidence from cosmogenic dating of alluvium-filled-cave in the French Pyrenees. Geomorphology 246, 617–633.

Calvet, M., Autran, A., Wiazemsky, M., Laumonier, B., Guitard, G., 2015. Carte géologique de la France, 1:50,000 scale, sheet Argelès-sur-Mer / Cerbère (1097). BRGM, Orléans. Handbook by Laumonier, B., Calvet, M., Barbey, P., Guennoc, P., Lambert J., Lenoble, J.L., Wiazemsky, M., 149 p.

Calvet, M., Hez, G., Gunnell, Y., Jaillet, S., 2019. Le karst du synclinal de Villefranche, enregistreur de l'incision de la vallée de la Têt. Bol/ Soc. Esp. Speleo. Sci. Karst 14, 15–32.

Cameselle, A.L., Urgeles, R., de Mol, B., Camerlenghi, A., Canning, J.C., 2014. Late Miocene sedimentary architecture of the Ebro Continental Margin (Western Mediterranean): implications to the Messinian Salinity Crisis. Int. J. Earth Sci., 103, 423–440.

Campanyà, J., Ledo, J., Queralt, P., Marcuello, A., Liesa, M., Muñoz, J.A. 2012. New geoelectrical characterisation of a continental collision zone in the West-Central Pyrenees: Constraints from long period and broadband magnetotellurics. Earth Planet. Sci. Lett. 333–334, 112–121.

Campanyà, J., Ledo, J., Queralt, P., Marcuello, A., Muñoz, J.A., Liesa, M., Jones, A.J., 2018. New geoelectrical characterization of a continental collision zone in the Central. Eastern Pyrenees: Constraints from 3-D joint inversion of electromagnetic data. Tectonophysics, 742–743, 168–179.

Canérot, J., 2006. Réflexions sur la "révolution danienne" dans les Pyrénées. C. R. Geoscience 338, 658–665.

Canérot, J., 2008. Les Pyrénées, vol. 1: Histoire géologique, vol. 2: Itinéraires de découverte. Atlantica and BRGM, Biarritz–Orléans, 516 and 127 p.

Canérot, J., 2017. The pull apart-type Tardets-Mauléon basin, a key to understand the formation of the Pyrenees. Bull. Soc. Géol. Fr. 188, 35. http://doi.org/10.1051/bsgf/2017198

Canérot, J., Hudec, M.R., Rockenbauch, K., 2005. Mesozoic diapirism in the Pyrenean orogen: salt tectonics on a transform plate boundary. Am. Assoc. Petrol. Geol. Bull. 89, 211–229.

Capdeville, J.P., Dubreuilh, J., 1990. Carte géologique de la France, 1:50,000 scale, sheet Mont-de-Marsan (951). BRGM, Orléans. Handbook by Capdeville, J.P., 41 p.

Capdeville, J.P., Gineste, M.C., Turq A., Vergain P., 1997. Handbook to the Carte géologique de la France, 1:50,000 scale, sheet Hagetmau (978). BRGM, Orléans, 70 p. Map by Capdeville, J.P.

Capdeville, J.P., Darboux, F., 1998. Carte géologique de la France, 1:50,000 scale, sheet Aire-sur-l'Adour (979). BRGM, Orléans. Handbook by Capdeville, J.P., D. Millet, D., F. Millet, F., 51 p.

Capdeville, J.P., Chalard, P., Jarry, M., Millet, D., O'yl, W., 1997. Le gisement acheuléen d'En Jacca. La Sauvegarde à Colomiers (Haute-Garonne) : nouvelles données. Paléo 9, 69–99.

Carballo, A., Fernandez, M., Jiménez-Munt, I., Torne, M., Vergés, J., Melchiorre, M., Pedreira, D., Afonso, J.C., Garcia-Castellanos, D., Díaz, J., Villaseñor, A., Pulgar, J.A., Quintana, L., 2015. From the North-Iberian margin to the Alboran Basin: a lithosphere geo-transect across the Iberian Plate. Tectonophysics 663, 399–418.

Carbon, D., Combes, P., Cushing, M., Granier, T., Grellet, B., 1995. Rupture de surface post-pléistocène moyen dans le bassin aquitain. C. R. Acad. Sci. Paris sér. IIa 320, 311–317.

Carcenac, C., Coinçon, R., Taillefer, F., 1969. Carte géomorphologique du Mas d'Azil. Rev. Géogr. Pyrén. Sud-Ouest 40, 329–351.

Carreras, J., Capella, I., 1994. Tectonic levels in the Paleozoic basement of the Pyrenees: a review and a new interpretation. J. Struct. Geol. 16, 1509–1524.

Carrigan, J.H., Anastasio, D.J., Kodama, K.P., Par, J.M., 2016. Fault-related fold kinematics recorded by terrestrial growth strata, Sant Llorenç de Morunys, Pyrenees Mountains, NE Spain. J. Struct. Geol. 91, 161–176.

Casanovas-Vilar, I., van den Hoek Ostende, L.W., Furió, M., Madern, P.A., 2014. The range and extent of the Vallesian Crisis (Late Miocene): new prospects based on the micromammal record from the Vallès-Penedès basin (Catalonia, Spain). J. Iberian Geol. 40, 29–48

Casas, J.M., Clariana, J., García-Sansegundo, J., Margalef, A., 2019. The Pyrenees. In: Quesada, C., Oliveira, J.T. (eds.), The geology of Iberia: a geodynamic approach, vol. 2, The Variscan cycle. Springer, pp. 335–337.

Casas-Sainz, A.M., de Vicente, G., 2009. On the tectonic origin of Iberian topography. Tectonophysics 474, 214–235.

Cavelier, C., Fries, G., Lagarigue, J.L., Capdeville, J.P., 1997. Sédimentation progradante au Cénozoïque inférieur en Aquitaine méridionale : un modèle. Géologie de la France 4, 69–79.

Chanvry, E., Deschamps, R., Joseph, P., Puigdefàbregas, C., Poyatos-Moré, M., Serra-Kiel, J., Garcia, D., Teinturier, S., 2018. The influence of intrabasinal tectonics in the stratigraphic evolution of piggyback basin fills: Towards a model for the Tremp–Graus–Ainsa Basin (South-Pyrenean Zone, Spain). Sed. Geol. 377, 34–62.

Chaput, E., 1927. Recherches sur l'évolution des terrasses de l'Aquitaine. Bull. Soc. Hist. Nat. Toulouse 56, 17–84.

Chevalier, M., 1909. Note sur la « cuencita » de la Seo de Urgell (Province de Lerida, Espagne). Bull. Soc. Géol. Fr., 158–178.

Chevalier, M., 1954a. Le relief glaciaire des Pyrénées du Couserans. I. Les cirques. Rev. Géogr. Pyrén. Sud-Ouest 25, 97–124.

Chevalier, M., 1954b. Le relief glaciaire des Pyrénées du Couserans. II. Les vallées. Rev. Géogr. Pyrén. Sud-Ouest 25, 189–220.

Chevrot, S., Sylvander, M., Delouis, B., 2011. A preliminary catalog of moment tensors for the Pyrenees. Tectonophysics 510, 239–251.

Chevrot, S., Villaseñor, A., Sylvander, M., Benahmed, S., Beucler, E., Cougoulat, G., Delmas, P., de Saint Blanquat, M., Diaz, J., Gallart, J., Grimaud, F., Lagabrielle, Y., Manatschal, G., Mocquet, A., Pauchet, H., Paul, A., Péquegnat, C., Quillard, O., Roussel, S., Ruiz, M., Wolyniec, D., 2014. High-resolution imaging of the Pyrenees and Massif Central from the data of the PYROPE and IBERARRAY portable array deployments. J. Geophys. Res. (Solid Earth) 119, 6399–6420.

Chevrot, S., Sylvander, M., Diaz, J., Ruiz, M., Paul, A. and the PYROPE Working Group, 2015. The Pyrenean architecture as revealed by teleseismic P-to-S converted waves recorded along two dense transects. Geophys. J. Int. 200, 1096–1107.

Chevrot, S., Sylvander, M., Diaz, J., Martin, R., Mouthereau, F., Manatschal, G., Masini, E., Calassou, S., Grimaud, F., Pauchet, H. Ruiz, M., 2018. The non-cylindrical crustal architecture of the Pyrenees. Sci. Rep., 8:9591, DOI:10.1038/s41598-018-27889-x

Choukroune, P., 1992. Tectonic evolution of the Pyrenees. Annu. Rev. Earth Planet. Sci. 20, 143–158.

Choukroune, P., Le Pichon, X., Séguret, M., Sibuet, J.C., 1973. The Pyrenees: subduction and collision? Earth Planet. Sci. Lett. 18, 109–118.

Cirac, P., Bourillet, J.F., Griboulard, R., Normand, A., Mulder, T., ITSAS' Team, 2001. Canyon of Capbreton: new morphostructural and morphosedimentary approaches, First results of the ITSAS cruise, C. R. Acad. Sci. Paris sér. IIa 332, 447–455.

Clauzon, G., 1990. Restitution de l'évolution géodynamique néogène du bassin du Roussillon et de l'unité adjacente des Corbières d'après les données écostratigraphiques et paléogéographiques. Paléobiol. Continent. (Montpellier) 17, 125–155.

Clauzon, G., Cravatte, J., 1985. Révision chronostratigraphique de la série marine pliocène traversée par le sondage Canet 1 (Pyrénées-Orientales) : apport à la connaissance du Néogène du Roussillon. C. R. Acad. Sc. Paris II 301, 1351–1354.

Clauzon, G., Aguilar, J.P., Michaux, J., 1987. Le bassin pliocène du Roussillon (Pyrénées-Orientales, France) : exemple d'évolution géodynamique d'une ria méditerranéenne consécutive à la crise de salinité messinienne. C. R. Acad. Sc. Paris II 304, 585–590.

Clauzon, G., Suc, J.P., Aguilar, J.P., Ambert, P., Capetta, H., Cravatte, J., Drivaliari, A., Domènech, R., Dubar, M., Leroy, S., Martinell, J., Michaux, J., Roiron, P., Rubino, J.L., Savoye, B., Vernet, J.L., 1990. Pliocene geodynamic and climatic evolutions in the French mediterranean region, Field Guidebook. In: Agustí, J., Domènech, R., Julià, R., Martinell, J. (eds), Iberian Neogene basins. Paleontol. Evol. (Sabadell), Spec. Publ. 2, pp. 131–186.

Clerc, C., Lagabrielle, Y., 2014. Thermal control on the modes of crustal thinning leading to mantle exhumation. Insights from the Cretaceous Pyrenean hot paleomargins. Tectonics 33, 1340–1359.

Clot, A., Duranthon, F., 1990. Les mammifères fossiles du Quaternaire dans les Pyrénées. Muséum d'Histoire Naturelle de Toulouse and Accord Editions, 80 p.

Clottes, J., 1999. La vie et l'art des Magdaléniens en Ariège. La maison des roches, Paris, 700 p.

Cochelin, B., Lemirre, B., Denèle, Y., de Saint Blanquat, M., Lahfid, A., Duchêne, S., 2018. Structural inheritance in the Central Pyrenees: the Variscan to Alpine tectonometamorphic evolution of the Axial Zone. J. Geol. Soc. (London) 175, 336–351.

Cocherie, A., Baudin, T., Guerrot, C., Autran, A., Fanning, M.C., Laumonier, B., 2005. Evidence of the Lower Ordovician intrusion age for metagranites in the Late Proterozoic Canaveilles Group of Pyrénées and Montagne noire (France): new U–Pb datings. Bull. Soc. Géol. Fr. 176, 269–282.

Collina-Girard, J., 1976. Les alluvions fluviatiles des fleuves côtiers dans le Roussillon. In: de Lumley, H. (Ed.), La Préhistoire française. CNRS Editions, Paris, t. 1, pp. 78–82.

Collina-Girard, J., 1986. Grille descriptive et évolution typologique des industries archaïques : le modèle catalan. Bull. Soc. Préhist. Fr. 83, pp. 383–403.

Coney, P.J., Muñoz, A.J., McClay, K.R., Evenchik, C.A., 1996. Syntectonic burial and post-tectonic exhumation of the southern Pyrenees foreland fold-thrust belt. J. Geol. Soc. (London) 153, 9–16.

Conway-Jones, B. W., Roberts, G. G., Fichtner, A., Hoggard, M., 2019. Neogene epeirogeny of Iberia. Geochem., Geophys., Geosyst. 20, 1138–1163.

Corbier, P., Karnay, G., Bourgine, B., Saltel, M., 2010. Gestion des eaux souterraines en région Aquitaine Reconnaissance des potentialités aquifères du Mio-Plio-Quaternaire des Landes de Gascogne et du Médoc en relation avec les SAGE. Rapport final, BRGM/RP-57813-FR. BRGM, Orléans, 187 p.

Cordier, S., Adamson, K., Delmas, M., Calvet, M., Harmand, D., 2017. Of ice and water: Quaternary fluvial response to glacial forcing. Quat. Sci. Rev. 166, 57–73.

Costa, J.M., Maestro-Maideu, E., Betzler, C., 1996. The Paleogene basin of the Eastern Pyrenees. In: Friend, P.F., Dabrio, C.J. (eds), Tertiary basins of Spain, the stratigraphic record of crustal kinematics. Cambridge University Press, Cambridge, pp. 106–113.

Costa, E., Garcés, M., López-Blanco, M., Beamud, E., Gómez-Paccard, M., Larrasoaña, J.C., 2010. Closing and continentalization of the South Pyrenean foreland Basin (NE Spain): magnetochronological constraints. Basin Res. 22, 904–917.

Costa, E., Garcés, M., Sáez, A., Cabrera, L., López-Blanco, M., 2011. The age of the “Grande Coupure” mammal turnover: new constraints from the Eocene–Oligocene record of the Eastern Ebro Basin (NE Spain). Palaeogeogr. Palaeoclim. Palaeoecol. 301, 97–107.

Costa, E., Garcés, M., López-Blanco, M., Serra-Kiel, J., Bernaola, G., Cabrera, L., Beamud, E., 2013. The Bartonian–Priabonian marine record of the eastern South Pyrenean foreland basin (NE Spain): a new calibration of the larger foraminifers and calcareous nannofossil biozonation. Geol. Acta 11, 177–193.

Costamagna, L.G., Schäfer, A., 2013. The Cixerri Fm (Middle Eocene–Early Oligocene): analysis of a "Pyrenean" continental molassic system in southern Sardinia. J. Medit. Earth Sci., Spec. Issue, pp. 41–44.

Cravatte, J., Dufaure, J.F., Prim, M., Rouaix, S., 1974. Les forages du Golfe du Lion : stratigraphie, sédimentologie. Notes et Mémoires du C.F.P. 11, 209–274.

Crest, Y., Delmas, M., Braucher, R., Gunnell, Y., Calvet, M., ASTER Team, 2017. Cirques have growth spurts during deglacial and interglacial periods: evidence from 10Be and 26Al nuclide inventories in the central and eastern Pyrenees. Geomorphology 278, 60–77.

Crochet, B., 1991. Molasses syntectoniques du versant nord des Pyrénées : la série de Palassou. Doc. BRGM 199, 387 p.

Crouzel, F., 1957. Le Miocène continental du bassin d'Aquitaine, Bull. Serv. Carte Géol. de la France. 248, LIV (1956), 264 p.

Crusafont, M., Villalta, J.F. de, Truyols, J., 1956. Caracterización del Eoceno continental en la cuenca de Tremp y edad de la orogenesis pirenaica. Actes du deuxième Congrès international d’études pyrénéennes, Luchon–Pau 1954. 2, I, pp. 39–53.

Crusafont, M., 1961. Sobre la probable presencia del Mioceno continental en la cuenca del Ampurdan. Actas III Congreso Int. Est. Pirenaicos, Gerona, 1958. 1, 1, pp. 57–65.

Crusafont, M., Hartenberger, J.L., Thaler, L., 1963. Sur des nouveaux restes de mammifères du gisement Eocène supérieur de Sossis, au nord de Tremp (Lérida, Espagne). C. R. Acad. Sci. Paris 257, 3014–3017.

Crusafont, M., Riba, O., Villena, J., 1966. Nota preliminar sobre un nuevo yacimiento de vertebrados aquitanienses en Santa Cília (río Formiga, provincia de Huesca), y sus consecuencias geológicas. Not. Com. Inst. Geol. Min. Esp. 83, 7–13.

Crusafont, M., Pons, J.M., 1969. Nuevos datos sobre el Aquitaniense del norte de la provincia de Huesca. Acta Geol. Hisp. 4, 124–125.

Crusafont, M., Golpe-Posse, J.M., 1973. Yacimientos del Eoceno Prepirenaico (nuevas localidades del Cuisiense). Acta Geol. Hisp. 8, 145–147.

Cuenca, G., Aranza, B., Canudo, J.I., Fuertes, V., 1989. Los micromamíferos del Mioceno inferior de Peñalba (Huesca). Implicaciones bioestratigráficas. Geogaceta 6, 75–77.

Cuenca, G., Canudo, J.I., Laplana, C., Andres, J.A., 1992. Bio y cronoestratigrafia con mamíferos en la Cuenca Terciaria del Ebro: ensayo de síntesis. Acta Geol. Hisp. 27 ("Homenaje a Oriol Riba Arderiu"), 127–143.

Cuesta, M.A., Checa, L., Casanovas, M.L., 2006. Los artiodáctilos del yacimiento ludiense de Sossís (Cuenca Prepirenaica, Lleida, España). Rev. Esp. Paleontol. 21, 123–144.

Curry, M.E., van der Beek, P., Huismans, R.S., Wolf, S.G, Muñoz, J.A., 2019. Evolving paleotopography and lithospheric flexure of the Pyrenean Orogen from 3D flexural modeling and basin analysis. Earth Planet. Sci. Lett. 515, 26–37.

Daignières, M., Séguret, M., Specht, M., ECORS Team, 1994. The Azarcq–Western Pyrenees ECORS Deep Seismic Profile. In: Mascle, A. (Ed), Hydrocarbon and petroleum geology of France, Spec. Publ. Eur. Assoc. Petrol. Geosci. 4, 199–208.

Damotte, B. (Ed.), 1998. The ECORS Pyrenean deep seismic surveys, 1985–1994. Mém. Soc. Géol. France 173, 108 p.

Dautria, J.M., Liotard, J.M., Bosch, D., Alard, O., 2010. 160 Ma of sporadic basaltic activity on the Languedoc volcanic line (Southern France): a peculiar case of lithosphere–asthenosphere interplay. Lithos 120, 202–222.

Debals, B., 2000. Mise au point sur la chronostratigraphie des dépôts alluviaux quaternaires de la Plaine du Roussillon : exemple de la vallée de la Têt (France). Quaternaire 11, 31–39.

Debroas, É.J., Azambre, B., 2012. Des brèches aux lherzolites. La mise en place des lherzolites dans les fosses du flysch albo-cénomanien de la Ballongue et d'Aulus (Zone Nord-Pyrénéenne, Ariège). Excursion AGSO, 9–10 June 2012, Guidebook, 120 p.

DeFelipe, I., Pedreira, D., Pulgar, J.A., van der Beek, P.A., Bernet, M., Pik, R., 2019. Unraveling the Mesozoic and Cenozoic tectonothermal evolution of the eastern Basque–Cantabrian Zone, western Pyrenees, by low-temperature thermochronology. Tectonics 38, 3436–3461.

Delmas, M., Calvet, M., Gunnell, Y., 2009. Variability of Quaternary glacial erosion rates—A global perspective with special reference to the Eastern Pyrenees. Quat. Sci. Rev. 28, 484–498.

Delmas, M., Gunnell, Y., Calvet, M., 2014. Environmental controls on alpine cirque size. Geomorphology 206, 318–329.

Delmas, M., Braucher, R., Gunnell, Y., Guillou, V., Calvet, M., Bourlès, D., 2015. Constraints on Pleistocene glaciofluvial terrace age and related soil chronosequence features from vertical ^{10}Be profiles in the Ariège River catchment (Pyrenees, France). Glob. Planet. Change 132, 39–53.

Delmas M., Calvet M., Gunnell Y., Voinchet P., Manel C., Braucher R., Tissoux H., Bahain J.J., Perrenoud C., Saos T, Aster Team, 2018. Terrestrial ^{10}Be and Electron Spin Resonance dating of fluvial terraces quantifies Quaternary tectonic uplift gradients in the eastern Pyrenees. Quat. Sci. Rev., 193, 188–211.

Deloule É., Alexandrov P., Cheilletz A., Laumonier B., Barbey P., 2002. In-situ U–Pb zircon ages for Early Ordovician magmatism in the eastern Pyrenees, France: the Canigou orthogneisses. Int. J Earth Sci., 91, 398–405.

Demory, F., Conesa, G., Oudet, J., Mansouri, H., Münch, P., Borgomano, J., Thouveny, N., Lamarche, J., Gisquet, F., Marié, L., 2011. Magnetostratigraphy and paleoenvironments in shallow-water carbonates: the Oligocene-Miocene sediments of the northern margin of the Liguro-Provençal basin (West Marseille, southeastern France). Bull. Soc. Géol. Fr. 182, 37–55.

Demoulin, A., Mather, A., Whittaker, A., 2017. Fluvial archives, a valuable record of vertical crustal deformation. Quat. Sci. Rev. 166, 10–37.

Dempster, T.J., Persano, C., 2006. Low temperature thermochronology: resolving geotherm shapes or denudation histories? Geology 34, 73–76.

Denizot G., 1928. Note sur la morphologie, sur l'évolution et sur l'âge des terrasses toulousaines. Bull. Soc. Hist. Nat. Toulouse 57, 346–356.

Depéret, C., 1885. Description géologique du basin tertiaire du Roussillon. Ann. Sci. Géol. 17, 1–136. Thèse, Paris. Description des vertébrés fossiles du terrain pliocène du Roussillon. Ann. Sci. Géol. 17, 137–268.

Depéret, C., 1912. Sur le grès éocène de Moulas, près le Boulou (Pyrénées-Orientales). C. R. somm. Soc. Géol. France, 21–22.

Depéret, C., 1923. Les glaciations des vallées pyrénéennes françaises et leurs relations avec les terrasses fluviales. C. R. Acad. Sci. 176, 1519–1524.

Dercourt, J., Ricou, L.E., Vrielynck, B. (eds)., 1993. Atlas Tethys: palaeoenvironmental maps. Gauthier-Villars, Paris, 307 p.

De Sitter, L.U., 1952. Pliocene uplift of Tertiary mountain chains. Am. J. Sci. 250, 297–307.

De Sitter, L.U., 1954. Note préliminaire sur la géologie du Val d'Aran. Leidse Geol. Med. 18, 272–280.

De Sitter L.U., 1961. La phase tectogénique pyrénéenne dans les Pyrénées méridionales. C. R. Somm. Soc. Géol. Fr. 8, 224–225.

De Vicente, G., Cloetingh, S., Muñoz-Martin, A., Olaiz, A., Stich, D., Vegas, R., Galindo-Zaldivar, J., Fernandez-Lozano, J., 2008. Inversion of moment tensor focal mechanisms for active stresses around the microcontinent Iberia: tectonic implications. Tectonics 27, TC1009, doi:10.1029/2006TC002093.

Diaz, J., Vergés, J., Chevrot, S., Antonio-Vigil, A. Ruiz, M., Sylvander, M., Gallart, J. 2018. Mapping the crustal structure beneath the eastern Pyrenees. Tectonophysics 744, 296–309.

Dieni, I., Massari, F., Médus, J., 2008. Age, depositional environment and stratigraphic value of the Cuccuru 'e Flores Conglomerate: insight into the Palaeogene to Early Miocene geodynamic evolution of Sardinia. Bull. Soc. Géol. Fr. 179, 51–72.

Donville, B., 1973a. Ages K–Ar des vulcanites du Haut Ampurdan (NE de l'Espagne). Implications stratigraphiques. C. R. Acad. Sci. Paris 276, 2497–2500.

Donville, B., 1973b. Ages K–Ar des vulcanites du Bas Ampurdan. C. R. Acad. Sci. Paris 276, 3253–3256.

Donville, B., 1973c. Ages K–Ar des roches volcaniques de la depression de La Selva (NE de l'Espagne). C. R. Acad. Sci. Paris 277, 1–4.

Donville, B., 1973d. Géologie néogène et âge des éruptions volcaniques de la Catalogne orientale. PhD thesis, Univ. of Toulouse, 3 vols.

Donville, B., 1976. Géologie néogène de la Catalogne orientale. Bull. BRGM 2, 177–210.

Donzeau-Wiazemsky, M., Laumonier, B., Guitard, G., Autran, A., Llac, F., Baudin, T., Calvet, M., 2010. Carte géologique de la France, 1:50,000 scale, sheet 1096 Céret. Handbook by Laumonier, B., Calvet, M., Donzeau-Wiazemsky, M., Barbey, P., Marignac, C., Lambert, A., Lenoble, J.L., Autran, A., Cocherie, A., Baudin, T., Llac, F., 2015, BRGM édit., Orléans, 164 p.

Douvillé, H., 1924. A propos du poudingue de Palassou. C. R. Somm. Soc. Géol. Fr. 15, 160–162.

Dubos-Sallée, N., Nivière, B., Lacan, P., Hervouët, Y., 2007. A structural model for the seismicity of the Arudy (1980) epicentral area (Western Pyrenees, France). Geophys. J. Int. 171, 259–270.

Dubreuilh, J., Capdeville, J.P., Farjanel, G., Karnay, G., Platel, J.P., Simon-Coinçon, R., 1995. Dynamique d'un comblement continental néogène et quaternaire : l'exemple du bassin d'Aquitaine. Géologie de la France 4, 3–26.

Dufréchou, G., Tiberi, C., Martin, R., Bonvalot, S., Chevrot, S., Seoane, L., 2018. Deep structure of Pyrenees range (SW Europe) imaged by joint inversion of gravity and teleseismic delay time. Geophys. J. Int. 214, 282–301.

Durand-Delga, M., Fontboté, J.M., 1980. Le cadre structural de la Méditerranée occidentale. In: Aubouin, J., Debelmas, J., Latreille, M. (eds.), Géologie des chaînes alpines issues de la Téthys. Mém. BRGM 115, 67–85.

Duranthon, F., 1991. Biozonation des molasses continentales oligo-miocènes de la région toulousaine par l'étude des mammifères. Apports à la connaissance du Bassin d'Aquitaine. C. R. Acad. Sc. Paris 313, 965–970.

Duranthon, F., 1992. Les mammifères fossiles recueillis par l'Abbé Pouech. Actes du colloque J.J. Pouech, Pamiers 16–17 oct. 1992. Soc. Hist. Archéol. Pamiers Basse Ariège, pp. 49–54.

Duranthon, F., 1993. Nouveaux gisements à rongeurs dans les molasses oligo-miocènes de la région toulousaine. Palaeovertebrata (Montpellier) 22, 113–136.

Duranthon, F., Cahuzac, B., 1997. Eléments de corrélation entre échelles marines et continentales : les données du bassin d'Aquitaine au Miocène. In: Aguilar, J.P., Legendre, S., Michaux J. (eds.), Actes du Congrès BiochronM'97. Mém. Trav. EPHE (Montpellier) 21, pp. 591–608.

Duvail, C., Le Strat, P., Alabouvette, B., Perrin, J. Seranne, M., 2000. Évolution géodynamique du bassin du Roussillon : analyse des profils sismiques calibrés par les sondages profonds de Elne 1 et de Canet 1. Rapport n° GTR/BRGM/1200-137, Montpellier, 23 p.

Duvail, C., Gorini, C., Lofi, J., Le Strat, P., Clauzon, G., Dos Reis, T., 2005. Correlation between onshore and offshore Pliocene–Quaternary systems tracks below the Roussillon basin (Eastern Pyrenees, France). Mar. Petrol. Geol. 22, 747–756.

Duval, M., Sancho, C., Calle, M., Guilarte, V., Peña-Monné, J.L., 2015. On the interest of using the multiple center approach in ESR dating of optically bleached quartz grains: some examples from the Early Pleistocene terraces of the Alcanadre River (Ebro basin, Spain). Quat. Geochron. 29, 58–69.

ECORS Pyrenees Team, 1988. The ECORS deep reflection seismic survey across the Pyrenees. Nature 331, 508–511.

Ellenberger, F., Gottis, M., 1967. Sur les jeux de failles pliocènes et quaternaires dans l'arrière-pays narbonnais. Rev. Géogr. Phys. Géol. Dyn. 9, 153–159.

Ellenberger, F., Freytet, P., Plaziat, J.C., Bessière, G., Viallard, P., Berger, J.M., Marchal, J.P., 1987. Handbook to the Carte géologique de la France, 1:50,000 scale, sheet Capendu (1060). BRGM, Orléans, 88 p.

Enjalbert, H., 1960. Les Pays Aquitains, le modelé et les sols. Impr. Bière, Bordeaux, 618 p.

Escarguel, G., Marandat, B., Legendre, S., 1997. Sur l'âge numérique des faunes de mammifères du Paléogène d'Europe occidentale, en particulier celles de l'Eocène inférieur et moyen. In: Aguilar, J.P., Legendre, S., Michaux J. (eds.), Actes du Congrès BiochronM'97. Mém. Trav. EPHE (Montpellier) 21, pp. 441–460.

Espurt, N., Angrand, P., Teixell, A., Labaume, P., Ford, M., de Saint Blanquat, M., Chevrot, S., 2019. Crustal-scale balanced cross-section of the Central Pyrenean belt (Nestes–Cinca transect): highlighting the structural control of Variscan belt and Permian–Mesozoic rift systems on mountain building. Tectonophysics 764, 25–45.

Etheve, N., Frizon de Lamotte, D., Mohn, G., Martos, R., Roca, E., Blanpied, C., 2016. Extensional vs contractional deformation in Ibiza (Balearic Promontory, Spain): integration in the West-Mediterranean back-arc setting. Tectonophysics 682, 35–55.

Faillat, J.P., Aguilar, J.P, Calvet, M., Michaux, J., 1990. Les fissures à remplissages fossilifères néogènes du plateau de Baixas (Pyrénées orientales, France), témoins de la distension oligo-miocène. C.R. Acad. Sci. Paris sér. II 311, 205–212.

Fernandes, R.M.S., Miranda, J.M., Meijninger, B.M.L., Bos, M.S., Noomen, R., Bastos, L., Ambrosius, B.A.C., Riva, R.E.M., 2007. Surface velocity field of the Ibero-Maghrebian segment of the Eurasia–Nubia plate boundary. Geophys. J. Int. 169, 315–324.

Filleaudeau P.Y., Mouthereau F., Pik R., 2011. Thermo-tectonic evolution of the south-central Pyrenees from rifting to orogeny: insights from detrital zircon U/Pb and (U–Th)/He thermochronometry. Basin Res. 23, 1–17.

Fillon, C., van der Beek, P., 2012. Post-orogenic evolution of the southern Pyrenees: constraints from inverse thermo-kinematic modelling of low-temperature thermochronology data. Basin Res. 23, 1–19.

Fillon, C., Gautheron, C., van der Beek, P., 2013. Oligocene–Miocene burial and exhumation of the Southern Pyrenean foreland quantified by low-temperature thermochronology. J. Geol. Soc. (London) 170, 67–77.

Fitzgerald, P.G., Muñoz, J.A., Coney, P.J., Baldwin, S.L., 1999. Asymmetric exhumation across the Pyrenean orogen: implications for the tectonic evolution of a collisional orogen. Earth Planet. Sci. Lett. 173, 157–170.

Fleta, J., Vergés, J., Escuer, J., Pujadas, J., 1994. Mapa geologico de España, escala 1:50,000, Figueras (258). Memoria IGME, Madrid, 83 p.

Fleta, J., Santanach, P., Goula, X., Martínez, P., Grellet, B., Masana, E., 2001. Preliminary geologic, geomorphologic and geophysical studies for the palaeoseismological analysis of the Amer fault, NE Spain. Netherl. J. Geosci. 80, 243–253.

Ford, M., Hemmer, L., Vacherat, A., Gallagher, K., Christophoul, F., 2016. Retro-wedge foreland basin evolution along the ECORS line, eastern Pyrenees, France. J. Geol. Soc. (London) 173, 419–437.

Ford M., Vergés J., 2020. Evolution of a salt-rich transtensional rifted margin, eastern North Pyrenees, France. J. Geol. Soc. (London), https://doi.org/10.1144/jgs2019-157;

Friend, P.F., Lloyd, M.J., Mcelroy, R., Turner, J., Van Gelder, A., Vincent, S.J., 1996. Evolution of the central part of the northern Ebro basin margin, as indicated by its Tertiary fluvial sedimentary infill. In: Friend, P.F. Dabrio, C.J. (eds), Tertiary basins of Spain, the stratigraphic record of crustal kinematics. Cambridge University Press, Cambridge, pp. 166–172.

Gallart, J., Daignières, M., Banda, E., Suriñach, E., Hirn, A. 1980. The eastern Pyrenean domain: lateral variations at crust-mantle level. Ann. Geophys. 36, 141–158.

Gallart, J., Olivera, C., Daignières, M., Hirn, A. 1982. Quelques données récentes sur la relation entre fractures crustales et séismes dans les Pyrénées orientales. Bull. Soc. Géol. Fr. 24, 293–298.

Gallart, J., Diaz, J., Nercessian, A., Mauffret, A., Dos Reis, T., 2001. The eastern end of the Pyrenees: seismic features at the transition to the NW Mediterranean. Geophys. Res. Lett. 28, 2277–2280.

Garcés, M., Cabrera, L., Agustí, J., Parés, J.M., 1997. Old World first appearance datum of “Hipparion” horses: late Miocene large mammal dispersal and global events. Geology 25, 19–22.

Garcés, M., López-Blanco, M., Valero, L., Beamud, E., Muñoz, J.A., Oliva-Urcia, B., Vinyoles, A., Arbués, P., Cabello, P., Cabrera, L., 2020. Paleogeographic and sedimentary evolution of the south-Pyrenean foreland basin. Mar. Petrol. Geol. 113, 104105.

García-Castellanos, D., Vergés, J., Gaspar-Escribano, J., Cloetingh, S., 2003. Interplay between tectonics, climate, and fluvial transport during the Cenozoic evolution of the Ebro Basin (NE Iberia). J. Geophys. Res. 108, 2347, doi:10.1029/2002jb002073.

García-Castellanos, D., Cloetingh, S., 2012. Modeling the interaction between lithospheric and surface processes in foreland basins. In: Busby, C., Azor, A. (eds), Tectonics of sedimentary basins: recent advances. Blackwell, pp. 152–181.

García-Castellanos, D., Larrasoaña, J.C., 2015. Quantifying the post-tectonic topographic evolution of closed basins: The Ebro basin (Northeast Iberia). Geology 43, 663–666.

García-Ruiz, J.M., Valero-Garcés, B.L., Martí-Bono, C., González-Sampériz, P., 2003. Asynchroneity of maximum glacier advances in the central Spanish Pyrenees. J. Quat. Sci. 18, 61–72.

García-Ruiz, J.M., Martí-Bono, C., Peña-Monné, J.L., Sancho, C., Rhodes, E., Valero, B., Gonzalez Samperiz, P., Moreno, A., 2013. Glacial and fluvial deposits in the Aragón Valley, central western Pyrenees: chronology of the Pyrenean late Pleistocene glaciers. Geogr. Ann., Ser. A Phys. Geogr. 95, 15–32.

García-Ruiz, J.M., Palacios, D., de Andrés, N., Valero-Garcés, B.L., López-Moreno, J., Sanjuán, Y., 2014. Holocene and ‘Little Ice Age’ glacial activity in the Marboré Cirque, Monte Perdido Massif, Central Spanish Pyrenees. The Holocene 24, 1439–1452.

García Sainz, L., 1940. Las superficies de erosión que preceden a los glaciares quaternarios del Pirineo central y sus recíprocas influencias. Estud. Geogr. 1, 45–73.

García Senz, J., Ramirez, J.I., Navarro, J.J., Rodríguez, R., Castaño, R.M., Leyva, F., García, J., Ramirez del Poeo, J., 2009. Mapa geológico de España, 1:50,000, Pont de Suert, sheet no. 213, and handbook (76 p). Instituto Geológico y Minero de España.

Gardère, P., 2002. Les Sables Fauves : dynamique sédimentaire et évolution morpho-structurale du Bassin d'Aquitaine au Miocène moyen. Strata (Toulouse) 40, 264 p.

Gardère, P., 2005. La Formation des Sables Fauves : dynamique sédimentaire au Miocène moyen et évolution morpho-structurale de l'Aquitaine (SW France) durant le Néogène. Eclog. Geol. Helv. 97, 201–217.

Gardère, P., Rey, J., Duranthon, F., 2002. Les « Sables Fauves », témoins de mouvements tectoniques dans le basin d'Aquitaine au Miocène moyen. C. R. Geoscience 334, 987–994.

Gardère, P., Pais J., 2007. Palynologic data from Aquitaine (SW France) Middle Miocene Sables Fauves Formation. Climatic evolution. Ciências da Terra (Lisboa) 15, 151–161.

Garwin, L.G., 1985. Fission-track dating and tectonics in the Eastern Pyrenees. PhD thesis (unpubl.), Univ. of Cambridge.

Gaspar-Escribano, J., van Wees, J.D., Ter Voorde, M., Cloetingh, S., Roca, E., Cabrera, L., Muñoz, J.A., Ziegler, P.A., 2001. Lithospheric structure of the Ebro Basin (NE Spain): constraints from 3D flexural modeling. Geophys. J. Int. 145, 349–367.

Gaudant, J., 1999. Présence du genre Lates Cuvier et Valenciennes dans les grès de Moulas (Pyrénées-Orientales). Géologie de la France 4, 67–75.

Gély, J.P., Sztrakos, K., 2000. L'évolution paléogéographique et géodynamique du Bassin aquitain au Paléogène : enregistrement et datation de la tectonique pyrénéenne. Géologie de la France 2, 31–57.

Genna, A., Lenotre, N., Capdeville, J.P., 1997. Proposition d'un modele d'inversion tectonique au Plio-Quaternaire dans les Corbieres et Ie Minervois (France). Consequences morphologiques et hydrologiques. C. R. Acad. Paris 325, 807–813.

Genti, M., 2015. Impact des processus de surface sur la déformation actuelle des Pyrénées et des Alpes. PhD thesis (unpubl.), Univ. of Montpellier, 247 p.

Gibert, J., Agustí, J., Moya, S., 1979. Bioestratigrafía de l'Emporda. Paleontol. Evol. (Sabadell) 9, 43–47.

Gibert, J., Agustí, J., Moya, S., 1980. Nuevos datos sobre la bioestratigrafía del Ampurdán. Bol. Geol. Min. (Madrid) 41–46, 705–712.

Gibson, M., Sinclair, H.D., Lynn, G.J., Stuart, F.M., 2007. Late- to post-orogenic exhumation of the Central Pyrenees revealed through combined thermochronological data and modelling. Basin Res. 19, 323–334.

Gillot, P.Y., 1974. Chronométrie par la méthode K/Ar des laves des Causses et du Bas-Languedoc. Interprétation. MPhil. Dissertation (unpubl.), Univ. Paris-Sud, 61 p.

Giménez, J., Surinach, E., Fleta, J. Goula, X., 1996. Recent vertical movements from high-precision leveling data in northeast Spain. Tectonophysics 263, 149–161.

Glangeaud, P., 1938. Sur la découverte d'un gisement stampien à Anthracothérium dans les argiles à lignites de Nassiet (Landes). P. V. Soc. Linn. (Bordeaux) 40, 16–22.

Golpe-Posse, J.M., 1981a. Paleobiologia dels jaciments amb vertebrats al transit Eocè-Oligocè a la Catalunya central. Bol. Inst. Catal. Hist. Nat. 48 (Sec. Geol. 3), 123–134.

Golpe Posse, J.M., 1981b. Los Mamíferos de las cuencas de Cerdanya y Seu de Urgell y sus yacimientos; Vallesiense Medio-Superior. Bol. Geol. Min. (Madrid) 42, 91–100.

Gómez de Soler, B., Campeny Vall-Llosera, G., Van der Made, J., Oms, O., Agustí, J., Sala, R., Blain, H.A., Burjachs, F., Claude, J., García Catalán, S., Riba, D., Rosillo, R., 2012. A new key locality for the Pliocene vertebrate record of Europe: the Camp dels Ninots maar (NE Spain). Geol. Acta 10, 1–17.

Gómez-Gras, D., Roigé,, M., Fondevilla, V., Oms, O., Boya, S., Remacha, E., 2016. Provenance constraints on the Tremp Formation paleogeography (southern Pyrenees): Ebro Massif vs Pyrenees sources. Cretaceous Res. 57, 414–427.

Gomis Coll, E., Parés, J.M., Cabrera, L., 1997. Nuevos datos magnetoestratigráficos del tránsito Oligoceno-Mioceno en el sector SE de la Cuenca del Ebro (provincias de Lleida, Zaragoza y Huesca, NE de España). Acta Geol. Hisp. 32, 185–199 (publ. in 1999).

Gong, Z., Langereis, C.G., Mullender, T.A.T., 2008. The rotation of Iberia during the Aptian and the opening of the Bay of Biscay. Earth Planet. Sci. Lett. 273, 80–93.

Gorini, C., Lofi, J., Duvail, C., Dos Reis, T., Guennoc, P., Le Strat, P., Mauffret, A., 2005. The Late Messinian salinity crisis and Late Miocene tectonism: interaction and consequences on the physiography and post-rift evolution of the Gulf of Lions margin. Mar. Petrol. Geol. 22, 695–712.

Goron, L., 1931. Un type de vallée pyrénéenne : La Barguillère (Pyrénées Ariègeoises). Rev. Géogr. Pyrén. Sud-Ouest 2, 59–94.

Goron, L., 1937. Les unités topographiques du Pays ariégeois : Le rôle des cycles d'érosion tertiaires et des glaciations quaternaires dans leur morphologie. Rev. Géogr. Pyrén. Sud-Ouest 8, 300–334.

Goron, L., 1941a. Les Pré-Pyrénées ariégeoises et garonnaises, essai d'étude morphogénique d'une lisière de montagne. Privat, Toulouse, 886 p.

Goron, L., 1941b. Le rôle des glaciations quaternaires dans le modelé des vallées maîtresses des Pré-Pyrénées ariégeoises et garonnaises et leur avant-pays. Privat, Toulouse, 460 p. Abridged in: Rev. Géogr. Pyrén. Sud-Ouest 12, pp. 5–61, 147–226, 322–356, 373–430.

Gottis, M., 1958. L'apport des travaux de la Compagnie d'Exploitation Pétrolière (CEP) dans la connaissance du bassin tertiaire du Roussillon. Bull. Soc. Géol. Fr. 6-VIII, 881–883.

Gottis, M., Lenguin, M., Sellier, E., Tavoso, A., 1972. Hypothèses sur les causes et la chronologie des défluviations dans la gouttière de Carcassonne entre Toulouse et Narbonne. Bull. Soc. Linn. Bordeaux 6, 125–132.

Goula, X., Olivera, C., Fleta, J., Grellet, B., Lindo, R., Rivera, L.A., Cisternas, A., Carbon, D., 1999. Present and recent stress regime in the eastern part of the Pyrenees. Tectonophysics 308, 487–502.

Gourinard, Y., 1971. Les moraines de la basse vallée du Carol entre Latour et Puigcerda (Pyrénées orientales franco-espagnoles). C. R. Acad. Sci. Paris D 272, 3112–3115.

Granado, P., Urgeles, R., Sàbat, F., Albert-Villanueva E., Roca, E., Muñoz, J.A., Nicoletta Mazzuca, N., Gambini, R., 2016. Geodynamical framework and hydrocarbon plays of a salt giant: the NW Mediterranean Basin. Petrol. Geosci. 22, 309–321.

Granger, D.E., Kirchner, J.W., Finkel, R.C., 1997. Quaternary downcutting rate of the New River, Virginia, measured from differential decay of cosmogenic ^{26}Al and ^{10}Be in cave-deposited alluvium. Geology 25, 107–110.

Granger, D.E., Muzikar, P., 2001. Dating sediment burial with cosmogenic nuclides: theory, techniques, and limitations. Earth Planet. Sci. Lett. 188, 269–281.

Grool, A.R., Ford, M., Vergés, J., Huismans, R.S., Christophoul, F., Dielforder, A., 2018. Insights into the crustal-scale dynamics of a doubly vergent orogen from a quantitative analysis of its forelands: a case study of the Eastern Pyrenees. Tectonics 37, 450–476.

Guennoc, P., Gorini, C., Mauffret, A., 2000. Histoire géologique du golfe du Lion et cartographie du rift oligo-aquitanien et de la surface messinienne. Géologie de la France 3, 67–97.

Guitard, G., 1970. Le métamorphisme hercynien mésozonal et les gneiss œillés du massif du Canigou (Pyrénées orientales). Mém. BRGM 63, 353 p.

Guitard, G., Geyssant, J., Laumonier, B., Autran, A., Fonteilles, M., Dalmayrac, M., Vidal, J.-C., Bandet, Y., 1992. Carte géologique de la France, 1:50 000 scale, sheet Prades (1095). BRGM, Orléans. Handbook by Guitard, G., Laumonier, B., Autran, A., Bandet, Y., Berger, G.-M. (1998), 198 p.

Gunnell, Y., 2000. Apatite fission track thermochronology: an overview of its potential and limitations in geomorphology. Basin Res. 12, 115–132.

Gunnell, Y., Calvet M., 2006. Comment on “Origin of the highly elevated Pyrenean peneplain”, by J. Babault et al. Tectonics 25, TC3003, doi:10.1029/2005TC001849.

Gunnell, Y., Zeyen, H., Calvet, M., 2008. Geophysical evidence of a missing lithospheric root beneath the Eastern Pyrenees: consequences for post-orogenic uplift and associated geomorphic signatures. Earth Planet. Sci. Lett. 276, 302–313.

Gunnell, Y., Calvet, M., Brichau, S., Carter, A., Aguilar, J.P., Zeyen, H., 2009. Low long-term erosion rates in high-energy mountain belts: insights from thermo- and biochronology in the Eastern Pyrenees. Earth Planet. Sci. Lett. 278, 208–218.

Harlé, E., 1893. Restes d’éléphants du sud-ouest de la France. Bull. Soc. Hist. Nat. Toulouse, pp. 28–34.

Hartevelt, J.J.A., 1970. Geology of the Upper Segre and Valira valleys, central Pyrenees, Andorra-Spain. Leid. Geol. Med. 45, 167–236.

Hernandez, M., Mercier, N., Bertran, P., Colonge, D., Lelouvier, L.A., 2012. Premiers éléments de datation des industries du Pléistocène moyen (Acheuléen–Paléolithique moyen ancien) de la région pyrénéo-garonnaise : une approche géochronologique pluri-méthodes (TL, OSL et TT-OSL) des sites de Duclos et Romentères. Paléo 23, 155–170.

Hérail, G., Hubschman, J., Jalut G., 1987. Quaternary glaciation in the French Pyrenees. Quat. Sci. Rev. 5, 397–402.

Hervouët, Y., 1997. Déformations alpines, inversion tectonique négative et karstogenèse : exemple de la Pierre Saint-Martin (Pyrénées-Atlantiques, France). Bull. Soc. Géol. Fr. 168, 663–674.

Hez, G., Jaillet, S., Calvet, M., Delannoy, J.J., 2015. Un enregistreur exceptionnel de l'incision de la vallée de la Têt : le karst de Villefranche, Pyrénées-orientales. France. Karstologia 65, 9–32.

Hilgen, F.J., Lourens, L.J., Van Dam, J.A., Beu, A.G., Boyes, A.E., Cooper, R.A., Krijgsman, W., Ogg, J.G., Piller, W.E., Wilson, D.S., 2012. The Neogene Period. In: Gradstein, F.M., Ogg, J.G., Schmitz, M.D., Ogg, G.M. (eds), The geologic time scale. Elsevier, pp. 923–978.

Hirst, J.P.P., Nichols, G.J., 1986. Thrust tectonic controls on the Miocene distribution patterns, southern Pyrenees. In: Allen, P.A., Homewood, P. (eds), Foreland basins. IAS Spec. Publ. 8, pp. 247–258.

Hogan, P.J., Burbank, D.W., 1996. Evolution of the Jaca piggyback basin and emergence of the External Sierra, southern Pyrenees. In: Friend, P.F., Dabrio, C.J. (eds), Tertiary basins of Spain, the stratigraphic record of crustal kinematics. Cambridge University Press, Cambridge, pp. 153–160.

Hourdebaigt, M.L., Villatte, J., Crochet, B., 1986. Le poudingue de Jurançon du Sud de Pau appartient à la série syntectonique de Palassou : preuve par la découverte d'une malacofaune éocène. C. R. Acad. Sci. Paris sér. II 303, 951–955.

Hourdebaigt, M.L., 1988. Stratigraphie et sédimentologie des molasses synorogéniques en Béarn et en Bigorre. PhD thesis (unpubl.), Univ. Paul-Sabatier, Toulouse, 240 p.

Hubschman J., 1973. Etablissement par l'étude des faciès d'altération, d'un schéma stratigraphique du Quaternaire garonnais et ariégeois. C. R. Acad. Sci. Paris D 277, 753–755.

Hubschman, J., 1975a. Morphogenèse et pédogenèse dans le piémont des Pyrénées garonnaises et ariégeoises. H. Champion, Paris, 745 p.

Hubschman, J., 1975b. Conclusion, évolution pédo-géochimique et interprétation paléobioclimatique du piémont quaternaire garonnais. Bull. Assoc. Fr. Étud. Quat. 3–4, 211–216.

Huyghe, D., Mouthereau, F., Castelltort, S., Filleaudeau, P.Y., Emmanuel, L., 2009. Paleogene propagation of the southern Pyrenean thrust wedge revealed by finite strain analysis in frontal thrust sheets: Implications for mountain building. Earth Planet. Sci. Lett. 288, 421–433.

Huyghe, D., Mouthereau, F., Emmanuel, L., 2012. Oxygen isotopes of marine mollusc shells record Eocene elevation change in the Pyrenees. Earth Planet. Sci. Lett. 345–348, 131–141.

Huyghe D., Mouthereau F., Ségalen, L., Furió, M., 2020. Long-term dynamic topographic support during post-orogenic crustal thinning revealed by stable isotope ($\delta^{18}O$) paleo-altimetry in eastern Pyrenees. Sci. Rep., doi.org/10.1038/s41598-020-58903-w.

Icole, M., 1968. Données nouvelles sur la formation de Lannemezan. C. R. Acad. Sci. Paris 267, 687–689.

Icole M., 1969. Age et nature de la formation dite « de Lannemezan ». Rev. Géogr. Pyrén. Sud-Ouest 40, 157–170.

Icole, M., 1973. Géochimie des altérations dans les nappes d'alluvions du piémont occidental nord-pyrénéen. Essai de paléopédologie quaternaire. Mém. Sci. Géol. 40, Univ. Louis Pasteur, Strasbourg, 201 p.

Jalut, G., Montserrat, J., Fontugne, M., Delibrias, G., Vilaplana, J.M., Julià, R., 1992. Glacial to interglacial vegetation changes in the northern and southern Pyrenees: deglaciation, vegetation cover and chronology. Quat. Sci. Rev. 11, 449–480.

Jammes, S., Manatschal, G., Lavier, L., Masini, E., 2009. Tectonosedimentary evolution related to extreme crustal thinning ahead of a propagating ocean: example of the western Pyrenees. Tectonics 28, TC4012, 24 p.

Jarman, D., Calvet, M., Corominas, J., Delmas, M., Gunnell, Y., 2014. Large-scale rock slope failures in the Eastern Pyrenees: identifying a sparse but significant population in paraglacial and parafluvial contexts. Geogr. Ann. Ser. A: Phys. Geogr. 96, 357–391.

Jolivet, M., Labaume, P., Monié, P., Brunel, M., Arnaud, N., Campani, M., 2007. Thermochronology constraints for the propagation sequence of the south Pyrenean basement thrust system (France–Spain). Tectonics 26, TC5007, doi:10. 1029 /2006 TC002080.

Jolivet, L., Romagny, A., Gorini, C., Maillard, A., Thinon, I., Couëffé, R., Ducoux, M., Séranne, M., 2020. Fast dismantling of a mountain belt by mantle flow: late-orogenic evolution of Pyrenees and Liguro-Provençal rifting. Tectonophysics 776, 228312, 15 p.

Jones, S.J., 2004. Tectonic controls on drainage evolution and development of terminal alluvial fans, southern Pyrenees, Spain. Terra Nova 16, 121–127.

Juez Larré, J., Andriessen, P.A.M., 2006. Tectonothermal evolution of the northeastern margin of Iberia since the break-up of Pangea to present, revealed by low-temperature fission-tracks and (U–Th)/He thermochronology, a case history of the Catalan Coastal Ranges. Earth Planet. Sci. Lett. 243, 159–180.

Karnay, G., Dubreuilh J., 1998. Carte géologique de la France, 1:50,000 scale, sheet Lembeye (1005). BRGM, Orléans. Handbook by Kamay, G., Mauroux, B., Châteauneuf, J.J., 50 p.

Kästle, E.D., Rosenberg, C., Boschi, L., Bellahsen, N., Meier, T., El-Sharkawy, A., 2019. Slab break-offs in the Alpine Subduction Zone. Solid Earth Discuss., 16 p., https://doi.org/10.5194/se-2019-17.

Kiden, P., Törnqvist, T.E., 1998. Can river terrace flights be used to quantify Quaternary tectonic uplift rates? J. Quat. Sci. 13, 573–574.

Kieken, M., 1973. Évolution de l'Aquitaine au cours du Tertiaire. Bull. Soc. Géol. Fr. 15, 51–60.

Kieken, M., Burger, J.J., Thibault, C., 1975. Handbook to the Carte géologique de la France, 1:50,000 scale, sheet Saint-Vincent-de-Tyrosse (975–976). BRGM, Orléans, 46 p.

Klein, C., 1990. L'évolution géomorphologique de l'Europe hercynienne occidentale et centrale. Aspects régionaux et essai de synthèse. CNRS Editions, Paris, 177 p.

Kleinsmiede, W.F.J., 1960. Geology of the Valle de Aran (Central Pyrenees). Leid. Geol. Med. 25, 129–245.

Labaume, P., Séguret, M., Seyve, C., 1985. Evolution of a turbiditic foreland basin and analogy with an accretionary prism: example of the Eocene South-Pyrenean basin. Tectonics 4, 661–685.

Labaume, P., Méresse, F., Jolivet, M., Teixell, A., Lahfid, A., 2016a. Tectonothermal history of an exhumed thrust-sheet-top basin: An example from the south Pyrenean thrust belt. Tectonics 35, 1280–1313.

Labaume, P., Meresse, P., Jolivet, M., Teixell, A., 2016b. Exhumation sequence of the basement thrust units in the west-central Pyrenees. Constraints from apatite fission track analysis. Geogaceta 60, 11–14.

Labaume, P., Teixell, A., 2018. 3D structure of subsurface thrusts in the eastern Jaca Basin, southern Pyrenees. Geol. Act, 16, 477–498.

Labaume, P., Teixell, A., 2020. Evolution of salt structures of the Pyrenean rift (Chaînons Béarnais, France): From hyper-extension to tectonic inversion. Tectonophysics, https://doi.org/10.1016/j.tecto.2020.228451.

Lacan, P., Ortuño, M., 2012. Active tectonics of the Pyrenees: a review. J. Iberian Geol. 38, 9–30.

Lacan, P., Nivière, B., Rousset, D., Sénéchal, P., 2012. Late Pleistocene folding above the Mail Arrouy Thrust, North-Western Pyrenees (France). Tectonophysics 541–543, 57–68.

Lacombe, O., Jolivet, L., 2005. Structural and kinematic relationships between Corsica and the Pyrenees–Provence domain at the time of the Pyrenean orogeny. Tectonics 24, TC1003, doi: 10.1029/2004TC001673.

Lagabrielle, Y., Labaume, P., de Saint Blanquat, M., 2010. Mantle exhumation, crustal denudation, and gravity tectonics during Cretaceous rifting in the Pyrenean realm (SW Europe): insights from the geological setting of the lherzolite bodies. Tectonics 29, TC4012, doi:10.1029/2009TC002588.

Lagabrielle, Y., Asti, R., Fourcade, S., Corre, B., Poujol, M., Uzel, J., Labaume, P., Clerc, C., Lafay, R., Picazo, S., Maury, R., 2019. Mantle exhumation at magma-poor passive continental margins. Part 1. 3D architecture and metasomatic evolution of a fossile exhumed mantle domain (Urdach lherzolite, north-western Pyrenees, France). Bull. Soc. Géol. Fr. 190, 8. https://doi.org/10.1051/bsgf/2019007

Lagasquie, J.J., 1969. Le Bassin de Saint-Girons et la vallée du Baup (Pyrénées du Couserans). Etude morphologique. Rev. Géogr. Pyrén. Sud-Ouest 40, 267–286.

Lagasquie, J.J., 1984a. Géomorphologie des granites, les massifs granitiques de la moitié orientale des Pyrénées françaises. Thèse doct. (1982), éd. Régionales du CNRS, Toulouse, 374 p.

Lagasquie, J.J., 1984b. Les relations piémont-montagne en Couserans et Bas-Salat. Actes du colloque « Montagnes et piémonts » (12–15 May 1982), Hommage à F. Taillefer. Rev. Géogr. Pyrén. Sud-Ouest, Travaux I, pp. 239–245.

Lagasquie, J.J., 1987. Signification géodynamique des formes et dépôts de piémont dans la moitié orientale des Pyrénées. Rev. Géomorph. Dyn. 36, 85–86.

Larena, Z., Arenas, C., Baceta, J.I., Murelaga, X., Suarez-Hernando, O., 2020. Stratigraphy and sedimentology of distal-alluvial and lacustrine deposits of the western-central Ebro Basin (NE Iberia) reflecting the onset of the middle Miocene Climatic Optimum. Geol. Acta 18, 1–26.

Larrasoaña, J.C., Murelaga, X., Garcés, M., 2006. Magnetobiochronology of Lower Miocene (Ramblian) continental sediments from the Tudela Formation (western Ebro basin, Spain). Earth Planet. Sci. Lett. 243, 409–423.

Larue, J.-P., 2001. Tectonique et dynamique fluviale quaternaires : l'exemple de la basse vallée de l'Aude (France). Quaternaire 12, 169–178.

Larue, J.P., 2007. Drainage pattern modifications in the Aude basin (France): tectonic and morphodynamic implications. Proc. Geol. Assoc. 118, 187–200.

Larue, J.P., 2008. Effects of tectonics and lithology on long profiles of 16 rivers of the southern Central Massif border between the Aude and the Orb (France). Geomorphology 93, 343–367.

Laumonier, B., 2008. Les Pyrénées pré-hercyniennes et hercyniennes. In : Canérot, J., Colin, J.-P., Platel, J.-P., Bilotte, M. (eds), Pyrénées d'hier et d'aujourd'hui, Pau, 20–21 septembre 2008. Atlantica and BRGM, Biarritz–Orléans, pp. 23–35.

Laumonier, B., Barbey, P., Denèle, Y., Olivier, P., Paquette, J.-L., 2014. Réconcilier les données stratigraphiques, radiométriques, plutoniques, volcaniques et structurales au Pennsylvanien supérieur (Stéphanien–Autunien p.p.) dans l'Est des Pyrénées hercyniennes (France, Espagne). Rev. Géol. Pyrén. 1, 10 pp. http://www.geologie-despyrenees.com/

Laumonier, B., 2015. Les Pyrénées alpines sud-orientales (France, Espagne) : essai de synthèse. Rev. Géol. Pyrén. 2, 44 pp. http://www.geologie-despyrenees.com/

Laumonier, B., Le Bayon, B., Calvet, M., 2015. Handbook to the Carte géologique de la France, 1:50.000 scale, sheet Prats-de-Mollo–La-Preste (1099). BRGM, Orléans, 189 p. Geological map by Laumonier, B. et al. (2015).

Laumonier, B., Calvet, M., Delmas, M., Barbey, P., Lenoble, J.-L., Autran, A. (2017). Handbook to the Carte géologique de la France (1:50,000 scale, sheet Mont-Louis (1094). BRGM, Orléans, 139 p. Geological map by Autran, A., Calvet, M., Delmas, M. (2005).

Legendre, S., Lévêque, F., 1997. Étalonnage de l'échelle biochronologique mammalienne du Paléogène d'Europe occidentale : vers une intégration à l'échelle globale. In: Aguilar, J.P., Legendre, S., Michaux J. (eds), Actes du Congrès BiochronM'97. Mém. Trav. EPHE (Montpellier) 21, pp. 461–473.

Legendre, S., Sigé, B., Astruc, J.G., de Bonis, L., Crochet, J-Y., Denys, C., Godinot, M, Hartenberger, J-L., Levêque, F., Marandat, B., Mourer-Chauviré, C., Rage, J.-C., Remy, J.A., Sudre, J., Vianey Liaud, M., 1997. The phosphorites of Quercy: 30 years of investigations, results and prospects. Geobios 20, 331–345.

Legigan, P., 1979. L'élaboration de la formation du Sable des Landes, dépôt résiduel de l'environnement sédimentaire pliocène–pléistocène centre aquitain. Mém. Inst. Géol. Bass. Aquit., 429 p.

Lenôtre, N., Fourniguet, J., 1987. Mouvements verticaux actuels : comparaison des nivellements. Synthèse géologique des Pyrénées, Rapport groupe de travail Tectonique récente et actuelle, 7 p. and 2 maps, Doc. BRGM–IGME (unpubl).

Le Pichon, X., Bonnin, J., Sibuet, J.-C., 1970. La faille nord-pyrénéenne : faille transformante liée à l'ouverture du Golfe de Gascogne. C. R. Acad. Sci. Paris sér. D 271, 1941–1944.

Leroux, E., Aslanian, D., Rabineau, M., Pellen, R., Moulin, M., 2018. The late Messinian event: a worldwide tectonic revolution. Terra Nova 30, 207–214.

Lewis, C.J., Vergés, J., Marzo, M., 2000. High mountains in a zone of extended crust: Insights into the Neogene-Quaternary topographic development of northeastern Iberia. Tectonics 19, 86–102.

Lewis, C.J., McDonald, E.V., Sancho, C., Peña, J.L., Rhodes, E.J., 2009. Climatic implications of correlated Upper Pleistocene and fluvial deposits on the Cinca and Gállego Rivers (NE Spain) based on OSL dating and soil stratigraphy. Glob. Planet. Change 67, 141–152.

Lewis, C.J., Sancho, C., McDonald, E.V., Peña-Monné, J.L., Pueyo, E.L., Rhodes, E., Calle, M., Soto, R., 2017. Post-tectonic landscape evolution in NE Iberia using staircase terraces: combined effects of uplift and climate. Geomorphology 292, 85–103.

Lofi, J., Rabineau, M., Gorini, C., Berné, S., Clauzon, G., de Clarens, P., dos Reis, T., Mountain, G.S., Ryan, W.B.F., Steckler, M.S., Fouchet, C., 2003. Plio-Quaternary prograding clinoformwedges of the western Gulf of Lion continental margin (NW Mediterranean) after the Messinian Salinity Crisis. Mar. Geol. 198, 289–317.

Lofi, J., Gorini, C., Berné, S., Clauzon, G., Dos Reis, T., Ryan, W.B.F., Steckler, M.S., 2005. Erosional processes and paleo-environmental changes in the Western Gulf of Lions (SW France) during the Messinian Salinity Crisis. Mar. Geol. 217, 1–30.

Londeix L., (Ed.), 2014. Stratotype Aquitanien. Muséum National d'Histoire Naturelle, Paris, 416 p.

López-Gómez, J. (Ed.), 2019. Permian-Triassic rifting stage. In: Quesada, C., Oliveira, J.T. (eds), The geology of Iberia: a geodynamic approach, vol. 3, The Alpine cycle. Springer, pp. 29–112.

López-Martínez, N., Civis, J., Casanovas, L., Daams, R. (eds), 1998. Geología y Paleontología del Eoceno de la Pobla de Segur (Lleida). Edicions Universitat de Lleida, Lleida, 267 p.

López-Martínez, N., 1998. Los yacimientos de mamíferos del Eoceno de la Pobla de Segur. In: López-Martínez, N., Civis, J., Casanovas, L., Daams, R. (eds), Geología y Paleontología del Eoceno de la Pobla de Segur (Lleida), Edicions Universitat de Lleida, Lleida, pp. 9–18.

López Ruiz, J., Rodríguez Badiola, E., 1985. La region volcanica mio-pleistocena del NE de España. Estud. Geol. 41, 105–126.

Losantos, M., Aragonès, E., Berástegui, X., Palau, J., Puigdefàbregas, C., 1989. Mapa geològic de Catalunya, 1:250,000 scale. Institut Cartogràfic de Catalunya, Barcelona.

Lustrino, M., Wilson, M., 2007. The circum-Mediterranean anorogenic Cenozoic igneous province. Earth-Sci. Rev. 81, 1–65.

Luzón, A., 2005. Oligocene–Miocene alluvial sedimentation in the northern Ebro Basin, NE Spain: tectonic control and palaeogeographical evolution. Sed. Geol. 177, 19–39.

Macchiavelli, C., Vergés, J., Schettino, A., Fernández, M., Turco, E., Casciello, E., Torné, M., Pierantoni, P.P., Tunini, L., 2017. A new southern North Atlantic isochron map: insights into the drift of the Iberian Plate since the late Cretaceous. J. Geophys. Res., Solid Earth 122, 9603–9626.

Macles, O., Vernant, P., Chéry, J., Camps, P., Cazes, G., Ritz, J.F., Fink, D., 2020. Determining the Plio-Quaternary uplift of the southern French Massif Central; a new insight for intraplate orogen dynamics. Solid Earth 11, 241–258.

Maestro-Maideu, E., Serra Roig, J., 1996. The Late Eocene–Early Oligocene deposits of the NE Ebro basin, west of the Segre River. In: Friend, P.F., Dabrio, C.J. (eds), Tertiary basins of Spain, the stratigraphic record of crustal kinematics. Cambridge University Press, Cambridge, pp. 134–143.

Magné, J., 1978. Études microstratigraphiques sur le Néogène de la Méditerranée nord-occidentale. vol. 1: Les

bassins néogènes catalans, 259 p.; vol. 2: Le Néogène marin du Languedoc méditerranéen, 435 p. Éd. CNRS, Toulouse.

Magné, J., Baudelot, S., Crouzel, F., Gourinard, Y., Wallez, M.J., 1985. La mer du Langhien inférieur a envahi le centre du bassin d'Aquitaine : arguments biostratigraphiques et géochronologiques. C. R. Acad. Sc. Paris II 300, 961–964.

Maire, R., 1990. La haute montagne calcaire : karsts, cavités, remplissages, Quaternaire, paléoclimats. Karstologia Mém. 3, 731 p.

Maire, R., Vanara, N., 2008. Les karsts du domaine pyrénéen, témoins des paléoenvironnements depuis le Paléozoïque (transect Zone axiale–Zone nord pyrénéenne dans les Pyrénées atlantiques). In: Canérot, J., Colin, J.-P., Platel, J.-P., Bilotte, M. (eds), Pyrénées d'hier et d'aujourd'hui. Atlantica and BRGM, Biarritz–Orléans, pp. 109–127.

Maldonado, A., Riba, O., Orche, E., Colombo, F., 1979. Mapa geologico de España al 1/50,000, sheet n° 255 Tortosa, Memoria explicativa. IGME, Madrid, 54 p.

Marandat, B., 1991. Mammifères de l'Ilerdien moyen (Eocène inférieur) des Corbières et du Minervois, systématique, biostratigraphie, corrélations. Palaeovertebrata (Montpellier) 20, 55–144.

Marandat, B., Adnet, S., Marivaux, L., Martinez, A., Vianey-Liaud, M., Tabuce, R., 2012. A new mammalian fauna from the earliest Eocene (Ilerdian) of the Corbières (Southern France): palaeobiogeographical implications. Swiss J. Geosci. 105, 417-434.

Marcet-Riba, J., Solé-Sabaris, L., 1949. Mapa geológico de España, escala 1:50,000, explicación de la hoja 334 Gerona. IGME, Madrid, 140 p.

Marcet-Riba, J., 1954. El Villafranquiense de la vertiente meridional de los Pirineos orientales en la provincia de Gerona (España). Actes du II Congrès int. Etudes pyrénéennes, Luchon–Pau. Privat, Toulouse, pp. 143–146.

Margerie, E. de, 1946. Études Pyrénéennes. In : Critique et Géologie, contribution à l'histoire des sciences de la terre (1882–1942), vol. III, A. Colin, Paris, pp. 1157–1714.

Martínez, A., Rivero, L., Casas, A., 1997. Integrated gravity and seismic interpretation of duplex structures and imbricate thrust systems in the southeastern Pyrenees (NE Spain). Tectonophysics 282, 303–329.

Martínez del Olmo, W., 1996. Depositional sequences in the Gulf of Valencia Tertiary basin. In: Friend, P.F., Dabrio, C.J. (eds), Tertiary basins of Spain, the stratigraphic record of crustal kinematics. Cambridge University Press, Cambridge, pp. 55–67.

Martínez-Rius, A., Tudela, M., Taliada, A., Copons, R., 2013. Mapa geologic de Catalunya, escala 1:25,000, La Pobla de Lillet, 255-1-2 (71-22). Institut Geologic de Catalunya-Institut Cartografic de Catalunya.

Martinius, A.W., 2012. Contrasting styles of siliciclastic tidal deposits in a developing thrust-sheet-top basin. the Lower Eocene of the central Pyrenees (Spain). In: Davis Jr., R.A., Dalrymple, R.W. (eds), Principles of tidal sedimentology. Springer, pp. 473–506.

Martonne, E. de, 1910. Remarque sur la communication de M. L. Carez, « Résumé de la géologie des Pyrénées », Séance du 2 mai 1910, C. R. séances Soc. Géol. Fr., p. 425.

Martí, J., 2004. La región volcánica de Gerona. In: Vera, J A. (Ed.), Geología de España. SGE–IGME, Madrid, pp. 672–675.

Martí, J., Mitjavila, J., Rocá, E., Aparicio, A., 1992. Cenozoic magmatism of the Valencia trough (western Mediterranean): relationship between structural evolution and volcanism. Tectonophysics 203, 145–165.

Martí Bono, C.E., Puigdefábregas, C., 1968. Estudio del Parque Nacional de Aigues Tortes y Lago de San Mauricio (Pirineos centrales): geología y morfología. Publ. Centro Piren. Biol. Exper. (Jaca) 2, 7–37.

Martí Bono, C.E., García Ruiz, J.M. (eds), 1994. El glaciarismo surpirenaico: nuevas aportaciones. Geoforma, Logroño, 142 p.

Martzluff, M., 2006. Entre Pebble Culture, bifaces et érosion, le « Tautavélien » des terrasses quaternaires en Roussillon. Archéo 66 (Bull. Assoc. Archéo. Pyrén. Orient.) 21, 89–112.

Masana, E., 1994. Neotectonic features of the Catalan Coastal Ranges, Northeastern Spain. Acta Geol. Hisp. 29, 107–121 (Publ. in 1996).

Masana, E., Villamarín, J.A., Sánchez Cabañero, J., Plaza, J., Santanach, P., 2001a. Seismogenic faulting in an area of low seismic activity: Paleoseismicity of the El Camp fault (Northeast Spain). Neth. J. Geosci. 80, 229–241.

Masana, E., Villamarín, J.A., Santanach, P., 2001b. Paleoseismic results from multiple trenching analysis along a silent fault: the El Camp fault (Tarragona, northeastern Iberian Peninsula). Acta Geol. Hisp. 36, 329–354.

Mattauer, M., 1968. Les traits structuraux essentiels de la chaîne pyrénéenne. Rev. Géogr. Phys. Géol. Dyn. 10, 3–12.

Mattauer, M., Henry, J., 1974. Pyrenees. In: Spencer, A.M. (Ed), Mesozoic–Cenozoic belts: data for orogenic studies, Geol. Soc. London, Spec. Publ. 4, 3–21.

Mauffret, A., Durand de Grossouvre, B., dos Reis, A.T., Gorini, C., Nercessian, A., 2001.Structural geometry in the eastern Pyrenees and western Gulf of Lion (Western Mediterranean). J. Struct. Geol. 23, 1701–1726.

Maurel, O., Monié, P., Pik, R., Arnaud, N., Brunel, M., Jolivet, M., 2008. The Meso-Cenozoic thermo-tectonic evolution of the eastern Pyrenees: an $^{40}Ar/^{39}Ar$ fission track and (U–Th)/He thermochronological study of the Canigou and Mont-Louis massifs. Int. J. Earth Sci. 97, 565–584.

Meigs, A.J., Vergés, J., Burbank, D.W., 1996. Ten-million-year history of a thrust sheet. Geol. Soc. Am. Bull. 108, 1608–1625.

Meigs, A., 1997. Sequential development of selected Pyrenean thrust faults. J. Struct. Geol. 19, 481–502.

Mellere, D., Marzo, M., 1992. Los depósitos aluviales sintectónicos de la Pobla de Segur: alogrupos y su significado tectonoestratigráfico. Acta Geol. Hisp. 27, 145–159.

Mencos, J., Carrera, N., Muñoz, J.A., 2015. Influence of rift basin geometry on the subsequent postrift sedimentation and basin inversion: The Organyà Basin and the Bóixols thrust sheet (south central Pyrenees). Tectonics 34, 1452–1474.

Menendez Amor, J., 1955. La depression ceretana Española y sus vegetales fósiles. Características fitopaleontológicas del Neogeno de la Cerdaña Española. Mem. Real Acad. Sci. ex., fis. y nat. 18, 345 p.

Mensua, S., Ibañez, J., Yetano, M., 1977. Sector central de la depresion del Ebro, mapa de terrazas fluviales y glacis (5 hojas al 1:100,000, Comentario a los mapas). Departamento de Geografia, Universidad de Zaragoza, 18 p.

Meresse, F., 2010. Dynamique d'un prisme orogénique intracontinental : évolution thermochronologique

(traces de fission sur apatite) et tectonique de la Zone Axiale et des piémonts des Pyrénées centro occidentales. PhD thesis (unpubl.), Univ. of Montpellier 2, 277 p.

Metcalf, J.R., Fitzgerald, P.J., Baldwin, S.L., Muñoz, J.A., 2009. Thermochronology of a convergent orogen: Constraints on the timing of thrust faulting and subsequent exhumation of the Maladeta Pluton in the Central Pyrenean Axial Zone. Earth Planet. Sci. Lett. 287, 488–503.

Miall A., 2016. Fluvial depositional systems. Springer, 316 p.

Michael, N.A., Carter, A., Whittaker, A.C., Allen, P.A., 2014. Erosion rates in the source region of an ancient sediment routing system: comparison of depositional volumes with thermochronometric estimates. J. Geol. Soc. (London) 171, 401–412.

Michaux, J., Lopez-Martínez, N., Beaumont, G. de, Ginsburg, L., Thomas, H., Eisenmann, V., Guérin, C., Tobien, H., Legendre, S., Sen, S., 1988. Contribution à l'étude du gisement du Miocène supérieur de Montredon (Hérault). Les grands mammifères. Palaeovertebrata (Montpellier), Mém. Extraordinaire, 192 p.

Millán, H., den Bezemer, T., Vergés, J., Zoetemeijer, R., Cloetingh, S., Marzo, M., Muñoz, J.A., Puigdefábregas, C., Roca, E., Cirés, J., 1995. Present-day and middle Lutetian flexural modeling in the eastern Pyrenees and Ebro basin. Mar. Petrol. Geol. 12, 917–928.

Miller, K.G., Mountain, G.S., Wright, J.D., Browning, J.V., 2011. A 180-million-year record of sea level and ice volume variations from continental margin and deep-sea isotopic records. Oceanography 24, 40–53.

Molliex, S., Rabineau, M., Leroux, E., Bourlès, D.L., Authemayou, C., Aslanian, D., Chauvet, F., Civeta, F., Jouët, G., 2016. Multi-approach quantification of denudation rates in the Gulf of Lion source-to-sink system (SE France). Earth Planet. Sci. Lett. 444,101–115.

Molnar P., England P., 1990. Late Cenozoic uplift of mountain ranges and global climate change: chicken or egg? Nature 346, 29–34.

Molnar, P., 2004. Late cenozoic increase in accumulation rates of terrestrial sediment: How might climate change have affected erosion rates? Ann. Rev. Earth Planet. Sci., 32, 67–89.

Monaco, A., Thommeret, J., Y., 1972. L'âge des dépôts quaternaires sur le plateau continental du Roussillon (golfe du Lion). C. R. Acad. Sci. Paris D 274, 2280–2283.

Monod, B., Regard, V., Carcone, J., Wyns, R., Christophoul, F., 2016. Postorogenic planar palaeosurfaces of the central Pyrenees: Weathering and neotectonic records. C. R. Géoscience 348, 184–193.

Montgomery, D.R., 1994. Valley incision and the uplift of mountain peaks. J. Geophys. Res. 99, 13,913–13,921.

Morris, R.G., Sinclair, H.D., Yelland, A.J., 1998. Exhumation of the Pyrenean orogen: implications for sediment discharge. Basin Res. 10, 69–85.

Mouchené, M., van der Beek, P., Carretier, S., Mouthereau, F., 2017a. Autogenic versus allogenic controls on the evolution of a coupled fluvial megafan–mountainous catchment system: numerical modelling and comparison with the Lannemezan megafan system (northern Pyrenees, France). Earth Surf. Dyn. 5, 125–143.

Mouchené, M., van der Beek, P., Mouthereau, F., Carcaillet, J., 2017b. Controls on quaternary incision of the northern Pyrenean foreland: chronological and geomorphological constraints from the Lannemezan megafan, SW France. Geomorphology 281, 78–93.

Mouline, M.P., 1967. Etude des poudingues dits de Puylaurens, leurs conditions de mise en place, les conséquences paléoclimatiques de ces phénomènes. Actes Soc. Linn. Bordeaux 104 B, 3–15.

Mouline, M.P., 1978. Les épandages conglomératiques de l'Eocène inférieur à l'Oligocène dans le Castrais et l'Albigeois : l'importance de l'orographie et ses conséquences climatiques dans une des principales manifestations de la rhexistasie paléopyrénenne d'origine tectonique. Bull. Soc. Géol. Fr. 20, 215–219.

Mouline, M.P., 1989. Sédimentation continentale en zone cratonique. Le Castrais et l'Albigeois au Tertiaire. PhD thesis (unpubl.), Univ. Bordeaux Montaigne, 878 p.

Mouline, M.P., Birot, P., Paquereau, M., 1969. Le rebord NE de la Montagne Noire dans la région de Revel. Livret guide excursion A6, Pyrénées orientales et centrales, Roussillon, Languedoc occidental. VIIIe Congrès INQUA, Paris, pp. 106–109.

Mourre, V., Colonge, D., 2007. Et si l'Acheuléen méridional n'était pas là où on l'attendait ? In: Evin, J. (Ed.), Un siècle de construction du discours scientifique en Préhistoire, Avignon 21–25 sept. 2004. Congrès du Centenaire de la Société Française de Préhistoire, vol. 3, pp. 68–78.

Mouthereau, F., Filleaudeau, P.Y., Vacherat, A., Pik, R., Lacombe, O., Fellin, M.G., Castelltort, S., Christophoul, F. Masini, E., 2014. Placing limits to shortening evolution in the Pyrenees: role of margin architecture and implications for the Iberia/Europe convergence. Tectonics 33, 2283–2314.

Muñoz, J.A., 1992. Evolution of a continental collision belt: ECORS-Pyrenees crustal balanced cross-section. In: McClay, K.R. (Ed.), Thrust tectonics. Chapman and Hall, New York, pp. 235–246.

Muñoz, J.A., 2002. The Pyrenees. In: Gibbons, W., Moreno, T. (eds), The Geology of Spain. Geol. Soc., London, 370–385.

Muñoz, J.A., 2019. Alpine Orogeny: Deformation and Structure in the Northern Iberian Margin (Pyrenees s.l.). In: Quesada, C., Oliveira, J.T. (eds.), The geology of Iberia: a geodynamic approach, vol. 3: The Alpine cycle. Springer Nature, 433–451.

Muñoz, J.A., Martínez, A., Vergés, J., 1986. Thrust sequences in the Eastern Spanish Pyrenees. J. Struct. Geol. 8, 399–405.

Muñoz, J.A., Carrera, N., Mencos, J., Beamud, E., Perea, H., Arbués, P., Rivas, G., Bausà, J., García, J.M., Solà, J., Montaner, J., Rivas, G., Serra, L., Picart, J., Caus, E., Boix, C., Villalonga, R., Martínez, R., Rosell, J., 2010. Mapa geológic de Catalunya, Aramunt 252-2-2 (66-22), 1:25,000. Institut Geológic de Catalunya-Institut Cartográfic de Catalunya, Generalitat de Catalunya.

Muñoz, J.A., Beamud, E., Fernández, O., Arbués, P., Dinarès-Turell, J., Poblet, J., 2013. The Ainsa fold and thrust oblique zone of the central Pyrenees: Kinematics of a curved contractional system from palaeomagnetic ans structural data. Tectonics 32, 1142–1175.

Muñoz, J.A., Mencos, J., Roca, E., Carrera, N., Gratacós, O., Ferrer, O., Fernández, O., 2018. The structure of the South-Central-Pyrenean fold and thrust belt as constrained by subsurface data. Geol. Acta 16, 439–460.

Muratet B., Cavelier C., 1992. Caractère séquentiel discontinu des molasses oligocènes à la bordure orientale du Bassin aquitain ; signification des conglomérats bordiers (Tarn, Tarn et Garonne, Sud-Ouest de la France). Géologie de la France, 1, 3–14.

Muratet B., Duranthon F., Lange-Badré B., Riveline J., 1992. Discontinuité d'origine eustatique dans les molasses oligocènes de l'Est du Bassin Aquitain (SW France). Apport de la biochronologie. C. R. Acad. Sci. Paris sér. II 315, 1113–1118.

Murelaga X., Pérez-Rivarés F.J., Vázquez-Urbez M., Zuluaga M.C., 2008. Nuevos datos bioestratigráficos y paleoecológicos del Mioceno medio-superior (Aragoniense) del área de Tarazona de Aragón (Cuenca del Ebro, provincia de Zaragoza, España). Ameghiniana, Buenos-Aires, 45, 393–406.

Murru, M., Farrara, C., da Pelo, S., Ibba, A., 2003. The Palaeogene–Middle Eocene deposits of Sardinia (Italy) and their palaeoclimatic significance. C. R. Geoscience 335, 227–238.

Murru, M., Ferrara, C., Matteucci, R., da Pelo, S., Vacc,a A., 2007. I depositi continentali ferruginosi del Maastrichtiano sommitale–Paleocene della Sardegna meridionale (Italia). Geol. Romana 40, 175–186.

Nercessian, A., Mauffret, A., dos Reis, A.T., Vidal, R., Gallart, J., Diaz, J., 2001. Deep reflection seismic images of the crustal thinning in the eastern Pyrenees and western Gulf of Lion. J. Geodyn. 31, 211–225.

Nguyen, H.N., Vernant, P., Mazzotti, S., Khazaradze, G., Asensio, E., 2016. 3D GPS velocity field and its implications on the present-day postorogenic deformation of the Western Alps and Pyrenees. Solid Earth 7, 1349–1363

Nichols, G.J., 2005. Tertiary alluvial fans at the northern margin of the Ebro Basin. In: Harvey, A.M., Mather, A.E., Stokes, M. (eds), Alluvial fans: geomorphology, sedimentology, dynamics. Geological Society, London, Spec. Publ. 251, pp. 187–206.

Nichols, G.J., 2018. High-resolution estimates of rates of depositional processes from an alluvial fan succession in the Miocene of the Ebro Basin, northern Spain. In: Ventra, D., Clarke, L.E. (eds), Geology and geomorphology of alluvial and fluvial fans: terrestrial and planetary perspectives. Geological Society, London, Spec. Publ. 440, pp. 159–173.

Nijman, W., 1989. Thrust sheet rotation? The South Pyrenean Tertiary basin configuration reconsidered. Geodin. Acta 3, 17–42.

Nijman, W., 1998. Cyclicity and basin axis shift in a piggyback basin: towards modelling of the Eocene Tremp–Ager Basin, South Pyrenees, Spain. In: Mascle A., Puigdefabregas C., Luterbacher H.P., Fernàndez M. (eds) Cenozoic foreland basins of Western Europe. Geological Society, London, Spec. Publ. 134, pp. 135–162.

Nivière, B., Lacan, P., Regard, V., Delmas, M., Calvet, M., Huyghe, D., Roddaz, B., 2016. Evolution of the late Pleistocene Aspe river (western Pyrenees, France). Signature of climatic events and active tectonics. C. R. Geoscience 348, 203–212.

Nocquet, J.M., Calais, E., 2003. The crustal velocity field in Western Europe from permanent GPS array solutions, 1996–2001. Geophys. J. Int. 154, 72–88.

Nocquet, J.M., Calais, E., 2004. Geodetic measurements of crustal deformation in the western Mediterranean and Europe. Pure Appl. Geophys. 161, 661–681.

Nussbaum, F., 1930. Morphologische studien in den östlichen Pyrenäen. Z. Ges. Erdkunde (Berlin), 200–210.

Nussbaum, F., 1931. Sur les surfaces d'aplanissement d'âge tertiaire dans les Pyrénées-Orientales et leurs transformations pendant l'époque quaternaire. C. R. Congrès Int. Géogr., Paris, pp. 529–534.

Nussbaum, F., 1943. Orographische und morphologische untersuchungen in den östlichen Pyrenäen. Jahr. Geogr. Ges. Bern 35, 1–148 (publ. in 1945).

Odlum, M.L., Stockli, D.F., Capaldi, T.N., Thomson, K.D., Clark, J., Puigdefabregas, C., Fildani, A., 2019. Tectonic and sediment provenance evolution of the South Eastern Pyrenean foreland basins during rift margin inversion and orogenic uplift. Tectonophysics 765, 226–248.

Oele, E., Sluiter, J., Pannekoek, A.J., 1963. Tertiary and Quaternary sedimentation in the Conflent. An intramontane rift valley in the Eastern Pyrenees. Leid. Geol. Med. 28, 297–319.

Oliva-Urcia, B., 2018. Thirty years (1988–2018) of advances in the knowledge of the structural evolution of the south-central Pyrenees during the Cenozoic collision, a summary. Rev. Soc. Geol. Esp. 31, 51–68.

Oliva-Urcia, B., Beamud, E., Garcés, M., Arenas, C., Soto, R., Pueyo, E.L., Pardo, G., 2016. New magnetostratigraphic dating of the Palaeogene syntectonic sediments of the west-central Pyrenees: tectonostratigraphic implications. In: Pueyo, E.L., Cifelli, F., Sussman, A.J., Oliva-Urcia, B. (eds), Palaeomagnetism in fold and thrust belts: new perspectives. Geological Society, London, Spec. Publ. 45, pp. 107–128.

Oliva-Urcia, B., Beamud, E., Arenas, C., Pueyo, E.L., Garcés, M., Soto, R., Valero, L., Pérez-Rivarés, F.J., 2019. Dating the northern deposits of the Ebro foreland basin; implications for the kinematics of the SW Pyrenean front. Tectonophysics 765, 11–34.

Ortiz, A., Guillocheau, F., Lasseur, E., Briais, J., Robin, C., Serrano, O., Fillon, C., 2020. Sediment routing system and sink preservation during the post-orogenic evolution of a retro-foreland basin: the case example of the North Pyrenean (Aquitaine, Bay of Biscay) basins. Mar. Petrol. Geol. 112, 104085.

Ortuño, M., Queralt, P., Martí, A., Ledo, J., Masana, E., Perea, H., Santanach, P., 2008. The North Maladeta Fault (Spanish Central Pyrenees) as the Vielha 1923 earthquake seismic source: recent activity revealed by geomorphological and geophysical research. Tectonophysics 453, 246–262.

Ortuño, M., Martí, A., Martin-Closas, C., Jimenéz-Moreno, G., Martinetto, E., Santanach, P., 2013. Palaeoenvironments of the Late Miocene Pruëdo Basin: implications for the uplift of the Central Pyrenees. J. Geol. Soc. (London) 170, 79–92.

Ortuño, M., Guinau, M., Calvet, J., Furdada, G., Bordonau, J., Ruiz, A., Camafort, M., 2017. Potential of airborne LiDAR data analysis to detect subtle landforms of slope failure: Portainé, Central Pyrenees. Geomorphology 295, 364–382.

Ortuño, M., Viaplana-Muzas, M., 2018. Active fault control in the distribution of elevated low relief topography in the Central-Western Pyrenees. Geol. Acta 16, 499–518.

Oudet, J., Münch, P., Borgomano, J., Quillevère, F., Melinte-Dobrinescu, M.C., Demory, F., Viseur, S., Cornée, J.J., 2010. Land and sea study of the northeastern Golfe du Lion rifted margin: the Oligocene–Miocene of southern Provence (Nerthe area, SE France). Bull. Soc. Géol. Fr. 181, 591–607.

Oudet, J., Münch, P., Verati, C., Ferrandini, M., Melinte-Dobrinescu, M., Gattacceca, J., Cornée, J.J., Oggiano, C., Quilévéré, F., Borgomano, J., Ferrandini, J., 2010. Integrated chronostratigraphy of an intra-arc basin:

$^{40}Ar/^{39}Ar$ datings, micropalaeontology and magnetostratigraphy of the early Miocene Castelsardo basin (northern Sardinia, Italy). Palaeogeogr. Palaeoclim. Palaeoecol. 295, 293–306.

Palassou, P.B., 1781. Essai sur la minéralogie des Monts-Pyrénées. Didot-A. Jombert, Esprit éditions, reprint La Découvrance, 2007, 367 p.

Palassou, P.B., 1815. Mémoire pour servir à l'histoire naturelle des Pyrénées et des pays adjacents. Imprimerie de Vignancour, Pau, 485 p.

Palassou, P.B., 1819. Suite des mémoires pour servir à l'histoire naturelle des Pyrénées et des pays adjacents. Imprimerie de Vignancour, Pau, 428 p.

Palassou, P.B., 1823. Nouveau mémoire pour servir à l'histoire naturelle des Pyrénées et des pays adjacents. Imprimerie de Vignancour, Pau, 192 p.

Panzer, W., 1926. Talentwicklung und Eiszeitklima in nord-östlichen Spanien. Abh. Senckenb. Naturforsch. Ges. (Frankfurt) 39, 141–182.

Panzer, W., 1933. Die Entwicklung der Täler Kataloniens. Géologie des Pays Catalans, III, 21, Barcelona.

Pannekoek, A.J., 1935. Évolution du bassin de la Têt dans les Pyrénées-Orientales pendant le Néogène : étude de morphotectonique. Univ. of Utrecht, 72 p.

Pardé, M., 1941. La formidable crue d'octobre 1940 dans les Pyrénées-Orientales. Rev. Géogr. Pyrén. Sud-Ouest 12, 237–279.

Parize, O., Mulder, T., Cahuzac, B., Fiet, N., Londeix, L., Rubino, J.L., 2008. Sedimentology and sequence stratigraphy of Aquitanian and Burdigalian stratotypes in the Bordeaux area (southwestern France). C. R. Geoscience 340, 390–399.

Parsons, A.J., Michael, N.A., Whittaker, A.C., Duller, R.A., Allen, P.A., 2012. Grain-size trends reveal the late orogenic tectonic and erosional history of the south–central Pyrenees, Spain. Journal of the Geological Society, London, 169, 111–114.

Pasumot, F., 1797. Voyages physiques dans les Pyrénées en 1788 et 1789, Histoire naturelle d'une partie de ces montagnes. Le Clère, Paris, 420 p.

Patin, J., 1967. L'évolution morphologique du plateau de Lannemezan. Rev. Géogr. Pyrén. Sud-Ouest 38, 325–337.

Payros, A., Tosquella, J., Bernaola, G., Dinarès-Turell, J., Orue-Etxebarria, X., Pujalte, V., 2009. Filling the North European Early/Middle Eocene (Ypresian/Lutetian) boundary gap: insights from the Pyrenean continental to deep-marine record. Palaeogeogr. Palaeoclim. Palaeoecol. 280, 313–332.

Pedreira, D., Pulgar, J.A., Gallart, J., Diaz, J., 2003. Seismic evidence of Alpine crustal thickening and wedging from the western Pyrenees to the Cantabrian Mountains (north Iberia). J. Geophys. Res. 108, 2204, doi.org/10.1029/2001JB001667

Pedreira, D., Pulgar, J.A., Gallart, J., Torné, M., 2007. Three-dimensional gravity and magnetic modeling of crustal indentation and wedging in the western Pyrenees-Cantabrian Mountains. J. Geophys. Res. 112, B12405, doi.org/10.1029/2007JB005021.

Pedreira, D., Afonso, J.C., Pulgar, J.A., Gallastegui, J., Carballo, A., Fernàndez, M., García-Castellanos, D., Jiménez-Munt, I., Semprich, J., 2015. Geophysical petrological modeling of the lithosphere beneath the

Cantabrian Mountains and North-Iberian margin: geodynamic implications. Lithos 230, 46–68.
Peña, J.L., 1984. La conca de Tremp y sierras prepirenaicas comprendidas entre los ríos Segre y Noguera Ribagorzana, estudio geomorphológico. Instituto de Estudios Ilerdenses, SCIC, 2 vols, 373 p.
Peña, J.L., Sancho, C., 1988. Correlación y evolución cuaternaria del sistema fluvial Segre-Cinca en su curso bajo (Provincias de Lerida y Huesca). Cuat. Geomorfol. 2, 77–83.
Peña, J.L., Turu, V., Calvet, M., 2011. Les terrasses fluvials del Segre i afluents principals: descripció d'afloraments i assaig de correlació. In: Turu, V., Constante, A. (eds), El Cuaternario en España y areas afines, avances en 2011. XIII Reunión Nacional de Cuaternario, Andorra, 4–7 July. Asociación Española para el Estudio del Cuaternario (AEQUA), pp. 51–55.
Penck, A., 1883. Die Eiszeit in den Pyrenäen. Mitteilungen Ver. für Erdkunde, Leipzig, pp. 163–231.
Penck, A., 1894. Studien uber das klima spaniens während der jungeren Tertiarperiod und diluvialperiode. Z Ges. Erdkunde (Berlin) 29, 109–141.
Pérez-Rivarés, F.J., Garcés, M., Arenas, C., Pardo, G., 2002. Magnetocronología de la sucesión miocena de la Sierra de Alcubierre (sector central de la Cuenca del Ebro). Rev. Soc. Geol. Esp. 15, 217–231.
Pérez-Rivarés, F.J., Garcés, M., Arenas, C., Pardo, G., 2004. Magnetostratigraphy of the Miocene continental deposits of the Montes de Castejón (central Ebro basin, Spain): geochronological and paleoenvironmental implications. Geol. Acta 2, 221–234.
Pérez-Rivarés, F.J., Arenas, C., Pardo, G., Garcés, M., 2018. Temporal aspects of genetic stratigraphic units in continental sedimentary basins: examples from the Ebro basin, Spain. Earth-Sci. Rev. 178, 136–153.
Perrouty, S., Moussirou, B., Martinod, J., Bonvalot, S., Carretier, S., Gabalda, G., Monod, B., Hérail, G., Regard, V., Remy, D., 2015. Geometry of two glacial valleys in the northern Pyrenees estimated using gravity data. C. R. Geoscience 347, 13–23.
Peybernès, B., Fondecave-Wallez, M.-J., Combes, J.-P, Eichène, P., 2001. Mise en évidence d'un sillon marin à brèches paléocènes dans les Pyrénées centrales (Zone interne métamorphique et Zone nord-pyrénéenne). C. R. Acad. Sci. Paris 332, 379–386.
Peybernès, B., Fondecave-Wallez, M.-J., Combes, J.-P., Séranne, M., 2007. Remplissages marins successifs, paléocènes et éocènes, de paléokarsts polyphasés dans les calcaires crétacés des nappes de l'Empordà (Pyrénées catalanes, Espagne) : relations tectonique-karstification. Bull. Soc. Géol. Fr. 178, 15–24.
Peybernès, B., Melinte-Dobrinescu, M.C., Fondecave-Wallez, M.-J., 2014. Découverte de nannofossiles calcaires paléocènes dans les brèches marines remplissant les paléokarsts du synclinal d'Amélie-les-Bains (couverture de la Haute-Chaîne Primaire, Pyrénées Orientales, France). Rev. Paléobio (Geneva) 33, 455–462.
Philip, H., Bousquet, J.C., Escuer, J., Fleta, J., Goula, X., Grellet, B., 1992. Présence de failles inverses d'âge quaternaire dans l'est des Pyrénées : implications sismotectoniques. C. R. Acad. Sci. Paris sér. II 314, 1239–1245.
Philip, H. (Ed.), 2018. Tectonique récente et actuelle — Synthèse géophysique et géologique des Pyrénées – Volume 3 : Cycle alpin : phénomènes alpins. AGSO and BRGM, Pau–Orléans, pp. 361–404.
Plaziat, J.C., 1981. Late Cretaceous to late Eocene paleogeographic evolution of southwest Europe. Palaeogeogr. Palaeoclim. Palaeoecol. 36, 263–320.

Plaziat, J.C., 1984. Stratigraphie et évolution paléogéographique du domaine pyrénéen de la fin du Crétacé (phase maastrichtienne) à la fin de l'Éocène (phase pyrénéenne). Thèse doct. État, Univ. Paris-Sud, 1362 p.

Potter, P.E., Szatmari, P., 2009. Global Miocene tectonics and the modern world. Earth-Sci. Rev. 96, 279–295.

Pouech, J.J., 1873. Note au sujet des restes d'un éléphant fossile découvert à Pamiers (Ariège). C.R. Somm. Bull. Soc. Géol. Fr., 8–14.

Pous, J., Julià, R., Sole Sugrañes, L., 1986. Cerdanya basin geometry and its implication on the Neogene evolution of the eastern Pyrenees. Tectonophysics 129, 355–365.

Pous, J., Solé Sugrañes, L., Badiella, P., 1990. Estudio geoeléctrico de la depresión de La Selva (Girona). Acta Geol. Hisp. 25, 261–269.

Pous, J., Ledo, J., Marcuello, A., Daignières, M., 1995a. Electrical resistivity model of the crust and upper mantle from a magnetotelluric survey through the central Pyrenees. Geophys. J. Int. 121, 750–762.

Pous, J., Muñoz, J.A., Ledo, J.J., Liesa, M., 1995b. Partial melting of subducted continental lower crust in the Pyrenees. J. Geol. Soc. (London) 152, 217–220.

Puigdefábregas, C., 1975. La sedimentación molásica en la cuenca de Jaca. Monografias del Instituto de Estudios Pirenaicos. Pirineos (Jaca) 104, 188 p.

Puigdefábregas, C., Soler, M., 1973. Estructura de las Sierras Exteriores Pirenaícas en el corte del río Gállego (prov. de Huesca). Pirineos (Jaca) 109, 5–15.

Puigdefàbregas, C., Souquet, P., 1986. Tecto-sedimentary cycles and depositional sequences of the Mesozoic and Tertiary from the Pyrenees. Tectonophysics 129, 173–203.

Pujadas, C., Casas, J.M., Muñoz, J.A., Sabat, F., 1989. Thrust tectonics and Paleogene syntectonic sedimentation in the Empordà area, Southeastern Pyrenees. Geodin. Acta 3, 195–206.

Pujalte, V., Baceta, J.I., Schmitz, B., Orue-Etxebarria, X., Payros, A., Bernaola, G., Apellaniz, E., Caballero, F., Robador, A., Serra-Kiel, J., Tosquella, J., 2009. Redefinition of the Ilerdian Stage (early Eocene). Geol. Acta 7, 177–194.

Pujos-Lamy, A., 1984. Foraminifères benthiques et bathymétrie : le Cénozoïque du Golfe de Gascogne. Palaeogeogr. Palaeoclim. Palaeoecol. 48, 39–60.

Quirantes, J., Riba, O., 1973. Materiales pirenaicos depositados en la Depresión tertiaria del Ebro. Actes du VI Congrès international d'Etudes pyrénéennes, Bagnères-de-Bigorre, 1971. Pirineos (Jaca) 107, 13–24.

Rahl, J.M., Haines, S.H., van der Pluijm, B.A., 2011. Links between orogenic wedge deformation and erosional exhumation: Evidence from illite age analysis of fault rock and detrital thermochronology of syn-tectonic conglomerates in the Spanish Pyrenees. Earth Planet. Sci. Lett. 307, 180–190.

Ramond de Carbonnières, L.F.E., 1789. Voyages et observations faites dans les Pyrénées ; pour servir de suite à des observations sur les Alpes, insérées dans une traduction des Lettres de W. Coxe sur la Suisse. Belin, Paris, 452 p.

Razin, P., 1989. Évolution tectono-sédimentaire alpine des Pyrénées basques à l'Ouest de la transformante de Pamplona (Province du Labourd). Unpubl. PhD thesis, Univ. of Bordeaux 3, 464 p.

Rehault, J.P., Boillot, G., Mauffret, A., 1984. The western Mediterranean basin geological evolution. Mar. Geol. 55, 447—477.

Reille, J.L., 1967. Subdivisions stratigraphiques et phases de plissement dans le Paléogène continental sud-pyrénéen (region de Barbastro, province de Huesca). C. R. Acad. Sci. Paris Sér. D 265, 852–854.

Reille, J.L., 1971. Les relations entre tectogenèse et sédimentation sur le versant sud des Pyrénées centrales d'après l'étude des formations tertiaires essentiellement continentales. Thèse de Doct. Etat, Univ. of Montpellier, 330 p.

Renaud, S., Michaux, J., Schmidt, D.N., Aguilar, J.P., Mein, P., Auffray, J.C., 2005. Morphological evolution, ecological diversification and climate change in rodents. Proc. Roy. Soc. B 272, 609–617.

Rey, J., Duranthon, F., Gardère, P., Gourinard, Y., Magné, J., Feinberg, H., Muratet, B., 1997. Découverte d'un encaissement entre dépôts de sables fauves dans la région de Sos (Miocène centre-aquitain). Géologie de la France 2, 23–29.

Riba, O., 1973. Las discordancias syntectónicas del Alto Cardener (Prepirineo catalán), ensayo de interpretación. Acta Geol. Hisp 8, 90–99.

Riba, O., 1976. Syntectonic unconformities of the Alto Cardener, Spanish Pyrenees: A genetic interpretation: Sed. Geol. 15, 213–233.

Richard, M., 1948. Contribution à l'étude du bassin d'Aquitaine. Les gisements de mammifères tertiaires. Mém. Soc. Géol. France 52, 380 p.

Rigo, A. Cushing, M., 1999. Effets topographiques sur les comparaisons de profils de nivellement : cas français de Saint-Paul-de-Fenouillet (Pyrénées-Orientales) et d'Arudy (Pyrénées-Atlantiques). C. R. Acad. Sci. Paris 329, 697–704.

Rigo, A., Vernant, P., Feigl, K.L., Goula, X., Khazaradze, G., Talaya, J., Morel, L., Nicolas, J., Baize, S., Chery, J., Sylvander, M., 2015. Present-day deformation of the Pyrenees revealed by GPS surveying and earthquake focal mechanisms until 2011. Geophys. J. Int. 201, 947–964.

Roca, E., 1996a. The Neogene Cerdanya and Seu d´Urgell intramontane basins (eastern Pyrenees). In: Friend, P.F., Dabrio, C.J. (eds), Tertiary basins of Spain, the stratigraphic record of crustal kinematics. Cambridge University Press, Cambridge, pp. 114–118.

Roca, E., 1996b. La evolución geodinámica de la Cuenca Catalano-Balear y áreas adyacentes desde el Mesozoico hasta la actualidad. Acta Geol. Hisp. 29, 3–25.

Roca, E., Sans, M., Cabrera, L., Marzo, M., 1999. Oligocene to Middle Miocene evolution of the central Catalan margin (northwestern Mediterranean). Tectonophysics 315, 209–233.

Rodríguez-Vidal, J., 1986. Geomorfología de las sierras exteriores oscenses y su piedemonte. PhD thesis (1983), Univ. de Zaragoza, Instit. Estud. Alto Aragoneses, CSIC, 172 p.

Roigé, M., Gómez-Gras, D., Remacha, E., Daza, R., Boya, S., 2016. Tectonic control on sediment sources in the Jaca basin (Middle and Upper Eocene of the South-Central Pyrenees). C. R. Geoscience 348, 236–245.

Roigé, M., Gómez-Gras, D., Remacha, E., Boya, S., Viaplana-Muzas, M., Teixell, A., 2017. Recycling an uplifted early foreland basin fill: An example from the Jaca basin (Southern Pyrenees, Spain). Sed. Geol. 360, 1–21.

Roigé, M., Gómez-Gras, D., Stockli, D.F., Teixell, A., Boya, S., Remacha, E., 2019. Detrital zircon U–Pb insights

into the timing and provenance of the South Pyrenean Jaca Basin. J. Geol. Soc. (London) 176, 1182–1190.
Rosell, J., Riba, O., 1966. Nota sobre la disposicion sedimentaria de los conglomerados de La Poble de Segur. Pirineos (Jaca) 81–82, 61–74.
Rosell Sanuy, J., 1967. Estudio geológico del sector del Prepirineo comprendido entre los ríos Segre y Noguera Ribagorzana. Pirineos (Jaca) 21, pp. 9–214.
Rosell, J., Linares, R., Llompart, C., 2001. El «Garumniense» prepirenaico. Rev. Soc. Geol. Esp. 14, 47–56.
Rosenbaum, G., Lister, G.S., Duboz, C., 2002. Relative motions of Africa, Iberia and Europe during Alpine orogeny. Tectonophysics 359, 117–129.
Rosset, C., 1964. Les formations du basin oligocène de Sigean–Portel et leur chronologie. C. R. Somm. Soc. Géol. Fr., 415–417.
Rougier, G., Ford, M., Christophoul, F., Bader, A.G., 2016. Stratigraphic and tectonic studies in the central Aquitaine Basin, northern Pyrenees: Constraints on the subsidence and deformation history of a retro-foreland basin. C. R. Geoscience 348, 224–235.
Roure, F., Choukroune, P., 1998. Contribution of the ECORS seismic data to the Pyrenean geology: crustal architecture and geodynamic evolution of the Pyrenees. In: Damotte B., The ECORS Pyrenean deep seismic surveys, 1985–1994. Mém. Soc. Géol. Fr. 173, 37–52.
Sancho, C., Calle M., Peña-Monné, J.L., Duval, M., Oliva-Urcia, B., Pueyo, E.L., Benito, G., Moreno, A., 2016. Dating the earliest Pleistocene alluvial terrace of the Alcanadre River (Ebro Basin, NE Spain): insights into the landscape evolution and involved processes. Quatern. Int. 407, 86–95.
Sanjuan, J., Martín-Closas, C., Serra-Kiel, J., Gallardo, H., 2012. Stratigraphy and biostratigraphy (charophytes) of the marine-terrestrial transition in the Upper Eocene of the NE Ebro Basin (Catalonia, Spain). Geol. Acta 10, 19–31.
Sartégou, A., Bourlès, D.L., Blard, P.H., Braucher, R., Tibari, B., Zimmermann, L., Leanni, L., Aumaître, G., Keddadouche, K., 2018. Deciphering landscape evolution with karstic networks: a Pyrenean case study. Quat. Geochron. 43, 12–29.
Saspiturry, N., Razin, P., Baudin, T., Serrano, O., Issautier, B., Lasseur, E., Allanic, C., Thinon, I., Leleu, S., 2019. Symmetry vs asymmetry of a hyper-thinned rift: Example of the Mauléon Basin (Western Pyrenees, France). Mar. Petrol. Geol. 104, 86–105.
Saula, E., Picart, J., Mató, E., Llenas, M., Losantos, M., Berástegui, X., Agustí, J., 1994. Evolución geodinámica de la fosa del Emporda y las Sierras Transversales. Acta Geol. Hisp. 29, 55–75.
Sauvage, J., 1969. Etude sporo-pollinique des formations miocènes d'Orignac (Pyrénées centrales françaises). Doc. Lab. Géol. Fac. Sci. Lyon 31, 1–19.
Schettino, A., Turco, E., 2011. Tectonic history of the western Tethys since Late Triassic. Geol. Soc. Am. Bull. 123, 89–105.
Schoeffler J., 1969. L'âge des molasses de Pau à Peyrehorade. Bull. Soc. Géol. Fr. 7, 28–34.
Schoeffler, J., 1971. Étude structurale des terrains molassiques du piémont nord des Pyrénées de Peyrehorade à Carcassonne. Thèse Doct. Etat (unpubl.), Univ. of Bordeaux 1, 323 p.

Schoeffler, J., 1973. Étude structurale des terrains molassiques du piémont nord des Pyrénées de Peyrehorade à Carcassonne. Rev. Inst. Fr. Pétrole 28, 515–549 and 639–665.

Séguret, M., 1972. Étude tectonique des nappes et séries décollées de la partie centrale du versant sud des Pyrénées. Caractère synsédimentaire, rôle de la compression et de la gravité. Publ. USTELA, Montpellier, Sér. Géol. Struct. 2, 162 p.

Sen, S., 1990. Hipparion datum and its chronologic evidence in the Mediterranean area. In: Lindsay, E.H., Fahlbusch, V., Mein, P. (eds), European Neogene mammal chronology. Plenum Press, New York, pp. 495–505.

Séranne, M., 1999. The Gulf of Lion continental margin (NW Mediterranean) revisited by IBS: an overview. In: Durand, B., Jolivet, L., Horvath, F., Séranne, M. (eds), The Mediterranean basins: Tertiary extension within the Alpine orogen. Geological Society, London, Spec. Publ. 156, pp. 15–36.

Sère, V., 1993. Analyse cinématique et évolution thermotectonique des mylonites de la faille de la Têt (versant nord du Canigou, Pyrénées-Orientales). MPhil Dissertation (unpubl.), Univ. of Montpellier 2, 51 p.

Sermet, J., 1950. Réflexions sur la morphologie de la Zone Axiale des Pyrénées. Pirineos (Jaca) 6, 323–404.

Serra-Kiel, J., Mato, E., Saula, E., Travé, A., Ferrandez-Cañadell, C., Busquets, P., Samso, J.M., Tosquella, J., Barnolas, A., Alvarez-Perez, G., Franquès, J., Romero, J., 2003. An inventory of the marine and transitional Middle/Upper Eocene deposits of the Southeastern Pyrenean Foreland Basin (NE Spain). Geol. Acta 1, 201–229.

Serrano, O., Guillocheau, F., Leroy, E., 2001. Évolution du bassin compressif Nord-Pyrénéen au Paléogène (bassin de l'Adour) : contraintes stratigraphiques. C. R. Acad. Sci. Paris 332, 37–44.

Serrano E., Agudo C., 2004. Glaciares rocosos y deglaciación en la alta montaña de los Pirineos aragoneses (España). Boletín Real Sociedad Española de Historia Natural (Sección Geología) 99, 159–172.

Serrano, E., Agudo, C., Delaloye, R., Gonzalez-Trueba, J.J., 2001. Permafrost distribution in the Posets massif, central Pyrenees. Norsk Geogr. Tidsskr. 55, 245–252.

Serrat, D., Bordonau, J., Bru, J., Furdada, G., Gomez, A., Marti, J., Marti, M., Salvador, F., Ventura, J., Vilaplana, J.M., 1994. Síntesis cartográfica del glaciarismo surpirenaico oriental. In: Martí Bono, C.E., García Ruiz, J.M. (eds), El glaciarismo surpirenaico: nuevas aportaciones. Geoforma, Logroño, pp. 9–15.

Sigé, B., 1997. Les mammifères insectivores des nouvelles collections de Sossis et sites associés (Éocène supérieur, Espagne). Geobios 30, 91–113.

Sinclair, H.D., Gibson, M., Naylor, M., Morris, R.G., 2005. Asymmetric growth of the Pyrenees revealed through measurement and modelling of orogenic fluxes. Am. J. Sci. 305, 369–406.

Sinclair, H.D., Gibson, M., Lynn, G., Stuart, F., 2009. The evidence for a Pyrenean resurrection: a response to Babault et al. (2008). Basin Res. 21, 143–145.

Sitzia, L., 2014. Chronostratigraphie et distribution spatiale des dépôts éoliens quaternaires du bassin Aquitain. PhD thesis, Univ. of Bordeaux I, 341 p.

Sitzia, L., Bertran, P., Bahain, J.J., Bateman, M.D., Hernandez, M., Garon, H., de Lafontaine, G., Mercier, N., Leroyer, C., Queffélec, A., Voinchet, P., 2015. The Quaternary coversands of southwest France. Quat. Sci. Rev. 124, 84–105.

Solé Sabaris, L., 1951. Los Pirineos, el medio y el hombre. Editorial Martin, Barcelona, 624 p.

Soler, D., Teixell, A., García-Sansegundo, J., 1998. Amortissement latéral du chevauchement de Gavarnie et sa relation avec les unités sud-pyrénéennes. C. R. Acad. Sci. Paris 327, 699–704.

Sorre, M., 1913. Les Pyrénées méditerranéennes, étude de géographie biologique. Thèse, A. Colin, Paris, 508 p.

Sorriaux, P., Delmas, M., Calvet, M., Gunnell, Y., Durand, N., Pons-Branchu, E., 2016-2018. Relations entre karst et glaciers depuis 450 ka dans les grottes de Niaux-Lombrives-Sabart (Pyrénées ariégeoises). Nouvelles datations U/Th dans la grotte de Niaux. Karstologia 67, 3–16.

Soto, R., Larrasoaña, J.C., Beamud, E., Garcés, M., 2016. Early–Middle Miocene subtle compressional deformation in the Ebro foreland basin (northern Spain); insights from magnetic fabrics. C. R. Geoscience 348, 213–223.

Souquet, P., Peybernès, B., Bilotte, M., Debroas, E.J., 1977. La chaîne alpine des Pyrénées. Géol. Alpine 53, 193–201.

Souquet, P., Rey, J., Peybernès, B., Cavaillé, A., Ternet, Y., 1977. Carte géologique de la France, 1:50,000 scale, sheet Le Mas-d'Azil (1056), BRGM, Orléans. Handbook by Souquet, P., Rey, J., Peybernès, B., Bilotte, M., Cosson, J., Cavaillé, A., Roche, J.H., Bambier, A., 39 p.

Souquet, P., Debroas, E.J., 1980. Tectorogenèse et évolution des bassins de sédimentation dans le cycle alpin des Pyrénées. I : Autran A., Dercourt J. (eds), Évolutions géologiques de la France, Mém. BRGM. 107, 213–233.

Souquet, P., Debroas, É.J., Boirie, J.M., Pons, P., Fixari, G., Roux, J.C., Dol, J., Thieuloy, J.P., Bonnemaison, M., Manivit, H., Peybernès, B., 1985. Le Groupe du Flysch noir (Albo-Cénomanien) dans les Pyrénées. Bull. Cent. Rech. Explor. Prod. Elf-Aquitaine 9, 183–252.

Souriau, A., Granet, M., 1995. A tomographic study of the lithosphere beneath the Pyrenees from local and teleseismic data. J. Geophys. Res. 100, 18,117–18,134.

Souriau, A., Pauchet, H., 1998. A new synthesis of the Pyrenean seismicity and its tectonic implications. Tectonophysics, 290, 221–224.

Souriau, A., Chevrot, S., Olivera, C., 2008. A new tomographic image of the Pyrenean lithosphere from teleseismic data. Tectonophysics 460, 206–214.

Stange, K.M., van Balen, R.T., Vandenberghe, J., Peña, J.L., Sancho, C., 2013a. External controls on Quaternary fluvial incision and terrace formation at the Segre River, southern Pyrenees. Tectonophysics 602, 316–331.

Stange, K.M., van Balen, R., Carcaillet, J., Vandenberghe, J., 2013b. Terrace staircase development in the Southern Pyrenees foreland: inferences from ^{10}Be terrace exposure ages at the Segre River, Glob. Planet. Change 101, 97–112.

Stange, K.M., van Balen, R.T., Kasse, C., Vandenberghe, J., Carcaillet, J., 2014. Linking morphology across the glaciofluvial interface: a 10Be supported chronology of glacier advances and terrace formation in the Garonne River, northern Pyrenees, France. Geomorphology 207, 71–95.

Stange, K.M., Van Balen, T., Garcia-Castellanos, D., Cloetingh, S., 2016. Numerical modelling of Quaternary terrace staircase formation in the Ebro foreland basin, southern Pyrenees, NE Iberia. Basin Res. 28, 124–146.

Stange, K.M., Midtkandal, I., Nystuen, J.P., Kuss, H.J., Spiegel, C., 2018. Direct response of small non-glaciated headwater catchments to Late Quaternary climate change: The Valle de la Fueva, southern Pyrenees. Geomorphology 318, 187–202.

Stehlin, H.G., 1910. Die Säugetiere des schweizerischen Eocaens. Mém. Soc. Paléont. Suisse 36, 838–1164.

Suc, J.P., Fauquette, S., 2012. The use of pollen floras as a tool to estimate palaeoaltitude of mountains: The eastern Pyrenees in the Late Neogene, a case study. Palaeogeogr. Palaeoclim. Palaeoecol. 321–322, 41–54.

Sudre, J., de Bonis, L., Brunet, M., Crochet, J.Y., Duranthon, F., Godinot, M., Hartenberger, J.L., Jehenne, Y., Legendre, S., Marandat, B., Remy, J.A., Ringeade, M., Sigé, B., Vianey-Liaud, M., 1992. La biochronologie mammalienne du Paléogène au Nord et au Sud des Pyrénées : état de la question. C. R. Acad. Sci. Paris sér. II 314, 631–636.

Sztrakos, K., Gély, J.P., Blondeau, A., Müller, C., 1998. L'Éocène du bassin sud-aquitain : lithostratigraphie, biostratigraphie et analyse séquentielle. Géologie de la France 4, 57–105.

Sztrakos, K., Steurbaut, E., 2017. Révision lithostratigraphique et biostratigraphique de l'Oligocène d'Aquitaine occidentale (France). Geodiversitas (Paris) 39, 741–781.

Taillefer, F., 1951. Le piémont des Pyrénées françaises, contribution à l'étude des reliefs de piémont. Privat, Toulouse, 383 p.

Taillefer, F., 1957. Le glaciaire pyrénéen : versant nord et versant sud. Rev. Géogr. Pyrén. Sud-Ouest 28, 221–244.

Taillefer, F., 1967. Extent of Pleistocene glaciation in the Pyrenees. In: Wright, H.E., Osborne, W.H. (eds), Arctic and Alpine environments. Indiana University Press, Bloomington, pp. 255–266.

Taillefer, F., 1969. Les glaciations des Pyrénées. Actes du VIII° Congrès international de l'INQUA, supplément au Bulletin de l'Association Française pour l'Etude du Quaternaire, Paris, pp. 19–32.

Taillefer, F., 1982. Les conditions locales de la glaciation pyrénéenne. Pirineos (Jaca) 116, 5–12.

Tassy, P., 1990. "The Proboscidean datum event": how many proboscideans and how many datum events. In: Lindsay E.H. et al. (eds), European Neogene mammal chronology. Plenum Press, New York, p. 237–252.

Tavani, S., Bertok, C., Granado, P., Piana, F., Salas, R., Vigna, B., Muñoz, J.A., 2018. The Iberia–Eurasia plate boundary east of the Pyrenees. Earth-Sci. Rev. 187, 314–337.

Teixell, A., 1990. Alpine thrusts at the western termination of the Pyrenean Axial zone. Bull. Soc. Géol. Fr. 8, 241–249.

Teixell, A., 1998. Crustal structure and orogenic material budget in the west-central Pyrenees. Tectonics 17, 395–406.

Teixell, A., García-Sansegundo, J., 1995. Estructura del sector central de la Cuenca de Jaca (Pirineos meridionales). Rev. Soc. Geol. Esp. 8, 215–228.

Teixell, A., Muñoz, J.A., 2000. Evolución tectonosedimentaria del Pirineo meridional durante el Terciario: una síntesis basada en la transversal del río Noguera Ribagorçana. Rev. Soc. Geol. Esp. 13, 251–264.

Teixell, A., Ayarza, P., Zeyen, H., Fernàndez, M., Arboleya, M.L., 2005. Effects of mantle upwelling in a compressional setting: the Atlas Mountains of Morocco. Terra Nova 17, 456–461.

Teixell, A., Zamorano Cáceres, M., Ramírez Merino, J., Navarro Juli, J.J., Rodríguez Santisteban, R. Castaño, R.M., Leyva, F., Ramírez del Pozo, J., Aguilar, P., Robador Moreno, A., 2016. Mapa Geológico de España, escala 1:50,000, Graus (n° 250), Memoria 71 p., serie Magna, IGME.

Teixell, A., Labaume, P., Lagabrielle, Y., 2016. The crustal evolution of the west-central Pyrenees revisited: Inferences from a new kinematic scenario. C. R. Geoscience 348, 257–267.

Teixell, A., Labaume, P., Ayarza, P., Espurt, N., de Saint Blanquat, M., Lagabrielle, Y., 2018. Crustal structure and evolution of the Pyrenean–Cantabrian belt: A review and new interpretations from recent concepts and data. Tectonophysics 724–725, 146–170.

Ternois, S., Odlum, M., Ford, M., Pik, R., Stockli, D., Tibari, B., Vacherat, A., Bernard, V., 2019. Thermochronological evidence of early orogenesis, eastern Pyrenees, France. Tectonics 38, 1308–1336.

Thiry, M., 2000. Palaeoclimatic interprétation of clay minerals in marine deposits: an outlook from the continental origin. Earth-Sci. Rev. 49, 201–221.

Thomson, K.D., Stockli, D.F., Clark, J.D., Puigdefabregas, C., Fildani, A., 2017. Detrital zircon (U–Th)/(He–Pb) double-dating constraints on provenance and foreland basin evolution of the Ainsa Basin, south-central Pyrenees, Spain. Tectonics 36, 1352–1375.

Tosquella, J., Samsó, J.M., 1996. Bioestratigrafía y litoestratigrafía del Paleoceno superior-Eoceno inferior del sector oriental de la cuenca surpirenaica. Acta Geol. Hisp. 31, 3–21.

Tricart, J., Hirsch, A.R., Griesbach, J.C., 1966. La géomorphologie du bassin du Touch (Haute-Garonne), ses implications pédologiques et hydrologiques. Rev. Géogr. Pyrén. Sud-Ouest 37, 5–46.

Tugend, J., Manatschal, G., Kusznir, N.J., Masini, E., Mohn, G., Thinon, I., 2014. Formation and deformation of hyperextended rift systems: insights from rift domain mapping in the Bay of Biscay–Pyrenees. Tectonics 33, 1239–1276.

Turner, J.P., 1990. Structural and stratigraphic evolution of the West Jaca thrust-top basin, Spanish Pyrenees. J. Geol. Soc. (London) 147, 177–184.

Turu, V., Boulton, G.S., Ros, X., Peña, J.L., Martí, C., Bordonau, J., Serrano-Cañadas, E., Sancho-Marcén, C., Constante-Orrios, A., Pous, J., Gonzalez-Trueba, J.J., Palomar, J., Herrero, R., Garcia-Ruiz, J.M., 2007. Structure des grands bassins glaciaires dans le nord de la péninsule ibérique : comparaison entre les vallées d'Andorre (Pyrénées orientales), du Gàllego (Pyrénées centrales) et du Trueba (Chaîne cantabrique). Quaternaire 18, 309–325.

Turu V., 2011. Los complejos morrenicos terminales del Valira (Andorra–Alt Urgell). Resúmenes XIII Reunion Nacional de Cuaternario, Andorra 2011, Simposio de glaciarismo, guía de campo, 1–8.

Turu, V., Vidal Romani, J.R., Fernández Mosquera, D., 2011. Dataciones con isótopos cosmogénicos (^{10}Be): el "LGM" (Last Glacial Maximum) y the "Last Termination" en los valles del Gran Valira y la Valira del Nord (Principado de Andorra, Pirineos orientales). Resúmenes XIII Reunion Nacional de Cuaternario, Andorra 2011, Simposio de glaciarismo, pp. 19–23.

Turu, V., Calvet, M., Bordonau, J., Gunnell, Y., Delmas, M., Vilaplana, J.M., Jalut, G., 2017. Did Pyrenean glaciers dance to the beat of global climatic events? Evidence from the Würmian sequence stratigraphy of an ice-dammed palaeolake depocentre in Andorra. In: Hughes, P.D., Woodward, J.C. (eds), Quaternary glaciation

in the Mediterranean mountains. Geological Society, London, Spec. Publ. 433, pp. 111–136.
Urgeles, R., Camerlenghi, A., Garcia-Castellanos, D., de Mol, B., Garcés, M., Vergés, J., Haslam, I., Hardman, M., 2011. New constraints on the Messinian sealevel drawdown from 3D seismic data of the Ebro Margin, western Mediterranean. Basin Res. 23, 123–145.
Uzel, J., Nivière, B., Lagabrielle, Y., 2020. Fluvial incisions in the North-Western Pyrenees (Aspe Valley): dissection of a former planation surface and some tectonic implications. Terra Nova 32, 11–22.
Vacca, A., Farrara, C., Matteucci, R., Murru, M., 2012. Ferruginous paleosols around the Cretaceous–Paleocene boundary in central-southern Sardinia (Italy) and their potential as pedostratigraphic markers. Quatern. Int. 265, 179–190.
Vacher, P., Souriau, A., 2001. A 3D-model of the Pyrenean deep structure based on gravity modelling, seismic images and petrological constraints. Geophys. J. Int. 145, 460–470.
Vacherat, A., Mouthereau, F., Pik, R., Bernet, M., Gautheron, C., Masini, E., Le Pourhiet, L., Tibari, B., Lahfid, A., 2014. Thermal imprint of rift-related processes in orogens as recorded in the Pyrenees. Earth Planet. Sci. Lett. 408, 296–306.
Vacherat, A., Mouthereau, F., Pik, R., Bellahsen, N., Gautheron, C., Bernet, M., Daudet, M., Balansa, J., Tibari, B., Pinna Jamme, R., Rada, J., 2016. Rift-to-collision transition recorded by tectono-thermal evolution of the northern Pyrenees. Tectonics 35, 907–933.
Vacherat, A., Mouthereau, F., Pik, R., Huyghe, D., Paquette, J.L., Christophoul, F., Loget, N., Tibari, B., 2017. Rift-to-collision sediment routing in the Pyrenees: A synthesis from sedimentological, geochronological and kinematic constraints. Earth-Sci. Rev. 172, 43–74.
Valero, L., Garcés, M., Cabrera, L., Costa, E., Sáez, L., 2014. 20 Myr of eccentricity-paced lacustrine cycles in the Cenozoic Ebro Basin. Earth Planet. Sci. Lett. 408, 183–193.
Vanara, N., Maire, R., Lacroix, J., 1997. La surface carbonatée du massif des Arbailles (Pyrénées Atlantiques) : un example de paléoréseau hydrographique néogéne déconnecté par la surrection. Bull. Soc. Géol. Fr. 168, 255–265.
Vanara, N., 2000. Le Karst des Arbailles. Karstologia Mém. 3, 320 p.
Vandenberghe, N., Hilgen, F.J., Speijer, R.P., Ogg, J.G., Gradstein, F.M., Hammer, O., 2012. The Paleogene period. In: Gradstein, F.M., Ogg, J.G., Schmitz, M.D., Ogg, G.M. (eds), The geologic time scale. Elsevier, pp. 855–921.
Vanderhaeghe, O., Grabkowiak, A., 2014. Tectonic accretion and recycling of the continental lithosphere during the Alpine orogeny along the Pyrenees. Bull. Soc. Géol. Fr. 185, 143–155.
Van der Made, J., Mazo, A.V., 2003. Proboscidean dispersals from Africa towards Western Europe. In: Reumer, J.W.F., de Vos, J., Mol, D. (eds), Advances in Mammoth research (Proceedings of the Second International Mammoth Conference, Rotterdam, May 16–20 1999). DEINSEA 9, 437–452.
Van der Meer, D.G., van Hinsbergen, D.J.J., Spakman, W., 2018. Atlas of the underworld: slab remnants in the mantle, their sinking history, and new outlook on mantle viscosity. Tectonophysics 723, 309–448.

Van Hinsbergen, D.J.J., Torsvik, T.H., Schmid, S.M., Maţenco, L.C., Maffione, M., Vissers, R.L.M., Gürer, D., Spakman, W., 2019. Orogenic architecture of the Mediterranean region and kinematic reconstruction of its tectonic evolution since the Triassic. Gond. Res. 81, 79–229.

Vázquez-Urbez, M., Arenas, C., Pardo, G., Pérez-Rivarés, J., 2013. The effect of drainage reorganization and climate on the sedimentologic evolution of intermontane lake systems: the final fill stage of the Tertiary Ebro Basin (Spain). J. Sed. Res. 83, 562–590.

Ventra, D., Clarke, L.E., 2018. Geology and geomorphology of alluvial and fluvial fans: current progress and research perspectives. In: Ventra, D., Clarke, L.E. (eds), Geology and geomorphology of alluvial and fluvial fans: terrestrial and planetary perspectives. Geological Society, London, Spec. Publ. 440, pp. 1–21.

Vergés, J., Martínez, A., 1988. Corte compensado del Pirineo oriental: Geometría de las cuencas de antepaís y edades de emplazamiento de los mantos de corrimiento. Acta Geol. Hisp. 23, 95–105.

Vergés, J., Muñoz, J.A., 1990. Thrust sequences in the southern central Pyrenees. Bull. Soc. Géol. Fr. 8, 265–271.

Vergés, J., Martínez-Rius, A., Domingo, F., Muñoz, J.A., Losantos, M., Gisbert, J., Fleta, J., 1994. Mapa geológico de España, 1:50 000 scale, sheet 225, La Pobla de Lillet. IGME, Madrid. Handbook by Vergés, J., Martínez-Rius, A., Fleta, J., Pujadas, J., Tosquella, J., Samsó, J.M., Sanz, J., Barberà, M., Berástegui, X.

Vergés, J., Millán, H., Roca, E., Muñoz, J.A., Marzo, M., Cirés, J., den Bezemer, T., Zoetemeijer, R., Cloetingh, S., 1995. Eastern Pyrenees and related foreland basins: pre-, syn- and post-collisional crustal scale cross-sections. Mar. Petrol. Geol. 12, 893–915.

Vergés, J., Burbank, D.W., 1996. Eocene–Oligocene thrusting and basin configuration in the eastern and central Pyrenees (Spain). In: Friend, P.F., Dabrio, C.J. (eds), Tertiary basins of Spain, the stratigraphic record of crustal kinematics. Cambridge University Press, Cambridge, pp. 120–133.

Vergés, J., Marzo, M., Santaeularia, T., Serra-Kiel, J., Burbank, D.W., Muñoz, J.A., Giménez-Montsant, J., 1998. Quantified vertical motions and tectonic evolution of the SE Pyrenean foreland basin. In: Mascle, A., Puigdefabregas, C., Luterbacher, H.R., Fernandez, M. (eds), Cenozoic foreland basins of Western Europe. Geological Society, London, Spec. Publ. 134, pp. 107–134.

Vergés, J., Fernàndez, M., Martínez, A., 2002. The Pyrenean orogen: pre-, syn-, and post-collisional evolution. In: Rosenbaum, G., Lister, G.S. (eds), Reconstruction of the evolution of the Alpine–Himalayan Orogen. J. Virtual Explorer 8, 55–74.

Vergés, M., Fernàndez, M., 2006. Ranges and basins in the Iberian Peninsula: their contribution to the present topography. In: Gee, D.G., Stephenson, R.A. (eds), European lithosphere dynamics. Geological Society, London, Memoir 32, pp. 223–234.

Vernant, P., 2018. Apports du karst du Cotiella aux débats scientifiques sur l'érosion dans les Pyrénées, Revista Cotiella, ACEC, Plan 6, 37–47.

Viers, G., 1960. Le relief des Pyrénées occidentales et leur piémont. Pays Basque français et Barétous. Privat, Toulouse, 604 p.

Viers, G., 1961. La tectonique post-pliocène sur le littoral atlantique entre Biarritz et Hendaye. Actes VI° congrès INQUA, Varsovie, vol. 1, pp. 539–544.

Villalta, J.F. de, Crusafont, M., 1943. Los vertebrados del Mioceno continental de la Cuenca del Vallés-Penedés. Bol. Inst. Geol. Min. Esp. 59, 147–336.

Villalta, J.F. de, Palli, L., 1973. Presencia del Mioceno continental bajo et cauce del rio Onyar en Gerona. Acta Geol. Hisp. 8, 109–110.

Villena, J., Gonzalez, A., Muñoz, A., Pardo, G., Perez, A., 1992. Síntesis estratigráfica del Terciario del borde Sur de la Cuenca del Ebro: unidades genéticas. Acta Geol. Hisp. 27 (Homenaje a Oriol Riba Arderiu), 225–245.

Vincent, S.J., Elliott, T., 1996. Long-lived fluvial palaeovalleys sited on structural lineaments in the Tertiary of the Spanish Pyrenees. In: Friend, P.F., Dabrio, C.J. (eds), Tertiary basins of Spain, the stratigraphic record of crustal kinematics. Cambridge University Press, Cambridge, pp. 161–165.

Vincent, S.J., 2001. The Sis palaeovalley: a record of proximal fluvial sedimentation and drainage basin development in response to Pyrenean mountain building. Sedimentology 48, 1235–1276.

Vinyoles, A., López-Blanco, M., Garcés, M., Arbués, P., Valero, L., Beamud, E., Oliva-Urcia, B., Cabello, P., 2020. 10 Myr evolution of sedimentation rates in a deep marine to non-marine foreland basin system: tectonic and sedimentary controls (Eocene, Tremp–Jaca Basin, Southern Pyrenees, NE Spain). Basin Res. 00, 1–31, https://doi: 10.1111/bre.12481.

Viret, J., 1938. Sur l'âge des argiles ligniteuses de Nassiet près Amou (Landes). C. R. Acad. Sci. Paris 207, 500–501.

Vissers, R.L.M., Meijer, P.T., 2012a. Mesozoic rotation of Iberia: subduction in the Pyrenees? Earth-Sci. Rev. 110, 93–110.

Vissers, R.L.M., Meijer, P.T., 2012b. Iberian plate kinematics and Alpine collision in the Pyrenees. Earth-Sci. Rev. 114, 61–83.

Vissers, R.L.M., van Hinsbergen, D.J.J., van der Meer, D.G., Spakman, W., 2016. Cretaceous slab break-off in the Pyrenees: Iberian plate kinematics in paleomagnetic and mantle reference frames. Gond. Res. 34, 49–59.

Wang, Y., Chevrot, S., Monteiller, V., Komatitsch, D., Mouthereau, F., Manatschal, G., Sylvander, M., Diaz, J., Ruiz, M., Grimaud, F., Benahmed, S., Pauchet, H., Martin, R., 2016. The deep roots of the western Pyrenees revealed by full waveform inversion of teleseismic P waves. Geology 44, 475–478.

Wehr, H., Chevrot, S., Courrioux, G., Guillen, A., 2018. A three-dimensional model of the Pyrenees and their foreland basins from geological and gravity data. Tectonophysics 734–735, 16–32.

Whitchurch, A.L., Carter, A., Sinclair, H.D., Duller, R.A., Whittaker, A.C., Allen, P.A., 2011. Sediment routing system evolution within a diachronously uplifting orogen: insights from detrital zircon thermochronological analyses from the South-Central Pyrenees. Am. J. Sci. 311, 442–482.

Wiazemsky, M., Calvet, M., Laumonier, B., Guitard, G., Autran, A., Llac, F., Baudin, T., 2010. Carte géologique de la France, 1:50,000 scale, sheet Céret (1096). BRGM, Orléans. Handbook by Laumonier, B., Calvet, M., Wiazemsky, M., Barbey, P., Marignac, C., Lambert, J., Lenoble, J.L. (2015), 164 p.

Willett, S.D., Brandon, M.T., 2002. On steady states in mountain belts. Geology 30, 175–178.

Winnock, E., Fried, E., Kieken, M., 1973. Les caractéristiques des sillons aquitains. Bull. Soc. Géol. Fr. 15, 51–60.

Yelland, A., 1990. Fission track thermotectonics in the Pyrenean orogen. Nuclear Tracks and Radiation Measurements, 17, 293–299.

Yelland, A., 1991. Thermo-tectonics of the Pyrenees and Provence from fission-track studies, PhD thesis (unpubl.), Univ. of London.

Yuste, A., Luzón, A., Bauluz, B., 2004. Provenance of Oligocene–Miocene alluvial and fluvial fans of northern Ebro Basin (NE Spain): an XRD, petrographic ans SEM study. Sed. Geol. 172, 251–268.

Zandvliet, J., 1960. The geology of the upper Salat and Pallaresa valleys, Central Pyrenees, France/Spain. Leid. Geol. Med. 25, 1–127.

Zeck, H.P., 1999. Alpine plate kinematics in the Western Mediterranean: a westward directed subduction regime followed by slab roll-back and slab detachment. In: Durand, F., Jolivet, L., Horvath, M., Séranne, M. (eds), The Mediterranean basins: Tertiary extension within the Alpine orogen. Geological Society, London, Spec. Publ. 156, pp. 109–120.

Figure captions

Fig. 1. Simplified geological map of the Pyrenees. 1: Paleogene reverse faults and thrusts. 2a: Neogene normal faults. 2b: probable Neogene faults. 2c: other faults. 3: Hercynian basement, folded Paleozoic sequences, metasedimentary and granitoid rocks (basement outcrops in the Axial Zone, North-Pyrenean and Sub-Pyrenean zones, Catalan Range, and Massif Central). 4: folded Mesozoic and Cenozoic cover rocks; Paleogene conglomerate beds. 5: Neogene sedimentary rocks. 6: Neogene and Quaternary volcanic rocks. Relief base map: SRTM digital elevation model (3 arcsec).

Fig. 2. Structural subdivisions of the Pyrenean crustal wedge. A: classic tectonostratigraphic zoning. Note that all the contacts between zones are tectonic, except partly in the southeast. B: map of tectonic units and their associated thrusts, classified according to their direction of travel (northwards in the European Pyrenees, southwards in the Iberian Pyrenees) and, for the Iberian domain, the home area of the major thrust units. In red and yellow: upper units rooted to the north of the Axial Zone and NPF (southern NPZ or Chaînons béarnais, Nogueres unit, and part of the SPZ). In green: intermediate units with their home areas in the Axial Zone and involving both Axial Zone rocks (Hercynian basement) and the SPZ (cover rocks). In blue: lower units rooted beneath the Axial Zone and with outcrops either within the Axial Zone (Hercynian basement) or the SPZ (cover rocks). White arrows indicate the

5981 southward displacement of the Cotiella–Organyà–upper-Pedraforca Cretaceous unit relative
5982 to its pre-orogenic home area situated above the northern part of the Axial Zone; and more
5983 generally the sense of displacement of the SPCU–Pedraforca units. After Laumonier (2015,
5984 modified).

5985 **Fig. 3. Tectonostratigraphic cross-sections through the eastern and central Pyrenees.** A:
5986 structural units encountered along the ECORS-Pyrenees profile, after Muñoz (1992). Note
5987 the prevalence of steeply dipping discontinuities in the northern and central part of the Axial
5988 Zone, and the southward tilt of similar structures in its southern part. These southward dips
5989 have given the Nogueres units their classic impression of a 'false syncline' (Séguret, 1972). B,
5990 C: two alternative interpretations of the Axial Zone along the ECORS-Pyrenees profile: the
5991 'standard' model according to Muñoz (1992) in B, and according to Laumonier (2015) in C,
5992 respectively. Muñoz (1992) considered that the Axial Zone was a huge anticlinal stack
5993 involving a major thrust, the Nogueres–Gavarnie Thrust, implying substantial depths of
5994 crustal denudation of the basement (up to 20 km). According to Laumonier's (2015)
5995 alternative model, an overspanning Supra-Axial Thrust, rooted north of the Axial Zone (i.e.,
5996 beneath the NPZ), transported the central SPZ (i.e., the SPCU) and the Nogueres units
5997 southward. There is no major antiformal hump except along the marginal flexure, and the
5998 magnitude of uplift of the Axial Zone basement core is less than in the 'standard' model. This
5999 alternative view is supported by a number of field constraints, including the preservation of
6000 residual, unmetamorphosed Triassic cover deposits at Pruëdo (red star; see location in Fig.
6001 2), which suggests comparatively much smaller depths of denudation than implied by the
6002 thickness of the Nogueres (Gavarnie) nappe in Fig. 3B. D: schematic structural cross-section
6003 through the eastern Pyrenees (after Laumonier, 2015, modified and updated). The domain
6004 affected by Cretaceous metamorphism (i.e., the IMZ on the European side) is a very early
6005 (latest Cretaceous) nappe. It was incorporated into the overspanning Supra-Axial Thrust
6006 which propagated southward over the future Axial Zone. This IMZ represents the inverted
6007 core of the mid-Cretaceous rift and its pop-up-style ejection.

6008 **Fig. 4. Geophysical imaging of the deep lithospheric structure of the Pyrenees.** A: location
6009 of geophysical swath profiles (lines 1 to 4) and seismic profiles (lines A to E). Relief base map:
6010 Copernicus EU-DEM v1.1. B: lithospheric cross-sections obtained from simultaneous best fits
6011 between free-air gravity, geoid, thermal, and topographic data (after Gunnell et al., 2008,

6012 modified); note lithospheric taper in the east (shallowing of lithosphere–asthenosphere
6013 boundary), along profiles 3 and 4. Profile 4 extends to the Massif Central and reveals the
6014 well-documented thinned lithosphere and shallow lithosphere–asthenosphere boundary
6015 explaining the volcanic activity and dynamic uplift in that region. C: map of the lithosphere–
6016 asthenosphere boundary interpolated from profiles 1 to 4 (after Gunnell et al., 2009,
6017 modified). D: crustal-scale cross-sections through the Pyrenees (data from Chevrot et al.,
6018 2018); note the thinner crust along profiles D and E, immediately east of the ECORS-
6019 Pyrenees profile (C).
6020
6021 **Fig. 5. Parallel tectono-sedimentary evolutions of the European retro-wedge and Aquitaine**
6022 **Basin, and Iberian pro-wedge and Ebro Basin.** These scaled diagrams are
6023 chronostratigraphic (indicate the age of sedimentary formations) and tectonostratigraphic
6024 (show the contents of tectonic units delimited by major thrusts). Horizontal scale is
6025 unspecified because the N–S widths of the tectonic domains narrowed progressively over
6026 time. The chronology of thrust activity (continuous or episodic) and apparent fission-track
6027 rock exhumation age ranges for a number of massifs are also indicated. The international
6028 stratigraphic scale includes the ELMA biozones. Three synthetic transects spanning the
6029 Pyrenees from foreland to retro-foreland include an eastern one from the Montagne Noire
6030 to NE Catalonia; a central one from Ariège to eastern Aragón; and a western one from Béarn
6031 to western Aragón through the western termination of the Axial Zone.
6032 Key to symbols, colours and ornaments. 1: marine sequences; 2: deltaic and base-level
6033 floodplain sequences; 3: continental sequences; 4a: proximal conglomerates; 4b: other
6034 coarse-textured debris-fan formations; 5: clay with decalcified pebbles; 6: sand- and clay-
6035 textured, carbonate-rich fluvial molasse; 7: other sand- and clay-textured molasse
6036 occurrences; 8: sand- and clay-textured deltaic facies; 9: other marine sandstones; 10: shelf
6037 limestone, and lacustrine or palustrine limestone; 11a: epipelagic carbonates; 11b: outer-
6038 shelf marls; 12: slope and abyssal flysch and turbidites; 13: marine or continental evaporites
6039 (gypsum, salt); 14a: main mammalian fossil site; 14b: stratigraphic type section; 15: main
6040 lithostratigraphic units; 16a: transverse drainage systems; 16b: strike-parallel drainage
6041 systems; 17a: apatite fission-track (AFT) age range; 17b: zircon fission-track (ZFT) age range;
6042 18: main thrusts (a) and/or faults (b). In red: main tectonic structures, thrusts, and thrust
6043 soles. AFT and ZFT apparent cooling ages after Yelland (1991), Maurel (2003), Maurel et al.

(2002, 2008), Gunnell et al. (2009), Rushlow et al. (2013), Vacherat et al. (2016), Fitzgerald et al. (1999), Sinclair et al. (2005), Jolivet et al. (2007), Bosch et al. (2016), DeFelipe et al. (2019).

Fig. 6. Map of elevated erosion surfaces and other diagnostic landforms in the Pyrenees, with correlated sedimentary deposits. The map is based on a systematic map and field survey of each individual topographic unit. 1: range-top surface S (late Oligocene to Aquitanian). 2: range-flank pediment P1 (middle Miocene); in the western Pyrenees S and P1 are indistinguishable. 3: base-level connections for P1; 3a: Langhian–Serravallian coastal deposits; 3b; Serravallian and Tortonian lacustrine limestones. 4: elevated massifs of the western Axial Zone never bevelled by S or P1. 5: late Neogene local pediments P2 and P3, also represented as karstic poljes when in limestone outcrops. 6: deposits relating to the generation of P2 or P3; 6a: Mediterranean Pliocene sediments, Lannemezan Formation (ancient range-front fluvial megafans), calcrete-capped upper wash pediments of the Ebro Basin; 6b: isolated vestiges of siliciclastic lag gravels capping P2; 6c: upper slope breccia deposits of the Cinca watershed (Merli Fm.). 7: main palaeovalleys associated with P1 (7a), with P2 (7b), and of middle Pleistocene age (7c).

Fig. 7. Diagnostic erosion surfaces of the Pyrenees: Axial Zone and northern retro-wedge. A. middle Miocene pediment in the eastern Corbières, cross-cutting folded Aptian/Barremian limestone beds (Urgonian facies). Note how the erosional surface grades to the top of the marine Miocene sequence of the Serre du Scorpion (consists of a Langhian littoral facies at its base and terminates with offlapping lacustrine limestones). Leucate lagoon and modern Mediterranean coastline in the background. B. Shore platform cut in the Urgonian limestone at the base of the marine Miocene outcrop and displaying fossil Gastrochaenolites (Serre du Scorpion). C. Summit surface at Roc Paradet (Corbières). Here the Pyrenean Frontal Thrust and the entire North-Pyrenean limestone sequence (visible in the walls of the Galamus canyon) have been cross-cut by this erosional surface. D. Panoramic view of the Fenouillèdes and the Agly massif; surface S cuts across all the geological structures of the North-Pyrenean Zone, and has been tilted from the Madrès massif (where S lies at 2400 m) to the Mediterranean. Miocene surface P1 extends at lower elevations, and in this area takes the form of anomalously wide, flat-floored valleys. On the

far horizon: late Neogene horsts of the Canigou and Albères. E. Erosion surfaces of the Carlit massif (eastern Pyrenees). Miocene pediment P1, here unscathed by glaciation, forms an extensive topographic bench in granite and gneiss sloping SSE (2350–2000 m); the Carlit massif rises as a residual mass capped by summit surface S (inset F), itself bearing an isolated monadnock (Pic Péric) and cutting across Cambrian schist and hornfels. G. Vestiges of pediment P1 below the more elevated surface S in the Aston massif (Ariège), all cut in gneiss. H. Vast sweep of pediment P1 at the Plateau de Beille, Aston massif (also shown in G). Note residual topographic masses rising above P1 in the Carlit and Hospitalet massifs.

Fig. 8. Diagnostic erosion surfaces of the Pyrenees: southern pro-wedge and western massifs. A. Summit surface, S, in the Port de Comte massif (eastern South-Pyrenean Zone). The land surface cuts across folds in the Upper Cretaceous and Eocene limestone beds as well as upturned breccia units attributed to the Priabonian–Oligocene boundary. Note the low-angle fault-drag deformation of the Oligocene conglomerate beds (Berga conglomerates) beneath the Vallfogona Thrust (i.e., the SPFT). Partial pediments (generation P2) have cut benches into the conglomerate sequence along the mountain front. B. Erosion surfaces at the Montsec thrust (SPCU). Summit surface, S (tilted), on the Montsec thrust-front ridgetop and on the Serra de Sant Mamet; pediment P1 cuts across deformed Oligocene conglomerate beds and the north-dipping Upper Cretaceous units at the eastern termination of the Montsec. C. Summit surface S cutting across Upper Cretaceous limestone beds in the Montsec massif. D. The Montsec rising as a residual inselberg above pediment P1 at the Col de Comiols. E. Summit surface at the Sierra de Sevil (eastern Sierra de Guara, i.e., Sierras Exteriores), cutting across the Balcez anticline (thick Eocene limestone) with beds vertically upturned at its western limb). Unconformable early Miocene conglomerate beds supplied by the eroding relief have partially buried the south-facing mountain flank and are ovelain by finer molasse deposits (Sariñena Fm.). This upward-fining sequence is consistent with the upland topography having attained gentle gradients towards the end of the local denudation history, thereby supplying finer debris. Note identical gradient between the slope of the erosion surface and the dip of the clastic beds. F. Erosion surface in the central Sierra de Guara. Note the numerous monadnocks rising above it; the surface (as in E) grades to the Sariñena clastic sequence at the southern mountain front and bevels the northward-dipping sandstone beds of the Campodarbe Fm. on the northern mountain flank. G. the N–S

Turbon anticline. The limestone structure and its subvertical limbs are completely bevelled by the ridgetop erosion surface. H. Summit surface in the Basque Pyrenees. The Okabé plateau cuts across the Hercynian basement rocks of the Iraty massif as well as its Cretaceous and Eocene envelopes. I. The Arres d'Anie: an erosion surface cutting across the folded and faulted Canyon Limestone. Note its pyramidal monadnocks.

Fig. 9. Cross-cutting relations between low-gradient topography, geological structure, and the unconformable syn-orogenic Paleogene conglomerate sequences of the south-central Pyrenees. The proximal facies of these conglomerate deposits, which consists of massive boulder beds, is incompatible with the scenario of an overfilled basin onlapping northward onto a low-gradient erosion surface in its final stages of completion and itself supplying those boulder beds. Rather than a low-relief, low-energy hinterland, such deposits document steep, high-energy, and perhaps tectonically active orogenic relief upstream. A: Col de Perves (outcrops around Tossal Gros, Antist allogroup); these are >> 1-m-sized boulders of granite and Devonian source-rocks; in the background, the Axial Zone is entirely devoid of documented summit erosion surfaces. Elevations in metres. B: western summit zone of Boumort (outcrops around Planell Ras, Pallaresa allogroup), displaying metre-sized boulders of grey limestone, red Devonian limestone ('calcaire griotte', in foreground), and Triassic sandstone; in the background: cupola of Cenomanian–Turonian limestone cut by the vestige of an erosion surface. C: from Boumort, view to the NE, showing tectonic deformations in the Cogomera alluvial conglomerate sequence and the summit erosion surface cross-cutting the massive Urgonian limestone of Serra de Prada. D: Planell Ras outcrop, close-up of a boulder of Triassic conglomerate (height: 1.6 m). E: Serrat Negre–Catllaras outcrop, here showing the terminal Priabonian conglomerates containing megaboulders of granite (long axis: 3 m). The Paleogene conglomerates in the area everywhere are tectonically deformed and cross-cut by the low-gradient erosion surface. F: view from Boumort to the west towards the outcrops of La Pobla de Segur; note tectonic deformation of the entire series, terminal Antist allogroup included; to the SW, also note the vestiges of low-gradient erosion surfaces at the top Serra de Sis, Turbon (see also Fig. 8G), St Gervas–Mt. d'Adons, and Serra de Comillini–Plan del Mont (elevations in metres); to the NW, elevated massifs of the Axial Zone (Aneto) and its cover rocks (Monte Perdido), neither bearing clearly definable erosion surfaces. G, H: geological cross-sections through the

Boumort massif, showing that the conglomerate deposits have buried a palaeolandscape of high relief and that the land surface cross-cuts these underlying structures as well as the deformed conglomerate sequences. Section G cuts across the eastern extremity of Boumort; section H cuts through the summit area, where residual conglomerate beds still occur; position of the conglomerate sequence before erosion also schematiclly represented (cross-sections from Peña, 1983, redrawn, augmented and modified in the light of more recent data concerning the dip of the conglomerate beds as measured in the field and/or depicted on the detailed geological map (sheet: Aramunt) authored by Muñoz et al., 2010.

Fig. 10. Low-temperature thermochronology in relation to range-top or range-flank erosion surfaces in the Pyrenees. A: AFT and AHe age–elevation plot (data from Gunnell et al., 2009). Abbreviated massif names: CMPC–Campcardos; CAN–Canigou; POMA–Pla de Pomarola; GUIL–Pla Guillem; CAR–Carlit; MAD–Madres; DONZ–Donnezan; BAS–Bassiès; AS-Aston; LLES–Tossa Plana de Llès; LPCH–Col de la Perche; MTBA–Massif de Montalba; AGLY–Massif de l'Agly. AFT ages produced by Yelland (1991) and Maurel et al. (2008) (marked Y and M, respectively) are given to show good agreement between independent workers. B: plot of mean fission-track length vs. topographic elevation. C: cooling paths obtained by forward thermal modelling of the AFT and AHe data. The best-fitting cooling trajectories pooled and scaled in this way highlight the residence times of individual samples at near-surface conditions since 35–25 Ma irrespective of their current elevations (after Gunnell et al., 2009, modified). D: cooling paths for the Aneto massif (after Gibson et al., 2007, modified); note similarities with cooling paths obtained in the eastern Pyrenees.

Fig. 11. Conceptual scenarios for explaining the observed distribution of range-top erosion surfaces in the Pyrenees. Scenarios A and C are the two end-member situations detailed in the text. Scenario B is a variant of A. In A, the range-top surface (peneplain S) occurs throughout the range. The population of pediment surfaces (P) were generated during the middle Miocene except in the Basque Pyrenees, where P and S are indistinguishable. In B, the altitudinal offset between S and P only exists in the east, and is a response to changes in base level caused by Mediterranean rifting; further west, the two surfaces merge but erosion has obliterated them in the central Pyrenees because of more intense crustal uplift in this segment of the orogen. In C, the altitudinal offset between S and P is again a response

to Mediterranean rifting. The elevation offset disappears further west, where the surfaces only occur as summit bevels across the outer fold and thrust belts. The distinction with scenario B is that, in scenario C, the high massifs of the Axial Zone in the central Pyrenees never were bevelled by the range-top 'peneplain'.

Fig. 12. Neotectonic record in the Pyrenees and foreland areas. 1: outcrops of Hercynian basement; 2: Pliocene continental and marine deposits; 3: early Pleistocene alluvial deposits, uppermost terraces; 4: middle and late Pleistocene and Holocene alluvial terraces; 5: Pleistocene glaciers; 6: late Miocene to late Pleistocene volcanic rocks; 7: continental shelf isobaths; 8a: main faults and thrusts of Hercynian and Pyrenean age; 8b: blind or probable faults and thrusts of Hercynian and Pyrenean age; 9a: main fold axis in the outer fold belts; 9b: Neogene normal fault. 10: neotectonic deformations affecting Pliocene deposits; 10a: reverse fault, 10b: normal fault; 10c: strike-slip fault; 10d: faulted karstic landform of deposit (unspecified). 11: neotectonic deformations affecting Pleistocene deposits; 11a: reverse fault, fold; 11b: normal fault; 11c: strike-slip fault; 11d: faulted karstic landform of deposit (unspecified); 11e: fault (unspecified). Places names of recorded deformation indices (some are logged under a single number given their close proximity); 1: Escandorgue, 2: Le Rièges; 3: Bize-Minervois; 4: Saint Chipoli–Dourgne; 5: Fabrezan; 6: Caramany–Le Mas; 7: Millas, Néfiach, Ille-sur-Têt; 8: Perpignan–Serrat d'en Vaquer; 9: Trouillas, Fourques; 10: Sorède, Laroque des Albères, Villelongue; 11: St Climent Sescebes; 12: Pontos, Fluvia; 13: Pedrinya, Incarcal; 14: Serinya; 15: Tortella, Rajolins, Burro; 16: Camp de Tarragona; 17: Baix Ebre; 18: Villefranche karst (ND de Vie, Faubourg); 19: Estavar; 20: Osséja; 21: Martinet; 22: La Seu d'Urgell–Montferrer; 23: Balaguer NE–Rio Sio; 24: Balaguer NW; 25: Alfarras; 26: Canelles; 27: Isaba; 28: Pierre-St-Martin karst; 29: Arbailles karst; 30: Lurbe–Asasp; 31: Capbis; 32: Arcizac; 33: Bastenne-Gaujac, Heugas; 34: Horsarieux; 35: Meilhan; 36: Côte Basque, Arcangue-Castagnet. After Philip (2018), Baize et al. (2002), Goula et al. (1999), Lacan and Ortuño (2012), and other references provided in the text. For the Plio-Pleistocene fluvial deposits, data sources: 1:1,000,000 scale geological map of France (BRGM), 1:400,000 map of Quaternary deposits of the Pyrenees (Barrère et al., 2009), 1:50,000 scale geological maps of Spain (IGME), with additional data from Mensua et al. (1977). Glacial extent after Calvet (2004) and Calvet et al. (2011).

6204 **Fig. 13. Seismic activity in the Pyrenees.** A: historical earthquakes since the Middle Ages. B:
6205 instrumentally measured seismicity since 1997 (source: Réseau de Surveillance Sismique des
6206 Pyrénées, Observatoire Midi-Pyrénées, Toulouse).
6207
6208 **Fig. 14. Aspects of the Pyrenean partial pediments (generation P2), suggesting a late**
6209 **Neogene lull in rates of base-level change.** A. Erosional piedmont of the Basque Country,
6210 here looking west from Isturitz. P2 cuts across Cretaceous flysch, massive and vertically
6211 upturned Malm to Aptian/Barremian limestone, and the Hercynian core of schist in the
6212 Ursuya–Baïgura massifs. In foreground: Pleistocene polje of Isturitz. In background: residual
6213 inselbergs rising above P2. B. Erosional piedmont of the Basque Country, here looking east
6214 from Isturitz. P2 cuts across Cretaceous flysch; vestiges of an older surface at higher
6215 elevation caps the foothills situated below the snowline (Ostabat–Ainharp). On the far
6216 horizon, and extending in topographic continuity from P2: top of the de Lannemezan Fm.,
6217 here preserved as strips of the Ossau and Ger megafans. C. Erosional piedmont P2 in the
6218 central Pyrenees of the Ariège, here seen from the village of Carla-Bayle. The erosion surface
6219 cuts across the Sub-Pyrenean folds of the Plantaurel–Mas d'Azil (Petite Pyrénées: Paleocene
6220 and Lower Eocene limestones), the NPT, the Cretaceous flysch of the Camarade Basin, and
6221 massive limestones of the North-Pyrenean Zone at the foot of the Arize massif. P2 displays a
6222 residual hill in flysch at Cabanères, and grades westward along the strike of the mountain
6223 front to the top of the residual Salat megafan (Lannemezan Fm.). Vestiges of this alluvial
6224 deposit cap the Miocene molasse outcrop in the foreground. D. Well-preserved example of
6225 pediment P2 at the Col de La Perche, between the Cerdagne and Conflent intermontane
6226 half-grabens (eastern Pyrenees). The erosion surface cuts across the basement rocks of the
6227 Axial Zone as well as across upturned Upper Miocene beds of the Cerdagne Basin fill
6228 sequence. P2 is deeply incised on the east side of La Perche by the Têt knickzone near Mont-
6229 Louis. In the background, note surfaces S and P1 present in massifs on either side of the
6230 Cerdagne Basin. E. P2 pediment in the Port de Comte massif (eastern South-Pyrenean Zone).
6231 The Pla de Riard is the top of a clastic accumulation considered here to be an Iberian
6232 equivalent of the Lannemezan Fm. F. Palaeovalley P2 at the Col du Puymorens (eastern Axial
6233 Zone), with palaeodrainage probably directed towards the Querol and Cerdagne but later
6234 captured by the Ariège River and thus diverted northward. G. Palaeovalley P2 at Pla de Beret

(central Pyrenees), at the source of the Noguera Pallaresa. The upper catchment was captured and diverted by the Garonne.

Plate I. Palaeogeography of the Pyrenees and its surrounding regions from the early Paleocene (65–60 Ma) to the Quaternary. These ten maps crafted from a geomorphological perspective indicate the relative distribution of eroding land areas (specifying their high, moderate or low relief) and of three main depositional domains: (i) continental (fluvial, lacustrine), and (ii) carbonate- or clastic-dominated marine in (iia) a shallow shelf environment or (iib) a deeper palaeobathymetric setting (lower shelf, continental slope, trough). Boundary fluctuations between these domains were caused by tectonic and/or eustatic drivers but are too numerous to all be illustrated on these highly synthetic maps. For the Pyrenean mountain belt, Ebro and Aquitaine basins, and Basque and Cantabrian regions, the maps are based on the detailed (but partly outdated) maps of the "Synthèse géologique et géophysique des Pyrénées" atlas, volume 2, produced in 1997 but only published in 2018 (see Barnolas et al., 2018). Like their excellent antecedents produced by Plaziat (1981), those atlas maps displayed the modern-day geology; whereas the maps here take account of Alpine tectonic movements and crustal shortening. They are thus retrotectonic as well as palaeogeographic, and conform to the tectonic model advocated in this study for the nappe stack on the south side of the range (see Figs. 2, 3). Other work used to reconstruct the Pyrenean mountain belt include Andeweg (2002), Barnolas et al. (2019), Garcés et al. (2020), Ortiz et al. (2020), and the many additional references cited in the text. Kinematics of the main crustal blocs (i.e., Aquitaine–Massif Central; Bay of Biscay; Cantabrian–Pyrenean Range; Ebro Basin; Catalan Coastal Ranges, or Catalanides; Iberian Range and central Iberia) were calibrated on the works of Roca et al. (2011), Vissers and Meijer (2012b), Tugend et al. (2014), and Nirrengarten et al. (2018). For the eastern area (Tethyan, then Mediterranean: Languedoc; Provence; Sardinia; Balearic Islands), the reconstructions are underpinned by Dercourt et al. (1993), Séranne (1999), Murru et al. (2003, 2007), Lacombe and Jolivet (2005), Dieni et al. (2008), Cherchi et al. (2008), Leleu et al. (2009), Bache et al. (2009, 2010), Barca and Costamagna (2010), Oudet et al. (2010a, 2010b), Costamagna and Schäfer (2013), Bestani et al. (2016), Etheve et al. (2016, 2018), and van Hinsbergen et al. (2020). For reasons of visual clarity, tectonic lineaments (thrusts,

normal faults) have generally not been depicted, but the regional tectonic stress field has been indicated with arrows.

A. 65–60 Ma, early Paleocene (Danian–Selandian). Sardinia is placed here according to the preferred model of Advokaat et al. (2014). The Danian–Selandian marine turbiditic trough model associated with karst development (see Peybernès et al., 2001, 2014) was not favoured here (see Canérot, 2006). Grey stars ('Ferruginous deposits', termed 'Sidérolithique' in the Massif Central) locate occurrences of tropical laterites (age: late Maastrichtian to early Paleocene; e.g., Thiry, 2000; Vacca et al., 2012). Extent of late Cretaceous deposits in the Proto-Pyrenees has been portrayed schematically; the eastern boundary of this domain corresponds to a hypothetical (intracontinental) transform fault generated during earlier Mesozoic kinematics. Areas above sea-level other than the Proto-Pyrenees are evolving in unspecified ways (but resulting in an early Paleocene erosion surface in the Massif Central — previously named 'surface éogène': Baulig, 1928, or 'surface éotertiaire': Klein, 1990).

B. 56–53, Ma early Ypresian (Ilerdian). The tectonically active domain (Ancestral Pyrenees) corresponds to the current eastern NPZ (some nummulites of probable Ypresian age have been reworked and included in Pliocene beds at Néfiach, between Prades and Perpignan, at the boundary between Axial Zone and NPZ; Astre, 1937). At the time, most of the northeastern AZ was located south of the rising Ancestral Pyrenees and drowned by the Ypresian transgression.

C. 45 Ma, middle Lutetian. The Ancestral Pyrenees have grown south- and westward, and the pro- and retro-foreland basins have narrowed; magnitudes of N–S crustal shortening reach ca. 50 km in the central Pyrenees; Sardinia has begun to rotate counterclockwise. The South-Pyrenean Basin is still open to the Atlantic. An elevated mountain range (Ancestral Pyrenees) is supplying conglomerate sequences to both forelands, north and south (Palassou and Bellmunt–Campanue formations, respectively).

D. 38–36 Ma, Bartonian–Priabonian transition. This period was a tectonic paroxysm in Languedoc and Provence ('Bartonian event') and involved the collision of Sardinia and Provence (ca. 40 km of total shortening since the latest Cretaceous). Between Iberia and Europe, shortening had exceeded ~100 km by the late Eocene. In the Pyrenees, the peak of uplift and denudation recorded by thermochronology begins around 37 Ma and coincides

with the formation of the basement nappe stack in the Axial Zone. By this time, the deep South-Pyrenean Basin (and its Hecho canyon) has nearly overfilled.

E. 30–28 Ma, late Rupelian. The Pyrenees are now continuous with the Cantabrian Range and form a narrow mountain belt, still feeding thick conglomerate sequences to the piedmonts. The Ebro Basin has been internally drained since ~36 Ma. The peak of uplift and denudation continues until ~30 Ma and then abates considerably. In the east, convergence ceases abruptly and gives way to an extensional regime in Provence, Languedoc, Sardinia, and even the Catalanides.

F. 25–24 Ma, Chattian. The Pyrenees form two contrasting domains: (i) continuing convergence in the west and centre drives southward fold propagation out into the Iberian foreland; thick syntectonic conglomerate beds continue to accumulate in the Ebro Basin, but not in the Aquitaine. The northeastern Catalan Range is still undergoing compressive tectonics, and piggyback basins are generated in the area corresponding to the future Valencia Trough. In contrast, (ii) the NE part of the Pyrenees undergoes crustal extension; this promotes the formation of a partial peneplain (surface S). Sea level rises across the Gulf of Lion in Chattian time and advances westward during Aquitanian time. In Aquitanian time, the sea-level highstand briefly reached as far as Agen from the west.

G. 20–18 Ma, early Burdigalian. The previously established E–W tectonic divide is maintained. Convergence in the west is nonetheless declining, and the last synorogenic conglomerates (Huesca Fm.) are deposited. Footwall uplifts in the Mediterranean extensional domain generate high mountain topography in the eastern Pyrenees and Catalanides, with very coarse clastic output as a result in the Roussillon, Conflent, and Vallès basins. Southward drift and rotation of the Corsica–Sardinia bloc generates the deep Liguro-Provençal Basin. The Valencia Basin had already switched to an extensional regime in Aquitanian time.

H. 14–12 Ma, middle Miocene. This is a period of crustal relaxation. All tectonic convergence in the Pyrenees has ceased (except perhaps in the west between the Sierra de la Demanda and the Cantabrian Range), and the Corsica–Sardinia bloc has approximately reached is current position. A widespread partial erosion surface, P1, while preserving often large residual ridges and ranges, has cut pediment bench systems throughout the Iberian Range, Pyrenees, Massif Central and Provence. The central and western parts of the Axial Zone, however, were unaffected by P1; as a result, these areas constitute the last upstanding

vestiges of the Ancestral Pyrenees. Marine incursions are advancing over the Aquitaine, Gulf of Lion and Provence. Continental sedimentation is dominated by lacustrine limestones and is relatively starved of clastic inputs.

I. 10–6 Ma, late Miocene. Progressive, regional uplift, reaching maxima over the Pyrenees but also affecting the Massif Central and the entire Iberian peninsula, is associated with intraplate volcanism from the Massif Central to northern Catalonia. The youngest (10 Ma) lacustrine carbonate beds recorded occur in the Ebro Basin and in Languedoc. Extensional grabens and horsts are forming across the Western Mediterranean and deep into the central Pyrenean Axial Zone. The Ebro Basin is reconnected to marine base levels and undergoing fluvial incision, all of this prior to the construction of the Lannemezan retro-foreland megafan in Aquitaine. Marine shorelines are receding in the Aquitaine Basin and the Mediterranean.

J. 5–2 Ma, Pliocene. This map captures the region immediately after the late Messinian Salinity Crisis (5.6–5.46 Ma), which generated thick evaporite deposits in the deeper bathymetric levels of the Mediterranean and deeply incising canyons around the edges. Regional uplift continues, interrupted by brief pauses (e.g., formation of generation P2 of local pediments during the late Pliocene); volcanic activity intensifies. The Ebro Basin is undergoing deep dissection but the Lannemezan Formation continues to aggrade along the North-Pyrenean mountain front. This geomorphological asymmetry of the Pyrenees promotes drainage capture of north-flowing rivers by their south-flowing counterparts. Coarse-textured clastic input to eastern coastal basins intensifies, generating thick siliciclastic depositional wedges offshore.

K. 2–0 Ma, Quaternary. As testified by widespread staircases of Quaternary alluvial terraces, mountain uplift continues in the Pyrenees and throughout the region. Volcanism is still very active from the Massif Central to Catalonia. Valley incision is also ubiquitous, except in the Landes area, which became an erg during cold and dry glacial stages. Most of the coarse clastic depocentres are very thick and now situated offshore. An icefield develops over the more humid massifs (Atlantic influence), and glacial–interglacial oscillations control the alluvial terrace aggradation/incision regime. Drainage captures occur in the piedmont zones rather than in the mountain-range headwaters, mostly benefiting the Mediterranean base level (e.g., Aude River catchment).

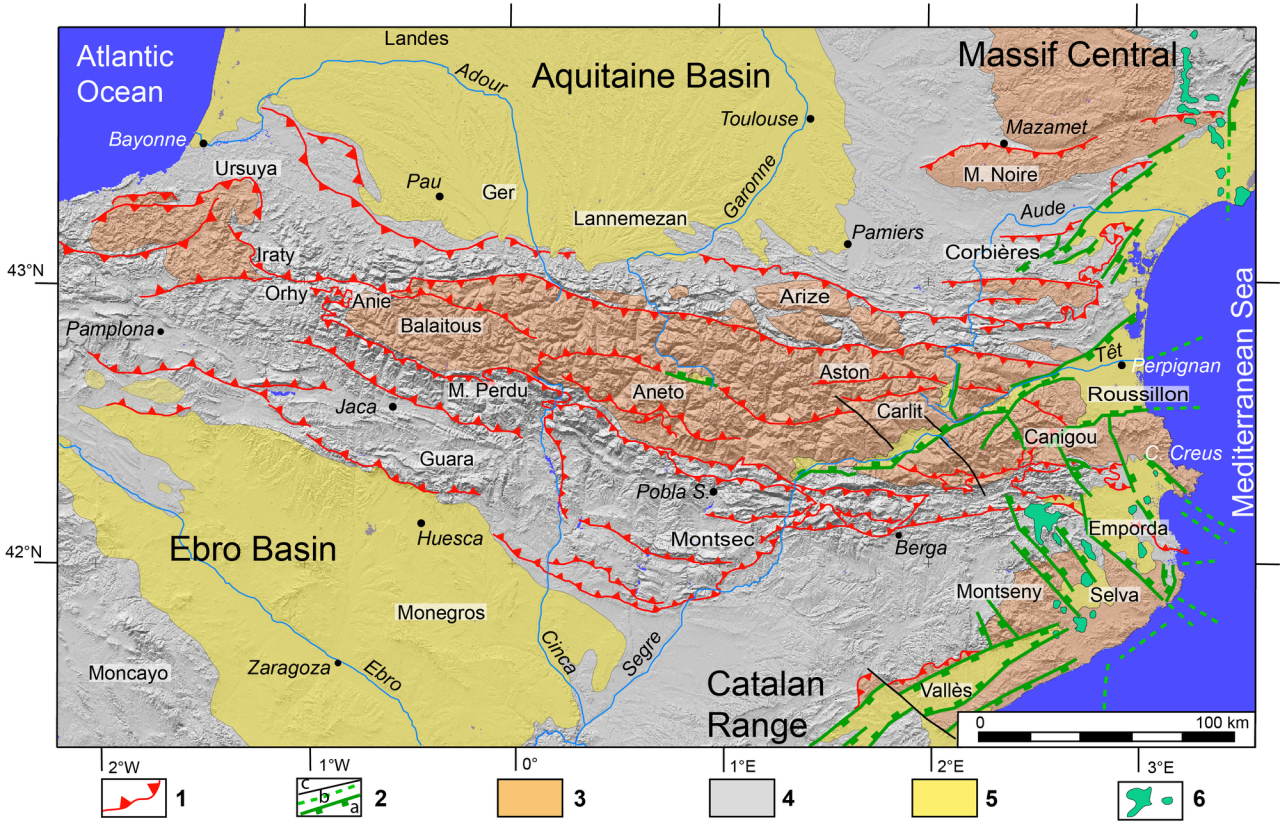
Atlantic Ocean
Landes
Adour
Aquitaine Basin
Massif Central
Toulouse
Mazamet
Bayonne
Ursuya
M. Noire
Pau
Ger
Garonne
Aude
Lannemezan
Pamiers
Corbières
Iraty
43°N
Orhy
Anie
Arize
Balaitous
Pamplona
Têt
Perpignan
Aston
Aneto
M. Perdu
Roussillon
Jaca
Carlit
Canigou
Guara
C. Creus
Pobla S.
Mediterranean Sea
Huesca
Montsec
Berga
Emporda
42°N
Ebro Basin
Montseny
Selva
Monegros
Cinca
Segre
Moncayo
Zaragoza
Ebro
Catalan Range
Vallès
0
100 km
2°W
1°W
0°
1°E
2°E
3°E
1
2
c
b
a
3
4
5
6

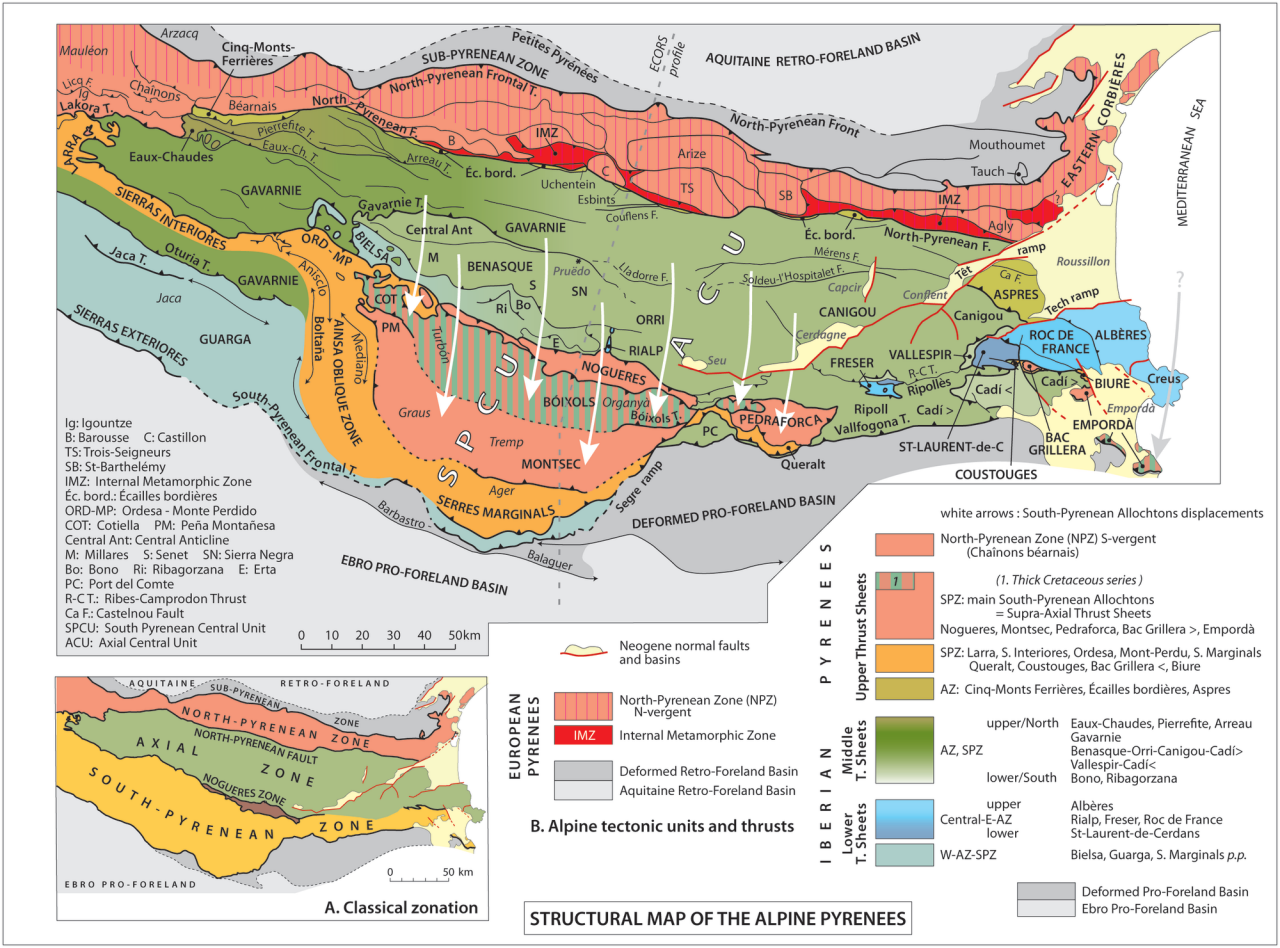
Mauléon
Arzacq
Cinq-Monts-Ferrières
Petites Pyrénées
SUB-PYRENEAN ZONE
ECORS profile
AQUITAINE RETRO-FORELAND BASIN
Licq F.
Ig
Chaînons
Béarnais
North-Pyrenean Frontal T.
Lakora T.
North-Pyrenean F.
North-Pyrenean Front
MEDITERRANEAN SEA
EASTERN CORBIÈRES
Pierrefite T.
Eaux-Ch. T.
Eaux-Chaudes
Arreau T.
Éc. bord.
IMZ
Arize
Mouthoumet
Tauch
LARRA
SIERRAS INTERIORES
GAVARNIE
Gavarnie T.
Central Ant
Uchentein
Esbints
TS
SB
Coufiens F.
Agly
Éc. bord.
North-Pyrenean F.
ramp
Roussillon
Jaca T.
Oturia T.
ORD-MP
BIELSA
M
BENASQUE
S
SN
Pruédo
Lladorre F.
Mérens F.
Soldeu-l'Hospitalet F.
Têt
Ca F.
ASPRES
Tech ramp
Jaca
Aniscio
Boltaña
Ri
Bo
E
COT
PM
Turbon
ORRI
RIALP
Seu
Capcir
Conflent
CANIGOU
Canigou
Cerdagne
ROC DE FRANCE
ALBÈRES
SIERRAS EXTERIORES
GUARGA
Mediano
AINSA OBLIQUE ZONE
NOGUERES
BOIXOLS
Organyà
Boixols T.
FRESER
VALLESPIR
R-C T.
Ripollès
Cadí <
Cadí >
BIURE
Creus
Graus
Tremp
PEDRAFORCA
Ripoll
Vallfogona T.
Empordà
EMPORDÀ
PC
ST-LAURENT-de-C
BAC GRILLERA
Queralt
COUSTOUGES
MONTSEC
Ager
SERRES MARGINALS
Segre ramp
DEFORMED PRO-FORELAND BASIN
Barbastro
Balaguer
EBRO PRO-FORELAND BASIN
0 10 20 30 40 50km
Ig: Igountze
B: Barousse C: Castillon
TS: Trois-Seigneurs
SB: St-Barthelémy
IMZ: Internal Metamorphic Zone
Éc. bord.: Écailles bordières
ORD-MP: Ordesa - Monte Perdido
COT: Cotiella PM: Peña Montañesa
Central Ant: Central Anticline
M: Millares S: Senet SN: Sierra Negra
Bo: Bono Ri: Ribagorzana E: Erta
PC: Port del Comte
R-C T.: Ribes-Camprodon Thrust
Ca F.: Castelnou Fault
SPCU: South Pyrenean Central Unit
ACU: Axial Central Unit
white arrows : South-Pyrenean Allochtons displacements
Neogene normal faults and basins
EUROPEAN PYRENEES
North-Pyrenean Zone (NPZ) N-vergent
IMZ
Internal Metamorphic Zone
Deformed Retro-Foreland Basin
Aquitaine Retro-Foreland Basin
B. Alpine tectonic units and thrusts
IBERIAN PYRENEES
Upper Thrust Sheets
North-Pyrenean Zone (NPZ) S-vergent (Chaînons béarnais)
(1. Thick Cretaceous series)
SPZ: main South-Pyrenean Allochtons = Supra-Axial Thrust Sheets
Nogueres, Montsec, Pedraforca, Bac Grillera >, Empordà
SPZ: Larra, S. Interiores, Ordesa, Mont-Perdu, S. Marginals Queralt, Coustouges, Bac Grillera <, Biure
AZ: Cinq-Monts Ferrières, Écailles bordières, Aspres
Middle T. Sheets
upper/North
AZ, SPZ
lower/South
Eaux-Chaudes, Pierrefite, Arreau Gavarnie
Benasque-Orri-Canigou-Cadí> Vallespir-Cadí<
Bono, Ribagorzana
Lower T. Sheets
upper
Central-E-AZ
lower
Albères
Rialp, Freser, Roc de France
St-Laurent-de-Cerdans
W-AZ-SPZ
Bielsa, Guarga, S. Marginals p.p.
Deformed Pro-Foreland Basin
Ebro Pro-Foreland Basin
AQUITAINE
SUB-PYRENEAN
RETRO-FORELAND
NORTH-PYRENEAN ZONE
NORTH-PYRENEAN FAULT
AXIAL ZONE
NOGUERES ZONE
SOUTH-PYRENEAN ZONE
EBRO PRO-FORELAND
0 50 km
A. Classical zonation
STRUCTURAL MAP OF THE ALPINE PYRENEES

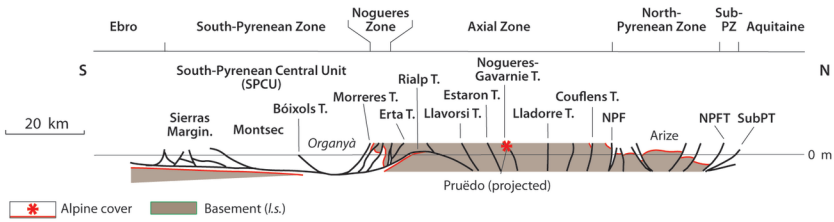

A – Structural elements along the ECORS-Pyrenees profile (from Muñoz, 1992)

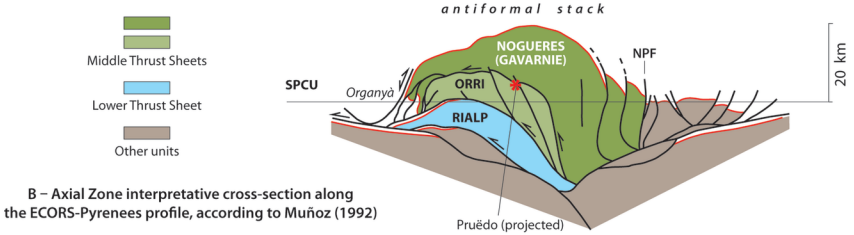

B – Axial Zone interpretative cross-section along the ECORS-Pyrenees profile, according to Muñoz (1992)

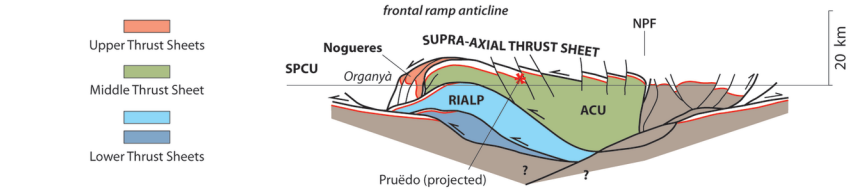

ACU: Axial Central Unit (Gavarnie + Orri)
SPCU: South-Pyrenean Central Unit
NPF: North-Pyrenean Fault

C – Interpretative cross-section through the central Axial Zone, along the ECORS-Pyrenees profile (Laumonier, 2015, this study)

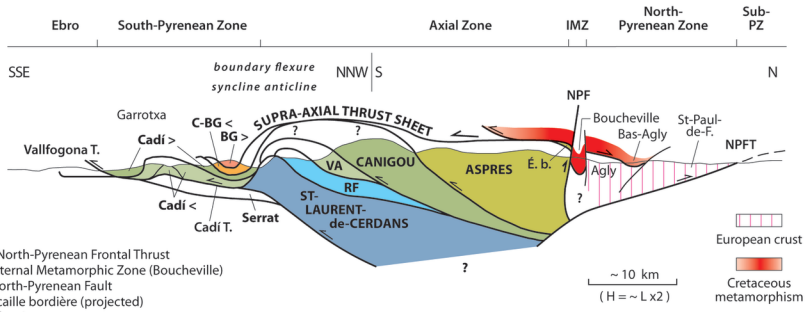

NPFT: North-Pyrenean Frontal Thrust
IMZ: Internal Metamorphic Zone (Boucheville)
NPF: North-Pyrenean Fault
É. b.: Écaille bordière (projected)
VA: Vallespir
RF: Roc de France
BG >: Upper Bac Grillera
C-BG <: Coustouges - Lower Bac Grillera

D – Schematic structural cross-section in the eastern Pyrenees

STRUCTURAL CROSS-SECTIONS OF THE CENTRAL AND EASTERN PYRENEES

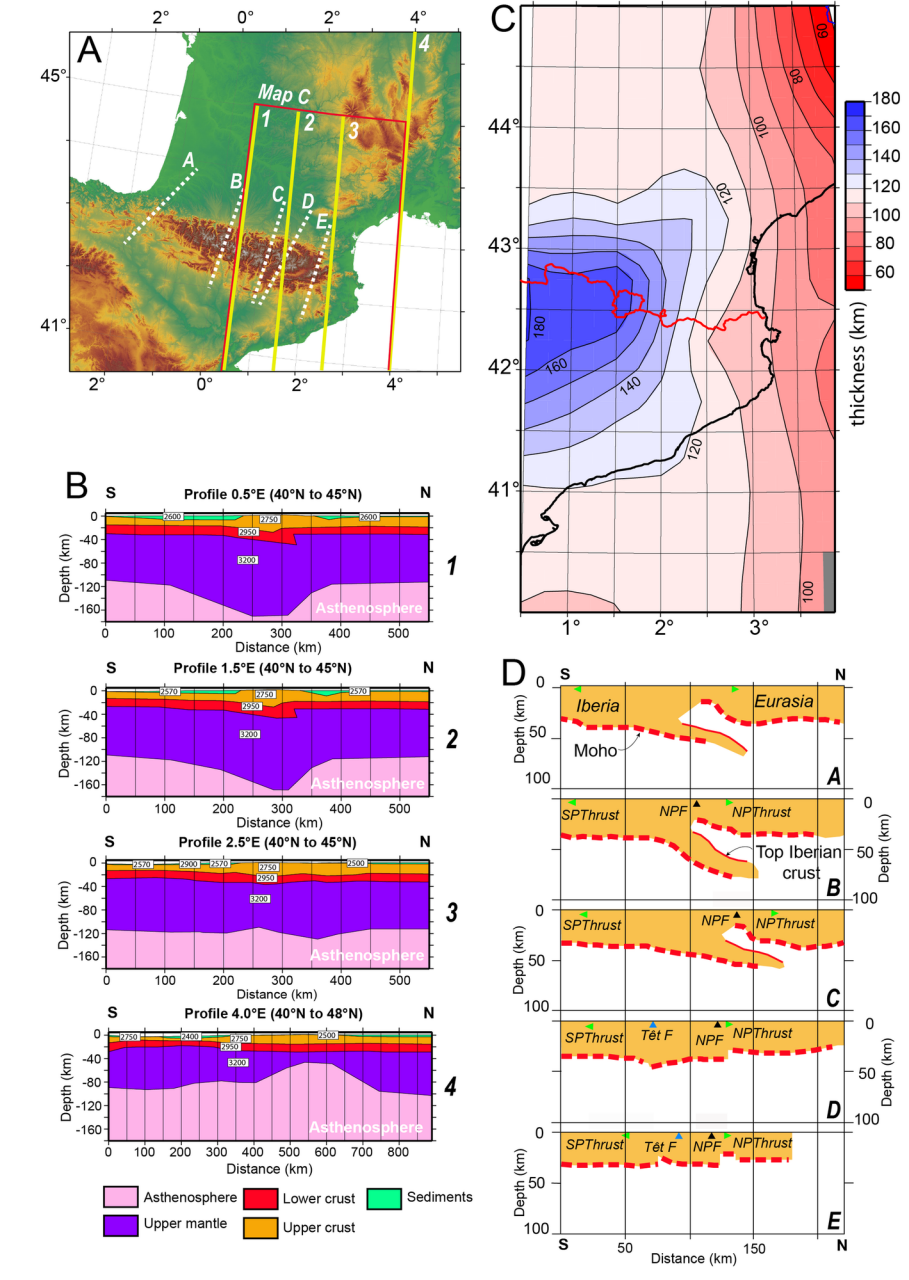
A
Map C
1
2
3
4
A
B
C
D
E
2°
0°
2°
4°
45°
41°
C
180
160
140
120
100
80
60
thickness (km)
44°
43°
42°
41°
1°
2°
3°
B
S
Profile 0.5°E (40°N to 45°N)
N
Depth (km)
Distance (km)
Asthenosphere
1
Profile 1.5°E (40°N to 45°N)
2
Profile 2.5°E (40°N to 45°N)
3
Profile 4.0°E (40°N to 48°N)
4
Asthenosphere
Upper mantle
Lower crust
Upper crust
Sediments
D
Iberia
Eurasia
Moho
SPThrust
NPF
NPThrust
Top Iberian crust
Tét F
A
B
C
D
E
Distance (km)

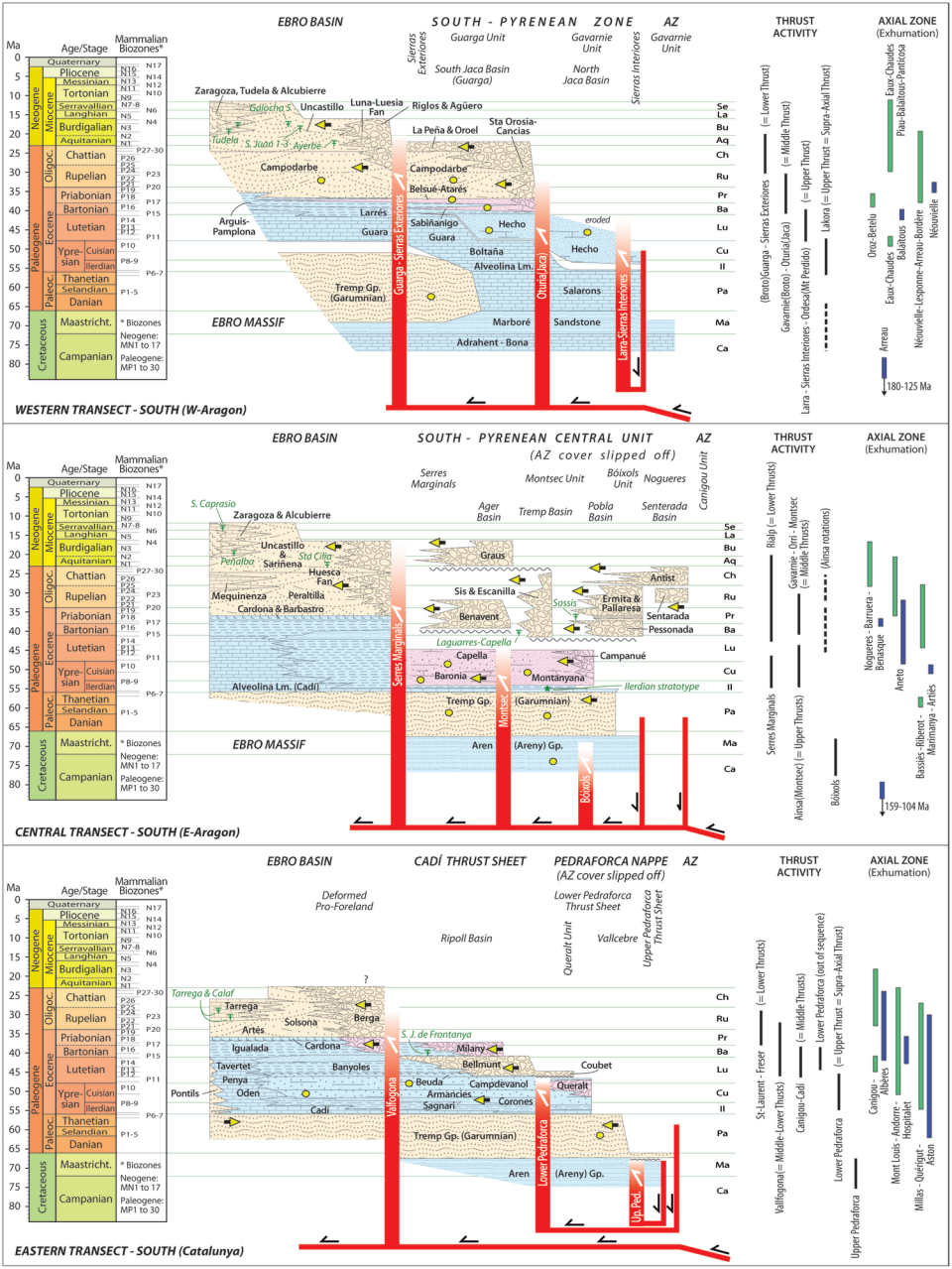
Ma
Age/Stage
Mammalian Biozones*
Quaternary
Pliocene
Messinian
Tortonian
Serravallian
Langhian
Burdigalian
Aquitanian
Chattian
Rupelian
Priabonian
Bartonian
Lutetian
Ypre-sian
Cuisian
Ilerdian
Thanetian
Selandian
Danian
Maastricht.
Campanian
Neogene
Paleogene
Cretaceous
Paleoc.
Miocene
Oligoc.
Eocene
* Biozones
Neogene: MNN1 to 17
Paleogene: MP1 to 30
EBRO BASIN
SOUTH - PYRENEAN ZONE
AZ
Sierras Exteriores
Guarga Unit
Gavarnie Unit
Gavarnie Unit
South Jaca Basin (Guarga)
North Jaca Basin
Sierras Interiores
Zaragoza, Tudela & Alcubierre
Galocha S.
Uncastillo
Luna-Luesia Fan
Riglos & Agüero
Tudela
S. Juan 1-3 · Ayerbe
La Peña & Oroel
Sta Orosia-Cancias
Campodarbe
Belsué-Atarés
Arguis-Pamplona
Larrés
Guara
Sabiñanigo
Hecho
eroded
Boltaña
Alveolina Lm.
Tremp Gp. (Garumnian)
Salarons
Oturia/Jaca
Guarga - Sierras Exteriores
Larra - Sierras Interiores
Marboré
Sandstone
Adrahent - Bona
EBRO MASSIF
Se
La
Bu
Aq
Ch
Ru
Pr
Ba
Lu
Cu
Il
Pa
Ma
Ca
THRUST ACTIVITY
AXIAL ZONE (Exhumation)
(= Lower Thrusts)
(= Middle Thrusts)
(= Upper Thrusts)
(= Upper Thrust = Supra-Axial Thrust)
(Broto)/Guarga - Sierras Exteriores
Gavarnie(Broto) - Oturia(Jaca)
Larra - Sierras Interiores - Ordesa(Mt Perdido)
Lakora
Eaux-Chaudes
Pic de Balaitous-Peñiscola
Oroz-Betelu
Eaux-Chaudes
Balaitous
Arrau
Néouvielle-Lesponne-Arreau-Bordère
Néouvielle
180-125 Ma
WESTERN TRANSECT - SOUTH (W-Aragon)
EBRO BASIN
SOUTH - PYRENEAN CENTRAL UNIT
(AZ cover slipped off)
AZ
Serres Marginals
Montsec Unit
Bóixols Unit
Nogueres
Canigou Unit
Ager Basin
Tremp Basin
Pobla Basin
Senterada Basin
S. Caprasio
Zaragoza & Alcubierre
Uncastillo & Sarinena
Peñalba
Sta Cilia
Huesca Fan
Mequinenza
Peraltilla
Cardona & Barbastro
Alveolina Lm. (Cadí)
Graus
Antist
Sis & Escanilla
Ermita & Pallaresa
Sossis
Benavent
Sentarada
Pessonada
Laguarres-Capella
Capella
Campanué
Baronia
Montanyana
Ilerdian stratotype
Tremp Gp.
(Garumnian)
Aren
(Areny) Gp.
Serres Marginals
Montsec
Bóixols
EBRO MASSIF
Se
La
Bu
Aq
Ch
Ru
Pr
Ba
Lu
Cu
Il
Pa
Ma
Ca
THRUST ACTIVITY
AXIAL ZONE (Exhumation)
(= Lower Thrusts)
(= Middle Thrusts)
(= Upper Thrusts)
(Ainsa rotations)
Rialp (= Lower Thrusts)
Gavarnie - Orri - Montsec
Serres Marginals
Ainsa(Montsec) (= Upper Thrusts)
Bóixols
Nogueres - Barrueta - Benasque
Aneto
Basàsis -Ilterot - Mammanya - Artíes
159-104 Ma
CENTRAL TRANSECT - SOUTH (E-Aragon)
EBRO BASIN
CADÍ THRUST SHEET
PEDRAFORCA NAPPE
AZ
Deformed Pro-Foreland
(AZ cover slipped off)
Lower Pedraforca Thrust Sheet
Upper Pedraforca Thrust Sheet
Ripoll Basin
Queralt Unit
Vallcebre
Tarrega & Calaf
Tarrega
Solsona
Berga
Artés
Igualada
Cardona
S. J. de Frontanya
Milany
Bellmunt
Coubet
Tavertet
Penya
Oden
Banyoles
Pontils
Beuda
Campdevanol
Querait
Armancies
Sagnari
Corones
Cadí
Vallfogona
Tremp Gp. (Garumnian)
Lower Pedraforca
Aren
(Areny) Gp.
Un Ped.
Ch
Ru
Pr
Ba
Lu
Cu
Il
Pa
Ma
Ca
THRUST ACTIVITY
AXIAL ZONE (Exhumation)
(= Lower Thrusts)
(= Middle Thrusts)
Lower Pedraforca (out of sequence)
(= Upper Thrust = Supra-Axial Thrust)
St-Laurent - Freser
Vallfogona (= Middle-Lower Thrusts)
Canigou - Cadí
Lower Pedraforca
Upper Pedraforca
Canigou - Albères
Mont Louis - Andorre - Hospitalet
Millas - Quéfigut - Axton
EASTERN TRANSECT - SOUTH (Catalunya)

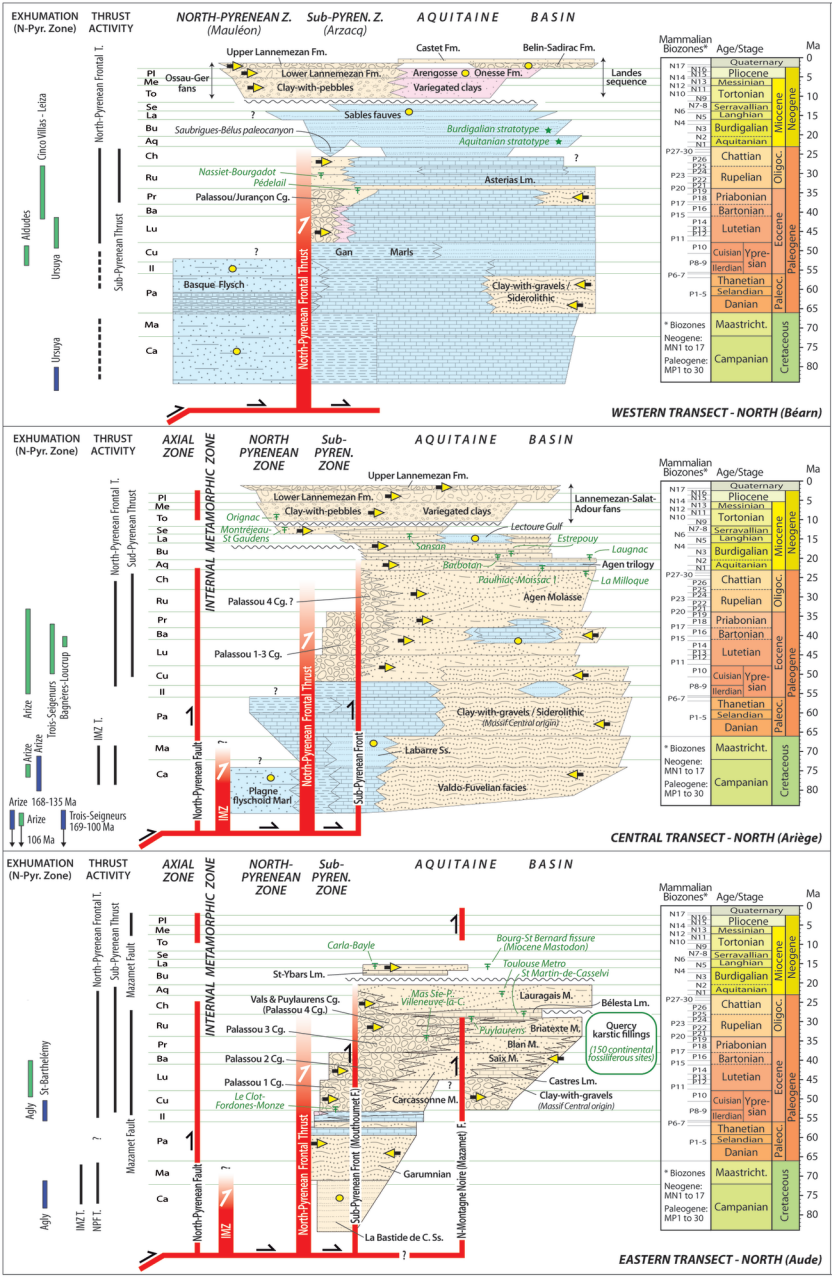
EXHUMATION (N-Pyr. Zone)
THRUST ACTIVITY
NORTH-PYRENEAN Z. (Mauléon)
Sub-PYREN. Z. (Arzacq)
AQUITAINE BASIN
Upper Lannemezan Fm.
Castet Fm.
Belin-Sadirac Fm.
Ossau-Ger fans
Lower Lannemezan Fm.
Clay-with-pebbles
Arengosse
Onesse Fm.
Variegated clays
Landes sequence
Sables fauves
Saubrigues-Bélus paleocanyon
Burdigalian stratotype
Aquitanian stratotype
Nassiet-Bourgadot
Pédelail
Palassou/Jurançon Cg.
Asterias Lm.
Gan
Marls
Basque Flysch
Clay-with-gravels / Siderolithic
North-Pyrenean Frontal Thrust
Sub-Pyrenean Thrust
Mammalian Biozones*
Age/Stage
Ma
Quaternary
Pliocene
Messinian
Tortonian
Serravallian
Langhian
Burdigalian
Aquitanian
Chattian
Rupelian
Priabonian
Bartonian
Lutetian
Cuisian
Ilerdian
Ypresian
Thanetian
Selandian
Danian
Maastricht.
Campanian
Neogene
Oligoc.
Eocene
Paleocene
Paleoc.
Cretaceous
* Biozones
Neogene: MN1 to 17
Paleogene: MP1 to 30
Aldudes
Cinco Villas - Leiza
Ursuya
WESTERN TRANSECT - NORTH (Béarn)
AXIAL ZONE
NORTH PYRENEAN ZONE
Sub-PYREN. ZONE
INTERNAL METAMORPHIC ZONE
Lannemezan-Salat-Adour fans
Lower Lannemezan Fm.
Clay-with-pebbles
Variegated clays
Orignac
Montréjeau-St Gaudens
Lectoure Gulf
Estrepouy
Sansan
Laugnac
Barbotan
Agen trilogy
Paulhiac-Monsac
La Milloque
Agen Molasse
Palassou 4 Cg.
Palassou 1-3 Cg.
Clay-with-gravels / Siderolithic
(Massif Central origin)
Labarre Ss.
Valdo-Fuvelian facies
Plagne flyschoid Marl
IMZ
North-Pyrenean Fault
Sub-Pyrenean Front
Arize
Trois-Seigneurs Bagnères-Loucrup
IMZ T.
Arize 168-135 Ma
Arize 106 Ma
Trois-Seigneurs 169-100 Ma
CENTRAL TRANSECT - NORTH (Ariège)
Carla-Bayle
Bourg-St Bernard fissure (Miocene Mastodon)
Toulouse Metro
St Martin-de-Casselvi
St-Ybars Lm.
Mas Ste-P.
Villeneuve-la-C.
Lauragais M.
Bélesta Lm.
Vals & Puylaurens Cg. (Palassou 4 Cg.)
Puylaurens
Briatexte M.
Quercy karstic fillings
(150 continental fossiliferous sites)
Palassou 3 Cg.
Blan M.
Palassou 2 Cg.
Saix M.
Palassou 1 Cg.
Castres Lm.
Le Clot-Fardones-Monze
Carcassonne M.
Clay-with-gravels
(Massif Central origin)
Garumnian
La Bastide de C. Ss.
N-Montagne Noire (Mazamet) F.
Mazamet Fault
Agly
St-Barthélemy
IMZ T.
WPF T.
EASTERN TRANSECT - NORTH (Aude)
Sansan
Palassou I Cg.
Bélesta Lm.
AFT
ZFT

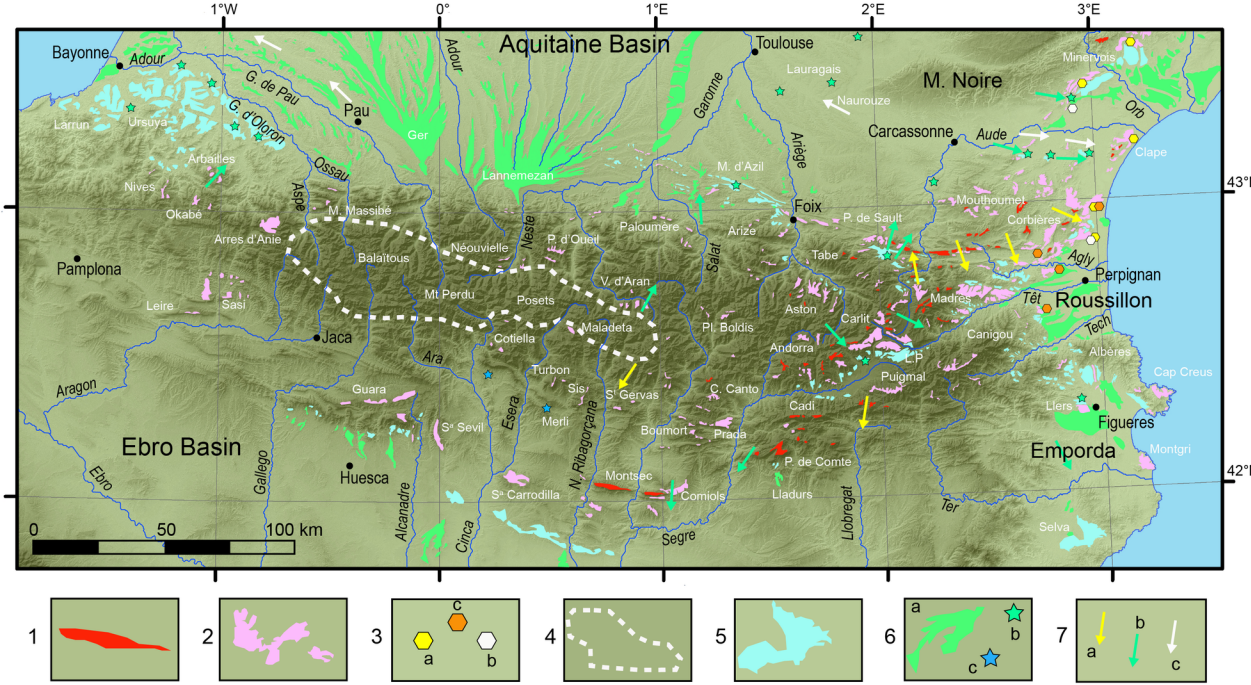
1°W
0°
1°E
2°E
3°E
43°N
42°N
Aquitaine Basin
Ebro Basin
M. Noire
Emporda
Roussillon
Bayonne
Adour
G. de Pau
G. d'Oloron
Pau
Larrun
Ursuya
Arbailles
Nives
Okabé
Ossau
Aspe
M. Massibé
Arres d'Anie
Pamplona
Balaïtous
Leire
Sasi
Jaca
Mt Perdu
Ger
Lannemezan
Adour
Garonne
Ariège
Toulouse
Lauragais
Naurouze
Carcassonne
Aude
Orb
Minervois
Clape
M. d'Azil
Foix
Arize
Salat
Nestie
Néouvielle
P. d'Oueil
Paloumère
V. d'Aran
Posets
Maladeta
Pl. Boldis
Aston
Carlit
Andorra
Puigmal
Tabe
P. de Sault
Mouthoumet
Corbières
Agly
Madres
Tét
Perpignan
Canigou
Tech
Albères
Cap Creus
Llers
Figueres
Montgri
Selva
Ter
Llobregat
Lladurs
P. de Comte
Cadi
Prada
Boumort
C. Canto
Sis
S. Gervas
Turbon
Merli
Cotiella
Ara
Esera
N. Ribagorçana
Montsec
Comiols
Segre
Cinca
Alcanadre
Gallego
Ebro
Aragon
Guara
S. Sevil
S. Carrodilla
Huesca
0
50
100 km
1
2
3
a
b
c
4
5
6
7

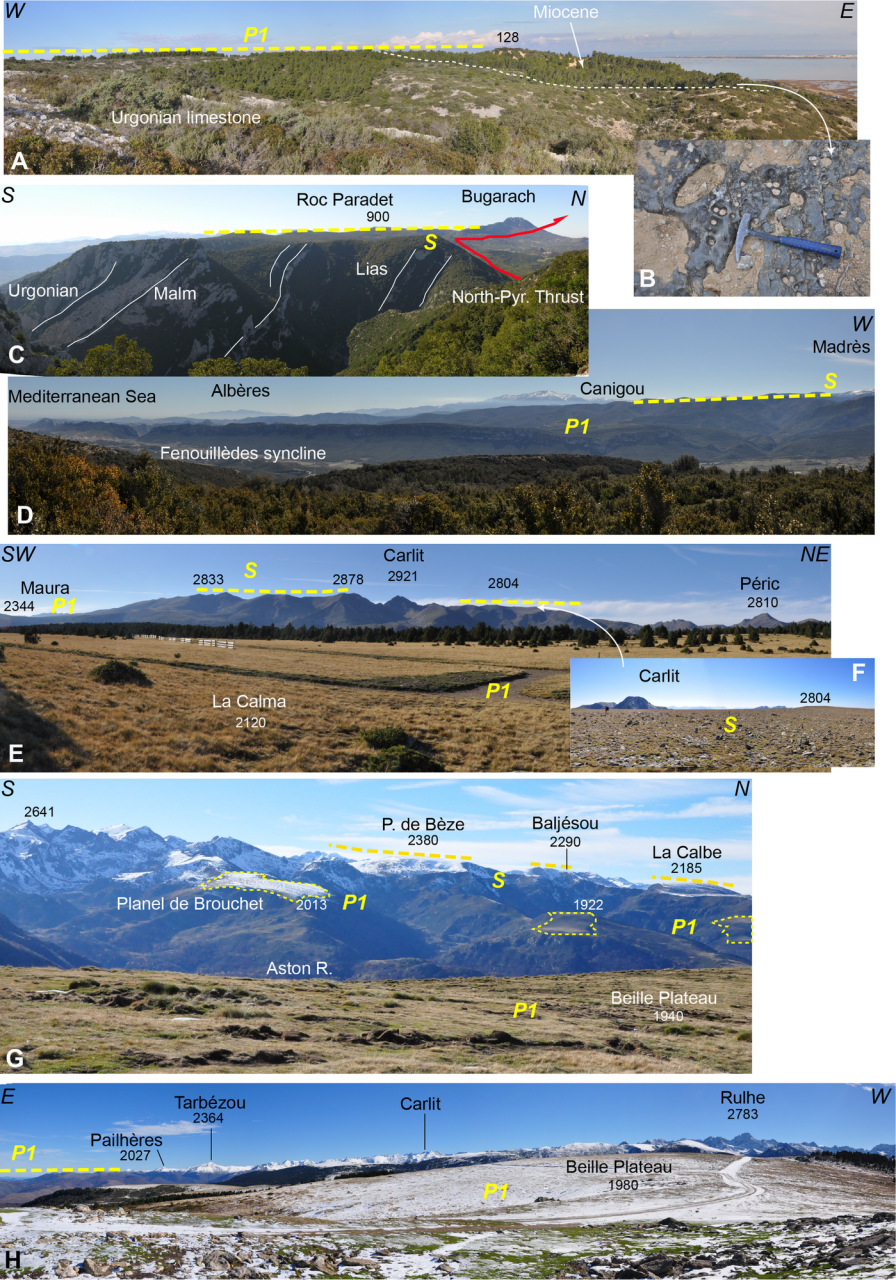
W
E
P1
128
Miocene
Urgonian limestone
A
B
S
N
Roc Paradet
900
Bugarach
S
Lias
Urgonian
Malm
North-Pyr. Thrust
C
W
Madrès
Mediterranean Sea
Albères
Canigou
S
P1
Fenouillèdes syncline
D
SW
NE
Carlit
Maura
2344
P1
2833
S
2878
2921
2804
Péric
2810
La Calma
2120
P1
E
Carlit
F
2804
S
S
N
2641
P. de Bèze
2380
Baljésou
2290
La Calbe
2185
Planel de Brouchet
2013
P1
S
1922
P1
Aston R.
P1
Beille Plateau
1940
G
E
Tarbézou
2364
Carlit
Rulhe
2783
W
P1
Pailhères
2027
Beille Plateau
1980
P1
H

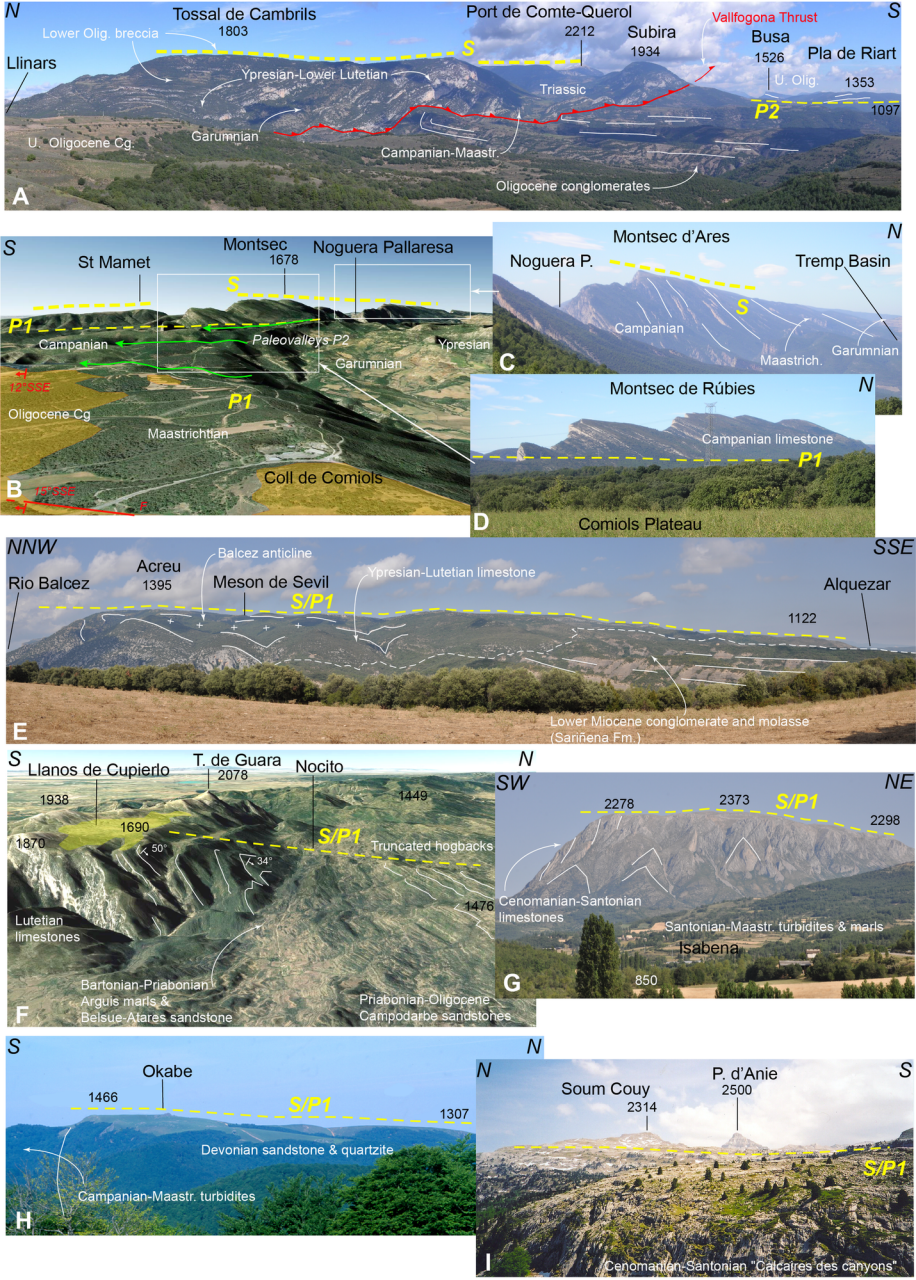
N
Tossal de Cambrils
1803
Lower Olig. breccia
S
Port de Comte-Querol
2212
Subira
1934
Vallfogona Thrust
S
Busa
1526
Pla de Riart
Llinars
Ypresian-Lower Lutetian
Triassic
U. Olig.
1353
P2
1097
U. Oligocene Cg.
Garumnian
Campanian-Maastr.
Oligocene conglomerates
A
S
St Mamet
Montsec
1678
Noguera Pallaresa
S
P1
Campanian
Paleovalleys P2
Ypresian
Garumnian
17°SSE
Oligocene Cg
P1
Maastrichtian
B
17°SSE
Coll de Comiols
Montsec d'Ares
N
Noguera P.
Tremp Basin
S
Campanian
Maastrich.
Garumnian
C
Montsec de Rúbies
N
Campanian limestone
P1
D
Comiols Plateau
NNW
SSE
Rio Balcez
Acreu
1395
Balcez anticline
Meson de Sevil
S/P1
Ypresian-Lutetian limestone
Alquezar
1122
E
Lower Miocene conglomerate and molasse
(Sariñena Fm.)
S
Llanos de Cupierlo
1938
T. de Guara
2078
Nocito
1449
1690
1870
S/P1
50°
34°
Truncated hogbacks
1476
Lutetian
limestones
Bartonian-Priabonian
Arguis marls &
Belsue-Atares sandstone
Priabonian-Oligocene
Campodarbe sandstones
F
N
SW
NE
2278
2373
S/P1
2298
Cenomanian-Santonian
limestones
Santonian-Maastr. turbidites & marls
Isabena
850
G
S
Okabe
1466
S/P1
1307
Devonian sandstone & quartzite
Campanian-Maastr. turbidites
H
N
N
S
Soum Couy
2314
P. d'Anie
2500
S/P1
Cenomanian-Santonian "Calcaires des canyons"
I

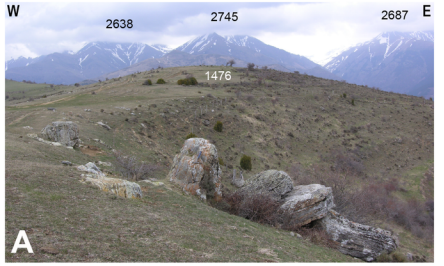
W
2638
2745
2687
E
1476
A

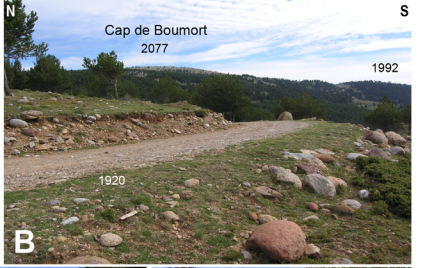
N
S
Cap de Boumort
2077
1992
1920
B

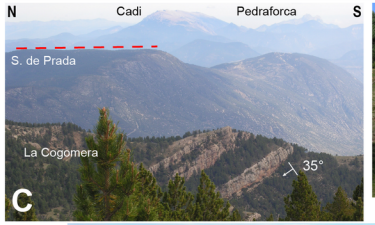
N
Cadi
Pedraforca
S
S. de Prada
La Cogomera
35°
C


D


E

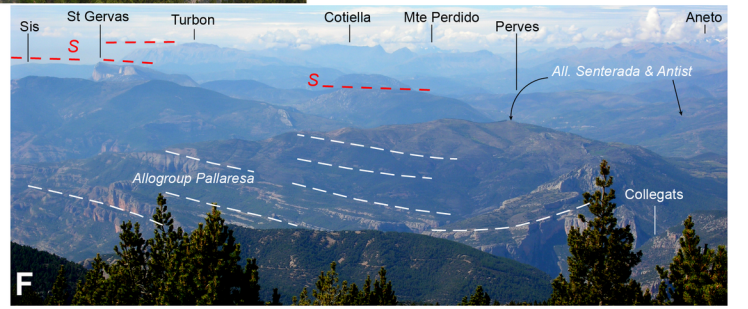
Sis
St Gervas
Turbon
Cotiella
Mte Perdido
Perves
Aneto
S
S
All. Senterada & Antist
Allogroup Pallaresa
Collegats
F

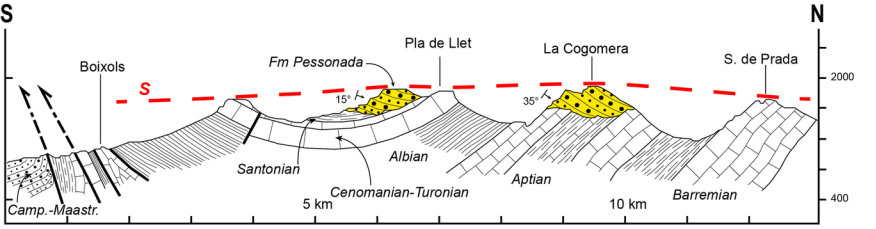
S
N
Boixols
S
Fm Pessonada
Pla de Llet
La Cogomera
S. de Prada
15°
35°
2000
400
Santonian
Albian
Aptian
Barremian
Cenomanian-Turonian
Camp.-Maastr.
5 km
10 km

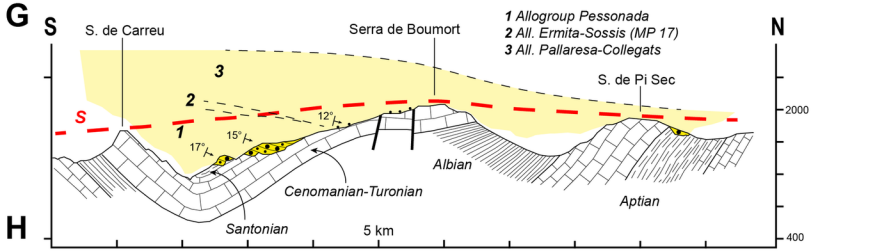
G
S
N
S. de Carreu
Serra de Boumort
S. de Pi Sec
1 Allogroup Pessonada
2 All. Ermita-Sossis (MP 17)
3 All. Pallaresa-Collegats
3
2
1
S
12°
17°
15°
2000
400
Albian
Aptian
Cenomanian-Turonian
Santonian
5 km
H

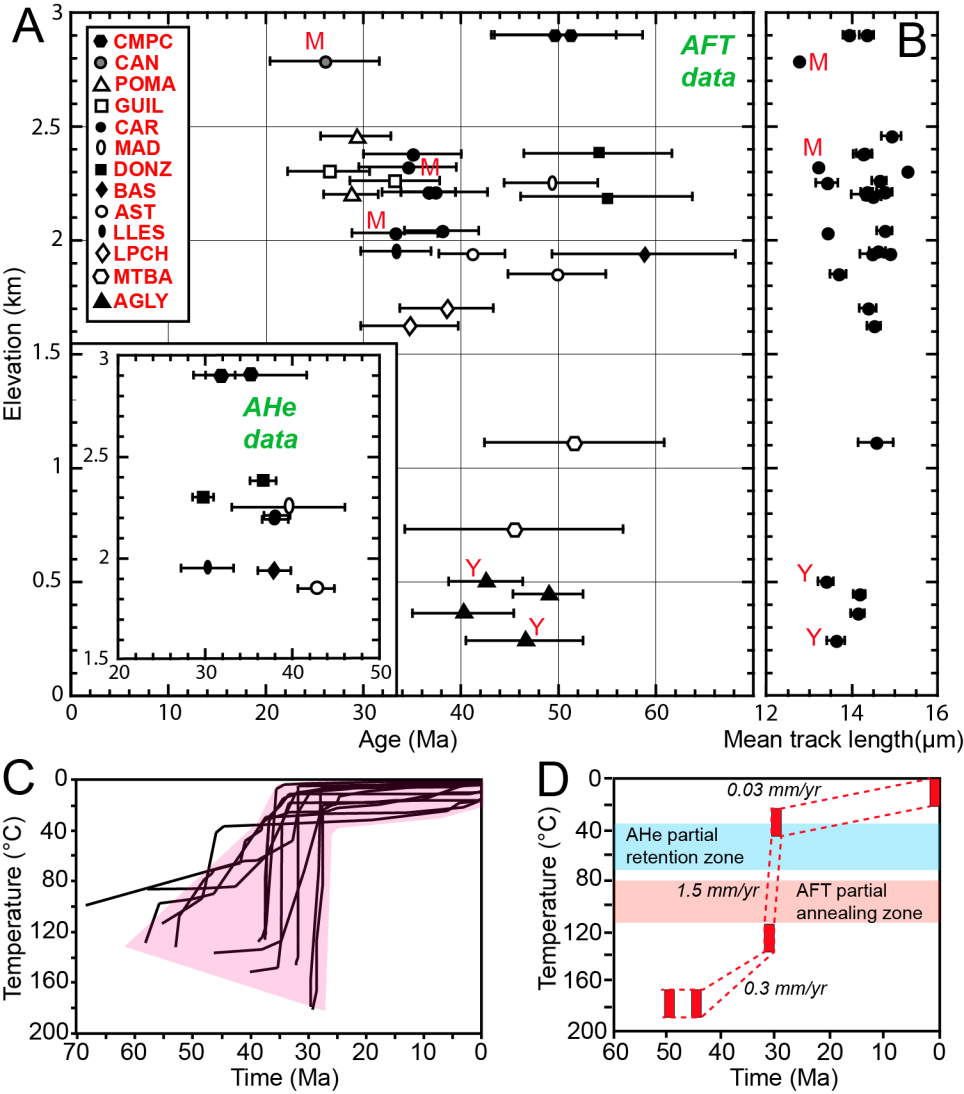
A
B
C
D
CMPC
CAN
POMA
GUIL
CAR
MAD
DONZ
BAS
AST
LLES
LPCH
MTBA
AGLY
AFT data
AHe data
M
Y
Elevation (km)
Age (Ma)
Mean track length(μm)
Temperature (°C)
Time (Ma)
0.03 mm/yr
AHe partial retention zone
1.5 mm/yr
AFT partial annealing zone
0.3 mm/yr

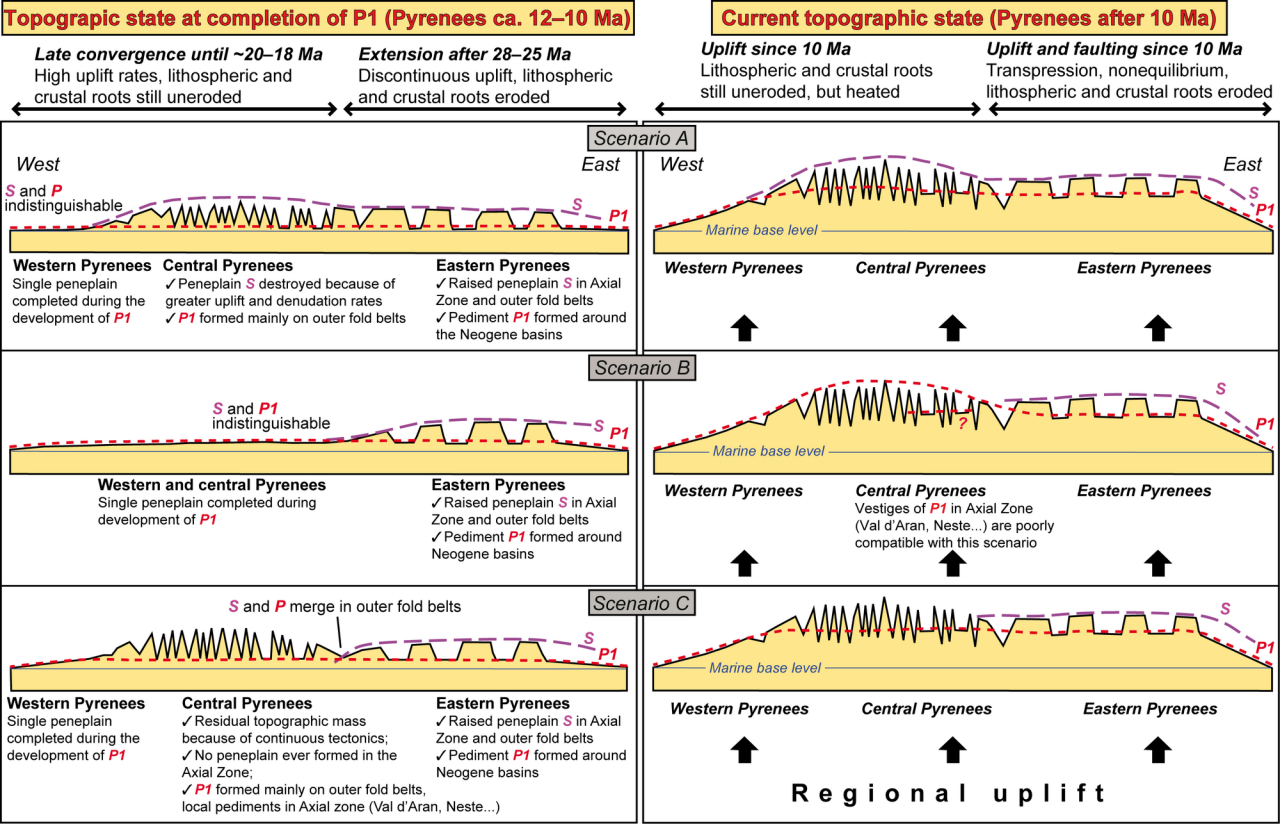
Topograpic state at completion of P1 (Pyrenees ca. 12–10 Ma)
Current topographic state (Pyrenees after 10 Ma)
Late convergence until ~20–18 Ma
High uplift rates, lithospheric and crustal roots still uneroded
Extension after 28–25 Ma
Discontinuous uplift, lithospheric and crustal roots eroded
Uplift since 10 Ma
Lithospheric and crustal roots still uneroded, but heated
Uplift and faulting since 10 Ma
Transpression, nonequilibrium, lithospheric and crustal roots eroded
Scenario A
West
East
S and P indistinguishable
S
P1
Western Pyrenees
Single peneplain completed during the development of P1
Central Pyrenees
✓Peneplain S destroyed because of greater uplift and denudation rates
✓P1 formed mainly on outer fold belts
Eastern Pyrenees
✓Raised peneplain S in Axial Zone and outer fold belts
✓Pediment P1 formed around the Neogene basins
Marine base level
Western Pyrenees
Central Pyrenees
Eastern Pyrenees
Scenario B
S and P1 indistinguishable
Western and central Pyrenees
Single peneplain completed during development of P1
Eastern Pyrenees
✓Raised peneplain S in Axial Zone and outer fold belts
✓Pediment P1 formed around Neogene basins
?
Central Pyrenees
Vestiges of P1 in Axial Zone (Val d'Aran, Neste...) are poorly compatible with this scenario
Scenario C
S and P merge in outer fold belts
Western Pyrenees
Single peneplain completed during the development of P1
Central Pyrenees
✓Residual topographic mass because of continuous tectonics;
✓No peneplain ever formed in the Axial Zone;
✓P1 formed mainly on outer fold belts, local pediments in Axial zone (Val d'Aran, Neste...)
Eastern Pyrenees
✓Raised peneplain S in Axial Zone and outer fold belts
✓Pediment P1 formed around Neogene basins
Regional uplift

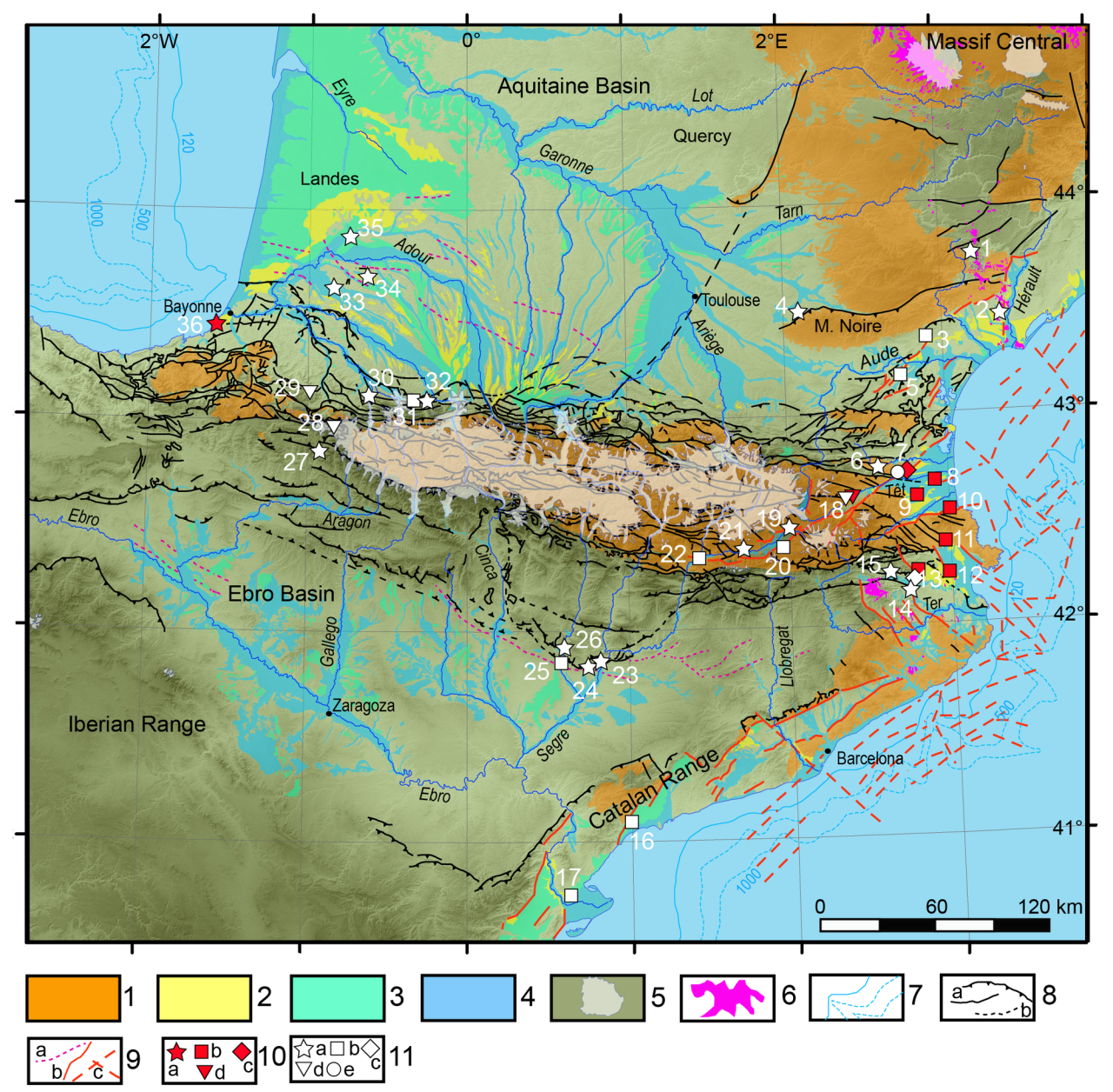
2°W
0°
2°E
Massif Central
Aquitaine Basin
Eyre
Lot
Quercy
Garonne
Landes
Tarn
44°
Adour
Hérault
Bayonne
Toulouse
M. Noire
Ariège
Aude
43°
Têt
Ebro
Aragon
Cinca
Ebro Basin
Gallego
Ter
42°
Llobregat
Iberian Range
Zaragoza
Segre
Barcelona
Catalan Range
Ebro
41°
0
60
120 km
1
2
3
4
5
6
7
8
9
10
11

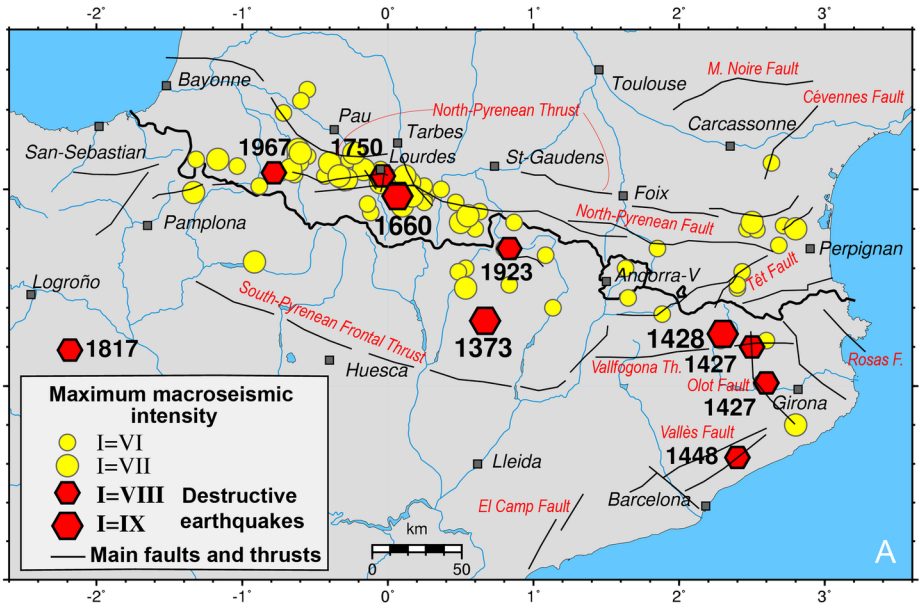
Bayonne
Pau
Tarbes
Lourdes
Toulouse
M. Noire Fault
Cévennes Fault
Carcassonne
San-Sebastian
1967
1750
North-Pyrenean Thrust
St-Gaudens
Foix
1660
Pamplona
North-Pyrenean Fault
Perpignan
1923
Logroño
Andorra-V
Tet Fault
South-Pyrenean Frontal Thrust
1817
1373
1428
Vallfogona Th.
1427
Rosas F.
Olot Fault
Huesca
1427
Girona
Vallès Fault
1448
Lleida
Barcelona
El Camp Fault
Maximum macroseismic intensity
I=VI
I=VII
I=VIII Destructive
I=IX earthquakes
Main faults and thrusts
km
0
50
A
-2°
-1°
0°
1°
2°
3°
43°
42°
41°

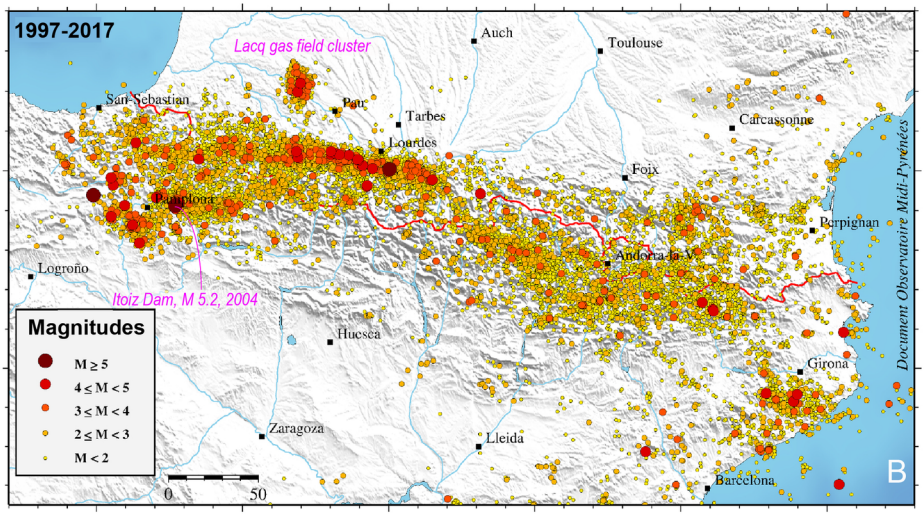
1997-2017
Lacq gas field cluster
Auch
Toulouse
San-Sebastian
Pau
Tarbes
Lourdes
Carcassonne
Foix
Pamplona
Perpignan
Andorra-la-V
Logroño
Itoiz Dam, M 5.2, 2004
Huesca
Girona
Zaragoza
Lleida
Barcelona
Magnitudes
M ≥ 5
4 ≤ M < 5
3 ≤ M < 4
2 ≤ M < 3
M < 2
0
50
B
Document Observatoire Midi-Pyrénées

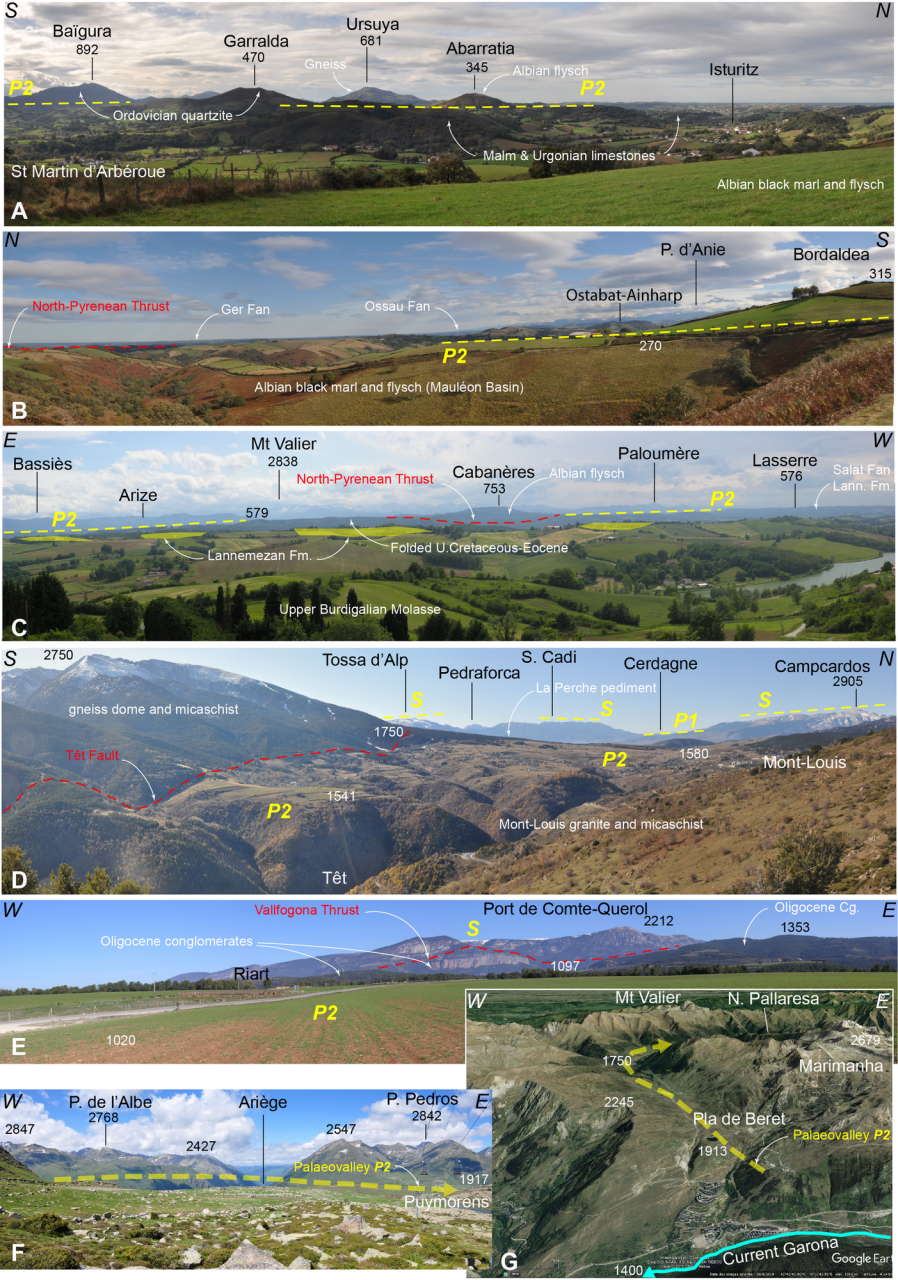
S
N
Baïgura
892
Garralda
470
Ursuya
681
Abarratia
345
Gneiss
Albian flysch
Isturitz
P2
Ordovician quartzite
Malm & Urgonian limestones
St Martin d'Arbéroue
Albian black marl and flysch
A
N
S
P. d'Anie
Bordaldea
315
Ostabat-Ainharp
270
North-Pyrenean Thrust
Ger Fan
Ossau Fan
P2
Albian black marl and flysch (Mauléon Basin)
B
E
W
Bassiès
Mt Valier
2838
Arize
579
North-Pyrenean Thrust
Cabanères
753
Albian flysch
Paloumère
Lasserre
576
Salat Fan
Lann. Fm.
P2
Lannemezan Fm.
Folded U.Cretaceous-Eocene
Upper Burdigalian Molasse
C
S
2750
Tossa d'Alp
Pedraforca
S. Cadi
La Perche pediment
Cerdagne
Campcardos
2905
N
gneiss dome and micaschist
S
P1
1750
Têt Fault
P2
1580
Mont-Louis
1541
Mont-Louis granite and micaschist
Têt
D
W
Vallfogona Thrust
Port de Comte-Querol
2212
Oligocene Cg.
1353
E
Oligocene conglomerates
S
1097
Riart
P2
1020
E
W
Mt Valier
N. Pallaresa
E
2679
1750
Marimanha
2245
Pla de Beret
Palaeovalley P2
1913
G
Current Garona
1400
Google Earth
W
P. de l'Albe
2768
Ariège
P. Pedros
2842
E
2847
2427
2547
Palaeovalley P2
1917
Puymorens
F